Improvements to Simulating the Carbon Cycle in Land Surface Models

BY

BETH AMY DREWNIAK
B.S., University of Illinois at Urbana-Champaign, 2002
M.S., University of Illinois at Urbana-Champaign, Champaign, 2006

THESIS

Submitted as partial fulfillment of the requirements
for the degree of Doctor of Philosophy in Biological Sciences
in the Graduate College of the
University of Illinois at Chicago, 2019

Chicago, Illinois

Defense Committee:

Miquel Gonzalez-Meler, Chair and Advisor
Joel Brown
Max Berkelhammer, Earth & Environmental Science
Jean Bogner, Earth & Environmental Science
V. Rao Kotamarthi, Argonne National Laboratory
Dr. Peter Snyder, University of Minnesota

For Mom and Dad, who taught me to aim for the stars

ACKNOWLEDGMENTS

I would like to thank my thesis advisor, Miquel Gonzalez-Meler for his guidance and patience throughout this process. I have learned more than I ever dreamed. Although I am still a modeler at heart, I have an appreciation for those "non-modeling" activities without which models would never exist. I would also like to thank my Argonne boss, Rao Kotamarthi, for encouraging me to start on this journey, and for all the words of wisdom when I ran into his office in "panic mode". Peter Snyder was also critical to my success, providing the first PhD seed in my head that persisted until I finally believed. I thank my committee for their advice and help steering my path through this new (to me) research area. I would also like to thank the Gonzalez-Meler lab at UIC for their council, feedback, and sharing an interest in my modeling endeavors.

Acknowledgements also go to Argonne National Laboratory and the Department of Energy, who supported much of this work through the Energy Exascale Earth System Model (E3SM) project. Numerical simulations were performed with high-performance computing resources provided by the National Energy Research Scientific Computing Center, a DOE Office of Science User Facility supported by the Office of Science of the U.S. Department of Energy and the cluster provided by the BER Earth System Modeling program operated by the Laboratory Computing Resource Center at Argonne.

Finally, I would like to thank my family, whose love and support helped me maintain my sanity as I clumsily tried to balance work, family, and school. I thank my parents, Vicki and

Stephen Bye, for a lifetime of encouragement and faith. I thank my husband, David Drewniak, who always believed in me, even when I had doubts. And my children, Emma and Abigail who waited up during those late-night work sessions for good night kisses and for giving me courage to keep plowing ahead.

BAD

CONTRIBUTION OF AUTHORS

Drewniak, B., Gonzalez-Meler, M. A., "Earth System Model needs for including the interactive representation of nitrogen deposition and drought effects on forested ecosystems", *Forests*, 8, doi:10.3390/f8080267 (2017).

This is a review manuscript that I conceived and primarily wrote. Miquel Gonzalez-Meler helped with writing and final revisions.

Drewniak, B. A., U. Mishra, J. Song, J. Prell, and V. R. Kotamarthi, "Modeling the impact of agricultural land use and management on US carbon budgets," *Biogeosciences*, 12: 2119-2129 (2015).

This manuscript I primarily wrote. J. Song, J. Prell and I performed all the code development in the model. I ran all the simulations and performed most of the data analysis. U. Mishra helped with data analysis compared with observations. All authors helped draft and edit the manuscript.

TABLE OF CONTENTS

TABLE OF CONTENTS (continued)

LIST OF TABLES

LIST OF FIGURES

LIST OF FIGURES (continued)

FIGURE PAGE

LIST OF FIGURES (continued)

LIST OF FIGURES (continued)

FIGURE PAGE

LIST OF FIGURES (continued)

LIST OF ABBREVIATIONS

ACME	Accelerated Climate Model for Energy
aDGVM	Adaptive Dynamic Global Vegetation Model
BDSB	Broadleaf Deciduous Shrub (Boreal)
BDST	Broadleaf Deciduous Shrub (Temperate)
BNF	Biological Nitrogen Fixation
C	Carbon
C3GA	C3 Arctic Grass
C3G	C3 Grass
C4G	C4 Grass
CABLE	CSIRO Atmospheric Biosphere Land Exchange
CESM	Community Earth System Model
CLM	Community Land Model
CONUS	contiguous United States
CTEM	Canadian Terrestrial Ecosystem Model
DBFT	Deciduous Broadleaf Forest (Temperate)
DOE	Department of Energy
E3SM	Energy Exascale Earth System Model
EBFT	Evergreen Broadleaf Forest (Temperate)
ED	Ecosystem Demography
ELM	E3SM Land Model
ENFB	Evergreen Needleleaf Forest (Boreal)
ENFT	Evergreen Needleleaf Forest (Temperate)

LIST OF ABBREVIATIONS (continued)

ENFTr	Evergreen Needleleaf Forest (Tropical)
ER	Ecosystem Respiration
ESM	Earth System Model
ET	Evapotranspiration
FUN	Fixation and Uptake of Nitrogen
GHG	Greenhouse Gases
GPP	Gross Primary Productivity
ISCN	International Soil Carbon Network
JeDi-DGVM	Jena Diversity-Dynamic Global Vegetation Model
LAI	Leaf Area Index
LSM	Land Surface Model
LUNA	Leaf Utilization of Nitrogen for Assimilation
N	Nitrogen
NEE	Net Ecosystem Exchange
NPP	Net Primary Productivity
ORCHIDEE	Organizing Carbon and Hydrology in Dynamic Ecosystems
PCC	Pearson Correlation Coefficient
PFT	Plant Functional Type
PRE	Percent Relative Error
RMSE	Root Mean Square Error
SD	Standard Deviation
SOC	Soil Organic Carbon

LIST OF ABBREVIATIONS (continued)

SWAT	Soil & Water Assessment Tool
TEC	Total Ecosystem Carbon
tRIBS + VEGGIE	TIN-based Real-Time Integrated Basin Simulator coupled to the Vegetation Generator for Interactive Evolution
Vcmax	maximum rate of carboxylation
WUE	Water Use Efficiency

SUMMARY

Earth System Models (ESMs) are the tools we use to experiment on the Earth, understand processes that drive climate, explore climate response to forcing, and project future climate. Their complexity has grown exponentially over the decades, and our understanding of the Earth, as a system, has advanced. The land surface model, one component of ESMs, allows us to analyze the interactions between vegetation and the carbon cycle. One important driver of model development has been addressing missing processes that impact the carbon cycle. In order to use ESMs more effectively, we must identify important pieces of biological systems that drive productivity and soil carbon storage that models currently lack.

One of the biggest uncertainties of climate change is determining the response of vegetation to many co-occurring stressors. In particular, many forests are experiencing increased nitrogen deposition and are expected to suffer in the future from increased drought frequency and intensity. Interactions between drought and nitrogen deposition are antagonistic and non-additive, which makes predictions of vegetation response dependent on multiple factors. Earth system models are ill-equipped to capture the physiological feedbacks and dynamic responses of ecosystems to these types of stressors. In chapter 2, I review the observed effects of nitrogen deposition and drought on vegetation as they relate to productivity, particularly focusing on carbon uptake and partitioning. I identify several areas of model development that can improve the predicted carbon uptake under increasing nitrogen deposition and drought. They include a more flexible framework for carbon and nitrogen partitioning, dynamic carbon allocation, better representation of root form and function, age and succession dynamics, competition, and plant

modeling using trait-based approaches. These areas of model development have the potential to improve the forecasting ability and reduce uncertainty of climate models. Two of the model developments, dynamic roots and dynamic carbon allocation, are then addressed in Chapter 3 and 4, respectively.

Roots are important contributors to plant development, functioning to provide nutrients and water for plant growth. However, roots and their functions are often simplified in earth system models, which limits the feedbacks of root foraging strategy on plant productivity, and their impacts on the carbon cycle. The goal of Chapter 3 is to introduce a new method to resolve the vertical structure of roots over time in the Energy Exascale Earth System Model. The method allows plasticity of rooting depth distribution under non-uniform profiles of water and nitrogen, which influences aboveground dynamics. The dynamic root model optimizes root distribution for both water and nitrogen uptake, but gives priority to plant water demands. The resulting root distribution maintains agreement with observations in most ecosystems, while marginally improving the gross primary productivity estimated by the model, compared to satellite observations. Increases in gross primary productivity are simulated in desert and boreal ecosystems, but decreased elsewhere. When the model distributes roots to uptake both nitrogen and water, a transfer of roots away from water resources toward nitrogen occurs, without a modeled benefit to nitrogen uptake. This results in the drop in GPP seen in most ecosystems. In addition, the model does not capture deep roots in the dry tropics, and therefore productivity losses are observed in parts of the Amazon and the African savannah. Sensitivity studies were performed that increased the amount of water stress experienced by the plant to explore the

model behavior in water-limited ecosystems. They showed, not surprisingly, as roots grew deeper, more water was available to the plant. This allowed GPP to increase in most ecosystems, with the exception of deserts, where the soil moisture was depleted and GPP decreased. The main conclusion of the study was additional model processes, such as climate dependent root depth, root hydraulics, root form and function, and better nitrogen uptake, should be considered to improve the root water and nitrogen uptake in ELM.

Most ESMs use simple allometric rules for carbon partitioning, which focus on fixed biomass ratios regardless of environmental conditions, with little to no attempt to capture plant plasticity. The lack of dynamics result in a limited capacity of models to predict vegetation response to climate change. Ideally, models should permit varying biomass ratios as a product of the co-limitation of resources. The work in Chapter 4 applies a new method of partitioning between above- and below-ground plant components using the Cobb-Douglas production function. The Cobb-Douglas production function is commonly used in economics to maximize an output given multiple inputs, analogous to a cost-benefit analysis. Here, we use the function in an optimization model to maximize GPP given inputs of carbon and nitrogen, where uptake of resources is governed by the production of leaves and roots, and a cost from the creation and maintenance of biomass. This allows a dynamic allocation of biomass between above and belowground components to simulate responsive plant development. The method is applied to the Energy Exascale Earth System Model (E3SM), a fully coupled climate-energy ESM, developed by DOE to investigate interactions between energy, climate, water, and land at high resolution. The model is tested using a single point resolution at various Fluxnet sites that

capture a diverse set of plant functional types. The usefulness of the approach is evaluated by the ability of the model to capture productivity at individual sites across numerous climate regions. The results indicate a strong dependence of fine root:leaf ratios on phenology. In particular, evergreen phenology vegetation has the highest fine root:leaf ratios, suggesting a more limited nitrogen environment. In contrast, deciduous phenology vegetation has the lowest fine root:leaf ratios, signaling these ecosystems are more carbon limited. In many ecosystems, the change in fine root:leaf ratios resulted in an increase in model simulated GPP, which also shows better agreement with observations at those sites. However, in nitrogen limited systems, GPP decreased because the nitrogen uptake in the model is not increasing. The results reveal additional model development activities that should be targeted to improve the dynamic carbon allocation model. However, the proof of concept shows promise for integrating dynamic allocation in ESMs.

Cultivation of the terrestrial land surface can create either a source or sink of atmospheric CO_2, depending on land management practices. The Community Land Model (CLM) was recently updated to include representation of managed lands growing maize, soybean, and spring wheat. In Chapter 5, the CLM-Crop model is used to investigate the impacts of various management practices, including fertilizer use and differential rates of crop residue removal, on the soil organic carbon (SOC) storage of croplands in the continental United States over approximately a 170-year period. Results indicate that total U.S. SOC stocks have already lost over 8 Pg C (10%) due to land cultivation practices (e.g., fertilizer application, cultivar choice, and residue removal), compared to a land surface composed of native vegetation (i.e., grasslands). After long periods of cultivation, individual subgrids (the equivalent of a field plot)

growing maize and soybean lost up to 65% of the carbon stored, compared to a grassland site. Crop residue management showed the greatest effect on soil carbon storage, with low and medium residue returns resulting in additional losses of 5% and 3.5%, respectively, in U.S. carbon storage, while plots with high residue returns stored 2% more carbon. Nitrogenous fertilizer can alter the amount of soil carbon stocks significantly. Under current levels of crop residue return, not applying fertilizer resulted in a 5% loss of soil carbon. Our simulations indicate that disturbance through cultivation will always result in a loss of soil carbon, and management practices will have a large influence on the magnitude of SOC loss.

1 INTRODUCTION

Carbon enters through the leaf.
Photosynthesis completes.
Growing, reaching, climbing high
toward the sunlight in the sky.
Till quietly falling to the ground;
crunching, munching can be found.
Here begins Decomposition,
Carbon stored in transition.
Freed as Respiration breath,
coming from soil depth.
There the cycle seems to end,
only to begin again.

Land matters. The land is tightly coupled to the atmosphere. The complex nature of the land's topography of mountains and rolling hills or vast stretches of sandy deserts help drive atmospheric processes. But those atmospheric processes also drive changes in the land by creating lush tropical rainforests teeming with biodiversity, rivers and lakes, ice and snow. The land surface can significantly alter atmosphere-land interactions through modifications to albedo, boundary layer, surface moisture, heat and energy fluxes. The land surface effects temperature and precipitation. The land surface has a large influence on hydrology and nutrient cycling. The land surface contributes to biogeochemical changes of soil organic carbon storage. Land matters.

Furthermore, climate change is expected to have a considerable effect on vegetation, influencing distribution, growth cycles, net primary productivity, and biodiversity (Sykes, 2009). Understanding how plants will respond to changes in temperature and precipitation is one of the primary concerns of biologists and climate scientists. Since elevated CO_2 and aerosol loading of the atmosphere will continue to disturb the balance of carbon, nitrogen, and water including

altered temperature and precipitation, understanding changes in vegetation behavior under these conditions is critical for successful simulation of historical and projected climate changes in ecosystems and their feedback to the earth system.

Edward Wilson (1999) states in his book The Diversity of Life, "one planet, one experiment". But, the creation of the Earth system model (ESM) has given scientists a tool to experiment on the whole earth so we can move forward and backward in time, learning from the past in order to predict the future. These ESMs have come a long way from their predecessors from 50 years ago. In a world facing climate change, focus was often on the atmosphere and the ocean. In fact, the first climate models to run on large scale computers, introduced in the 1960s, only included an atmosphere (Edwards, 2011). Ocean models were added soon after, but these atmosphere-ocean models (or General Circulation Models as they are now known) weren't coupled to land models until the 1980s. This oversite is understandable, given the small portion of the planet occupied by land – 30% compared to the 70% of ocean. But, the remaining 30% that makes up land and ice influences albedo, energy fluxes, carbon, nutrient and water cycles. And, when we consider the soil and vegetation store over three time more carbon than the atmosphere, it is obvious, land matters.

Fortunately, the climate community recognized the important role the land surface plays in driving atmospheric and climate processes. To that extent, many climate models began incorporating increasingly complex representations of the land surface, including vegetation, hydrological, and biogeochemical processes. And still, the land model continues to evolve. It is beyond the scope of this thesis to provide a history of land surface modeling, or even a

theoretical overview of current land surface models. For these, see the works of Pitman (2003) and Sato et al. (2015). It is, however, the introduction of the carbon cycle where things really got interesting in climate models.

Uncertainty in the carbon cycle contributes 40% or more of the spread in temperature from climate model simulations (Huntingford et al., 2009). Most uncertainty comes from the differences in model setup and complexity (Friedlingstein et al., 2014). Yet there is also uncertainty from within the models. For example, one great source of uncertainty in the carbon cycle is from how soil moisture stress is represented in models (Trugman et al., 2018). The cause is largely due to the way models handle water uptake through root systems (Warren et al., 2015). Another example of uncertainty is in land use land cover or dynamic vegetation (Yu et al., 2016). Bloom et al. (2016) suggested that the carbon stocks and residence times have not been properly captured in models. Given the importance of feedbacks between the carbon cycle and the atmosphere, land surface models (LSMs) should strive to capture the full carbon cycle. But developing processes, calibrating those processes, and validating the models is a challenge.

Therefore, this thesis serves to improve a small number of processes in land surface models to better predict impacts on the carbon cycle. I will begin in Chapter 2 with a discussion of ecosystem response to stress and highlight opportunities for future model development to improve model prediction. Then in Chapters 3, 4, and 5, I will undertake some major model developments to integrate some of the missing processes in ESMs.

While there are multiple studies that address the effects of a single stress (e.g., drought, elevated CO_2, nitrogen deposition, etc.), there are relatively few studies that address multiple co-occurring stressors. This subject is approached in Chapter 2 in a published manuscript in the journal Forests. Two types of stress are chosen, one from climate (drought) and the other from humans (nitrogen deposition). They are chosen because the ecosystem response to these two stresses are antagonistic (Meyer-Grünefeldt et al., 2013). For example, nitrogen deposition increases nutrient availability which causes trees to invest more biomass in stems (Pregitzer et al., 2008), but vegetation response to drought typically results in more root growth (Hertel et al., 2013). The manuscript identifies the processes responsible for vegetation response to these co-occurring stresses. The resulting discussion lists focus areas of model development for ESMs to capture the response of ecosystems.

Two of the model development recommendations that are discussed in Chapter 2, dynamic roots and dynamic carbon allocation, will be addressed in Chapters 3 and 4, respectively, in the E3SM Land Model (ELM). Previous work integrating dynamic vegetation into climate models only considered changes in vegetation distribution based on known ranges of temperature or precipitation regimes, with relatively narrow opportunities for vegetation to respond to nutrient limits except through photosynthesis downscaling, despite strong evidence that vegetation responds to the environment (Medlyn et al., 2015; De Kauwe et al., 2014; Thomas et al., 2009; Hermans et al., 2006; Ainsworth and Long, 2004). For example, most LSMs have fixed allocation rules governing carbon and nitrogen partitioning between leaves, stem, and roots (Franklin et al., 2012). This treatment restricts the plant response to changes in environment. Additionally, roots are represented with static depth and distribution dependent

only on plant functional type, greatly simplifying one of the most significant contributors to the carbon and hydrological cycles (Warren et al., 2015).

To address root dynamics, in Chapter 3 I introduce a new method of root distribution in the ELM. There have been some advances in dynamic root modeling to optimize water uptake (Sivandran and Bras et al., 2013), nitrogen uptake (McMurtie et al., 2012), or allow root distribution to shift with age (Arora and Boer, 2003). The new approach is designed to respond to both water and nitrogen limitations, with more emphasis on water uptake. I then compare the model response of gross primary productivity (GPP), total ecosystem carbon, evapotranspiration, and nitrogen uptake with and without dynamic roots. The manuscript concludes with a discussion of additional model development needed to fully utilize dynamic roots. This manuscript was published in the Journal of Advances in Modeling Earth Systems.

Next, in Chapter 4, I present an optimization method to dynamically allocate plant carbon in ELM. Using parallels between economics and ecology, plants are allowed to optimize productivity by choosing where to invest biomass such that water, nutrient, and carbon uptake are maximized. The result can expand the ability of the coupled biosphere-atmosphere model to respond to resource availability and improve predictions of critical exchanges of energy, water, and carbon between land use and the atmosphere.

But as much effort is given to improving the vegetation response to climate, we often forget that perhaps the most important driver are humans. Humans have managed the land by converting forests, prairies, and deserts to agriculture fields and urban centers, diverted rivers,

depleted lakes, and fragmented the landscape. And yet, human influence on the landscape has largely gone unnoticed in earth system models. We are aware that we have perturbed the load of carbon in the atmosphere through our emissions of fossil fuels. As such, we include the effect of elevated CO_2 in the atmosphere, but the scarred land surface does not show any indication of human consumption. Therefore, in Chapter Five, I confront the largest uncertainty of the Earth system – humans. For this effort, I will bring managed lands into the Community Land Model (CLM) through agriculture representation.

This effort introduces three new plant functional types into the model framework: corn, soybean, and spring wheat. The analysis is not on the performance of the model, that is discussed in previous work by Drewniak et al. (2013). However, the effects of management, specifically the harvest of non-grain plant components for cellulosic ethanol, are evaluated for soil carbon storage. The model establishes a baseline approximation of the soil carbon that is lost in the US from agriculture practices, and estimates the amount of carbon that would be lost from different scenarios of harvest (from 10% to 90%). This manuscript was published in the journal Biogeochemistry.

All the model development discussed in the main chapters of this thesis relate to the carbon cycle. Chapters 2, 3 and 4 demonstrate the impacts on GPP. Chapter 3 also includes some discussion on total carbon storage. Chapter 5 includes soil carbon storage. Therefore, Chapter 6 serves to synthesize the results from the studies included in this thesis, and provides an overview of the broader impacts.

1.1 References

Ainsworth, E. A., and Long, S. P. (2005), What have we learned from 15 years of free-air CO2 enrichment (FACE)? A meta-analytic review of the responses of photosynthesis, canopy properties and plant production to rising CO2. *New Phytol.*, 165(2), 351-371.

Arora, V. K., Boer, G. J. (2003), A Representation of Variable Root Distribution in Dynamic Vegetation Models. *Earth Interact.*, *7*, 1–19.

Bloom, A. A., Exbrayat, J.-F., van der Velde, I. R., Feng, L., and Williams, M. (2016), The decadal state of the terrestrial carbon cycle: Global retrievals of terrestrial carbon allocation, pools, and residence times. *Proc. Nat. Acad. Sci.*, 113(5), 1285-1290.

De Kauwe, M.G.; Medlyn, B.E.; Zaehle, S.; Walker, A.P.; Dietze, M.C.; Wang, Y.P.; Luo, Y.; Jain, A.K.; El-Masri, B.; Hickler, T., Wårlind, D., Wang, E., Parton, W. J., Thornton, P. E. Wang, S., Prentice, I. P., Asao, S., Smith, B., McCarthy, H. R., Iversen, C. M., Hanson, P. J., Warren, J. M., Oren, R., and Norby, R. J. (2014), Where does the carbon go? A model-data intercomparison of vegetation carbon allocation and turnover processes at two temperate forest free-air CO2 enrichment sites. *New Phytol.*, 203, 883–899.

Drewniak, B., Song, J., Prell, J., Kotamarthi, V. R., and Jacob, R. (2013), Modeling agriculture in the Community Land Model. *Geosci. Model Dev.*, 6, 495–515. doi:10.5194/gmd-6-495-2013.

Edwards, P. N. (2011), History of climate modeling. *WIREs Climate Change*, 2(1), 128-139.

Franklin, O., Johansson, J., Dewar, R. C., Dieckmann, U., McMurtrie, R. E., Brännström, A. K., Dybzinski, R. (2012), Modeling carbon allocation in trees: A search for principles. *Tree Physiol.*, *32*, 648–666.

Friedlingstein, P., Meinshausen, M., Arora, V.K., Jones, C.J., Anav, A., Liddicoat, S.K., Knutti, R. (2014), Uncertainties in CMIP5 climate projections due to carbon cycle feedbacks. *J. Clim.*, 27, 511–526.

Hermans, C., Hammond, J. P., White, P. J., and Verbruggen, N. (2006), How do plants respond to nutrient shortage by biomass allocation? *TRENDS in Plant Science*, 11(12),610-617.

Huntingford, C., Lowe, J. A., Booth, B. B. B., Jones, C. D., Haris, G. R., Gohar, L. K., and Meir, P. (2009), Contributions of carbon cycle uncertainty to future climate projection spread. *Tellus*, 61B, 355-360.

McMurtrie, R. E., Iversen, C. M., Dewar, R. C., Medlyn, B. E., Näsholm, T., Pepper, D. A., Norby, R. J. (2012), Plant root distributions and nitrogen uptake predicted by a hypothesis of optimal root foraging. *Ecol. Evol.*, *2*, 1235–1250.

Medlyn, B. E., Zaehle, S., De Kauwe, M. G., Walker, A. P., Dietze, M. C., Hanson, P. J., Hickler, T., Jain, A. K., Luo, Y., Parton, W., Prentice, I. C., Thornton, P. E., Wang, S., Wang, Y.-P., Weng, E., Iversen, C. M., McCarthy, H. R., Warren, J. M., Oren, R., Norby, R. J. (2015), Using ecosystem experiments to improve vegetation models. *Nat. Clim. Chang.*, *5*, 528–534.

Pitman, A. J. (2003), The evolution of, and revolution in, land surface schemes designed for climate models. *International Journal of Climatology*, 23: 479-510.

Sato, H., Ito, A., Ito, A., Ise, T., and Kato, E. (2015), Current status and future of land surface models. *Soil Science and Plant Nutrition*, 61:1, 34-47.

Sivandran, G., Bras, R. L. (2013), Dynamic root distributions in ecohydrological modeling: A case study at Walnut Gulch Experimental Watershed. *Water Resour. Res.*, *49*, 3292–3305.

Sykes, M. T. (2009), Climate change impacts: Vegetation. *Encyclopedia of Life Sciences*, doi: 10.1002/9780470015902.a0021227.

Thomas, R. Q., Canham, C.D., Weathers, K.C., Goodale, C.L. (2010), Increased tree carbon storage in response to nitrogen deposition in the US. *Nat. Geosci*, 3, 13–17.

Trugman, A. T., Medvigy, D., Mankin, J. S., and Anderegg, W. R. L. (2018), Soil moisture stress as a major driver of carbon cycle uncertainty. *Geophysical Research Letters*, 45, 6495-6503.

Warren, J.M., Hanson, P.J., Iversen, C.M., Kumar, J., Walker, A.P., Wullschleger, S.D. (2015), Root structural and functional dynamics in terrestrial biosphere models—Evaluation and recommendations. *New Phytol.*, 205, 59–78.

Wilson, E. O. (1999), The Diversity of Life, New York, NY: W. W. Norton & Company.

Yu, M., Wang, G., and Chen, H. (2016), Quantifying the impacts of land surface schemes and dynamic vegetation on the model dependency of projected changes in surface energy and water budgets. *Journal of Advances in Modeling Earth Systems*, 8(1), 370-386.

2 EARTH SYSTEM MODEL NEEDS FOR INCLUDING THE INTERACTIVE REPRESENTATION OF NITROGEN DEPOSITION AND DROGHT EFFECTS ON FORESTED ECOSYSTEMS

This chapter was previously published as Drewniak, B., and Gonzalez-Meler, M. A. 2017. Earth System Model needs for including the interactive representation of nitrogen deposition and drought effects on forested ecosystems. *Forests*, 8, 267: doi:10.3390/f8080267.

2.1 Introduction

Earth system models (ESMs) have been used to predict the climate's response to increased CO_2 emissions (or concentrations), but uncertainty in land carbon (C) feedbacks results in a wide spread of uncertainty in model results (Friedlingstein et al., 2014). Part of this uncertainty lies in a general lack of knowledge of the physical processes responsible for the land feedbacks on the C cycle, which makes estimating the land C sink difficult. Adding to this uncertainty is the response of ecosystems in the face of multiple stressors, the impacts of which may be non-additive and will certainly be highly variable across ecosystems. One prime example is the current increase in nitrogen (N) deposition and the predicted increase in drought (Seneviratne et al., 2012). Most field studies isolate one environmental component (e.g., drought, elevated CO_2, N deposition) to study plant behavior. This results in an incomplete knowledge of an ecosystem's reaction to multiple stressors, which limits our forecasting capability. Vegetation responses have a strong influence on C storage. As plants adjust their partitioning strategy for C and other nutrients to optimize uptake while limiting costs to ensure survival, the quantity and quality of C stored and the way nutrients are recycled will change.

Anthropogenic production of reactive N from fossil fuel combustion and fertilizer synthesis has led to an increased availability of reactive N in ecosystems, and this has become a global problem (Vitousek et al., 1997). The current N deposition rate in some systems is over 10 kg ha^{-1} $year^{-1}$ (Galloway et al., 2008), which is well over the deposition rate from natural sources at 0.5 kg ha^{-1} $year^{-1}$ (Dentener et al., 2006). Nitrogen deposits from industrial and agriculture activities have led to significant N loading in soils, particularly in regions of Europe and the eastern United States (Aber et al., 2003; Bobbink et al., 2010). These N additions are within the critical load of N for sensitive ecosystems (Pardo et al., 2011; Bobbink and Roelofs, 1995). This N loading may be further exacerbated by increases in N availability from climate influences (i.e., warming and elevated CO_2) on internal N cycling, which can increase decomposition, mineralization, and biological nitrogen fixation (BNF) (Melillo et al., 2002; Pastor and Post, 1988; Peterjohn et al., 1994). The consequences of N loading are well known and include changes in biodiversity (Bobbink et al., 2010; Clark and Tilman, 2008; Simkin et al., 2016), composition (BassiriRad et al., 2015; Minocha et al., 2015), productivity (Matson et al., 2002), leaching (Fang et al., 2009; Dise and Wright, 1995), and possibly nitrification (Matson et al., 2002). Since N is strongly tied to C, understanding the impact of increased N availability in ecosystems in the context of climate change is crucial if we are to understand whether increased N availability will strengthen or weaken the land's C sink capacity.

Understanding the vegetative response to N deposition is increasingly difficult due a wide variability of responses between and within species and across climate and soil regimes, as well as contrasting behavior when faced with other elements of climate change (e.g., elevated CO_2 or

drought). For example, increased N availability generally results in an increase in aboveground woody biomass and a decrease in root biomass, but experiments with drought indicate an increase in root biomass at the expense of aboveground tissue (Broeckx et al., 2014; Hertel et al., 2013; Martin-St. Paul et al., 2013; Padilla et al., 2009). This has led to the conclusion that N deposition may increase ecosystem vulnerability to drought (Friedrich et al., 2012), but some studies find that N deposition may enhance the recovery of some species post drought (Kinugasa et al., 2012). Therefore, a large uncertainty exists for vegetation response to increased N deposition under drought, especially because many of these antagonistic responses exhibit nonlinear behavior.

Predictions of climate change indicate an increase in the frequency and severity of drought (Seneviratne et al., 2012) in many regions that are already water stressed. For example, in the Amazon, the dry season is expected to lengthen and intensify, and the area affected by seasonal drought is expected to expand by up to 0.75 million km^2 by the end of the century (Boisier et al., 2015). The southwest and central United States are forecast to experience increases in drought severity that exceed the severest mega drought events at millennial scales (Cook et al., 2015). Areas that do not experience a change in total precipitation may still experience changes in the timing and intensity of rainfall events. Plants under drought stress can experience hydraulic failure, C starvation, and increased vulnerability to disease, pests, and fire. Drought during peak growth periods will likely be more detrimental; juvenile and shallow-rooted plants are most susceptible to drought, whereas plants that are able to modify biogeochemical feedbacks will increase their chance of survival (Hanson and Weltzin, 2000). In general, drought results in decreased stomatal conductance and decreased net primary productivity (Cook et al.,

2015). In the past, drought events over the Amazon have reduced C storage through mortality and slowed growth (Phillips et al., 2009); increased events in the future could result in a weaker C sink of boreal, temperate, and tropical biomes across the globe (He et al., 2014). This would contrast with the increased productivity that can result from high N deposition. Most ecosystems have experienced an extreme drought in the past, but extreme drought in combination with other climate impacts such as N deposition can put unprecedented amounts of stress on ecosystems. Given that the co-occurrence of drought and increased N availability are highly probable, these climate effects must be considered together to predict ecosystem behavior.

To answer questions about the future of the terrestrial C sink, we need to understand the behavior of ecosystems under long-term chronic N deposition and drought, as well as the interactions between these phenomena. ESMs are important tools for exploring the relationships between climate and vegetation responses, but current models might not be able to capture these processes.

The ESM community has made great strides in improving the C cycle in land surface models (LSMs) due to improvements to biogeochemical and hydrological cycles. Some of these advances constrain land C sequestration by imposing N limitations on C fertilization (Thornton et al., 2009), water table, and inundation dynamics (Koirala et al., 2014) and even hydraulic redistribution (Yan and Dickinson, 2014). However, these models still cannot capture mortality in trees from drought, changes in biomass partitioning due to nutrient limitations, or even acclimation (Leuzinger and Thomas, 2011). For example, Ukkola et al. (2016) found that 14 LSMs overestimate seasonal drought, due partly to how models handle soil hydrology and plant

moisture stress. De Kauwe et al. (2015) also found that LSMs exaggerate drought effects because most models assume the same drought sensitivity for all vegetation types. Adding the N cycle to LSMs results in productivity decreases that range from 7% to 64% (Fisher et al., 2012), but the feedbacks between C and N are weak once a steady state is reached (Gerber et al., 2010). This suggests that ESMs still lack key processes. In order to simulate N deposition-drought interactions, we hypothesize that additional model developments are necessary to mimic ecosystem stress responses, particularly if ESMs are to represent the C cycle accurately.

This review seeks to determine whether the current ESM framework of the C cycle is sufficient to capture the vegetation response to the combined effects of drought and growing N loading in ecosystems. To that end, this paper will review the observed impacts on C uptake and allocation due to increased N availability, drought, and their combined effects. Next will be a review of how current ESMs represent the coupled carbon-nitrogen model for C uptake and partitioning. We will present recent developments in several state-of-the-art LSMs, including the limitations of the representations for capturing interactions from N deposition and drought stress. Finally, we will discuss which additional processes should be the focus of future model developments to reduce uncertainty and improve predictive power.

2.2 Observations of N Inputs

Nitrogen is a critical component in ecosystems; it drives productivity through photosynthesis processes (Evans, 1989). Increased N deposition results in increased production because N is generally the most limiting nutrient for growth (Fisher et al., 2012, Davidson and

Howarth, 2007). Bala et al. (2013) estimate that an additional 175 PgC has been stored since the pre-industrial period due to increased N deposition. This increase results mostly from changes in photosynthesis (i.e., increase in foliar N) or shifts in C allocation to increase light availability (Figure 2.1 and Table I, Appendix A). Several mechanisms will allow plants to respond to changes in N such as the ability to increase photosynthetic capacity, plasticity to alter C partitioning of resources, and the presence or absence of other limiting factors in the system (e.g., water, P, mycorrhizal associations, etc.). An overview of some of the consequences of N deposition in ecosystems is included in Figure 2.1.

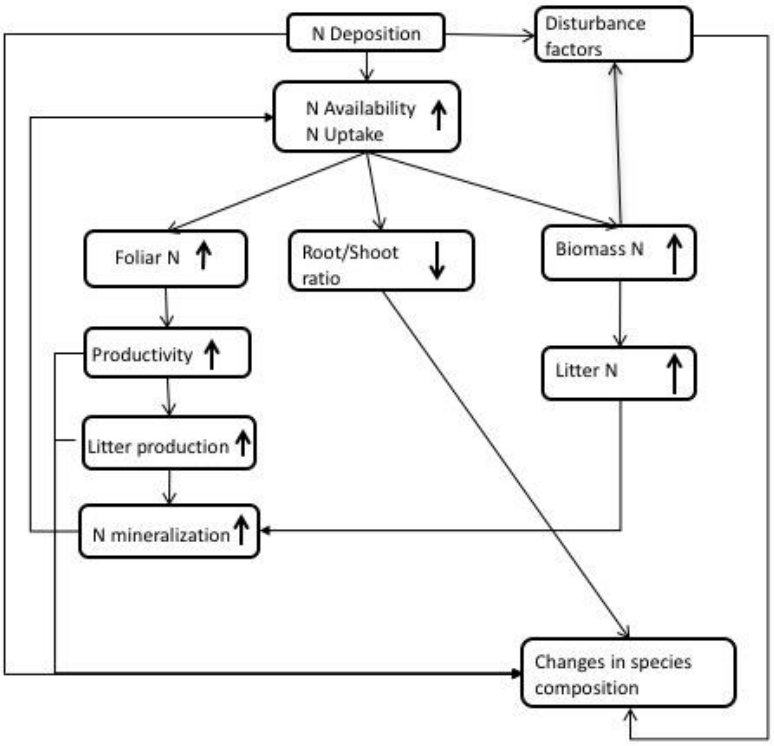

Figure 2.1. Effects of N deposition on ecosystems, based on the concepts of Bobbink et al. (2010). Up arrows represent an increase, and down arrows represent a decrease. Three main pathways exist: changes in foliar or leaf N, changes to biomass partitioning, and increases in biomass N. Changes in leaf or plant N generally lead to a positive feedback by increasing N in the litter pool. Changes in the partitioning of biomass can lead to changes in competition for resources that will ultimately affect species distribution. In general, the impacts of N deposition occur over short timescales (<5 years), while changes to species composition and disturbance occur over longer timescales (Bobbink et al., 2010).

Nitrogen deposition studies frequently find an increase in foliar N that results in decreased C:N ratios of leaves (Pregitzer et al., 2008; Elvir et al., 2005; Boggs et al., 2005). This relationship between N deposition and foliar N content has even been used to estimate critical

loads of N in Europe (Pitcairn et al., 2001). Pregitzer et al. (2008) suggested that the increase in foliar N is responsible for the increase in aboveground net primary productivity (ANPP) that is found under elevated N availability, considering the relationship N plays in photosynthetic capacity and C assimilation (Evans, 1989; Fleischer et al., 2013). However, reductions in N use efficiency and C allocation shifts away from mycorrhizae may also result in increases in ANPP (Talhelm et al., 2011). Increases in productivity can also lead to increases in litter production that can ultimately lead to increased N in soils.

Gains in productivity can be the result of changes in patterns of C partitioning within the plant, and they often seem to be correlated with increases in above ground biomass (Pregitzer et al., 2008; Wang et al., 2012; Thomas et al., 2012). Most increases in aboveground biomass from increased N deposition are allocated to stems (Pregitzer et al., 2008; De Vries et al., 2014; Xia et al., 2008), particularly for small-diameter trees (Ibáñez et al., 2016). This response results in faster biomass accumulation, which produces taller, skinnier trees (Ibáñez et al., 2016). Although this is more likely to affect young trees or seedlings exposed to elevated N, Du and Fang (2014) also found weak growth in a mature forest. This may increase the mortality of young trees as a result of light limitation or the respiratory costs of early rapid growth (Ibáñez et al., 2016). However, the increase in growth is not consistent or linear for all species. For example, de Vries et al. (2014) found that tropical forests had the least response to N deposition compared to temperate and boreal forests, and in some cases a negative growth relationship exists at high N inputs (Thomas et al., 2010). Herbaceous plants also experience biomass increases from N deposition (Wang et al., 2012; Verma et al., 2014), and under low levels of N deposition they can increase aboveground biomass more than trees (Xia et al., 2008).

The increase in aboveground biomass is expected to come at the expense of belowground inputs Wang et al., 2012). However, it is unclear how roots respond to increased N availability; this response can include increases in productivity, even though decreases in biomass occur (Brassard et al., 2009). This occurs when increases in root turnover with N availability result in root biomass decreases over long time scales, even though C allocated to the roots likely increases. The root response is strongly associated with root sensitivity (Smithwick et al., 2013); the heterogeneity of the soil, substrate, and climate can result in different root responses that will increase root vulnerability to damage or mortality.

Finally, increases in N deposition can increase N in forest biomass (Zhu et al., 2015). This increase in biomass will lead to changes in N cycling as biomass eventually flows from the canopy into the litter pool. The enhanced amount of N in the litter pool can cause faster decomposition (Zhu et al., 2015) and increase N mineralization on the forest floor.

Nitrogen deposition can also increase susceptibility to disturbance factors. An increase in biomass N can lead to lowered resistance to pathogen infection or herbivory (Bobbink and Lamers, 2002). This increased vulnerability to pests can result in increased wildfires (Grulke et al., 2009). Ultimately, these changing conditions could lead to changes in species composition and biodiversity as a result of shifts in nutrient availability or toxicity, environment favorability, and competition Bobbink et al. (2010).

2.3 Observations of Drought Impacts

Under drought conditions, plants typically undergo C starvation or hydraulic failure (Mcdowell et al., 2008) (Figure 2.2. and Table I, Appendix A). Either condition can be fatal. Carbon starvation occurs when stomata close to constrain water loss, resulting in significantly lower C assimilation that will not only halt growth, but also risk insufficient reserves to sustain plant maintenance requirements. Hydraulic failure occurs when xylems become damaged or collapse, limiting a plant's ability to extract water. The timing of drought and phenology will play a key role that drives plant response (Weißhuhn et al., 2011). For example, a drought event that coincides with the peak growth period will result in higher plant mortality than drought during a less active growth period. Another important consideration is drought intensity versus drought frequency (Klein et al., 2011). A severe drought with a long duration will have a different impact on plant response and survival than short, frequent droughts. The length of time a plant has been exposed to drought cycles is an important driver of trait changes that increase drought tolerance. Over short time scales, stomata regulate water loss, but, over longer time scales, changes in allometry will occur to optimize hydraulic conductance (Martin-St. Paul et al., 2013). Plant traits may change similarly across short and long drought intervals; for example, leaf area may decrease with decreasing precipitation, while other processes may be delayed (i.e., partitioning changes between the leaf and roots) or homeostatic (e.g., xylem vulnerability) (Martin-St. Paul et al., 2013). Figure 2.2. shows some of the effects forests may experience under drought.

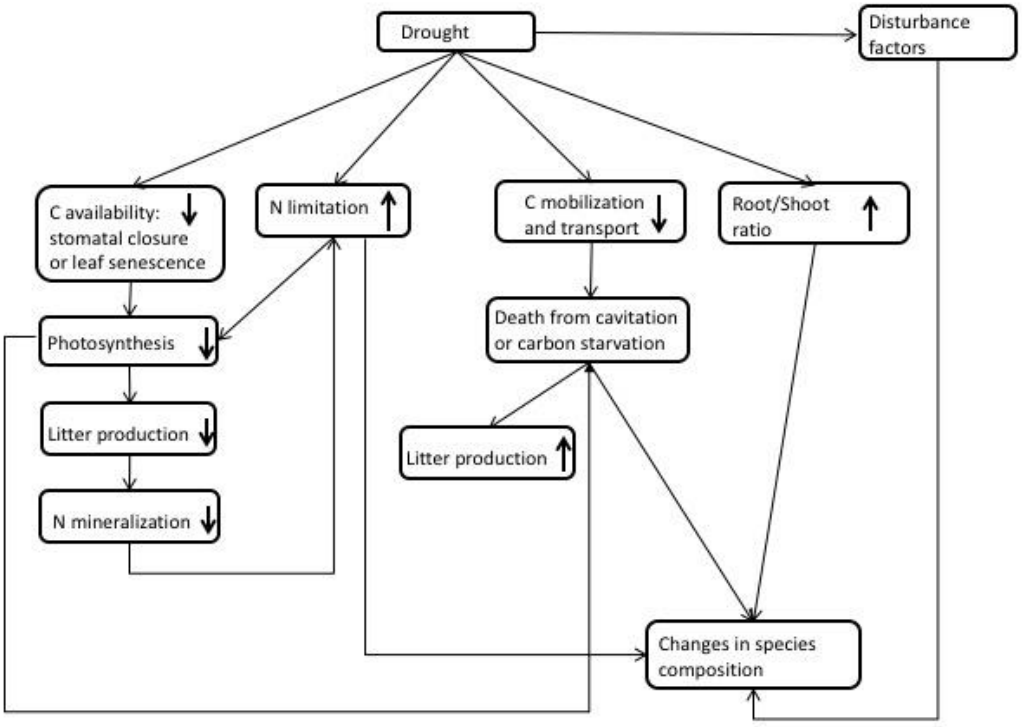

Figure 2.2. Effects of drought on ecosystems. Up arrows represent an increase, and down arrows represent a decrease. Four main pathways exist: changes in C availability, increases in N limitation, changes to C mobilization and transport, and changes to biomass partitioning (i.e., root:shoot). Changes in C availability and N limitation both lead to decreases in photosynthesis, which has a positive feedback on N limitation when less biomass is contributing N to litter pools. Changes in C availability and a lack of C mobilization can lead to death from carbon starvation. Several pathways result in altered species composition from shifts in nutrient availability and competition. In general, the impacts from drought occur over short timescales (<5 years), while changes to species composition and disturbance occur over longer timescales.

There are many ecological traits that can make a system more or less tolerant to drought, thereby leading to improved water use efficiency, including control over stomatal conductance, allometric plasticity, hydraulic redistribution (Baker et al., 2008), or even long-term acclimation.

To survive drought, plants may also reduce C demand, which can be achieved by leaf senescence and the down-regulation of respiration (Sala et al., 2010).

Many field studies have observed increased stomatal closure (Broeckx et al., 2014; Hanson and Weltzin, 2000; Cardoso et al., 2015) and increased water use efficiency during droughts (Broeckx et al., 2014). However, observations also found species that have less stomatal control and may continue to transpire well into a drought event (Cardoso et al., 2015). This may provide an advantage during short-term droughts but not necessarily during longer, more intense drought events. The ability to moderate water uptake and growth may be absent in the tropics; Rowland et al. (2015) found no change in the growth rate of trees in the Amazon under a long-term drought.

Stomata closure will reduce photosynthesis and, over long periods, lead to lower biomass accumulation, litter production, and ultimately N mineralization in the soil (Schimel et al., 2007). Additional nutrient limitations can occur during drought because of low soil moisture levels, which act to reduce nutrient flow and diffusion in soils. These N limitations can exacerbate the effects of drought by limiting photosynthesis further.

Since plants continue to demand C for metabolic respiration, when stomata close during drought, plants rely on reserves to meet C requirements. The ability to mobilize and transport stored C may be impaired by drought but is critical for species survival (Sala et al., 2010). Carbon reserves can help trees avoid C starvation. As these reserves are depleted, a tree may

suffer from C starvation. Although this theory lacks testing, McDowell et al. (2008) suspects that C starvation may result in the mortality of isohydric species under drought conditions.

Another adaptation to drought is through increases in the root-to-shoot ratio to maintain respiration during the early stages of drought, as suggested by the optimal partitioning theory. Hertel et al. (2013) found a doubling of root production and an increase in root-to-leaf biomass and production under drought in a mature beech forest. Even under significant decreases in a plant's relative growth rate, its root growth may remain constant (Lotter et al., 2014). The ability to re-translocate biomass from leaves and stems or utilize stored nonstructural carbohydrates can increase survival chances (Klein et al., 2011). Furthermore, altering the morphological characteristics of roots (e.g., length and surface area) can also aid in fulfilling water demands (Meier and Leuschner, 2008).

The ability to extend root systems to deep soil layers (Hanson et al., 2007) or move water through the soil column from depth via hydraulic redistribution can also increase a plant's chance of surviving a drought. Not only can this effect transfer water upward into dry soils, allowing plants to maintain transpiration and photosynthesis during dry seasons or at night, it can move water downward to be protected from evaporation or competition. The obvious benefit of hydraulic redistribution is maintaining water potential below hydraulic failure limits, but neighboring plants can also take advantage of the new water that is available (Prieto et al., 2012). The quantity of water hydraulically transferred ranges from 0.04 mm H_2O d^{-1} up to 1.3 mm H_2O d^{-1} and may be as much as 80% of the water that the plant transpires (Neumann and Cardon, 2012).

Several other mechanisms can also play a role in drought mortality such as increased vulnerability to pests or fungal infection and fire (He et al., 2014; Allen et al., 2010). These disturbances can have a devastating impact on forest mortality and the C cycle. Similar to N deposition impacts on vegetation, changes in biomass, composition, mortality, and nutrient cycling can lead to shifts in species competition and distribution (McDowell et al., 2008) and the impairment of the mobilization and transport of stored C (Sala et al., 2010; Allen et al., 2010).

2.4 Interactions between N and Drought

The interactions between N and drought are difficult to determine because (1) the effects can depend on the timing of N deposition relative to drought; (2) most experiments are done with young trees or herbaceous plants and not with mature vegetation; (3) many studies impose only weak drought conditions that might not result in drought–N feedbacks (Kleczewski et al., 2012); and (4) the impacts vary with ecosystem and plant traits. However, in general, the effects from drought and N deposition are interdependent (Friedrich et al., 2012) and not always additive Meyer-Grünefeldt et al., 2013; Meyer-Grünefeldt et al., 2015). A list of studies that have examined N deposition-drought interactions is included in Table I, Appendix A.

Drought seems to negate the increase in productivity observed from increased N deposition (Liu et al., 2013; Wang et al., 2012), although the effects of N addition may alleviate some of the impacts of drought on growth (Wang et al., 2012). This can be partially attributed to the countering effects of N and drought on photosynthesis; in particular, N deposition tends to

increase photosynthetic capacity, while drought limits photosynthesis. Other interactions between these two types of stress also occur. For example, N deposition tends to increase water use efficiency (WUE), but, during a severe drought, plants may lose the ability to utilize N, leading to a loss of biomass (Liu et al., 2013). Some ecosystems experience a decline in above- and belowground biomass (Friedrich et al., 2012; Palátová, 2004) and a loss of root functionality Palátová et al., 2004). In some cases, changes in allocation between above- and belowground biomass result in higher root-to-shoot ratios (Meyer-Grünefeldt et al., 2015).

The timing of a drought event is also an important factor considering N level effects. Plants are more susceptible to drought when N availability increases before drought because it leads to higher productivity, thereby increasing evaporative demands (Friedrich et al., 2012). This can even result in a loss of N allocation control and adaptive strategies to mitigate drought effects (Friedrich et al., 2012). Finally, increased N availability can lower concentrations of compounds that are important for stress tolerance, which could also increase mortality under more severe drought conditions (Zhou et al., 2011).

Plant age also plays a role in determining the response of N deposition combined with drought. Palátová (2002) found that the reduction in root biomass due to combined N deposition and drought was more severe for young seedlings than older trees. Trees tend to allocate more biomass to roots as they age, so younger trees are more susceptible to drought, and drought following N deposition further increases sensitivity to drought (Meyer-Grünefeldt et al., 2013). However, N deposition during drought may not always be detrimental. For example, drought can lock nutrients in an immobilized state by reducing the soil water available for

decomposition Hanson and Weltzin, 2000), but N deposition can increase available nutrients. Increased N deposition can also aid the recovery after drought of some species (Kinugasa et al., 2012). For trees that preferentially shift allocations to stems under N deposition and drought (Albuquerque et al., 2013), water stress may be alleviated by the extra water storage in the tree. In desert systems, N deposition relieved some of the negative effects of water stress through increases in root weight, leaf number, leaf area, biomass, and decreased root-to-shoot ratios (Zhou et al., 2011; Verburg et al., 2014).

2.5 Earth System Models

ESMs are designed to predict the climate state by integrating feedback between the atmosphere, land, and ocean. One goal of these models is to capture biosphere-atmosphere interactions in order to understand what will be the vegetation response to changing environmental conditions. The land component has undergone considerable growth over the last decade and now has complexity that rivals atmospheric models. This growth has greatly improved the climate forecasting ability of ESMs, but these models still fall short of providing a good estimate of the land C sink. The following section and Table II details some important processes already included in many LSMs that are necessary to capture vegetation responses to increased N and drought. The limitations of these model advances are also highlighted.

Table II. Representation of key model features from a subset of terrestrial ecosystem models.

Process	Model			
	CLM4.5	**CABLE**	**CTEM**	**LM3**
Reference	Oleson et al., 2013	(Wang et al., 2010)	(Arora and Boer, 2005; Arora et al., 2009)	(Gerber et al., 2010; Shevliakova et al., 2009)
Time step	30 min to one hour	30 min	30 min to one day	30 min
Plant Functional Type (PFTs)	14 natural and two generic crop types	15 natural and one crop type	7 natural and 2 crop types (C3 and C4)	five natural
Dynamic vegetation	Dependent on climate or prescribed	NA	Dependent on climate or prescribed	Dependent on climate and light
Plant C				
Photosynthesis	(Farquhar et al., 1980; Collatz et al., 1991)	(Farquhar et al., 1980)	(Farquhar et al., 1980; Collatz et al., 1991)	(Farquhar et al., 1980; Collatz et al., 1991)
Phenology	Evergreen, stress deciduous, seasonal deciduous, and crop	Biome dependent, four states, input from remote sensing	Four leaf states: maximum growth, normal growth, leaf fall, and dormancy	Drought and cold deciduous seasonal
Allocation	Fixed fraction	Fixed fraction	Dependent on light, water, phenological status	Functional balance to maintain root-to-shoot ratio
Plant N				
Uptake	Dependent on N pool size, plant demand	Dependent on N pool size, plant demand	NA	Michaelis-Menten kinetics, dependent on N pool size and root biomass; priority given to immobilization
Fixation	Function of Net Primary Productivity (NPP)	External input	NA	Dependent on plant N demand, NPP, and light availability; C cost paid for biological nitrogen fixation (BNF)
Stoichiometry (C:N)	Flexible (within 0.8 N:C)	Fixed (PFT dependent)	NA	Fixed (PFT dependent)
Plant water				
Uptake	Dependent on plant demand, root profile, and soil matric potential	Dependent on plant demand, root fraction, and soil water content	Dependent on soil moisture content	NA
Root architecture	Double exponential for water uptake (Zeng et al., 2001); single exponential for soil C/N cycling (Jackson et al., 1996)	Exponential (Arora and Boer, 2005)	Prescribed maximum rooting depth, root distribution dependent on time and PFT (Arora and Boer, 2003)	NA

Process	Model			
	ORCHIDEE	**O-CN**	**JULES**	**LPJ-GUESS**
Reference	(Krinner et al., 2005)	(Krinner et al., 2005; Zaehle and Friend, 2010)	(Best et al., 2011; Clark et al., 2011)	(Smith et al., 2001; Smith et al., 2014)
Time step	30 min to one day	30 min to one day	30 min to one day	1 day
PFTs	10 natural and two agricultural grasses	10 natural and two agricultural grasses	5 natural	11 natural
Dynamic vegetation	Dependent on climate, stand structure, and light	Dependent on climate, stand structure, and light	Dependent on NPP and tree-shrub-grass hierarchy from the Lotka-Volterra competition approach	Dependent on climate, stand structure, light and soil resources, disturbance, and succession
Plant C				
Photosynthesis	(Farquhar et al., 1980; Collatz et al., 1991)	(Friend et al., 2005)	(Collaz et al., 1991; Collatz et al., 1992)	(Collaz et al., 1991; Collatz et al., 1992)
Phenology	Drought and cold deciduous seasonal	Drought and cold deciduous seasonal	Cold deciduous	Evergreen, drought, and cold deciduous
Allocation	Rule-based response to external limits; dependent on light, water, and N	Pipe model to maintain root-to-shoot ratio	Fixed fraction	Functional balance to maintain root-to-shoot ratio
Plant N				
Uptake	Implicit, dependent on soil humidity and soil temperature	Michaelis-Menten kinetics, dependent on fine root biomass, plant N status, N pool size, and soil temperature	NA	Dependent on N pool size, plant demand, root mass, and soil temperature
Fixation	NA	Calculate potential N fixation from evapotranspiration	NA	Calculate potential N fixation from evapotranspiration
Stoichiometry (C:N)	Prescribed	Flexible (provided range)	Fixed fraction	Flexible (provided range)
Plant water				
Uptake	Dependent on plant demand, root fraction, and soil water content	Dependent on plant demand, root fraction, and soil water content	Dependent on plant demand, root fraction, and available soil moisture	Dependent on plant demand and soil water in root zone
Root architecture	Exponential root profile	Exponential root profile	Double exponential	Two soil layers; more roots in lower layer (except grass)

2.5.1 Nitrogen

An obvious and crucial component for capturing N deposition impacts on plants is the treatment of N, but early versions ESMs only considered the C cycle and neglected the N cycle completely. Carbon-only models miss a significant N deficit and therefore overestimate C sequestration by ecosystems under climate change (Zaehle et al., 2015; Peñuelas et al., 2013). Many of the latest versions of ESMs now include N (and a rare few include phosphorus). However, because N is often a limiting nutrient in ecosystems, the focus is on plant response under limited N conditions and on the effects of the progressive N limitation (Luo et al., 2004) that is expected under elevated CO_2. Although some models offer prescribed N, more sophisticated ones employ an N pool (bulk or speciated) that is available to both plants and decomposers. Nitrogen additions come from sources including lightning, deposition, mineralization, and biological fixation. Losses are from plant uptake, immobilization, leaching, and nitrification/denitrification processes. Models can represent N limitation in different ways, including using N to scale photosynthesis (Zaehle et al., 2014); Ghimire et al., 2016), downscaling potential gross primary productivity (GPP) to reflect N availability (Gerber et a., 2010; Oleson et al., 2013; Wang et al., 2010; Parida, 2011), defining a C cost of N uptake (Fisher et al., 2010a), optimizing N allocation for leaf processes (Ali et al., 2015), or adapting a flexible C:N ratio for N allocation (Ghimire et al., 2016). Nitrogen uptake is scaled depending on demand, based on stoichiometry (see section 5.2) and availability, where photosynthesis and decomposition may be downscaled. More recent developments have led to the development of the Fixation and Uptake of Nitrogen (FUN) model (Fisher et al., 2010a), which expands N acquisition to include processes of passive uptake, active uptake, re-translocation, and symbiotic

N fixation through a C cost. Other advances in the Community Land Model (CLM) expand N uptake to include methods using Michaelis-Menten equations (Ghimire et al., 2016; Thomas et al., 2013) or equilibrium chemistry approximation (Zhu et al., 2017; Tang and Riley, 2013). Additional processes such as abiotic (i.e., mineral surface) competition for soil nutrients (Nutrient COMpetition model, (Zhu et al., 2017)) are anticipated for the next generation of the CLM and the Accelerated Climate Model for Energy (ACME).

2.5.2 Allometry

ESMs rarely include dynamic responses to changes in resource availability. The most common allocation approach assigns C to each plant component (usually leaf, stem, and root) via fixed ratios that vary with plant functional type (PFT), but not spatially or temporally (Gerber et al., 2010; Wang et al., 2010; Shevliakova et al., 2009; Zaehle et al., 2010; Parida, 2011; Tjiputra et al., 2013; Franklin et al., 2010; Goll et al., 2012). For models that include N (and less often P), N uptake plays a strong role in governing C assimilation and drives competition between plants and decomposers. In these cases, C allocation requires an additional constraint of fulfilling C:N:P ratios. Nitrogen uptake is controlled by plant demand and decomposition requirements determined from fixed C partitioning and C:N stoichiometry. When N and P demands to maintain stoichiometric C:N:P are unmet, photosynthesis is downscaled (Zaehle and Dalmonech, 2011; Thornton et al., 2007). This simple approach works well for regions that have relatively stable environments, but it does not permit plant plasticity responses to changing nutrients. This method of C allocation has been highlighted as a weakness of these models (Medlyn et al., 2015; De Dauwe et al., 2014) and has resulted in some models swapping to more dynamic allocation

schemes that allow responses to stress, as in Friedlingstein et al. (1999). Carbon allocation in two ESMs (CTEM (Arora and Boer 2005; Arora et al., 2009) and ORCHIDEE (Krinner et al., 2005)) is governed by the most limiting resource; light limitation results in more biomass being allocated to the stem, and water and N limitations result in more biomass being allocated to the roots. However, because N is not explicit in these models, the N limitation is parameterized.

The simple representation of plant allometry in ESMs can have a significant influence on biogeochemistry since the allocation of biomass in the form of C to woody versus non-woody (or photosynthetic versus non-photosynthetic) plant components drives biogeochemical cycling, the quality and quantity of litter, and the duration of C storage. Our ability to model C uptake and subsequent storage therefore depends on including C allocation relationships and their responses under changes in resource availability.

2.5.3 Roots

Another component of ESMs that is oversimplified is root forms and function. For example, most root algorithms in ESMs consist of a fixed rooting depth and distribution (Arora and Boer, 2003). This constrains water uptake to the root zone (weighted by effective root fraction in each layer) and does not allow differential water uptake from soil layers due to changes in root kinetics and morphology, nor does it allow changes in root distribution or depth to increase the water available to the plant. Water uptake is generally a function of plant demand (for evapotranspiration needs), root distribution, and soil water content (Warren et al., 2015). The most common model approach to determine water limitation is to calculate a water stress scalar, which can be a function of soil water matric potential, matric potential when stomata are open or

closed, or soil water content (Warren et al., 2015). That water stress scalar is then multiplied by physiological variables such as transpiration, stomatal conductance, photosynthetic capacity, and maintenance respiration to capture water stress on plants. One approach to improve the evapotranspiration in the CLM is to add root hydraulic redistribution (Tang et al., 2015), which can transport water either up or down the soil column. Hydraulic redistribution does not influence root growth or distribution, but it does enhance water uptake by shifting the water distribution in the root zone.

Nitrogen uptake (when included) is often less complex in ESMs; most N uptake is from a bulk N mineralization pool that depends on supply and demand rather than root biomass or profile, although some recent work has focused on uptake as a function of root biomass (Ghimire et al., 2016). Essentially, plants are given every opportunity to extract all available N necessary for growth. Although this allows an implicit metric for allowing roots an opportunity to adjust their uptake, it is not realistic and lacks feedbacks on the biogeochemistry from changes in the root profile.

Recently, studies focused on modeling root growth to maximize various plant traits have been conducted. For example, Sivandran and Bras (2013) used optimization techniques for root growth in the TIN-based Real-Time Integrated Basin Simulator coupled to the Vegetation Generator for Interactive Evolution (tRIBS + VEGGIE) model to maximize plant transpiration. The improved root parameterizations allowed more root C to be allocated to soil layers with high soil moisture, increased water uptake, and decreased plant water stress. Another study by McMurtrie et al. (2012) altered the vertical distribution of root mass to maximize N uptake.

However, the underlying limitation in all studies is that they focus on maximizing only one limiting resource, namely, water or N. This limits the studies' relevance to environments that share those resource limitations so they may not reflect the future state of those regions or be suitable for global application.

2.6 Model Development Priorities

While ESMs have advanced considerably, there are several processes that still require attention if we are to capture the effects from N deposition and drought as shown in the pathways in Figure 2.1 and Figure 2.2. Future model development should focus on the following goals (see Table III for summary): (1) allow a more flexible coupling of C and N in models; (2) integrate a dynamic C partitioning algorithm; (3) improve the structure and function of roots; (4) include succession and age classes; (5) include intra-plant competition; and (6) develop methods of trait-based modeling rather than the traditional PFT approach. Some of these developments are being addressed, at least in part, for the next generation of models. For others, support needs to come from observation and the empirical community to develop robust methodology for inclusion in models.

Table III. Summary of recommendations for model development.

Recommendation	Description	Impact	Example(s)
Flexibility of CN coupling	• Allows C:N ratios in the leaf to vary with N availability • Dynamic partitioning of N in the plant	• Effects N in the leaf with influences on photosynthesis	Fixation and Uptake of Nitrogen (FUN) model (Fisher et al., 2010a) Leaf Utilization of Nitrogen for Assimilation (LUNA) (Ali et al., 2015) Community Land Model (CLM) / Accelerated Climate Model for Energy (ACME) (Ghimire et al., 2015)
Adaptive dynamics approach to C partitioning	• Flexibility in C allocation to account for plant plasticity across environmental conditions	• Optimize nutrient uptake • Increase tissue allocation to respond to limiting resource	CLM/ACME (Ghimire et al., 2015)
Improve form and function of roots	• Time varying root structure (depth and distribution) • Variable root depth, traits, plasticity, and hydraulics that scale across space and time	• Adapt to heterogeneity of water and nutrients in soil • Optimizes below ground resource uptake	Dynamic root depth (El Masri et al., 2015) Maximize N (McMurtrie et al., 2012) Maximize evapotranspiration (ET) (Sivandran and Bras, 2013)
Succession	• Representing age class • Variable growth dynamics and response to stress with age	• Capture disturbance and recovery • Heterogeneity in plant distribution, improved canopy light dynamics	Ecosystem Demography (ED) model (Fisher et al., 2015)
Competition	• Inter- and intra-species competition for resources (e.g., light, water, N, etc.) • Allows competition both within and between PFTs	• Alters allocation of resources to outcompete neighbors • Possibly altering productivity or shift vegetation distribution	Triple Tragedy of Commons (McNickle et al., 2016) Competition with consumers (Zhu et al., 2017)
Trait-based modeling	• Varying morphology, physiology, or phenology characteristics of individuals across an environmental gradient • Environment acts as filter for trait composition	• Adaptation and evolution of species to environmental conditions • Dynamic vegetation moves beyond simple rules of existence and/or establishment	Adaptive Dynamic Global Vegetation Model (aDGVM) (Scheiter et al., 2013) Jena Diversity-Dynamic Global Vegetation Model (JeDi-DGVM) (Pavlick et al., 2013) CSIRO Atmospheric Biosphere Land Exchange (CABLE) (Lu et al., 2016)

2.6.1 Flexibility of C:N Coupling in Models

Given the increase in foliar N under increased N, allowing adaptations in the stoichiometry of C and N would improve model responses (Mendlyn et al., 2015). The main impact of this will be to decrease C:N in leaves, driving increases in productivity and changes to soil and litter N content that would be present under increasing N deposition. Changes in C:N ratios occur not just over the lifecycle of the plant, but also in response to changes in nutrient availability, which are not captured in models. Changes in resource availability will result in changes to plant C allocation and partitioning. Furthermore, plant responses will be limited under fixed C:N ratios, which in turn drive changes in belowground biogeochemistry and ultimately C uptake and storage. However, our understanding of how C:N ratios change with plant age and resource status is limited. Therefore, more observations of how C:N is partitioned within the plant over optimal conditions and under climate change are needed.

2.6.2 Adaptive Dynamics Approach to C Allocation

Possibly the most challenging improvement that would likely provide the most benefit for models predicting C uptake would be to address how C is partitioned within the plant and how that varies over time and with changes to the environment. According to Franklin et al. (2012), the difficulty is that C allocation is the result of several processes, which makes a mechanistic approach to represent C allocation difficult. The most robust approach for modeling allocation is adaptive dynamics that include evolution strategies that can emerge through population dynamics and can result in an evolutionary stable strategy (Franklin et al., 2012). This type of

implementation will be difficult in an ESM, given the complexity of integrating dynamic C allocation and the computational demand required to run at high resolution over global scales. However, optimization techniques such as those proposed by Lynch (2015) may be an alternative; vegetation may be able to take on the form of optimal response through a cost-benefit approach or game theoretical optimization (Franklin et al., 2012). This approach allows a flexible plant response to local and regional environmental conditions and nutrient availability. In addition, this functionality would allow PFTs in models to optimize nutrient capture by focusing resources to improve the uptake of the most limiting resources. In a scenario with N deposition and drought, a PFT would be able to alter its root:shoot ratio to increase allocation to roots to increase water uptake or to the stem to increase light competition.

2.6.3 Improving Form and Function of Roots

In order to allow ecosystems to respond to changes in the environment such as climate change, roots must be allowed to adapt to the heterogeneity of water and nutrients in the soil. Improving the form and function of roots will allow PFTs the opportunity to respond to the heterogeneity of resources, thus increasing the potential for N and/or water uptake. Increasing root depth alone is not sufficient to improve modeled water uptake in water-stressed systems; models also need to consider root distribution, plasticity, and hydraulics (Nippert and Holdo, 2015). At a minimum, root profiles should include time-varying structures as leaves and stems. Although models tend to have homogeneous soil horizontally (in a grid cell), the vertical structure of resources is dynamic. Allowing roots to proliferate in soil layers where resources are concentrated gives PFTs the chance to adapt to changes in environment and can further change

the vertical distribution of C and N. Baker et al. (2008) improved the modeled Net Ecosystem Exchange cycle in the Simple Biosphere Model compared with observations in the Amazon by adding hydraulic redistribution and soil depth to 10 m. Other elements of root systems that should be included in models are root order and classification (which will differ in respiration, uptake, turnover, and storage capacity), root phenology and turnover, and resource uptake response to heterogeneity of resources (Smithwick et al., 2014). Warren et al. (2015) provided additional suggestions for improving root representation in models, including scaling root function across temporal and spatial scales and including root traits that inform function and hydraulic redistribution. Although most work in ESM development has focused on improving aboveground productivity, some effort has targeted belowground activities. For example, recent work used optimization techniques to modify root growth to maximize plant transpiration (Sivandran and Bras, 2013) and N uptake (McMurtrie et al., 2012). Arora and Boer (2003) developed a method to represent root distribution as a function of root biomass, which is a proxy for plant age, to allow root depth to increase when plants are young but grow horizontally when plants are mature. This was implemented in the Integrated Science Assessment Model (El Masri et al., 2015) to capture seasonal leaf area index and GPP in northern high-latitude ecosystems. These methods should be expanded to optimize the most limiting resource, rather than focusing on only one limiting resource.

2.6.4 Succession

Most models do not consider succession or stand age, despite the evidence that old-growth forests do not respond as strongly as young trees to short-term changes in soil moisture or

N availability (Odum, 1969). This results in a homogeneous distribution of vegetation rather than the heterogeneous plant cover that occurs due to the variation of soils and climate across landscapes. This also limits a model's ability to capture disturbance and recovery events, which are major drivers of C and nutrient cycling. Including succession could help models capture different responses to N and drought stress as a result of tree age by, for example, simulating the higher mortality of young trees. A method to capture succession was implemented by Fisher et al. (2010b) in the Community Land Model by separating vegetation into cohorts of age, PFT, and height; this method was tested against deciduous–evergreen forest boundaries (Fisher et al., 2015). These techniques can capture the variability of individual PFTs within a grid cell, adding large-scale heterogeneity in plant distribution, and can be the first step toward a more trait-based modeling approach (see section 6.6).

2.6.5 Competition

In many LSMs, plants compete for resources such as light, water, and nutrients within a grid cell based on their weight on the grid cell. In these cases, the competition is between different PFTs and not within a PFT. Dynamic vegetation models can force one PFT to replace another when climate conditions are favorable (Quillet et al., 2010). A few LSMs have adopted Lotka-Volterra predator/prey equations (Arora and Boer, 2006) to represent colonization rates. However, no model currently implements a game-theoretic approach to the competition for resources that can produce an overabundance of biomass for resource uptake to outcompete neighbors. This method has the potential to improve estimates of plant production, respond to changing resources, and lead to an evolutional stable strategy (McNickle and Brown, 2012).

PFTs would have the opportunity to alter biomass allocation (i.e., shifts in the root:shoot ratio) to outcompete neighbors for limiting resources, which would lead to shifts in productivity and vegetation species distribution. Although it is hindered by the current model's resolution, as continuously expanding computational capabilities move toward high-resolution models (DOE, 2017), game theory is an achievable target.

2.6.6 Trait-Based Modeling

The current PFT approach to modeling vegetation is limited to feedback that results from changes in species distribution since most models assume that attributes within a PFT do not change with climate (Van Bodegom et al., 2012). To capture the adaptation and evolution of vegetation, the concept of trait-based modeling was introduced by Lavorel and Garnier (2002). Trait-based modeling links plant traits that act as plant responses to the environment with plant traits that represent the effect of plants on the ecosystem in order to capture the plant assemblage of a region. A trait can be defined as a feature that describes the morphology, physiology, or phenology characteristics of an individual, which can vary across an environmental gradient (Garnier and Navas, 2012). Trait based modeling allows dynamic vegetation to move beyond simple climate based temperature controls on vegetation existence and establishment. Therefore, species distribution would be a response to N and drought in the ecosystem. This approach has been used to improve two dynamic vegetation models (aDGVM, (Scheiter et al., 2013); JeDi-DGVM, (Pavlick et al., 2013)). The Jedi-DGVM outperformed other leading dynamic vegetation models for Leaf Area Index (LAI), NPP, CO_2 seasonality, C fluxes, and, in some regions, C stocks (Pavlick et al., 2013). Incorporating plant traits in the CSIRO Atmospheric Biosphere

Land Exchange (CABLE) model improved the biogeographical distribution of major forests that have multiple dominant PFTs (Lu et al., 2016). Using plant traits to capture whole-plant hydraulics has even been suggested to improve C and water use responses to drought (Matheny et al., 2016). The benefit of trait-based modeling is that the environment acts as a filter for trait composition, analogous to evolutional selection processes (Van Bodegom et al., 2012), and is not limited by climate and geography. This is particularly important considering that McNeil et al. (2005) found that species' foliar N responses to N deposition were dependent on two main plant traits, leaf mass area and shade tolerance. Matheny et al. (2016) also suggested several plant traits that could influence the availability of water to a plant that span across leaves, stems, and roots. The challenge is finding data to support the choice of traits and how different traits co-vary.

2.7 Conclusions

We have provided a review of the impacts of N and drought on ecosystems and a list of future model recommendations that serves to address the missing processes needed in LSMs to capture those interactions. While this list is extensive, it is by no means exhaustive. Our suggestions target two co-occurring stressors, but additional stresses will also be present that should be considered such as warming, elevated CO2, and herbivory. For example, herbivory could reduce the N benefits of elevated productivity from consumption (Throop et al., 2005) or be a source of N deposition. Effects from elevated CO2 can vary; CO2 fertilization can help mitigate extreme heat and drought (Roy et al., 2016), or fertilization effects on productivity may be eliminated during drought and nutrient limitation (Reich et al., 2014). These additional

impacts on ecosystems are important, considering that CO2 fertilization currently plays a larger role than N deposition in increasing productivity (Los et al., 2013).

Another example is the interactions that exist between N availability, drought, and air temperature. It is thought that forest productivity should increase with temperature at the global scale, but droughts often associated with increases in temperature have lowered the NPP potential in some regions (Zhao and Running, 2010). For instance, tropical forests can increase Net Ecosystem Exchange (NEE) with modest increases in air temperature, and drought effects could be ameliorated with increases in atmospheric CO_2 (Gonzalez-Meler et al., 2014). The interactions of temperature with drought and N can also affect the surface properties of forests beyond evapotranspiration. Drought sensitive forests (deciduous forests) tend to have a higher surface albedo than drought resistant ones (e.g., conifer forests), affecting the regional energy balance (Jackson et al., 2008). Further, increases in temperature can increase decomposition and N mineralization rates in the absence of drought, but N mineralization will not respond to temperature if moisture is the limiting factor (Hyvönen et al., 2007). These biophysical properties are important in understanding the global net effect of drought and N deposition on biosphere climate interactions (Anderson et al., 2011) and are not the focus of this work. It is important to note that, in most elevated temperature ecosystem experiments, drought is a secondary effect caused by elevated temperature treatments (Wu et al., 2011; Gonzalez-Meler et al., 2017), making it difficult to distinguish primary from integrated responses of forests to drought and temperature on biogeochemical and biophysical processes.

This study only focused on two stressors to ecosystems, N and drought. Although some of the identified processes targeted by this manuscript may help models to capture impacts from other climate-related effects, additional ecosystem processes will need to be addressed in the future. As the community integrates additional processes in models to capture vegetation responses to N inputs, we can revisit the resulting C uptake to evaluate the sink capacity of the terrestrial surface. However, special care should be taken when implementing additional parameters and processes into models, particularly so that models are not over-parameterized and so that the resulting C cycle response is not constrained by incomplete observational data. In the near term, model sensitivity studies can be used to determine the most sensitive parameters and processes that drive changes in C and nutrient cycles. More research on the structural uncertainty of models can provide insight on those processes that have strong feedbacks or introduce instability. Finally, when rigorous model testing through benchmarking is complete, we can focus on additional questions related to the fate of C in the land.

Improving estimates of the global terrestrial C sink is a priority for ESM development. In order to improve the predictions and reduce uncertainty, model development should focus on the processes that will be affected by multiple co-occurring stressors such as N deposition and drought. We have suggested avenues of model improvement that are possible in the near future with hopes that future generations of models can benefit and capture the response to increased N availability and drought.

2.8 References

Aber, J. D., Goodale, C. L., Ollinger, S. V., Smith, M.-L., Magill, A. H., Martin, M. E., Hallett, R. A., Stoddard, J. L. (2003), Is Nitrogen deposition altering the nitrogen status of northeastern forests? *Bioscience*, 53, 375–389.

Albuquerque, W. G., Severino, L. S., Beltrao, N. E. M., Azevedo, C. A. V., Da Silva Filho, J. L. (2013), Growth and biomass allocation of Jutropha curcas plants as influenced by nitrogen under different soil moisture regimes. *Res. Crop.*, 14, 928–934.

Ali, A. A., Xu, C., Rogers, A., McDowell, N. G., Medlyn, B. E., Fisher, R. A., Wullschleger, S. D., Reich, P. B., Vrugt, J. A., Bauerle, W. L., Santiago, L. S., and Wilson, C. J. (2015), Global-scale environmental control of plant photosynthetic capacity. *Ecol. Appl.*, 25, 2349–2365.

Allen, C. D., Macalady, A. K., Chenchouni, H., Bachelet, D., McDowell, N., Vennetier, M., Kitzberger, T., Rigling, A., Breshears, D. D., Hogg, E. H., Gonzalez, P., Fensham, R., Zhang, Z., Castro, J., Demidova, N., Lim, J.-H., Allard, G., Running, S. W., Semerci, A., and Cobb, N. (2010), A global overview of drought and heat-induced tree mortality reveals emerging climate change risks for forests. *For. Ecol. Manag.*, 259, 660–684.

Anderson, R. G., Canadell, J. G., Randerson, J. T., Jackson, R. B., Hungate, B. A., Baldocchi, D. D., Ban-Weiss, G. A., Bonan, G. B., Caldeira, K., Cao, L., Diffenbaugh, N. S., Gurney, K, R., Kueppers, L. M., Law, B. E., Luyssaert, S., O'Halloran, T. L. (2011), Biophysical considerations in forestry for climate protection. *Front. Ecol. Environ.*, 9, 174–182.

Arora, V. K., Boer, G. J. (2003), A representation of variable root distribution in dynamic vegetation models. *Earth Interact.*, 7, 1–19.

Arora, V. K., Boer, G. J. (2005), A parameterization of leaf phenology for the terrestrial ecosystem component of climate models. *Glob. Chang. Biol.*, 11, 39–59.

Arora, V. K., Boer, G. J. (2006), Simulating competition and coexistence between plant functional types in a dynamic vegetation model. *Earth Interact.*, 10, 1–30.

Arora, V. K., Boer, G. J., Christian, J. R., Curry, C. L., Denman, K. L., Zahariev, K., Flato, G. M., Scinocca, J. F., Merryfield, W. J., Lee, W. G. (2009), The effect of terrestrial photosynthesis down regulation on the twentieth-century carbon budget simulated with the CCCma Earth System Model. *J. Clim.*, 22, 6066–6088.

Baker, I. T., Prihodko, L., Denning, A. S., Goulden, M., Miller, S., Da Rocha, H. R. (2008), Seasonal drought stress in the amazon: Reconciling models and observations. *J. Geophys. Res. Biogeosci.*, 113, doi:10.1029/2007JG000644.

Bala, G., Devaraju, N., Chaturvedi, R. K., Caldeira, K., Nemani, R. (2013), Nitrogen deposition: How important is it for global terrestrial carbon uptake? *Biogeosciences*, 10, 7147–7160.

BassiriRad, H., Lussenhop, J. F., Sehtiya, H. L., Borden, K. K. (2015), Nitrogen deposition potentially contributes to oak regeneration failure in the Midwestern temperate forests of the USA. *Oecologia*, 177, 53–63.

Best, M. J., Pryor, M., Clark, D. B., Rooney, G. G., Essery, R. L. H., Ménard, C. B., Edwards, J. M., Hendry, M. A., Porson, A., Gedney, N., Mercado, L. M., Sitch, S., Blyth, E., Boucher, O., Cox, P. M., Grimmond, C. S. B., and Harding, R. J. (2011), The Joint UK Land Environment Simulator (JULES), model description—Part 1: Energy and water fluxes. *Geosci. Model Dev.*, 4, 677–699.

Bobbink, R., Roelofs, J. G. M. (1995), Nitrogen critical loads for natural and semi-natural ecosystems: The empirical approach. *Water. Air. Soil Pollut.*, 85, 2413–2418.

Bobbink, R., Lamers, L. P. M. (2002), Effects of increased nitrogen deposition. In Air Pollution and Plant Life; Bell, J.N.B., Treshow, M., Eds.; John Wiley and Sons: Chichester, UK,; pp. 201–235.

Bobbink, R., Hicks, K., Galloway, J., Spranger, T., Alkemade, R., Ashmore, M., Bustamante, M., Cinderby, S., Davidson, E., Dentener, F., Emmett, B., Erisman, J. W., Fenn, M., Giliam, F., Nordin, A., Pardo, L., De Vries, W. (2010), Global assessment of nitrogen deposition effects on terrestrial plant diversity: A synthesis. *Ecol. Appl.*, 20, 30–59.

Boggs, J. L., Mcnulty, S. G., Gavazzi, M. J., Myers, J.M. (2005), Tree growth, foliar chemistry, and nitrogen cycling across a nitrogen deposition gradient in southern Applachian deciduous forests. *Can. J. For. Res.*, 35, 1901–1913.

Boisier, J. P., Ciais, P., Ducharne, A., Guimberteau, M. (2015), Projected strengthening of Amazonian dry season by constrained climate model simulations. *Nat. Clim. Chang.*, 5, 656–660.

Brassard, B. W., Chen, H. Y. H., Bergeron, Y. (2009), Influence of environmental variability on root dynamics in northern forests. *CRC Crit. Rev. Plant Sci.*, 28, 179–197.

Broeckx, L. S., Verlinden, M. S., Berhongaray, G., Zona, D., Fichot, R., Ceulemans, R. (2014), The effect of a dry spring on seasonal carbon allocation and vegetation dynamics in a poplar bioenergy plantation. *GCB Bioenergy*, 6, 473–487.

Cardoso, J. A., Pineda, M., de la Cruz Jiménez, J., Vergara, M. F., Rao, I. M. (2015), Contrasting strategies to cope with drought conditions by two tropical forage C4 grasses. *AoB Plants*, 7, doi: 10.1093/aobpla/plv107.

Clark, C. M., Tilman, D. (2008), Loss of plant species after chronic low-level nitrogen deposition to prairie grasslands. *Nature*, 451, 712–715.

Clark, D. B., Mercado, L. M., Sitch, S., Jones, C. D., Gedney, N., Best, M. J., Pryor, M., Rooney, G. G., Essery, R. L. H., Blyth, E., Boucher, O., Harding, R. J., Huntingford, C., Cox, P. M. (2011), The Joint UK Land Environment Simulator (JULES), model description—Part 2: Carbon fluxes and vegetation dynamics. *Geosci. Model Dev.*, 4, 701–722.

Collatz, G. J., Ball, J. T., Grivet, C., Berry, J. A. (1991), Physiological and environmental regulation of stomatal conductance, photosynthesis and transpiration: A model that includes a laminar boundary layer. *Agric. For. Meteorol.*, 54, 107–136.

Collatz, G. J., Ribas-Carbo, M., Berry, J. A. (1992), Coupled photosynthesis-stomatal conductance model for leaves of C4 plants. *Aust. J. Plant Physiol.*, 19, 519–538.

Cook, B. I., Ault, T. R., Smerdon, J. E. (2015), Unprecedented 21st century drought risk in the American Southwest and Central Plains. *Sci. Adv.*, 1, e1400082.

Davidson, E. A., Howarth, R. W. (2007), Nutrients in synergy. *Nature*, 449, 1000–1001.

De Kauwe, M. G., Medlyn, B. E., Zaehle, S., Walker, A. P., Dietze, M. C., Wang, Y. P., Luo, Y., Jain, A. K., El-Masri, B., Hickler, T., Wårlind, D., Weng, E., Parton, W. J., Thornton, P. E., Wang, S., Prentice, I. C., Asao, S., Smith, B., Mccarthy, H. R., Iversen, C. M., Hanson, P. J.; Warren, J. M.; Oren, R.; Norby, R. J. (2014), Where does the carbon go? A model-data intercomparison of vegetation carbon allocation and turnover processes at two temperate forest free-air CO2 enrichment sites. *New Phytol.*, 203, 883–899.

De Kauwe, M. G., Zhou, S. X., Medlyn, B. E., Pitman, A. J., Wang, Y. P., Duursma, R. A., Prentice, I. C. (2015), Do land surface models need to include differential plant species responses to drought? Examining model predictions across a mesic-xeric gradient in Europe. *Biogeosciences*, 12, 7503–7518.

De Vries, W., Du, E., Butterbach-Bahl, K. (2014), Short and long-term impacts of nitrogen deposition on carbon sequestration by forest ecosystems. *Curr. Opin. Environ. Sustain.*, 9–10, 90–104.

Dentener, F., Drevet, J., Lamarque, J.-F., Bey, I., Eickhout, B., Fiore, A. M., Hauglustaine, D., Horowitz, L. W., Krol, M., Kulshrestha, U. C., Lawrence, M., Galy-Lacaux, C., Rast, S., Shindell, D., Stevenson, D., Van Noije, T., Atherton, C., Bell, N., Bergman, D., Butler, T., Cofala, J., Collins, B., Doherty, R., Ellingsen, K., Galloway, J., Gauss, M., Montanaro, V., Müller, J. F., Pitari, G., Rodriguez, J., Sanderson, M., Solmon, F., Strahan, S., Schultz, M., Sudo, K., Szopa, S., Wild, O. (2006), Nitrogen and sulfur deposition on regional and global scales: A multimodel evaluation. *Glob. Biogeochem. Cycles*, 20, doi:10.1029/2005GB002672.

Department of Energy. (2017, May 2). ACME Overview Brochure. Retrieved from: https://climatemodeling.science.energy.gov/sites/default/files/ACME_Overview_Brochure.pdf.

Dise, N. B., Wright, R. F. (1995), Nitrogen leaching from European forests in relation to nitrogen deposition. *For. Ecol. Manag.*, 71, 153–161.

Du, E., Fang, J. (2014), Weak growth response to nitrogen deposition in an old-growth boreal forest. *Ecosphere*, 5, doi:10.1890/ES14-00109.1.

El Masri, B., Shu, S., Jain, A. K. (2015), Implementation of a dynamic rooting depth and phenology into a land surface model: Evaluation of carbon, water, and energy fluxes in the high latitude ecosystems. *Agric. For. Meteorol.*, 211–212, 85–99.

Elvir, J. A., Rustad, L., Wiersrna, G. B., Fernandez, I., White, A. S., White, G. J. (2005), Eleven-year response of foliar chemistry to chronic nitrogen and sulfur additions at the Bear Brook Watershed in Maine. *Can. J. For. Res.*, 35, 1402–1410.

Evans, J. R. (1989), Photosynthesis and nitrogen relationship in leaves of C3 plants. *Oecologia*, 78, 9–19.

Fang, Y. T., Yoh, M., Mo, J. M., Gundersen, P., Zhou, G. Y. (2009), Response of nitrogen leaching to nitrogen deposition in disturbed and mature forests of southern China. *Pedosphere*, 19, 111–120.

Farquhar, G. D., Von Caemmerer, S., Berry, J. A. (1980), A biochemical model of photosynthetic CO2 assimilation in leaves of C3 species. *Planta*, 149, 78–90.

Fisher, J. B., Sitch, S., Malhi, Y., Fisher, R. A., Huntingford, C., Tan, S. Y. (2010a), Carbon cost of plant nitrogen acquisition: A mechanistic, globally applicable model of plant nitrogen uptake, retranslocation, and fixation. *Global Biogeochem. Cycles*, 24, doi:10.1029/2009GB003621.

Fisher, R., Mcdowell, N., Purves, D., Moorcroft, P., Sitch, S., Cox, P., Huntingford, C., Meir, P., Woodward, F. I. (2010b), Assessing uncertainties in a second-generation dynamic vegetation model caused by ecological scale limitations. *New Phytol.*, 187, 666–681.

Fisher, J. B., Badgley, G., Blyth, E. (2012), Global nutrient limitation in terrestrial vegetation. *Glob. Biogeochem. Cycles*, 26, doi:10.1029/2011GB004252.

Fisher, R. A., Muszala, S., Verteinstein, M., Lawrence, P., Xu, C., McDowell, N. G., Knox, R. G., Koven, C., Holm, J., Rogers, B. M., Spessa, A., Lawrence, D., Bonan, G. (2015), Taking off the training wheels: The properties of a dynamic vegetation model without climate envelopes, CLM4.5(ED). *Geosci. Model Dev.*, 8, 3593–3619.

Fleischer, K., Rebel, K. T., Van Der Molen, M. K., Erisman, J. W., Wassen, M. J., Van Loon, E. E., Montagnani, L., Gough, C. M., Herbst, M., Janssens, I. A., Gianelle, D., Dolman, A. J. (2013), The contribution of nitrogen deposition to the photosynthetic capacity of forests. *Glob. Biogeochem. Cycles*, 27, 187–199.

Franklin, O., Johansson, J., Dewar, R. C., Dieckmann, U., McMurtrie, R. E., Brännström, A. K., Dybzinski, R. (2012), Modeling carbon allocation in trees: A search for principles. *Tree Physiol.*, 32, 648–666.

Friedlingstein, P., Meinshausen, M., Arora, V. K., Jones, C. J., Anav, A., Liddicoat, S. K., Knutti, R. (2014), Uncertainties in CMIP5 climate projections due to carbon cycle feedbacks. *J. Clim.*, 27, 511–526.

Friedrich, U., von Oheimb, G., Kriebitzsch, W. U., Schleßelmann, K., Weber, M. S., Härdtle, W. (2012), Nitrogen deposition increases susceptibility to drought—Experimental evidence with the perennial grass Molinia caerulea (L.) Moench. *Plant Soil*, 353, 59–71.

Friedlingstein, P., Joel, G., Field, C. B., Fung, I. Y. (1999), Toward an allocation scheme for global terrestrial carbon models. *Glob. Chang. Biol.*, 5, 755–770.

Friend, A. D., Kiang, N. Y. (2005), Land surface model development for the GISS GCM: Effects of improved canopy physiology on simulated climate. *J. Clim.*, 18, 2883–2902.

Galloway, J. N., Townsend, A. R., Erisman, J. W., Bekunda, M., Cai, Z., Freney, J. R., Martinelli, L. A., Seitzinger, S. P., Sutton, M. A. (2008), Transformation of the nitrogen cycle: Recent trends, questions, and potential solutions. *Science*, 320, 889–892.

Garnier, E., Navas, M. L. (2012), A trait-based approach to comparative functional plant ecology: Concepts, methods and applications for agroecology. A review. *Agron. Sustain. Dev.*, 32, 365–399.

Gerber, S., Hedin, L. O., Oppenheimer, M., Pacala, S. W., Shevliakova, E. (2010), Nitrogen cycling and feedbacks in a global dynamic land model. *Glob. Biogeochem. Cycles*, 24, doi:10.1029/2008GB003336.

Ghimire, B., Riley, W. J., Koven, C. D., Mu, M., Randerson, J. T. (2016), Representing leaf and root physiological traits in CLM improves global carbon and nitrogen cycling predictions. J. *Adv. Model. Earth Syst.*, 8, 598–613.

Goll, D.S., Brovkin, V., Parida, B. R., Reick, C. H., Kattge, J., Reich, P. B., Van Bodegom, P.M., Niinemets, U. (2012), Nutrient limitation reduces land carbon uptake in simulations with a model of combined carbon, nitrogen and phosphorus cycling. *Biogeosciences*, 9, 3547–3569.

Gonzalez-Meler, M. A., Rucks, J. S., Aubanell, G. (2014), Mechanistic insights on the responses of plant and ecosystem gas exchange to global environmental change: Lessons from Biosphere 2. *Plant Sci.*, 226, 14–21.

Gonzalez-Meler, M. A., Silva, L. B. C., Dias-De-Oliveira, E., Flower, C. E., Martinez, C. A. (2017), Experimental air warming of a Stylosanthes capitata, vogel dominated tropical pasture affects soil respiration and nitrogen dynamics. *Front. Plant Sci.*, 8, 46, doi:10.3389/fpls.2017.00046.

Grulke, N. E., Minnich, R. A., Paine, T., Riggan, P. (2009), Air pollution increases forest susceptibility to wildfires: A case study for the San Bernardino Mountains in southern California. In Bytnerowicz, A., Arbaugh, M., Riebau, A., Anderson, C., (Eds.), *Wildland Fires and Air Pollution* (pp. 365–403), New York, NY, USA: Elsiver.

Hanson, P. J., Weltzin, J. F. (2000), Drought disturbance from climate change: Repsonse of United States forests. *Sci. Total Enivron.*, 262, 205–220.

Hanson, P. J., Tschaplinski, T. J., Wullschleger, S. D., Todd, D. E., Augé, R. M. (2007), The Resilience of Upland-Oak Forest Canopy Trees to Chronic and Acute Precipitation Maniuplations, Buckley, D.S., Clatterbuck, W.K., Eds., U.S. Department of Agriculture: Morgantown, WV, USA, Southern Research Station: Asheville, NC, USA.

He, B., Cui, X., Wang, H., Chen, A. (2014), Drought: The most important physical stress of terrestrial ecosystems. *Acta Ecol. Sin.*, 34, 179–183.

Hertel, D., Strecker, T., Müller-Haubold, H., Leuschner, C. (2013), Fine root biomass and dynamics in beech forests across a precipitation gradient—Is optimal resource partitioning theory applicable to water-limited mature trees? *J. Ecol.*, 101, 1183–1200.

Hyvönen, R., Ågren, G. I., Linder, S., Persson, T., Cotrufo, M. F., Ekblad, A., Freeman, M., Grelle, A., Janssens, I. A., Jarvis, P. G., Kellomäki, S., Lindroth, A., Loustau, D., Lundmark, T., Norby, R. J., Oren, R., Pilegaard, K., Ryan, M. G., Sigurdsson, B. D., Strömgren, M., van Oijen, M., and Wallin, G. (2007), The likely impact of elevated CO2, nitrogen deposition, increased temperature and management on carbon sequestration in temperate and boreal forest ecosystems: A literature review. *New Phytol.*, 173, 463–480.

Ibáñez, I., Zak, D. R., Burton, A. J., Pregitzer, K. S. (2016), Chronic nitrogen deposition alters tree allometric relationships: Implications for biomass production and carbon storage. *Ecol. Appl.*, 26, 913–925.

Jackson, R. B., Canadell, J., Ehleringer, J. R., Mooney, H. A., Sala, O. E., Schulze, E. D. (1996), A global analysis of root distributions for terrestrial biomes. *Oecologia*, 108, 389–411.

Jackson, R. B., Randerson, J. T., Canadell, J. G., Anderson, R. G., Avissar, R., Baldocchi, D. D., Bonan, G. B., Caldeira, K., Diffenbaugh, N. S., Field, C. B. (2008), Protecting climate with forests. *Environ. Res. Lett.*, 3, doi:10.1088/1748-9326/3/4/044006.

Kinugasa, T., Tsunekawa, A., Shinoda, M. (2012), Increasing nitrogen deposition enhances post-drought recovery of grassland productivity in the Mongolian steppe. *Oecologia*, 170, 857–865.

Kleczewski, N. M., Herms, D. A., Bonello, P. (2012), Nutrient and water availability alter belowground patterns of biomass allocation, carbon partitioning, and ectomycorrhizal abundance in Betula nigra. *Trees*, 26, 525–533.

Klein, T., Cohen, S., Yakir, D. (2011), Hydraulic adjustments underlying drought resistance of Pinus halepensis. *Tree Physiol.*, 31, 637–648.

Koirala, S., Yeh, P. J. F., Hirabayashi, Y., Kanae, S., Oki, T. (2014), Global-scale land surface hydrologic modeling with the representation of water table dynamics. J. *Geophys. Res. Atmos.*, 119, 75–89.

Krinner, G., Viovy, N., de Noblet-Ducoudré, N., Ogée, J., Polcher, J., Friedlingstein, P., Ciais, P., Sitch, S., Prentice, I. C. (2005), A dynamic global vegetation model for studies of the coupled atmosphere-biosphere system. *Glob. Biogeochem. Cycles*, 19, doi:10.1029/2003GB002199.

Lavorel, S., Garnier, E. (2002), Predicting changes in community composition and ecosystem functioning from plant traits: Revisiting the Holy Grail. *Funct. Ecol.*, 16, 545–556.

Leuzinger, S., Quinn Thomas, R. (2011), How do we improve Earth system models? Integrating Earth system models, ecosystem models, experiments and long-term data. *New Phytol.*, 191, 15–18.

Liu, X., Fan, Y., Long, J., Wei, R., Kjelgren, R., Gong, C., Zhao, J. (2013), Effects of soil water and nitrogen availability on photosynthesis and water use efficiency of Robinia pseudoacacia seedlings. *J. Environ. Sci.*, 25, 585–595.

Los, S. O. (2013), Analysis of trends in fused AVHRR and MODIS NDVI data for 1982-2006: Indication for a CO2 fertilization effect in global vegetation. *Glob. Biogeochem. Cycles*, 27, 318–330.

Lotter, D., Valentine, A. J., Archer Van Garderen, E., Tadross, M. (2014), Physiological responses of a fynbos legume, Aspalathus linearis to drought stress. *S. Afr. J. Bot.*, 94, 218–223.

Lu, X., Wang, Y.-P., Wright, I.J., Reich, P.B., Shi, Z., Dai, Y. (2016), Incorporation of plant traits in a land surface model helps explain the global biogeographical distribution of major forest functional types. *Glob. Ecol. Biogeogr*., 26, 304–317.

Luo, Y., Su, S., Currie, W. S., Dukes, J. S., Finzi, A., Hartwig, U., Hungate, B., McMurtrie, R. E., Oren, R., Parton, W. J., Pataki, D. E., Shaw, M. R., Zak, D. R., Field, C. B. (2004), Progressive nitrogen limitation of ecosystem responses to rising atmospheric carbon dioxide. *Bioscience*, 54, 731–739.

Lynch, D. J. (2015), Impacts of Fine-Roots on Terrestrial Net Primary Productivity and Soil Nutrient Cycling (Ph.D. Thesis). University of Illinois at Chicago, Chicago, IL, USA.

Martin-St Paul, N. K., Limousin, J. M., Vogt-Schilb, H., Rodríguez-Calcerrada, J., Rambal, S., Longepierre, D., Misson, L. (2013), The temporal response to drought in a Mediterranean evergreen tree: Comparing a regional precipitation gradient and a throughfall exclusion experiment. *Glob. Chang. Biol.*, 19, 2413–2426.

Matheny, A. M., Mirfenderesgi, G., Bohrer, G. (2016), Trait-based representation of hydrological functional properties of plants in weather and ecosystem models. *Plant Divers.*, 39, 1–12.

Matson, P., Lohse, K. A., Hall, S. J. (2002), The globalization of nitrogen deposition: Consequences for terrestrial ecosystems. *Ambio*, 31, 113–119.

Mcdowell, N., Pockman, W. T., Allen, C. D., Breshears, D. D., Cobb, N., Kolb, T., Plaut, J., Sperry, J., West, A., Williams, D. G., Yepez, E. A. (2008), Mechanisms of plant survival and mortality during drought: Why do some plants survive while others succumb to drought? *New Phytol.*, 178, 719–739.

McMurtrie, R. E., Iversen, C. M., Dewar, R. C., Medlyn, B. E., Näsholm, T., Pepper, D. A., Norby, R. J. (2012), Plant root distributions and nitrogen uptake predicted by a hypothesis of optimal root foraging. *Ecol. Evol.*, 2, 1235–1250.

McNeil, B. E., Read, J. M., Driscoll, C. T. (2007), Foliar nitrogen responses to elevated atmospheric nitrogen deposition in nine temperate forest canopy species. *Environ. Sci. Technol.*, 41, 5191–5197.

McNickle, G. G., Brown, J. S. (2012), Evolutionarily stable strategies for nutrient foraging and below-ground competition in plants. *Evol. Ecol. Res.*, 14, 667–687.

Mcnickle, G. G., Gonzalez-meler, M. A., Lynch, D. J., Baltzer, J. L., Brown, J. S. (2016), The world's biomes and primary production as a triple tragedy of the commons foraging game played among plants. *Proc. R. Soc. B*, 283, doi:10.1098/rspb.2016.1993.

Medlyn, B. E., Zaehle, S., De Kauwe, M. G., Walker, A. P., Dietze, M. C., Hanson, P. J., Hickler, T., Jain, A. K., Luo, Y., Parton, W., Prentice, I. C., Thornton, P. E., Wang, S., Wang, Y.-P., Weng, E., Iversen, C. M., McCarthy, H. R., Warren, J. M., Oren, R., Norby, R. J. (2015), Using ecosystem experiments to improve vegetation models. *Nat. Clim. Chang.*, 5, 528–534.

Melillo, J., Steudler, P., Aber, J., Newkirk, K., Lux, H., Bowles, F., Catricala, C., Magill, A., Ahrens, T., Morrisseau, S. (2002), Soil warming and carbon-cycle feedbacks to the climate system. *Science*, 298, 2173–2176.

Meier, I. C., Leuschner, C. (2008), Belowground drought response of European beech: Fine root biomass and carbon partitioning in 14 mature stands across a precipitation gradient. *Glob. Chang. Biol.*, 14, 2081–2095.

Meyer-Grünefeldt, M., Friedrich, U., Klotz, M., Von Oheimb, G., Härdtle, W. (2013), Nitrogen deposition and drought events have non-additive effects on plant growth—Evidence from greenhouse experiments. *Plant Biosyst.*, 149, 424–432.

Meyer-Grünefeldt, M., Calvo, L., Marcos, E., Von Oheimb, G., Härdtle, W. (2015), Impacts of drought and nitrogen addition on Calluna heathlands differ with plant life-history stage. *J. Ecol.*, 103, 1141–1152.

Minocha, R., Turlapati, S. A., Long, S., McDowell, W. H., Minocha, S. C. (2015), Long-term trends of changes in pine and oak foliar nitrogen metabolism in response to chronic nitrogen amendments at Harvard Forest, MA. *Tree Physiol.*, 35, 894–909.

Neumann, R. B., Cardon, Z. G. (2012), The magnitude of hydraulic redistribution by plant roots: A review and synthesis of empirical and modeling studies. *New Phytol.*, 194, 337–352.

Nippert, J. B., Holdo, R. M. (2015), Challenging the maximum rooting depth paradigm in grasslands and savannas. *Funct. Ecol.*, 29, 739–745.

Odum, E. P. (1969), The strategy of ecosystem development. *Science*, 164, 262–270.

Oleson, K. W., Lawrence, D. M., Bonan, G. B., Drewniak, B., Huang, M., Koven, C. D., Levis, S., Li, F., Riley, W. J., Subin, Z. M., Swenson, S. C., Thornton, P. E., Bozbiyik, A., Fisher, R., Heald, C. L., Kluzek, E., Lamarque, J.-F., Lawrence, P. J., Leung, L. R., Lipscomb, W., Muszala, S., Ricciuto, D. M., Sacks, W., Sun, Y., Tang J., and Yang Z.-L. (2013), Technical Description of version 4.5 of the Community Land Model (CLM). Boulder, Colorado.: NCAR.

Padilla, F. M., Miranda, J. D., Jorquera, M. J., Pugnaire, F. I. (2009), Variability in amount and frequency of water supply affects roots but not growth of arid shrubs. *Plant Ecol.*, 204, 261–270.

Palátová, E. (2002), Effect of increased nitrogen depositions and drought stress on the development of scots pine (Pinus sylvestris L.)—II. Root system response. *J. For. Sci.*, 48, 237–247.

Palátová, E. (2004), Effect of increased nitrogen depositions and drought stress on the development of young Norway spruce Picea abies (L.) Karst. stands. *Dendrobiology*, 51, 41–45.

Pardo, L.H., Fenn, M.E., Goodale, C.L., Geiser, L.H., Driscoll, C.T., Allen, E.B., Baron, J.S., Bobbink, R., Bowman, W.D., Clark, C.M., Emmett, B., Gilliam, F. S., Greaver, T. L., Hall, S. J., Lilleskov, E. A., Liu, L., Lynch, J. A., Nadelhoffer, K. J., Perakis, S. S., Robin-Abbott, M. J., Stoddard, J. L., Weathers, K. C., Dennis, R. L. (2011), Effects of nitrogen deposition and empirical nitrogen critical loads for ecoregions of the United States. *Ecol. Appl.*, 21, 3049–3082.

Parida, B.R. (2011). The Influence of Plant Nitrogen Availability on the Global Carbon Cycle and NO Emissions (Ph.D. Thesis). University of Hamburg, Hamburg, Germany.

Pastor, J., Post, W. (1988), Response of northern forests to CO2-induced climate change. *Nature*, 334, 55–58.

Pavlick, R., Drewry, D. T., Bohn, K., Reu, B., Kleidon, A. (2013), The Jena Diversity-Dynamic Global Vegetation Model (JeDi-DGVM): A diverse approach to representing terrestrial biogeography and biogeochemistry based on plant functional trade-offs. *Biogeosciences*, 10, 4137–4177.

Peñuelas, J., Poulter, B., Sardans, J., Ciais, P., van der Velde, M., Bopp, L., Boucher, O., Godderis, Y., Hinsinger, P., Llusia, J., Nardin, E., Vicca, S., Obersteiner, M., Janssens, I. (2013), Human-induced nitrogen-phosphorus imbalances alter natural and managed ecosystems across the globe. *Nat. Commun.*, 4, doi:10.1038/ncomms3934.

Peterjohn, W. T., Melillo, J. M., Steudler, P. A., Newkirk, K. M., Bowles, F. P., Aber, J. D. (1994), Responses of trace gas fluxes and N availability to experimentailly elevated soil temperatures. *Ecol. Appl.*, 4, 617–625.

Phillips, O. L., Aragão, L. E. O. C., Lewis, S. L., Fisher, J. B., Lloyd, J., López-González, G., Malhi, Y., Monteagudo, A., Peacock, J., Quesada, C. a, van der Heijden, G., Almeida, S., Amaral, I., Arroyo, L., Aymard, G., Baker, T. R., Bánki, O., Blanc, L., Bonal, D., Brando, P., Chave, J., de Oliveira, A. C. A., Cardozo, N. D., Czimczik, C. I., Feldpausch, T. R., Freitas, M. A., Gloor, E., Higuchi, N., Jiménez, E., Lloyd, G., Meir, P., Mendoza, C., Morel, A., Neill, D. A, Nepstad, D., Patiño, S., Peñuela, M. C., Prieto, A., Ramírez, F., Schwarz, M., Silva, J., Silveira, M., Thomas, A. S., ter Steege, H., Stropp, J., Vásquez, R., Zelazowski, P., Dávila, E. A., Andelman, S., Andrade, A., Chao, K., Erwin, T., Di Fiore, A., Honorio C, E., Keeling, H., Killeen, T. J., Laurance, W. F., Peña Cruz, A., Pitman, N. C. A., Núñez Vargas, P., Ramírez-Angulo, H., Rudas, A., Salamão, R., Silva, N., Terborgh, J., Torres-Lezama, A. (2009), Drought sensitivity of the Amazon rainforest. *Science*, 323, 1344–1347.

Pitcairn, C. E. R., Leith, I. D., Fowler, D., Hargreaves, K. J., Moghaddam, M., Kennedy, V. H., Granat, L. (2001), Foliar nitrogen as an indicator of nitrogen deposition and critical loads exceedance on a European scale. *Water. Air. Soil Pollut.*, 130, 1037–1042.

Pregitzer, K. S., Burton, A. J., Zak, D. R., Talhelm, A. F. (2008), Simulated chronic nitrogen deposition increases carbon storage in northern temperate forests. *Glob. Chang. Biol.*, 14, 142–153.

Prieto, I., Armas, C., Pugnaire, F. I. (2012), Water release through plant roots: New insights into its consequences at the plant and ecosystem level. *New Phytol.*, 193, 830–841.

Quillet, A., Peng, C. H., Garneau, M. (2010), Toward dynamic global vegetation models for simulating vegetation-climate interactions and feedbacks: Recent developments, limitations, and future challenges. *Environ. Rev.*, 18, 333–353.

Rowland, L., da Costa, A. C. L., Galbraith, D. R., Oliveira, R. S., Binks, O.J., Oliveira, A. A. R., Pullen, A. M., Doughty, C. E., Metcalfe, D. B., Vasconcelos, S. S., Ferreira, L. V, Malhi, Y., Grace, J., Mencuccini, M., Meir, P. (2015), Death from drought in tropical forests is triggered by hydraulics not carbon starvation. *Nature*, 528, 119–122.

Roy, J., Picon-Cochard, C., Augusti, A., Benot, M.-L., Thiery, L., Darsonville, O., Landais, D., Piel, C., Defossez, M., Devidal, S., Escape, C., Ravel, O., Fromin, N., Volaire, F., Milcu, A., Bahn, M., Soussana, J.-F. (2016), Elevated CO2 maintains grassland net carbon uptake under a future heat and drought extreme. *Proc. Natl. Acad. Sci. USA*, 113, 6224–6229.

Reich, P. B., Hobbie, S. E., Lee, T. D. (2014), Plant growth enhancement by elevated CO2 eliminated by joint water and nitrogen limitation. *Nat. Geosci.*, 7, 920–924.

Sala, A., Piper, F., Hoch, G. (2010), Physiological mechanisms of drought-induced tree mortality are far from being resolved. *New Phytol.*, 186, 274–281.

Scheiter, S., Langan, L., Higgins, S. I. (2013), Next-generation dynamic global vegetation models: Learning from community ecology. *New Phytol.*, 198, 957–969.

Schimel, J., Balser, T. C., Wallenstein, M. (2007), Microbial stress-response physiology and its implications for ecosystem function. *Ecology*, 88, 1386–1394.

Seneviratne, S.I., Nicholls, N., Easterling, D., Goodess, C.M., Kanae, S., Kossin, J., Luo, Y., Marengo, J., McInnes, K., Rahimi, M., Reichstein, M., Sorteberg, A., Vera, C., Zhang, X. (2012). Changes in climate extremes and their impacts on the natural physical environment. In Field, C. B., V. Barros, T.F. Stocker, D. Qin, D.J. Dokken, K.L. Ebi, M.D. Mastrandrea, K.J. Mach, G.-K. Plattner, S.K. Allen, M. Tignor, and P.M. Midgley (Eds.), Managing the Risks of Extreme Events and Disasters to Advance Climate Change Adaptation (pp. 109–230), Cambridge, UK: Cambridge University Press.

Shevliakova, E., Pacala, S. W., Malyshev, S., Hurtt, G. C., Milly, P. C. D., Caspersen, J. P., Sentman, L. T., Fisk, J. P., Wirth, C., Crevoisier, C. (2009), Carbon cycling under 300 years of land use change: Importance of the secondary vegetation sink. *Glob. Biogeochem. Cycles*, 23, doi:10.1029/2007GB003176.

Simkin, S. M., Allen, E. B., Bowman, W. D., Clark, C. M., Belnap, J., Brooks, M. L., Cade, B. S., Collins, S. L., Geiser, L. H., Gilliam, F. S., Jovan, S. E., Pardo, L. H., Schulz, B. K., Stevens, C. J., Suding, K. N., Throop, H. L., Waller, D. M. (2016), Conditional vulnerability of plant diversity to atmospheric nitrogen deposition across the United States. *Proc. Natl. Acad. Sci. USA*, 113, 4086–4091.

Sivandran, G., Bras, R. L. (2013), Dynamic root distributions in ecohydrological modeling: A case study at Walnut Gulch Experimental Watershed. *Water Resour. Res.*, 49, 3292–3305.

Smith, B., Prentice, I. C., Sykes, M. T. (2001), Representation of vegetation dynamics in the modelling of terrestrial ecosystems: Comparing two contrasting approaches within European climate space. *Glob. Ecol. Biogeogr.*, 10, 621–637.

Smith, B., Wärlind, D., Arneth, A., Hickler, T., Leadley, P., Siltberg, J., Zaehle, S. (2014), Implications of incorporating N cycling and N limitations on primary production in an individual-based dynamic vegetation model. *Biogeosciences*, 11, 2027–2054.

Smithwick, E. A. H., Eissenstat, D. M., Lovett, G. M., Bowden, R. D., Rustad, L. E., Driscoll, C. T. (2013), Root stress and nitrogen deposition: Consequences and research priorities. *New Phytol.*, 197, 712–719.

Smithwick, E. A. H., Lucash, M. S., McCormack, M. L., Sivandran, G. (2014), Improving the representation of roots in terrestrial models. *Ecol. Model.*, 291, 193–204.

Talhelm, A. F., Pregitzer, K. S., Burton, A. J. (2011), No evidence that chronic nitrogen additions increase photosynthesis in mature sugar maple forests. *Ecol. Appl.*, 21, 2413–2424.

Tang, J. Y., Riley, W. J. (2013), A total quasi-steady-state formulation of substrate uptake kinetics in complex networks and an example application to microbial litter decomposition. *Biogeosciences*, 10, 8329–8351.

Tang, J., Riley, W. J., Niu, J. (2015), Incorporating root hydraulic redistribution in CLM4.5: Effects on predicted site and global evapotranspiration, soil moisture, and water storage. *J. Adv. Model. Earth Syst.*, 7, 1828–1848.

Thomas, R. Q., Canham, C. D., Weathers, K. C., Goodale, C. L. (2010), Increased tree carbon storage in response to nitrogen deposition in the US. *Nat. Geosci.*, 3, 13–17.

Thomas, R. Q., Zaehle, S., Templer, P. H., Goodale, C. L. (2013), Global patterns of nitrogen limitation: Confronting two global biogeochemical models with observations. *Glob. Chang. Biol.*, 19, 2986–2998.

Thornton, P. E., Lamarque, J.-F., Rosenbloom, N. A., Mahowald, N. M. (2007), Influence of carbon-nitrogen cycle coupling on land model response to CO2 fertilization and climate variability. *Glob. Biogeochem. Cycles*, 21, doi:10.1029/2006GB002868.

Thornton, P. E., Doney, S. C., Lindsay, K., Moore, J. K., Mahowald, N., Randerson, J. T., Fung, I., Lamarque, J.-F., Feddema, J. J., Lee, Y. H. (2009), Carbon-nitrogen interactions regulate climate-carbon cycle feedbacks: Results from an atmosphere-ocean general circulation model. *Biogeosciences*, 6, 2099–2120.

Throop, H. L. (2005), Nitrogen deposition and herbivory affect biomass production and allocation in an annual plant. *Oikos*, 111, 91–100.

Tjiputra, J. F., Roelandt, C., Bentsen, M., Lawrence, D. M., Lorentzen, T., Schwinger, J., Seland, Ø., Heinze, C. (2013), Evaluation of the carbon cycle components in the Norwegian Earth System Model (NorESM). *Geosci. Model Dev.*, 6, 301–325.

Ukkola, A. M., De Kauwe, M. G., Pitman, A. J., Best, M. J., Abramowitz, G., Haverd, V., Decker, M., Haughton, N. (2016), Land surface models systematically overestimate the intensity, duration and magnitude of seasonal-scale evaporative droughts. *Environ. Res. Lett.*, 11, doi:10.1088/1748-9326/11/10/104012.

Van Bodegom, P. M., Douma, J. C., Witte, J. P. M., Ordoñez, J. C., Bartholomeus, R. P., Aerts, R. (2012), Going beyond limitations of plant functional types when predicting global ecosystem-atmosphere fluxes: Exploring the merits of traits-based approaches. *Glob. Ecol. Biogeogr.*, 21, 625–636.

Verburg, P. S. J., Kapitzke, S. E., Stevenson, B. A., Bisiaux, M. (2014), Carbon allocation in Larrea tridentata plant-soil systems as affected by elevated soil moisture and N availability. *Plant Soil*, 378, 227–238.

Verma, P., Sagar, R., Verma, H., Verma, P., Singh, D. K. (2014), Changes in species composition, diversity and biomass of herbaceous plant traits due to N amendment in a dry tropical environment of India. *J. Plant Ecol.*, 8, 321–332.

Vitousek, P. M., Aber, J., Howarth, R. W., Likens, G. E., Matson, P. A., Schindler, D. W., Schlesinger, W. H., Tilman, G. D. (1997), Human alteration of the global nitrogen cycle: Causes and consequences. *Issues Ecol.*, 1, 1–17.

Wang, Y. P., Law, R. M., Pak, B. (2010), A global model of carbon, nitrogen and phosphorus cycles for the terrestrial biosphere. *Biogeosciences*, 7, 2261–2282.

Wang, D., Maughan, M. W., Sun, J., Feng, X., Miguez, F., Lee, D., Dietze, M. C. (2012), Impact of nitrogen allocation on growth and photosynthesis of Miscanthus (Miscanthus × giganteus). *GCB Bioenergy*, 4, 688–697.

Wang, M., Shi, S., Lin, F., Hao, Z., Jiang, P., Dai, G. (2012), Effects of soil water and nitrogen on growth and photosynthetic response of Manchurian Ash (Fraxinus mandshurica) seedlings in northeastern China. *PLoS ONE*, 7, e30754.

Warren, J. M., Hanson, P. J., Iversen, C. M., Kumar, J., Walker, A. P., Wullschleger, S.D. (2015), Root structural and functional dynamics in terrestrial biosphere models—Evaluation and recommendations. *New Phytol.*, 205, 59–78.

Weißhuhn, K., Auge, H., Prati, D. (2011), Geographic variation in the response to drought in nine grassland species. *Basic Appl. Ecol.*, 12, 21–28.

Wu, Z., Dijkstra, P., Koch, G. W., Peñuelas, J., Hungate, B. A. (2011), Responses of terrestrial ecosystems to temperature and precipitation change: A meta-analysis of experimental manipulation. *Glob. Chang. Biol.*, 17, 927–942.

Xia, J., Wan, S. (2008), Global response patterns of terrestrial plant species to nitrogen addition. *New Phytol.*, 179, 428–439.

Yan, B., Dickinson, R. E. (2014), Modeling hydraulic redistribution and ecosystem response to droughts over the Amazon Basin using Community Land Model 4.0 (CLM4). *J. Geophys. Res. Biogeosci.*, 119, 2130–2143.

Zaehle, S., Friend, A. D. (2010), Carbon and nitrogen cycle dynamics in the O-CN land surface model: Model description, site-scale evaluation, and sensitivity to parameter estimates. *Glob. Biogeochem. Cycles*, 24, doi:10.1029/2009GB003521.

Zaehle, S., Dalmonech, D. (2011), Carbon-nitrogen interactions on land at global scales: Current understanding in modelling climate biosphere feedbacks. *Curr. Opin. Environ. Sustain.*, 3, 311–320.

Zaehle, S., Medlyn, B. E., De Kauwe, M. G., Walker, A. P., Dietze, M. C., Hickler, T., Luo, Y., Wang, Y.-P., El-masri, B., Thornton, P., Jain, A., Wang, S., Warlind, D., Weng, E., Parton, W., Iversen, C. M., Gallet-budynek, A., McCarthy, H., Finzi, A., Hanson, P. J., Prentice, I. C., Oren, R., Norby, R. J. (2014), Evaluation of 11 terrestrial carbon-nitrogen cycle models against observations from two temperate free-air CO2 enrichment studies. *New Phytol.*, 202, 803–822.

Zaehle, S., Jones, C. D., Houlton, B., Lamarque, J. F., Robertson, E. (2015), Nitrogen availability reduces CMIP5 projections of twenty-first-century land carbon uptake. *J. Clim.*, 28, 2494–2511.

Zeng, X. (2001), Global vegetation root distribution for land modeling. *J. Hydrometeorol.*, 2, 525–530.

Zhao, M., Running, S. W. (2010), Drought-induced reduction in global terrestrial net primary production from 2000 through 2009. *Science*, 329, 940–943.

Zhou, X., Zhang, Y., Ji, X., Downing, A., Serpe, M. (2011), Combined effects of nitrogen deposition and water stress on growth and physiological responses of two annual desert plants in northwestern China. *Environ. Exp. Bot.*, 74, 1–8.

Zhu, X., Zhang, W., Chen, H., Mo, J. (2015), Impacts of nitrogen deposition on soil nitrogen cycle in forest ecosystems: A review. *Acta Ecol. Sin.*, 35, 35–43.

Zhu, Q., Riley, W. J., Tang, J. (2017), A new theory of plant-microbe nutrient competition resolves inconsistencies between observations and model predictions. *Ecol. Appl.*, 27, 875–886.

3 SIMULATING DYNAMIC ROOTS IN THE ENERGY EXASCALE EARTH SYSTEM LAND MODEL

This chapter was previously published as Drewniak, B. A. 2019. Simulating dynamic roots in the Energy Exascale Earth System Land Model. *Journal of Advances in Modeling Earth Systems*, doi:10.1029/2018MS001334.

3.1 Introduction

Fine roots are responsible for water and nutrient uptake for plant needs (Jackson et al., 1997), functioning to couple aboveground and belowground ecosystems. Roots control surface energy fluxes through soil interactions that affect water availability to the plant, and by extension evapotranspiration (ET). Roots also moderate photosynthesis and biomass acclamation. As such, roots play an important role in the carbon cycle through respiration and carbon storage (Raich and Schlesinger, 1992; Lee et al., 2005; Nepstad et al., 1994; Balesdent and Balabane, 1996; Clemmensen et al., 2013).

Roots respond to their environment with foraging strategies to improve nutrient acquisition (de Kroon and Mommer, 2006). Examples of such behavior are increased root density in soil regions where resources are high (Hodge, 2004), increased productivity under elevated nutrients (Yuan and Chen, 2012), or changes in biomass allocation under nutrient shortage (Hermans et al., 2006). Barley plants responded to low nutrient soils by increasing resources to roots and increasing roots in soil regions with the highest nutrient concentration

(Grossman and Rice, 2012). Increased rooting depth, biomass, and production enhanced nutrient uptake under elevated CO_2 conditions (Iversen, 2010; Iversen et al., 2011; Finzi et al., 2007).

Plants also respond to moisture heterogeneity to enhance water uptake (Wilcox et al., 2004). Plants with root plasticity in their rooting depth distribution can alter the source of water uptake depending on the season (Dawson and Pate, 1996; Knight, 1999; Zencich et al., 2002; Zhu et al., 2016; Wang et al., 2017). Or, when surface soils dry, some species of plants can compensate by efficiently taking up water for plant transpiration from deep roots (Lai and Katul, 2000; Yang et al., 2015). Bao et al. (2014) found that plant roots grew asymmetrically toward a water source as sensed from microscale differences in environment. It is important that models allow roots to adapt to heterogeneity of water and nitrogen in the soil, in order to allow ecosystems to respond to changes in environment, especially those associated with climate change. However, roots have one of the simplest representations in Earth system models (ESMs).

Root systems have largely been ignored in ESMs for several reasons. First, ESMs can capture aboveground productivity fairly well without explicitly modeling roots. Second, there are limited data available for benchmarking root models. Belowground studies are more difficult (and destructive) than aboveground studies. Finally, there is a significant scale discrepancy between the model resolution (typically 1° or higher) and the heterogeneity of the environment as experienced by the root (millimeters for the rhizosphere). In a typical ESM, all the vegetation growing on the grid cell share the soil column, and the only heterogeneity occurs across vertical soil layers (if they exist). Root water uptake across small scales with heterogeneous water distribution has been addressed (Couvreur et al., 2012; Couvreur et al., 2014) but has not been

incorporated into an ESM. Recently, the possibility of including root system architecture in the Community Land Model (CLM) was tested by Bouda and Saiers (2017) and showed promising improvements in root water uptake in a grid cell.

Most root algorithms in ESMs consist of a fixed maximum rooting depth and distribution (Arora and Boer, 2003). The Energy Exascale Earth System Land Model (ELM) distinguishes between fine roots and coarse roots for woody vegetation (Oleson et al., 2013). Fine roots generally refer to roots that are less than 2 mm in diameter, and coarse roots make up the remaining root biomass, although this division is not explicit in models. Fine roots have the primary role of nutrient and water uptake (Jackson et al., 1997), while coarse roots provide structural support and serve as transporters (Tobin et al., 2007; Reubens et al, 2007). The ELM does not distinguish between these roles but does include different growth, respiration, and decomposition for coarse versus fine roots (Oleson et al., 2013). Although models generally recognize that root traits vary with plant functional type (PFT), they represent most root profiles with an exponential distribution similar to that found in Jackson et al. (1996; hereafter J96). This method works, in general, for many ecosystems, but there are several regions (e.g., arid and boreal) where root distribution is either overestimated or underestimated, resulting in stress-induced lost gross primary productivity (GPP). This approach also results in an inconsistency, as pointed out by Arora and Boer (2003); for example, small and large trees have the same root distribution, root depth, and root fraction in each soil layer. Fixed root distribution is also problematic in agricultural systems, where plant growth begins from a seed and experiences rapid growth to maturity over a short growing season. At a minimum, root profiles should include time-varying structure (i.e., distribution) as leaves and stems.

Root function is also poorly represented in most ESMs. For example, many ESMs do not include or parameterize nutrient uptake. When nitrogen is included, uptake is from a bulk nitrogen mineralization pool dependent on supply and demand rather than root biomass. Although water supply is handled within the soil column more explicitly, without a robust root distribution, water stress can result in an unrealistic downscaling of physiology (Warren et al., 2015). Furthermore, root function, production, and resource uptake are highly variable between models (Warren et al., 2015).

Despite the many advances in our understanding of root function, turnover, and distribution (Matamala and Stover, 2013), ESMs continue to represent roots in a rudimentary way (Warren et al., 2015), although some recent work has focused on improving belowground processes in ESMs, including root developments. For example, recent work simulated root growth using optimization techniques to maximize plant transpiration (Sivandran and Bras, 2013) and nitrogen uptake (McMurtrie et al. 2012). Arora and Boer (2003) developed a method to represent root distribution as a function of root biomass, which was tested against boreal (El Masri et al., 2015) and agricultural systems (Song et al., 2013). Finally, Yang et al. (2016) estimated effective rooting depth using a carbon cost-benefit model of water uptake. These efforts to improve root representation are still limited, because they focus on maximizing only one limiting resource: water or nitrogen. This limits the relevancy to environments that share those resource limitations and may not reflect the future state of those regions or may not be suitable for global application.

The goal of this work is to develop a new dynamic root approach for the Energy Exascale Earth System Model (E3SM; formerly known as the Accelerated Climate Model for Energy) Land Model (ELM), which accounts for both water and nutrient limitations, such that plants can adjust for whichever resource is limiting. I anticipate that this approach will improve plant response to drought and/or nutrient limitation, since plants can adapt to their environment, moderating the carbon cycle and storage of an ecosystem. Specifically, I expect that allowing roots to dynamically respond to resources will improve plant productivity in regions that are arid or have seasonal dry periods. In tropics and subtropics, I do not expect plant productivity to change much because I assume that water availability is sufficient and only nitrogen uptake can increase. The original model design, introduced in Drewniak et al. (2013) for agriculture, is expanded to take advantage of new developments in the below ground biogeochemistry introduced in ELM, in particular the vertically resolved nitrogen profile. I will analyze the resulting GPP, total ecosystem carbon storage (TEC), ET, and nitrogen uptake. It should also be noted that this model does not include phosphorus (which is now included ELM), which will be important in phosphorus limited regions such as the tropics. A description of the model is outlined in section 2. The resulting root distribution is presented in section 3, followed by a discussion in section 4.

3.2 Materials and Methods

3.2.1 Model Description

The E3SM is a fully coupled ESM developed by the U.S. Department of Energy (DOE) to simulate the atmosphere, ocean, and land. The E3SM shares lineage with the Community Earth System Model (CESM) v1.2, and thus, the E3SM Land Model (ELM) v0 is based on the CLM (CLM4.5). The ELM v1, which is used in this study, had additional development including improvements to the biogeochemistry model.

The current root distribution in ELM is an exponential profile with the root fraction in each soil layer based on Zeng (2001):

$$r_i = \begin{cases} 0.5\begin{bmatrix} exp(-r_a z_{h,i-1}) + exp(-r_b z_{h,i-1}) - \\ exp(-r_a z_{h,i}) - exp(-r_b z_{h,i}) \end{bmatrix} & for\ 1 \le i < N_{levsoi} \\ 0.5\left[exp(-r_a z_{h,i-1}) + exp(-r_b z_{h,i-1})\right] & for\ i = N_{levsoi} \end{cases} \quad (1)$$

where $z_{h,i}$ is the depth between the soil surface and the interface between the current and next soil layer and r_a and r_b are the root distribution parameters dependent on PFT (see Table 8.3 in Oleson et al., 2013). The ELM v1 has up to 10 soil layers with increasing thickness with depth, and root depth at the bottom of the soil layer (3.8 m). The exponential distribution of roots agrees well with global observations but does not allow changes in root distribution in response to changes in water or nutrients, nor does it capture the rooting profile of ecosystems in arctic or arid regions.

The new rooting profile is updated as new carbon inputs are allocated to roots. This algorithm is similar to that of Drewniak et al. (2013), which was implemented for crops to capture the rapid growth and development of agriculture root systems. Fine root carbon, C, in each soil layer *i* is calculated each time step as

$$C_i = C_{i,t-1} + r_{i,t} C_{new} \quad (2)$$

where C_{new} is the new carbon allocated to the roots at time t and $C_{i,t-1}$ represents the root carbon in layer i during the previous time step, which includes senescence due to turnover, calculated as the loss of carbon proportional to the root fraction in the soil layer. Just as the previous model of Drewniak et al. (2013), the senescence term does not influence the final root distribution, however, in future versions of this algorithm could represent turnover weighted toward soil layers that lack resources. Finally, $r_{i,t}$ is the new root fraction in each soil layer at time t:

$$r_{i,t} = (1 - f) * rw_i + f * rn_i \quad (3)$$

The root fraction is weighted by the water availability summed across the number of soil layers (*nlevsoi*) in the rooting zone (f),

$$f = \sum_1^{nlevsoi} max(0,\ w_i * r_{i,t-1}) \quad (4)$$

where the plant wilting factor, w_i, is defined as (Oleson et al., 2013)

$$w_i = \frac{\Psi_c - \Psi_i}{\Psi_c - \Psi_o} * p_{eff} \quad (5)$$

Ψ_i is the soil matrix potential (mm) in soil layer, i; Ψ_c is soil water potential at stomatal closure; and Ψ_o is the soil water potential at full stomatal opening. The plant wilting factor is weighted by the effective porosity, p_{eff}, which takes into account the soil ice fraction. The relative available soil moisture in each soil layer (rw_i) is then calculated as

$$rw_i = \frac{R_{w,i}}{\sum_1^{nlevsoi} R_w} \quad (6)$$

where

$$R_{w,i} = max(0, w_i) * dz_i \quad (7)$$

and the relative nutrient distribution in each soil layer (rn_i) is

$$rn_i = \frac{sminn_i * dz_i}{\sum_1^{nlevsoi} sminn_i * dz_i} \quad (8)$$

where $sminn_i$ is the soil mineral nitrogen in layer i and dz_i is the soil thickness of layer i. If the vertical nitrogen profile is not active, then a nitrogen profile is prescribed as an exponential decay with a decay constant of 3/m, consistent with Jobbágy and Jackson (2001) and Batjes (1996). Once the new root carbon in each soil layer is calculated, the new root fraction in each soil layer is determined by normalizing the root carbon over all the soil layers.

Crops have an additional root component that determines changes in rooting depth over the growing season to allow the rapid development of roots over short time scales (i.e., one growth cycle). Crop root depth is initialized at the bottom of the second soil layer (~4 cm). Root depth increases linearly with growing degree days over the growing cycle and reaches maximum depth at the beginning of the grain fill stage. Maximum rooting depth for crops varies with crop type: 120, 160, and 90 cm for corn, soybean, and wheat, respectively (Mayaki et al., 1976; Araki and Iijima, 2001; Amos and Walters, 2006). A maximum rooting depth is also assigned to other PFTs, although the depth does not change over the growing season. Table IV lists the maximum rooting depths for all PFTs, calculated using the asymptotic equation and extinction coefficients in J96 with a cumulative root fraction of 0.99. Tropical plants were assumed to have deeper root depths (Nepstad et al., 1994; Fan et al., 2017) and therefore were given a default depth of 3 m.

Table IV. Maximum rooting depth of PFTs in ELM.

PFT	Maximum rooting depth (m)
Needleleaf evergreen temperate tree	1.89
Needleleaf evergreen boreal tree	1.17
Needleleaf deciduous boreal tree	1.17
Broadleaf evergreen tropical tree	3.00
Broadleaf evergreen temperate tree	1.89
Broadleaf deciduous tropical tree	3.00
Broadleaf deciduous temperate tree	1.33
Broadleaf deciduous boreal tree	1.17
Broadleaf evergreen shrub	1.25
Broadleaf deciduous temperate shrub	1.25
Broadleaf deciduous boreal shrub	0.73
C3 arctic grass	0.51
C3 nonarctic grass	1.17
C4 grass	1.62
C3 generic crop	1.15
C3 generic crop – irrigated	1.15
Corn	1.20
Spring wheat	0.90
Soybean	1.60

The new root fraction impacts on ELM are demonstrated in Figure 3.1. The direct impact from the new root fraction is to soil moisture via shifts in water uptake in the root column. Changes to soil moisture content can influence both soil moisture stress and nitrogen availability. Although not shown in Figure 3.1, soil moisture stress and nitrogen availability are the components that drive changes in root fraction. Stomatal conductance and the maximum rate of carboxylation (Vcmax) are weighted by soil moisture stress, which can reduce photosynthesis and ET. Photosynthesis is also downscaled by nitrogen stress. Finally, changes to ET and photosynthesis will impact energy fluxes, productivity, and ultimately the amount of carbon that

can be stored in the ecosystem, or TEC. TEC includes the combined carbon in the litter, vegetation, and soil mineral pools, and can be considered the carbon storage for the land.

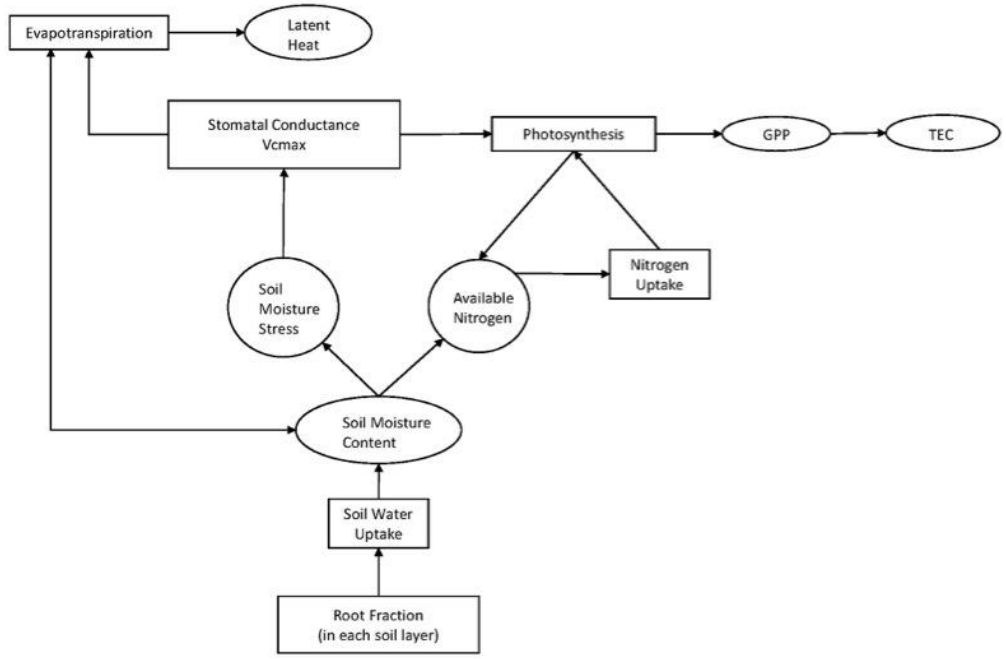

Figure 3.1. Schematic demonstrating the influence of root fraction on resource uptake, energy fluxes, and productivity in the Energy Exascale Earth System Land Model (ELM).

3.3 Model Simulations

The ELM was run off line using the accelerated spin-up procedure described in Koven et al. (2013) with modifications from D. Ricciuto (personal communication, February 2, 2016) with atmospheric data from 1972 to 2004 (Qian et al., 2006) cycled for a total of 1,000 model years. Following the accelerated spin-up, atmospheric forcing was cycled three times from 1972 to 2004 from Qian et al. (2006). The final 33 years were used for model evaluation to test the

behavior of root structure and to examine the impact of dynamic roots on vegetation productivity, nutrient, and water uptake.

Three additional experiments were performed to explore the sensitivity of productivity to water availability. The first sensitivity simulations set water availability, f in equation (3), to 0, so the vegetation was always considered to be fully water stressed and the resulting root profile was dependent only on water availability and not nitrogen availability. The goal was to examine how much water limitation was still playing a role in vegetation development and productivity after a dynamic rooting depth distribution was added. The second sensitivity experiment allowed f to range between 0 and a maximum of 0.5 to ensure that at least half of the root growth was focused in soil layers with water availability. Finally, a simulation that allowed f to range between 0 and a maximum of 0.9 forced the vegetation to have a minimal water demand. Table V summarizes the various model simulations that were performed.

Table V. Summary of simulations.

Simulation	Dynamic roots	Water stress	Nitrogen stress
CONTROL	No	NA	NA
DYNROOT	Yes	Dynamic	Yes
DYNROOT-W	Yes	Always stressed, set $f = 0$ in equation (3)	No
DYNROOT-50W	Yes	Max. 50%, set $f \leq 0.5$ in equation (3)	Yes
DYNROOT-90W	Yes	Max. 10%, set $f \leq 0.9$ in equation (3)	Yes

3.4 Results

3.4.1 Root Distribution

Root distribution with the dynamic root model compares well with observations of root profiles. Grid cells that have inactive vegetation are included in the analysis; however, the root profiles of the inactive vegetation are set to the default distribution in equation (1). Here I compare the output from the DYNROOT and CONTROL simulations with observational data from J96 and Schenk and Jackson (2002a). Observations from J96 consist of a database of 250 root studies across 11 biomes, used to solve the extinction coefficient in the asymptotic equation of cumulative root fraction proposed by Gale and Grigal (1987). Schenk and Jackson (2002a) expand that study further with a database of 475 root profiles, which were used to extrapolate the 50% and 95% root depth and analyze the relationships between rooting depths and climate, soil, and vegetation. Figure 3.2 shows the percent of root biomass above the top 30 cm of soil (similar to Figure 3.2 from J96). In agreement with J96, boreal and arctic regions include nearly 80–100% of root biomass in the top 30 cm of soil. Croplands also have a large percentage of roots (~80%) in the top 30 cm of soil, although this is somewhat higher than the J96 observations. The Amazon basin, the African Congo, and the island chain of Malaysia and Indonesia, as well as other moist climate regions, also have over 70% of roots in the top 30 cm. Dry and desert regions, such as Australia, south Africa, and east Brazil, tend to have fewer roots (60–70%) in the top 30 cm of soil. However, there are other regions that tend to overestimate or underestimate the fraction of roots in the top 30 cm. ELM underestimates root biomass in regions like the Sahel, western India, and northern Australia. ELM overestimates root biomass in the western United States, in the African savannahs, along the plains and the Brazilian highlands in South America, and in eastern China.

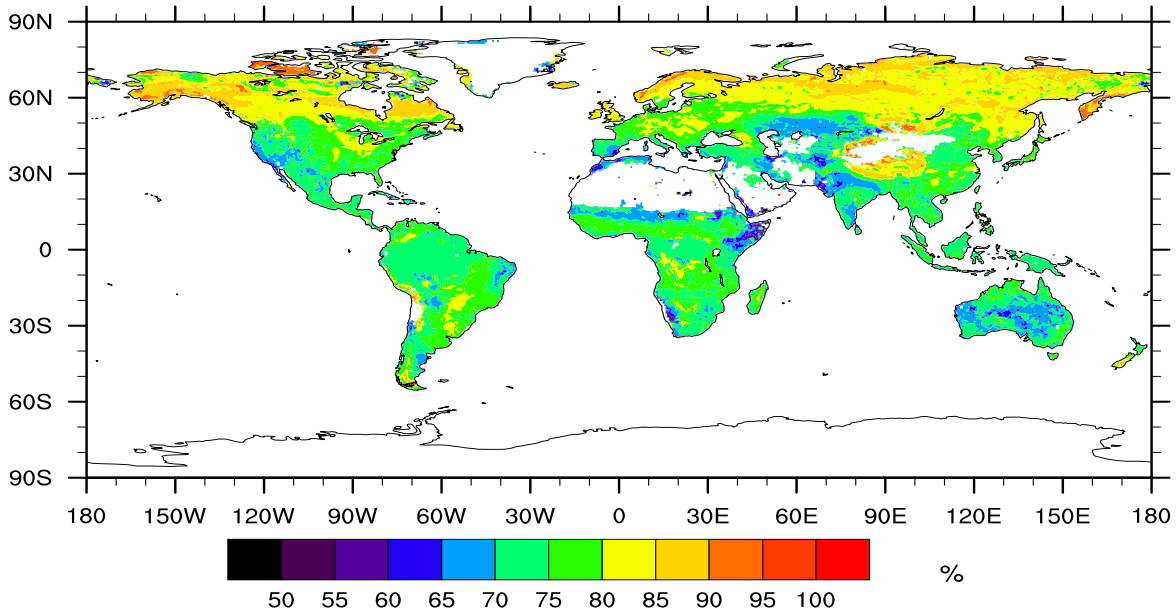

Figure 3.2. Percent of root biomass above 30 cm depth.

Another way of looking at the root distribution is the depth at which 50% (D50) and 95% (D95) of the root biomass exists. Figure 3.3 and Figure 3.4 show this, broken down by climate classification (see Figure 3.5, Appendix B, for the breakdown of climate zones based on Peel et al., 2007, downloaded from ORNL DAAC 2017; note that the crop biome includes all grid cells that have more than 50% crop cover and can include any of the other biomes). In much of the world, D50 is above 10 cm, and almost globally (with some exceptions), D50 is within the top 20 cm. This is somewhat shallower than observations; the range of D50 was generally between 0.09 and 0.16 m, with an average depth of 0.13 m in ELM, but Schenk and Jackson (2002a) suggest that the average should be closer to 0.18 m, with a range between 0.05 and 0.28 m. The variability of D50 is quite low, but there are exceptions, particularly for some tropical and desert biomes that have the shallowest and deepest D50 extremes. In general, the mean depth of D50 is lower for colder and drier biomes and higher for warmer and wetter biomes, but there is

considerable overlap. A global map of D50 and the difference in D50 between DYNROOT and CONTROL are shown in Figure 3.6 and Figure 3.7, Appendix B, respectively. In most regions, the dynamic root model predicts shallower depths, but some regions (i.e., the western United States, eastern Africa, and Australia) have a slightly deeper depth.

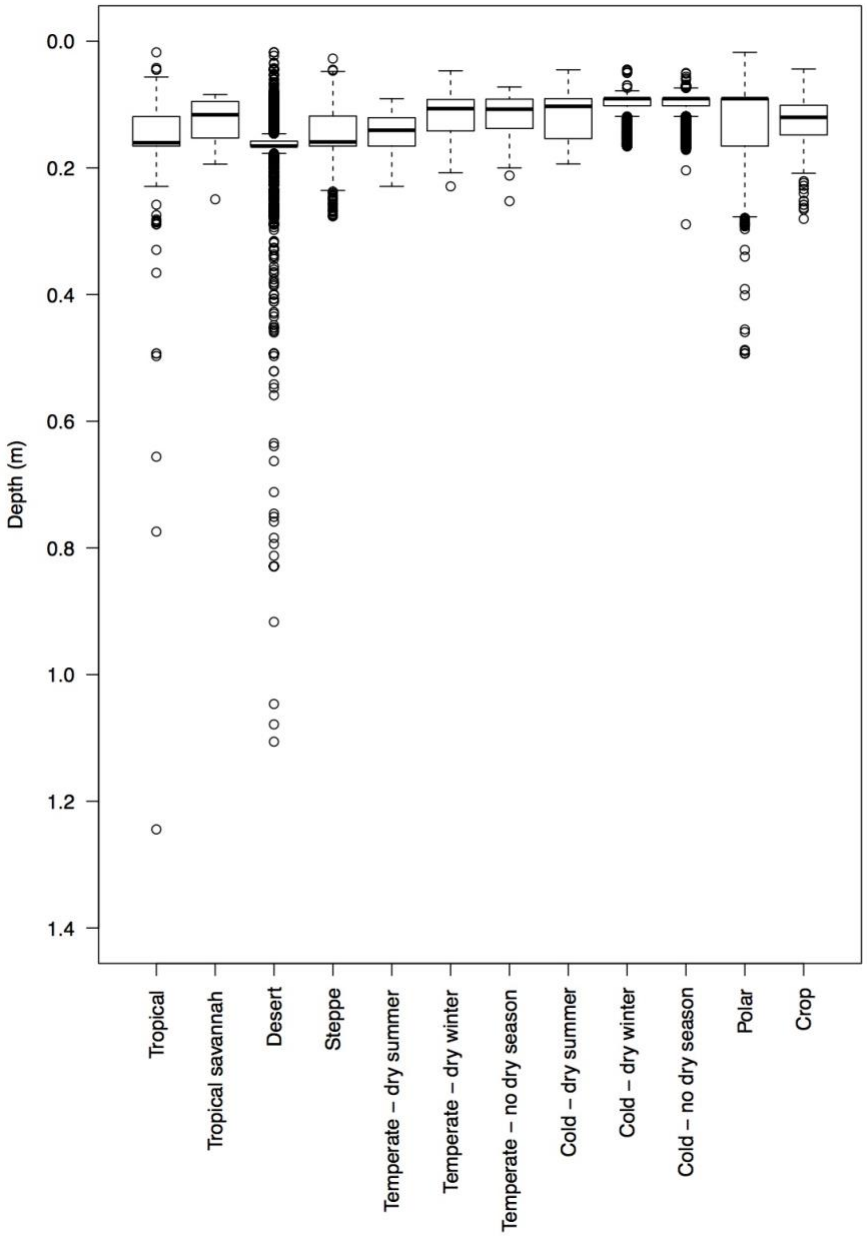

Figure 3.3. Box plot of soil layer depth (m) above which 50% root biomass exists for different climate classification zones from Figure 3.5, Appendix B.

The depth of 95% of root biomass is quite variable (Figure 3.4). This is in part due to the difference in maximum root depths between different vegetation types (e.g., tropical vegetation has a maximum rooting depth of 3 m, whereas boreal grass only has a 0.5 m maximum rooting depth). The same pattern of deeper depths of D95 occurs for warm and tropical or desert regions and shallower depths for cold or dry climates and is consistent with observations (Schenk and Jackson, 2002b). The average D95, which is modeled at 0.98 m, is much closer to observational estimates of 1.02 m (Schenk and Jackson, 2002a). The range of D95 is generally between 0.62 and 1.12 m, whereas Schenk and Jackson (2002a) found a range of 0.40 and 1.5 m. Table VI lists the D95 in each of the climate zones shown in Figure 3.4. Figure 3.6, Appendix B, shows the global map of soil depth to 95% root biomass. In general, high latitudes have shallower depths of D95 than tropical regions. This is also clear in the difference plot between the dynamic root model and the control (see Figure 3.7, Appendix B), which shows shallower root depths in boreal and tropical regions but deeper depths for drier and desert regions. Part of this difference is the result of the shallower soil depths in ELM for boreal vegetation combined with the permafrost soil layers that restrict root growth in arctic regions. In these regions, D95 is located above 0.65 m. This contrasts with tropical regions that have D95 of 1.5 m, or in some cases, such as Australia, below 2 m. The strong gradient that exists in Australia in Figure 3.6, Appendix B, is due to the sharp transition from temperate to tropical vegetation (arbitrarily chosen to be along the 23.25°S latitude). In the northern half of the continent, the majority of the PFTs are broadleaf deciduous tropical trees, while the southern half has mostly broadleaf deciduous temperate shrubs. D95 captures some of the maximum rooting depths estimated by Fan et al. (2017), in polar regions and in the western United States. However, the model does not capture the deepest roots that are expected to occur in the eastern United States, the dry season Amazon, India, and

central South America, mainly due to the limited root depth prescribed in ELM. Figure 3.8 shows the relationship of D95 with latitude. There is no relationship for low latitudes that encompass mostly tropical vegetation types, but for temperate latitudes, D95 decreases with increasing latitude. This relationship is in agreement with Schenk and Jackson (2002a). The increase in rooting depth at high latitudes (above 75°) is an artifact of vegetation that is present in grid cells but is not active; therefore, the root distribution reverts back to the default model value.

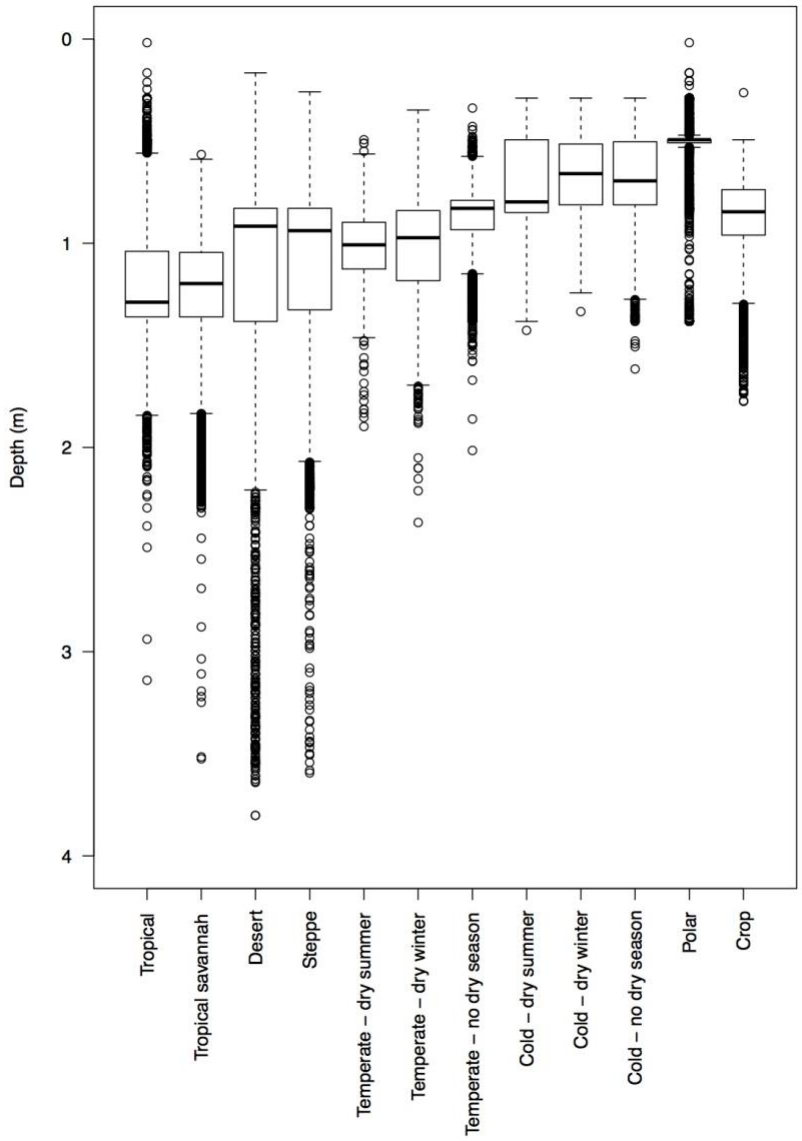

Figure 3.4. Box plot of soil layer depth (m) above which 95% root biomass exists for different climate classification zones from Figure 3.5, Appendix B.

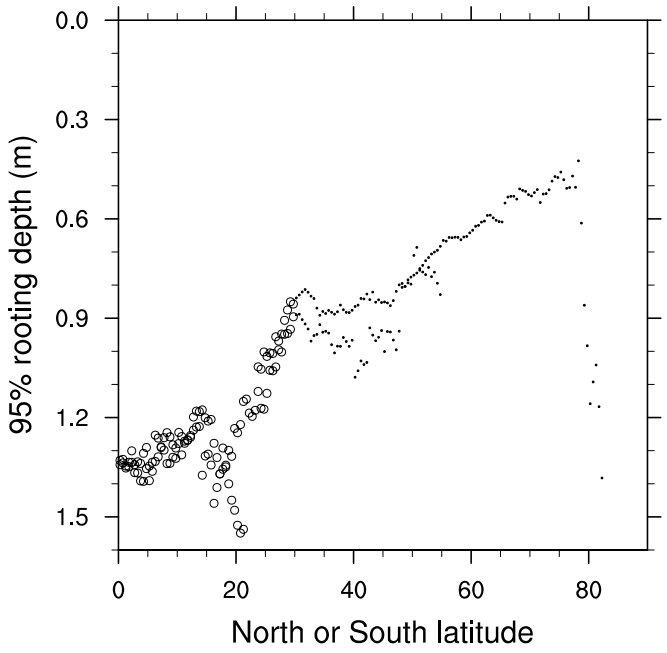

Figure 3.8. Soil layer depth above which 95% of root biomass exists as a function of latitude. The open circles represent latitudes between 30° north and south, and the closed circles are latitudes higher than 30° north or south.

Table VI. Climate zone averaged D95 (soil depth above which 95% of root biomass exists) and GPP (gross primary productivity) for the CONTROL, DYNROOT, AND DYNROOT-50W simulations. Values in parenthesis represent the percent change from CONTROL.

Ecosystem	D95 (m)		
	CONTROL	DYNROOT	DYNROOT-50W
Tropical	1.57	1.01	1.97
Tropical savannah	1.47	1.24	2.25
Desert	1.33	1.24	1.41
Steppe	1.31	1.13	1.43
Temperate—dry summer	1.36	1.00	1.55
Temperate—dry winter	1.35	1.03	1.74
Temperate—no dry season	1.47	0.92	1.82
Cold—dry summer	1.34	0.73	1.13
Cold—dry winter	1.31	0.66	1.07
Cold—no dry season	1.30	0.73	1.19
Polar	1.45	0.68	1.03
Crop	1.04	0.94	1.46
Global	1.44	0.99	1.61

	GPP (g C m^{-2} $year^{-1}$)		
	CONTROL	DYNROOT	DYNROOT-50W
Tropical	1396	1371 (1.8)	1425 (2.1)
Tropical savannah	1429	1385 (-3.1)	1513 (5.8)
Desert	222	222 (-0.1)	222 (-0.1)
Steppe	475	474 (-0.2)	480 (0.9)
Temperate—dry summer	903	881 (-2.4)	936 (3.7)
Temperate—dry winter	1152	1097 (-4.7)	1183 (2.7)
Temperate—no dry season	1576	1530 (-2.9)	1604 (1.8)
Cold—dry summer	443	434 (-2.1)	445 (0.5)
Cold—dry winter	711	703 (-1.2)	708 (-0.4)
Cold—no dry season	782	773 (-1.1)	783 (0.1)
Polar	413	408 (-1.4)	416 (0.7)
Crop	1198	1180 (-2.0)	1237 (2.1)
Global	832	815 (-2.0)	849 (2.1)

The distribution of roots as measured by the cumulative root fraction (Figure 3.9) for PFTs falls between the Zeng (2001) and J96 profiles. The cumulative root fraction from ELM is found from the PFT-weighted root profile, averaged across all simulated years (i.e., 1972-2004). For the observations, the root profile is taken from the asymptotic equation and corresponding ß found in J96. While the simulated root profile from DYNROOT does not always show improvement from CONTROL compared with observations, the purpose of these comparisons is to demonstrate that even though roots are allowed to change dynamically, the model can still produce root distributions that are acceptable. Trees tend to have more shallow roots under the dynamic root profile, but they also have roots at the depths seen in J96. This response is strong due to the grouping of all trees together, as results from individual tree PFTs vary (see Figure 3.10, Appendix B). For example, boreal forests in DYNROOT have root distributions that follow the J96 curve (Figure 3.10a, Appendix B), while the default root profile in ELM has too many roots at depth and too deep a root profile. Temperate evergreen forests (Figure 3.10b, Appendix B) also have too many shallow roots, but the cumulative root fraction curve follows the Zeng (2001) profile more closely than the J96 profile, while deciduous and tropical evergreen forests (Figure 3.10c–e, Appendix B) fall somewhere in between. Shrubs have shallower root profiles, but this is largely the result of the shallow root depth in ELM compared with that from J96. Grasses seem to fall between the Zeng (2001) and J96 profiles (Figure 3.8 and Figure 3.10f–g, Appendix B). Finally, crops (Figure 3.9 and Figure 3.10h, Appendix B) always have shallower root profiles than J96, although this could be the result of differences in the rooting depth modeled by DYNROOT as compared to observations.

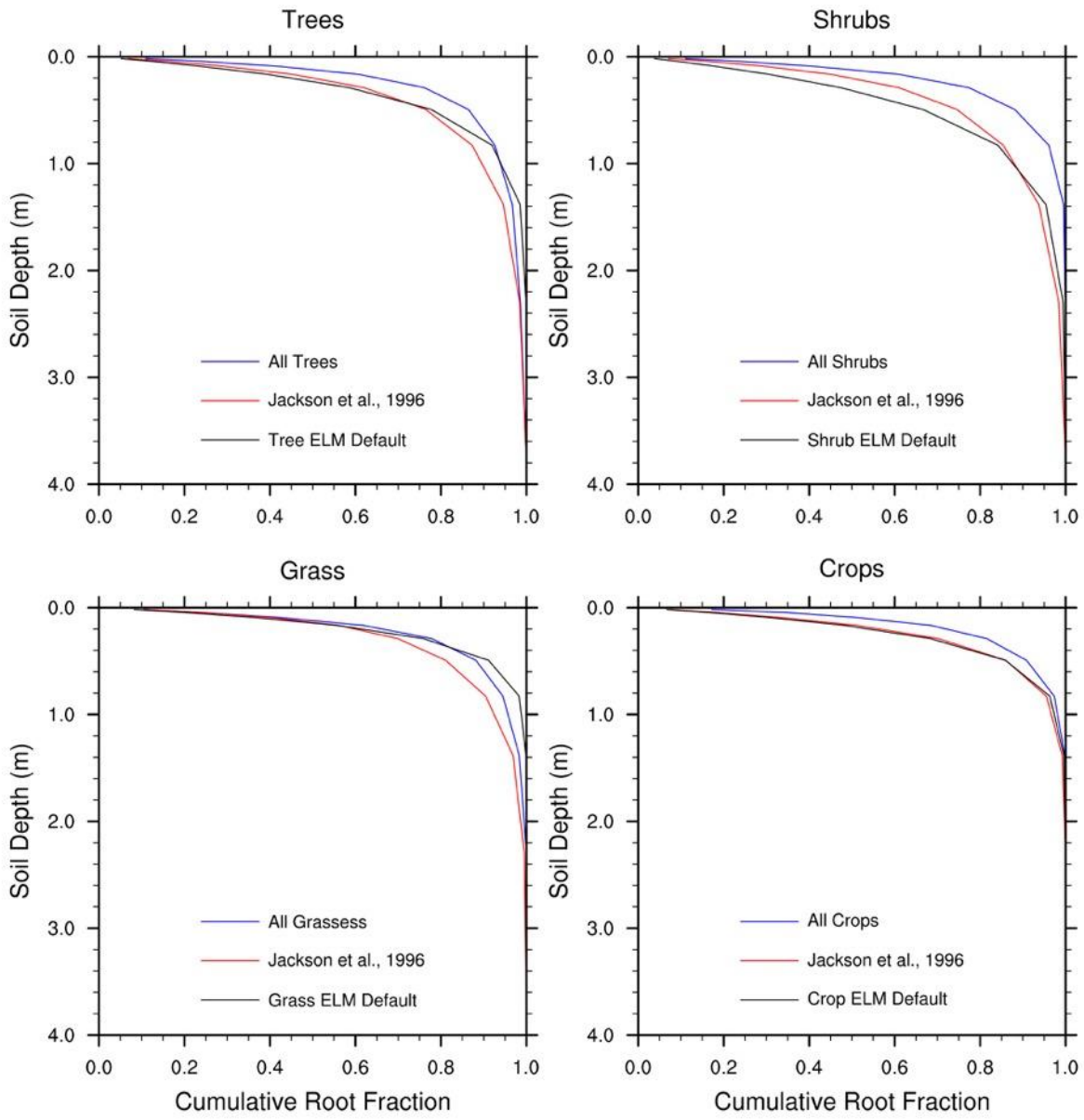

Figure 3.9. Cumulative root fraction of (top left) trees, (top right) shrubs, (bottom left) grasses, and (bottom right) crops for DYNROOT (blue line), CONTROL (black line), and J96 (red line).

3.4.2 Plant Productivity and Uptake

Changes to the root distribution result in altered ET and nitrogen uptake by the plant. Figure 3.11 shows the difference between DYNROOT and CONTROL (note that all difference plots are represented as experiment—control) for ET and nitrogen uptake. Increases occur in regions that are water limited. These include regions such as the western United States, South Africa, along the Sahel, India, Australia, and many boreal regions. However, there are more regions that have a loss in both ET and nitrogen uptake. Those regions include parts of South America, Central Africa, southern China, and Vietnam.

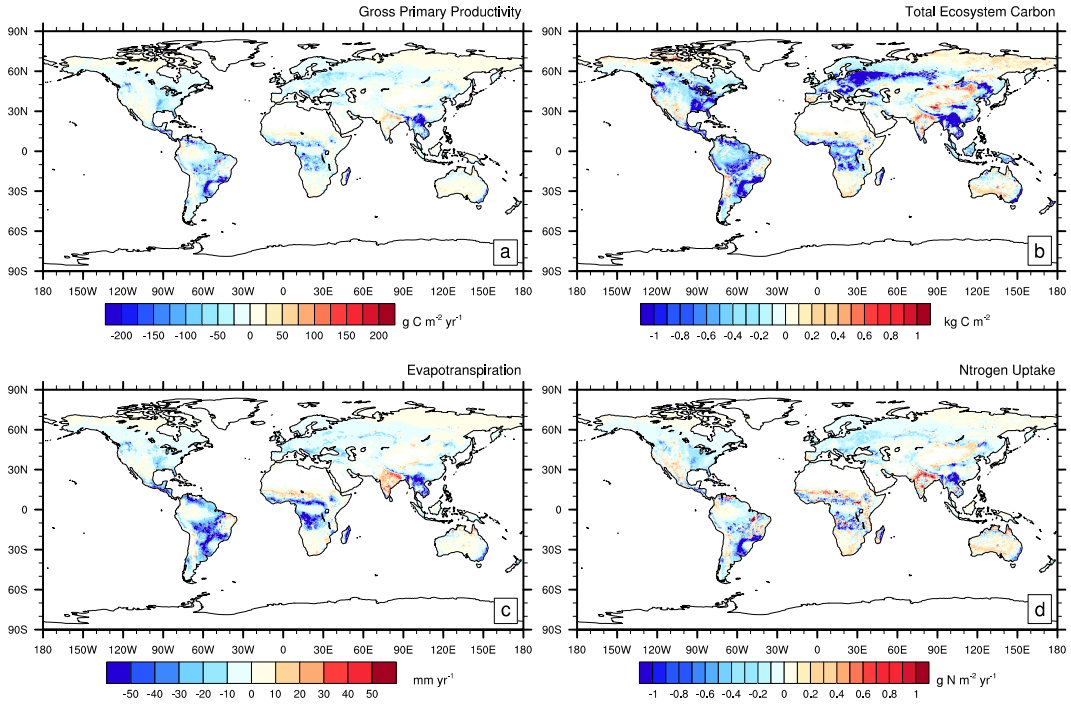

Figure 3.11. Difference between DYNROOT and CONTROL of (a) gross primary productivity (g C m^{-2} $year^{-1}$); (b) total ecosystem carbon (kg C/m^2); (c) evapotranspiration (mm/year); and (d) nitrogen uptake (g N m^{-2} $year^{-1}$).

Observed increases or decreases in productivity are generally correlated with increases or decreases in ET and nitrogen uptake. Although all climate zones experience on average a decrease in GPP (see Table VI), this varies regionally. Figure 3.11a shows the GPP difference between DYNROOT and the CONTROL. Most regions that experience small increases in GPP are in arid or dry ecosystems, but because the GPP in these systems is small, the percent increase can be as large as 50%. Regions with GPP losses tend to be in more productive areas, and thus, the percent loss of GPP is small. For example, in South America losses of GPP occur in some grasslands that are greater than 200 g C/year, but the percent loss of GPP is less than 10%. Globally, the percent decrease in GPP is 2%, or 2.1 Gt C/year.

Despite the modest decrease in global GPP, the dynamic root model improves ELM GPP bias compared with the Moderate Resolution Imaging Spectroradiometer (MODIS) GPP data product (Zhao and Running, 2010). A comparison between the model performance and MODIS is shown in Table VII for each season during the period of 2000–2004, the time period when the model and MODIS data overlapped. The data are presented as the seasonal average for each climate zone (Figure 3.5, Appendix B). The seasons are broken down as follows: winter includes December, January, and February; spring includes March, April, and May; summer includes June, July, and August; and fall includes September, October, and November.

The statistics that were used to examine model performance in Table VII are the average root mean square error (RMSE) and bias of GPP for each biome in each season. RMSE is calculated as

$$RMSE = \sqrt{\frac{\sum_{i=1}^{n} \hat{y}_i - y_i}{n}} \quad (9)$$

where y_i are the observed values, $\hat{y}_i$ are the model simulated values, and n is the number of samples. Bias is calculated as

$$Bias = \hat{y}_i - y_i \quad (10)$$

All the improvements in model performance are marginal. Improvements in RMSE occur during all seasons in cold climate and temperate-no dry season zones, whereas tropical savannah and temperate-dry winter zones are always worse. Other climate zones vary with season. Changes in model bias are similar, with a lower bias in DYNROOT for tropics, deserts, and cold climate zones during all seasons. All other regions vary in bias with season except for tropical savannah, which always performs worse in DYNROOT. To understand how the bias varies spatially, a map of the change in percent relative error (PRE) is shown in Figure 3.12. The PRE in this case is calculated as

$$PRE = 100 * \left| \frac{\hat{y}_i - y_i}{y_i} \right| \quad (11)$$

and the change in PRE is defined in Figure 3.12 as

$$\Delta PRE = PRE_{DRYNROOT} - PRE_{CONTROL} \quad (12)$$

The largest improvements are in the eastern United States, parts of Europe and eastern Asia, Australia, and the Amazon tropics. The regions where the model performance is worse in DYNROOT are the seasonally dry areas of the Amazon, African tropics, and southern Asia.

Table VII. The RMSE and Bias of model simulations compared with MODIS GPP.

DJF	**RMSE**		**Bias**	
	DYNROOT	CONTROL	DYNROOT	CONTROL
Tropical	84.75	84.79	17.54	18.44
Tropical savannah	72.13	70.57	-12.03	-9.57
Desert	20.65	20.81	-37.79	-38.85
Steppe	33.03	33.09	-26.84	-26.79
Temperate-dry summer	51.08	50.85	-13.00	-10.78
Temperate-dry winter	74.59	71.93	-23.38	-18.37
Temperate-no dry season	55.60	56.42	5.35	9.71
Cold-dry summer	8.48	9.21	88.20	107.89
Cold-dry winter	23.20	23.97	329.10	350.18
Cold-no dry season	5.79	6.13	42.47	53.03
Polar	51.32	52.29	-7.88	-6.68
Crop	37.82	38.04	7.54	8.02

MAM	**RMSE**		**Bias**	
	DYNROOT	CONTROL	DYNROOT	CONTROL
Tropical	83.08	82.55	14.61	15.33
Tropical savannah	73.37	71.18	-14.48	-11.84
Desert	22.81	22.94	-43.06	-43.79
Steppe	38.62	38.78	-22.85	-22.07
Temperate-dry summer	60.20	61.28	-3.84	-2.24
Temperate-dry winter	84.53	82.47	-17.39	-11.90
Temperate-no dry season	68.42	68.95	15.08	17.92
Cold-dry summer	45.70	46.42	76.50	80.81
Cold-dry winter	49.05	50.68	80.20	82.86
Cold-no dry season	44.65	46.22	51.14	55.13
Polar	35.72	36.79	30.97	33.61
Crop	61.59	62.58	28.63	30.43

JJA	RMSE		Bias	
	DYNROOT	CONTROL	DYNROOT	CONTROL
Tropical	78.69	78.75	12.21	12.90
Tropical savannah	71.22	70.03	-15.26	-11.85
Desert	24.55	24.42	-39.94	-41.02
Steppe	39.25	38.85	-14.96	-16.09
Temperate-dry summer	72.92	73.87	-35.49	-36.06
Temperate-dry winter	80.49	80.27	2.11	6.42
Temperate-no dry season	80.88	81.68	18.59	21.03
Cold-dry summer	55.83	54.80	-22.16	-20.49
Cold-dry winter	66.49	68.03	4.90	5.90
Cold-no dry season	61.99	62.78	-10.85	-9.80
Polar	42.12	42.63	-56.77	-57.87
Crop	89.56	90.13	40.61	41.04

SON	RMSE		Bias	
	DYNROOT	CONTROL	DYNROOT	CONTROL
Tropical	75.76	75.19	9.98	11.00
Tropical savannah	69.83	67.70	-12.22	-9.29
Desert	20.41	20.52	-38.67	-39.67
Steppe	30.87	30.78	-15.22	-15.97
Temperate-dry summer	56.71	56.49	-26.35	-25.40
Temperate-dry winter	69.22	68.33	-2.36	2.88
Temperate-no dry season	62.26	62.85	8.28	11.57
Cold-dry summer	22.48	22.32	14.81	16.29
Cold-dry winter	40.50	41.76	65.16	68.29
Cold-no dry season	18.77	19.12	17.92	20.07
Polar	23.62	23.74	-6.50	-6.73
Crop	48.79	48.55	24.06	25.47

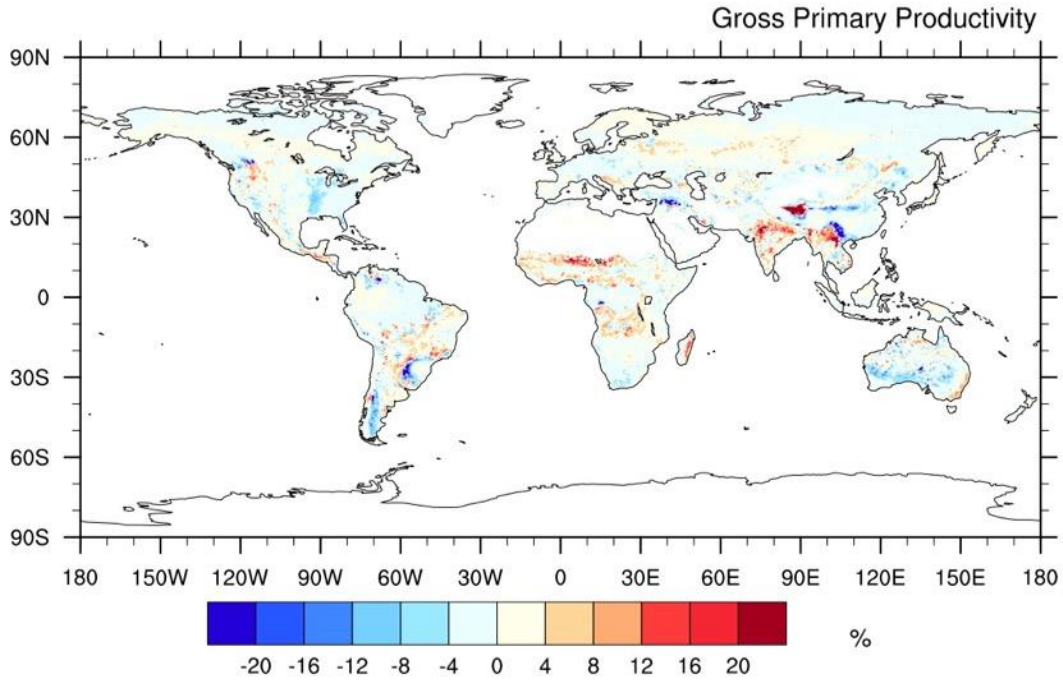

Figure 3.12. The change in percent relative error calculated as $PRE_{DYNROOT} - PRE_{CONTROL}$.

Dynamic roots also decreased the bias in modeled ET as compared with the MODIS ET data product (Zhao et al., 2013) in most ecosystems (Table VIII). Table VIII lists the average RMSE and bias of ET for each biome in each season. RMSE and bias are calculated as in equation (9) and (10). Again, all improvements from dynamic roots are marginal. Tropical regions do not have an improved RMSE or bias during any season. Tropical savannah has improved RMSE during fall and improved bias during all seasons. Crops have lower RMSE and bias during fall and winter (not typically active growing periods). Regions with cold seasons have improved fit with observations during spring, summer, and fall. Regions where agreement with observations improved include the central United States, the southern half of South America, and central Africa. Although these regions experienced decreased ET, the high bias of

ET was reduced. However, regions such as northern and central South America, southern Asia, and parts of central Africa show decreased agreement with observations due to a decrease in ET in already low-biased regions.

Table VIII. The RMSE and Bias of model simulations compared with MODIS ET.

DJF	**RMSE**		**Bias**	
	DYNROOT	CONTROL	DYNROOT	CONTROL
Tropical	23.71	23.64	-4.51	-3.89
Tropical savannah	33.73	33.54	10.47	11.72
Desert	23.10	23.39	32.96	35.38
Steppe	28.05	28.17	18.42	19.42
Temperate-dry summer	18.51	18.44	-21.70	-19.33
Temperate-dry winter	27.59	27.44	3.26	5.14
Temperate-no dry season	34.53	35.58	9.92	11.99
Cold-dry summer	17.47	17.24	-109.92	-108.31
Cold-dry winter	13.59	13.46	-86.44	-85.63
Cold-no dry season	12.27	12.17	-129.86	-128.53
Polar	10.98	10.93	-121.43	-120.26
Crop	21.83	21.75	-29.45	-28.45

MAM	**RMSE**		**Bias**	
	DYNROOT	CONTROL	DYNROOT	CONTROL
Tropical	24.42	24.07	-3.72	-3.38
Tropical savannah	37.49	37.11	13.29	14.59
Desert	19.20	19.21	78.88	78.73
Steppe	25.24	25.16	45.34	45.83
Temperate-dry summer	24.38	25.32	21.79	23.33
Temperate-dry winter	30.27	29.86	13.01	15.50
Temperate-no dry season	20.73	21.08	-0.76	0.02
Cold-dry summer	25.25	25.49	-21.52	-20.99
Cold-dry winter	21.68	21.95	-26.43	-26.22
Cold-no dry season	22.71	22.72	-55.07	-54.94
Polar	20.85	20.92	-96.97	-97.34
Crop	32.34	31.76	31.83	31.17

JJA	RMSE		Bias	
	DYNROOT	CONTROL	DYNROOT	CONTROL
Tropical	31.52	31.48	-8.15	-7.83
Tropical savannah	32.13	31.47	0.64	2.20
Desert	24.05	23.85	104.02	103.07
Steppe	32.13	31.77	77.84	76.70
Temperate-dry summer	23.48	23.86	-2.53	-2.63
Temperate-dry winter	27.64	27.30	10.57	10.82
Temperate-no dry season	21.70	22.12	1.06	2.15
Cold-dry summer	28.60	29.04	-7.29	-4.91
Cold-dry winter	29.16	29.19	-8.43	-8.00
Cold-no dry season	25.43	25.73	-17.04	-16.35
Polar	44.86	45.07	-66.33	-66.78
Crop	33.31	33.34	32.29	32.90

SON	RMSE		Bias	
	DYNROOT	CONTROL	DYNROOT	CONTROL
Tropical	25.28	24.89	-5.35	-4.81
Tropical savannah	39.77	40.20	16.86	18.49
Desert	19.00	19.03	80.28	80.06
Steppe	26.91	27.04	59.18	59.09
Temperate-dry summer	17.30	17.40	3.90	4.29
Temperate-dry winter	29.08	29.39	15.68	17.00
Temperate-no dry season	27.16	27.99	11.37	12.69
Cold-dry summer	14.55	14.44	-30.32	-30.33
Cold-dry winter	13.06	13.13	-22.70	-22.22
Cold-no dry season	11.94	11.90	-50.07	-49.67
Polar	16.71	16.73	-98.99	-99.12
Crop	23.39	23.83	15.72	16.66

Changes in GPP ultimately lead to changes in the carbon uptake and storage in vegetated and soil systems. Under DYNROOT, changes in plant productivity translate to lower TEC globally of 2.5%, or 34.4 Gt C, and the pattern generally coincides with the differences in GPP.

DYNROOT has higher TEC in regions such as the western United States, South Africa, India, southern Australia, and the Arctic. Lower TEC is concentrated in South America along the highlands, the Congo Basin in Africa, and South Asia, with up to 30% of the ecosystem carbon being lost. The bulk of the difference is in the vegetation and soil carbon pools with relatively small decreases in the litter pool.

3.4.3 Sensitivity to Water Column Profile

When the dynamic root algorithm is modified to have an increased water stress factor, the model response is quite different. When the water stress is high, root allocation is focused more strongly in soil layers with water, which shifts the bulk of root distribution, in general, to deeper soil layers. DYNROOT-W produced a significant amount of root biomass in deep soil layers, resulting in highly dimorphic (in this case, root biomass increases with depth) root profiles in all ecosystems. DYNROOT-W had a global root profile with significant roots at depth, including a deeper D50 (0.5 m) and D95 (1.6 m). The DYNROOT-50W global root profile also had significant roots at depth, producing dimorphic roots that result in a deep D50 (0.22 m) and D95 (1.6 m). However, increases in root depth did not occur everywhere. In polar and arid regions, roots are still shallower than CONTROL. However, the root profiles in DYNROOT-50W are deeper than DYNROOT (Table VI), demonstrating that imposing water stress in these regions drives deeper root growth. Root profiles for DYNROOT-90W were similar to DYNROOT, suggesting that the water stress imposed was not significant enough to alter the root profiles.

The impacts of perceived water stress on root profiles are seen in GPP. Figure 3.13 and Figure 3.14, Appendix B, show the difference between DYNROOT-W and CONTROL and DYNROOT-50W and CONTROL, respectively. When water stress is high, arid and semiarid regions experience a decrease in GPP, whereas humid and tropical regions experience an increase in GPP. The increase in global GPP for the high-water stress DYNROOT-W (DYNROOT-50W) scenarios results in an increase in GPP of 4.5 Gt C/year (2.1 Gt C/year) and an increase in TEC of 12 Gt C (1.8 Gt C) stored compared with the control simulation. The increases in GPP do not always coincide with increases in nitrogen uptake (Figure 3.13 and Figure 3.14, Appendix B). When water stress is low, as in DYNROOT-90W (Figure 3.15, Appendix B), results are similar to those of DYNROOT, suggesting that the mild water stress imposed is fairly typical in many regions. Globally, GPP decreases 1.4 Gt C/year and TEC decreases 27 Gt C/year.

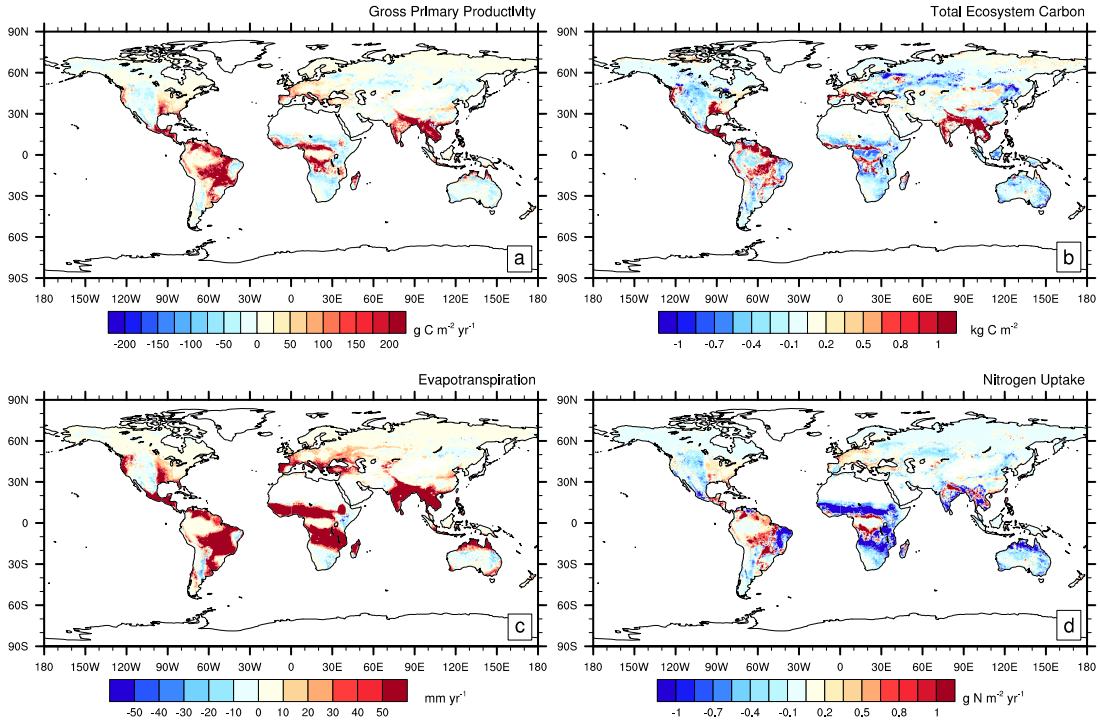

Figure 3.13. Difference between DYNROOT-W and CONTROL of (a) gross primary productivity (g C m^{-2} $year^{-1}$); (b) total ecosystem carbon (kg C/m^2); (c) evapotranspiration (mm/year); and (d) nitrogen uptake (g N m^{-2} $year^{-1}$).

3.5 Discussion

Allowing roots in ELM to shift their rooting depth distribution with resource demands and availability has resulted in root profiles that vary with region and PFT with implications for the carbon cycle. Regionally, GPP increases in arid and polar climate zones and GPP decreases in many of the tropics and subtropics. Globally, the net effect is a loss of productivity and carbon storage.

The model behavior can be explained as follows. Referring back to Figure 3.1, the fraction of roots in each soil layer affects the soil moisture content and the soil moisture stress, which has a direct influence on GPP through modifications to stomatal conductance and Vcmax. The water stress factor (equation (4)) determines the weight of the root distribution emphasized toward water uptake. Higher values of *f* result in more weight in soil layers with nitrogen, whereas lower values of *f* result in more weight toward soil layers with water. Figure 3.16 shows the distribution of *f*-values overlaid with the nitrogen stress factor. Regions that have nitrogen stress and water stress factors close to 1 (small or no stress) experience little change or increased GPP (Figure 3.11). Also, regions that have moderate to strong water stress, but no nitrogen stress also have increases in GPP. This is because the model is distributing roots to increase water availability, which has a strong influence on GPP. However, regions with moderate (but not strong) water stress and low nitrogen availability experience decreases in GPP. In these areas, the model is trying to compensate for both limiting factors: water and nitrogen, and therefore distributes roots accordingly. In ELM, root nitrogen uptake is based on the availability of nitrogen in the soil layer, and not where the root biomass is located in the soil layers. Therefore, nitrogen uptake is highest in soil layers where nitrogen is in the largest quantity, which may not correlate with root biomass. As such, the transfer of root biomass away from water toward nitrogen could result in a loss of water uptake without a benefit of nitrogen uptake. This translates to a stronger modeled response to water stress on GPP than nitrogen stress.

Much of the model behavior (i.e., large-scale reductions in GPP) is the result of missing processes or limitations in ELM. First, the capping of root depths could limit water available by restricting uptake to shallow soil layers. This effect would deny the plant available water in deep

soil layers (if the plant could establish roots at depth) and is important at dry sites (Nepstad et al., 1994; Knight, 1999). The lack of hydraulic redistribution, which is widely observed in semiarid ecosystems (Bleby et al., 2010), will reduce the amount of water available for plant use. Second, root water uptake is based on fixed parameters and not dependent on root functionality (Warren et al., 2015). Although roots are allowed to shift distribution, water uptake is still dependent on plant demand and soil matric potential. Roots are not allowed to modify function by shifting water uptake from shallow dry soil layers to deep wet soil layers during drought as observations indicate (Warren et al., 2005; Lai and Katul, 2000). This functional specialization has also been seen in variable nutrient uptake with depth (da Silva et al., 2011). Third, the way nitrogen uptake is modeled in ELM limits the dynamic root capability. Allowing nitrogen uptake based on root weight rather than total nitrogen availability could increase nitrogen uptake. Additionally, allowing roots to obtain nitrogen from biological nitrogen fixers or mycorrhizal associations is also not included further limiting nitrogen availability. Finally, this model does not include phosphorus (which is now included ELM), which will be important in phosphorus-limited regions such as the tropics. This could be addressed in future modifications to the dynamic root model.

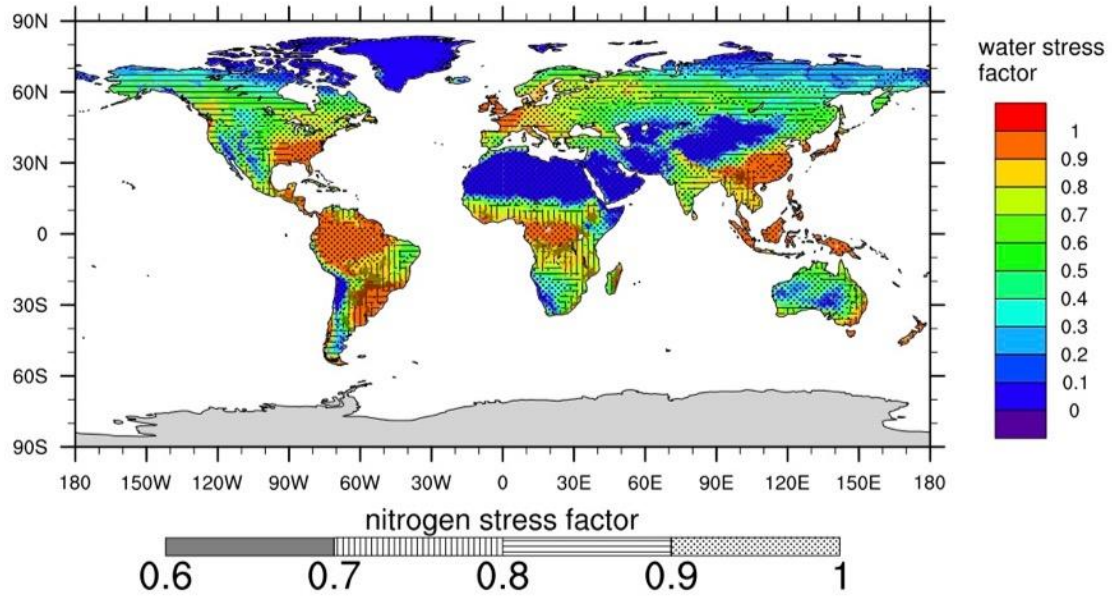

Figure 3.16. Overlay of water stress factor (in color) and the nitrogen stress factor (textured) from the DYNROOT simulation.

The model response has implications for climate change and how ecosystem roots should be represented in models. Not allowing roots to respond to environmental stresses could result in an overestimate or underestimate of modeled plant productivity. Plants have several means of adjusting to water stress. For example, seasonal water variability can lead to seasonal shifts in root production (Peek et al., 2006). In semiarid regions, isotope studies have found that root plasticity in rooting depth distribution allows water extraction from shallow soil depths during the rainy season and deep soil depths during the dry season (Wang et al., 2017; Yang et al., 2015; Dawson and Pate, 1996). Furthermore, hydrology often determines effective rooting depth. Roots in saturated soils are often limited by anoxic conditions, while roots in well-drained soils may not be able to overcome the dry gap between precipitation-wetted surface soils and the capillary fringe above the water table (Fan et al., 2017).

The new dynamic root model shows a strong hydrological response to reductions in precipitation with a deepening of root systems to counter water stress. An example can be seen in the relationship between effective rooting depth (here defined as D95) and precipitation over the 33-year period of DYNROOT. Figure 3.17 shows the Pearson's correlation coefficient (PCC) between precipitation and D95. In most regions, there is a negative correlation, which indicates that as rainfall increases, effective rooting depth decreases. During years with higher rainfall, soil water and nitrogen would be concentrated near the surface, resulting in more roots in shallow layers.

Tropical and some boreal regions (including wetlands/bogs and tundra) exhibit no or very low correlation between rainfall and D95. The lack of water stress in the wet tropics, wetlands, and humid ecosystems leads to shallower rooting profiles that depend more on nitrogen and respond less to precipitation events. In boreal and tundra systems permafrost limits the depth that roots can penetrate and restricts water movement, thus limiting roots to shallow soil layers. This could result in a stronger stress response to short-term drought events for these ecosystems. This is demonstrated by a drying of shallow soil layers in Figure 3.18, Appendix B. However, the deepening root structure in arid ecosystems suggests that over long-term droughts, the model can respond to available water in deeper soils.

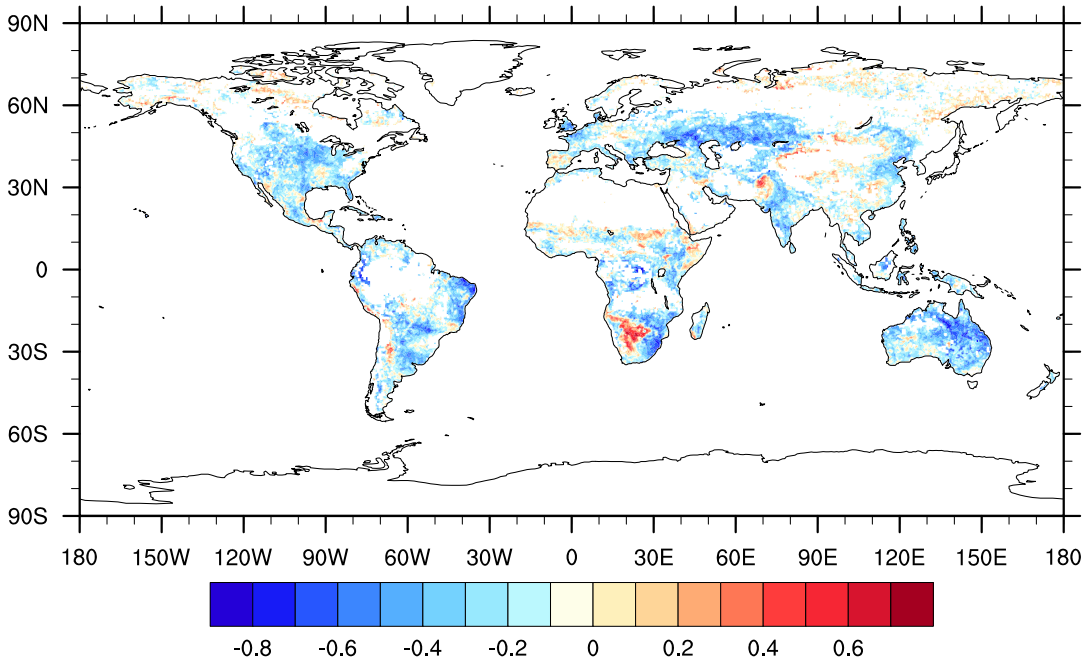

Figure 3.17. Pearson's correlation coefficient between D95 and rain for the last 33 years of the DYNROOT simulation.

Positive correlations occur in some desert regions, but mostly at high latitudes or high-elevation areas. These regions correspond to areas that receive low amounts of precipitation, so roots would be more dependent on water stored in deeper soil layers. The deepening of root structure during drought is consistent with observations (Grossiord et al., 2017). With dryland area already expanding from climate change (Huang et al., 2017), not allowing roots to respond to water stress will result in missed opportunities to capture climate feedback from changes to vertical root structure.

Finally, most seasonally dry tropic regions have a negative correlation with rainfall, simulating shallower rooting depths that rely too heavily on precipitation events. This behavior is

not consistent with observations that suggest deeper root profiles are commonly used to tap into groundwater and continue transpiration throughout the dry season (O'Grady et al., 1999 Juárez et al., 2007; Karam and Bras, 2008). This could be a result of a poor root response for stress-deciduous plants in those regions, which results in a shallow root profile that dries the top of the soil column quickly following the rainy season. Since stress phenology PFTs in ELM rely on soil moisture in the top 10 cm to trigger leaf onset and leaf-off, lack of soil water would force the PFT into dormancy. Indeed, the number of active growing days (not shown) for stress phenology PFTs in DYNROOT is less than in the control simulation, resulting in lower GPP and transpiration. This behavior is a problem in other models as well, the cause from equal weighting of soil moisture content in all soil layers (De Kauwe et al., 2015), and results in an abrupt transition to drought. De Kauwe et al. (2015) found that varying the contribution of soil water potential such that the weight shifts from the upper layers when wet to lower layers as the soil dried greatly improved the model response to drought. Another solution to address the lack of growth during the dry-season tropics is to redefine the rooting depth in these regions to allow deeper roots, perhaps through a minimum water stress parameter to encourage deeper root profiles. In addition, hydraulic lift allows deep rooted plants to bring water from deep soil layers to supply the water needs of shallow-rooted grasses and shrubs, which could improve the performance in tropical savannahs (Ludwig et al., 2003; Oliveira et al., 2005; Kurz-Besson et al., 2006). Finally, rethinking the moisture stress trigger for stress deciduous plants would improve the response of dry-season tropics, particularly by allowing the stress trigger to be dependent on total root-available water and not just the surface soil moisture.

Although observed increases or decreases in modeled ET correspond with increases or decreases in GPP, there are some ecosystems in ELM where ET is biased high but GPP is biased low, particularly dry seasonal ecosystems. Therefore, the decrease in ELM estimated GPP and ET result in an improvement in ET, but a degraded GPP agreement. Some reasons these regions are difficult to model is ELM has a high ET bias in semiarid regions, caused by too strong soil evaporation, particularly for grass PFTs (Swenson and Lawrence, 2014), the lack of root hydraulic redistribution (Tang et al., 2015), and poor hydraulic parameterizations (Tang et al., 2015). This suggests that the improvements in ET are for the wrong reasons and additional processes should be considered. Particularly, Swenson and Lawrence (2014) added a dry surface layer as a resistance to water movement out of the soil. Schultz et al. (2016) found that soil moisture was depleted in dry tropics and hypothesized that the root system and parameterizations should be modified in addition to revisions to the stomatal conductance model. However, Bouda and Saiers (2017) suggested that the root distribution might be fine, but the formulation for root water uptake should not allow increasing amounts of soil water to be removed from the deepest soil depths during drought. Finally, Tang et al. (2015) suggest that there are additional approaches to refine water uptake through hydraulic redistribution but should include better below ground representations of deep roots, soil texture, hydraulic parameters, and water table dynamics.

When I force the model to acknowledge some water stress, rooting depth responds with deeper root profiles. In humid regions and the tropics, water availability may increase, particularly if the shallow surface soils, which tend to store more nitrogen than deep soils, dry out occasionally or do not hold sufficient water to meet plant demands. Indeed, these regions

experience some increases in GPP and ET in the DYNROOT-W and DYNROOT-50W simulations. This is also obvious in the soil volumetric water content (Figure 3.18, Appendix B), which shows the DYNROOT-50W having more water in the top 0.5 m of soil but less in deeper soils than DYNROOT. However, the largest increases in GPP occur in seasonally dry regions. The deep dimorphic root structure allows these PFTs to decouple from precipitation by tapping into deep soil water, thereby allowing the plants to increase productivity. In contrast, arid and desert regions experience a drop in GPP and ET. This response is driven by interactions between soil water availability and the stress deciduous plant phenology in the model, which dominate these regions. Forcing water stress causes PFTs to deepen root systems that tend to deplete water through a deeper layer of the soil column, triggering moisture stress and leaf-off. This is also seen in the differences in soil volumetric water content (Figure 3.18, Appendix B). Both DYNROOT and DYNROOT-50W have fairly constant soil water in the shallow soil layers, but below the top 10–20 cm the soil, volumetric water decreases sharply in the DYNROOT-50W compared to the other simulations.

The relationship between effective rooting depth and productivity can be further examined with the PCC between the annual average of GPP and D95 across four simulations: CONTROL, DYNROOT, DYNROOT-50W, and DYNROOT-90W. These simulations were chosen because their root distributions were the most realistic when compared with observations. Figure 3.19 shows the PCC map. Most humid and seasonally dry regions have a strong positive relationship between D95 and GPP, meaning GPP increases as root depth increases. In addition, dry, arid, and boreal regions (including northern Canada, Siberia, the western United States, southern Australia, and parts of western and southern Africa) tend to have a strong negative

relationship between D95 and GPP. There are only a few regions where there is a weak relationship between D95 and GPP, for example, in the Amazon tropics and along transition zones.

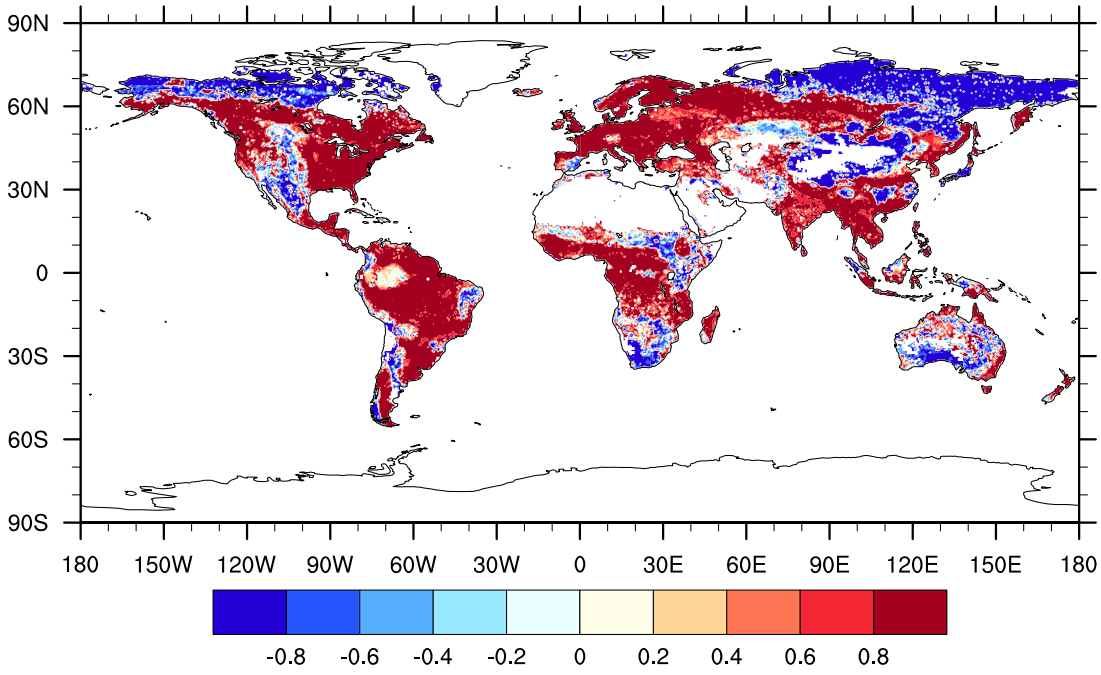

Figure 3.19. Pearson's correlation coefficient between gross primary productivity and D95 with CONTROL, DYNROOT, DYNROOT-50W, and DYNROOT-90W.

Since water availability increases with soil depth, forcing water stress results in a deepening, dimorphic root profile. In the tropics and dry-seasonal tropics, deepening roots allow increased access to water, which results in an increase in transpiration and GPP. It also allows PFTs in the dry tropics to continue growth longer during the dry season by delaying the drying of the shallow soil layer. In deserts, the deepening roots dry out the soil column. This drying effect

results in a decrease in water use efficiency (WUE; not shown) and causes a decline in transpiration and GPP. However, the dimorphic root profile is not realistic in many regions and does not match with the majority of observations. Furthermore, it can lead to decreases in soil water in deep soil layers, which can have consequences over time (e.g., plant die-off), particularly if the water table is not replenished as quickly as it is depleted.

There are several model developments that can be performed to improve the dynamic rooting model. One consideration for future model improvement is to allow maximum rooting depth to vary not just as function of PFT, but perhaps as a function of climate zone. Climate-dependent rooting depth could address limitations in the root model presented here, such as the lack of deep roots in the arid or dry-season tropical regions. Deep roots are important drivers of plant hydraulic lift and redistribution, nutrient uptake, and soil weathering, and they can contribute to soil carbon sequestration (Maeght et al., 2013). In many of the dry-season tropics, ELM simulates shallow roots where observations indicate deeper roots are present (J96; Schenk and Jackson, 2002a; Yang et al., 2016; Fan et al., 2017). A deeper root profile should be used in these regions, which could act to increase the opportunity for root foraging in deep soil layers and enhance productivity and ET by continuing growth during the dry season. This would allow roots to access the water table, which is quite deep in these regions, and improve water uptake ability. In addition, in many arid regions, such as the southwestern United States, hydrology regulates root depth and restricts growth to shallow layers (Fan et al., 2017). Creating a variable rooting depth that is dependent on climate and soil thickness may be one way to capture the variability in rooting depth better in the dynamic root algorithm.

One model improvement to support variable root depth is removing soil depth constraints. Although the majority of root biomass is in the top 1 m of soil (Schenk and Jackson, 2002a), in arid and semiarid climates, periodic drought can result in rooting depths much deeper than the 3.8 m soil column in models, in some cases to depths of tens of meters. In other regions, such as in high-latitude systems, shallow soil thickness limits rooting depth. The variable soil depth to bedrock data set developed by Brunke et al. (2016) prescribes estimates of global soil thickness. Combining the Brunke et al. (2016) data set with dynamic roots and variable root depth could improve the dynamic rooting model. For example, shallow soil thickness would put a cap on the rooting depth, while deep soil thickness would prevent some roots from foraging too deeply in a dry soil gap. However, care should be taken to avoid root foraging in the water table, which would limit necessary oxygen requirements for root respiration and could potentially cause an unrealistic buildup of soil carbon in deep soil layers as roots die.

There are other considerations for future model development that can improve the representation of roots in ESMs. Some of these include allowing different root forms for different functions (i.e., water versus nitrogen uptake). In addition, including a representation for root surface area and increased root length under drought (Padilla et al., 2015; Padilla et al., 2009) would have a significant influence on nutrient and water uptake with the same quantity of biomass. Root function could allow roots to distinguish water sources such that vegetation could focus water extraction from specific depths, allowing some plants to pull water from deep soil depths and not from surface layers, thus removing competition with shallower rooted vegetation. This could also include variable weights given to soil layers to shift water uptake from shallow to deep roots depending on water availability similarly to De Kauwe et al. (2015). In addition,

adding root hydraulics that would transport water from wet soil layers to dry soil layers to compensate for dry zones (Zhu et al., 2017) can increase plant available water during dry seasons and can be a major source of transpiration (Lee et al., 2018; Neumann and Cardon, 2012). Hydraulic lift has been found in all types of biomes (Prieto et al., 2012) and can also work in reverse, moving water from shallow soil layers to deep soil layers, which can protect that water from evaporation and can also give some plants a competitive advantage (Lee et al., 2018). Finally, allowing interactions from biological nitrogen fixers or mycorrhizal associations, and their influence on carbon allocation within the plant, might allow for greater uptake of nutrients at a lower expense of root investment for plants. This has been proposed in the Fixation and Uptake of Nitrogen (FUN) model (Fisher et al., 2010).

3.6 Conclusions

The new dynamic root model allows the dynamic allocation of fine roots to soil layers to reflect water and nitrogen needs while maintaining sufficient root distributions as compared with observations reported by Jackson et al. (1996) and Schenk and Jackson (2002a). The resulting changes in productivity favor increases in regions that are water limited, but not in regions with sufficient water during the active growing seasons. The model captures the shallow rooting depth of arid and polar ecosystems and improves the GPP agreement with observations but fails to produce the dimorphic root structure that allows plants in the dry season tropics to grow during the dry season. However, when a minimum water stress is included in the root module, the effective rooting depth increases, causing increases in transpiration and GPP for the dry season

tropics, but this dries out the soil column in desert regions. This result indicates that changes in precipitation regime can lead to shifts in rooting profiles.

The form and function of root systems is an important driver of aboveground productivity. Capturing the response of roots to heterogeneity of water and nutrients in the soil profile is critical to predict the carbon sink capacity of the terrestrial surface. I provide a new method for representing the changing distribution of roots in the ELM that includes interactions with both water and nitrogen, two of the most limiting resources in ecosystems. The approach allows root plasticity (i.e., shifts in biomass distribution) to changes in environment (i.e., water and nitrogen availability), and in most systems, results in small reductions in productivity, water, and nutrient uptake, while maintaining the observed distribution of roots over many different biomes. These modest changes in productivity help to reduce model bias of GPP in some ecosystems but fail in seasonally dry regions. The resulting behavior of the model sheds light on model processes regarding water and nitrogen uptake, providing incite on shortcomings of model representation and possible new avenues of research to improve vegetation response to resource limitations.

3.7 References

Amos, B., and Walters, D. T. (2006), Maize root biomass and net rhizodeposited carbon. *Soil Sci. Soc. Am. J.*, 70, 1489–1503.

Araki, H., and Iijima, M. (2001), Deep rooting in winter wheat: rooting nodes of deep roots in two cultivars with deep and shallow root system. *Plant Prod. Sci.*, 4, 215–219.

Arora, V. K., and Boer, G. J. (2003), A representation of variable root distribution in dynamic vegetation models. *Earth Interactions*, 7(6), 1–19.

Balesdent, J., and Balabane, M. (1996), Major contribution of roots to soil carbon storage inferred from maize cultivated soils. *Soil Biol. Biochem.*, 28(9), 1261–1263.

Bao, Y., Aggarwal, P., Robbins II, N. E., Sturrock, C. J., Thompson, M. C., Tan, H. Q., Tham, C., Duan, L., Rodriguez, P. L., Vernoux, T., Mooney, S. J., Bennett, M. J., and Dinney, J. R. (2014), Plant roots use a patterning mechanism to position lateral root branches toward available water. *Proceedings of the National Academy of Sciences*, doi/10.1073/pnas.1400966111.

Batjes, N. H. (1996), Total carbon and nitrogen in the soils of the world. *European Journal of Soil Science*, 47, 151–163.

Bleby, T. M., McElrone, A. J., and Jackson, R. B. (2010), Water uptake and hydraulic redistribution across large woody root systems to 20 m depth. *Plant, Cell & Environment*, 33, 2132-2148.

Bouda, M., and Saiers, J. E. (2017), Dynamic effects of root system architecture improve root water uptake in 1-D process-based soil-root hydrodynamics. *Advances in Water Resources*, 110, 319-334.

Brunke, M. A., Broxton, P., Pelletier, J., Gochis, D., Hazenberg, P., Lawrence, D. M., Leung, L. R., Niu, G.-Y., Troch, P. A., and Zeng, X. (2016), Implementing and evaluating variable soil thickness in the Community Land Model, Version 4.5 (CLM4.5). *Journal of Climate*, 29, 3441–3461. doi:10.1175/JCLI-D-15-0307.1.

Clemmensen, K. E., Bahr, A., Ovaskainen, O., Dahlberg, A., Ekblad, A., Wallander, H., Stenlid, J., Finlay, R. D., Wardle, D. A., and Lindahl, B. D. (2013), Roots and associated fungi drive long-term carbon sequestration in boreal forest. *Science*, 339(6127), 1615–1618. doi:10.1126/science.1231923

Couvreur, V., Vanderborght, J., and Javaux, M. (2012), A simple three-dimensional macroscopic root water uptake model based on the hydraulic architecture approach. *Hydrol. Earth Syst. Sci.*, 16, 2957-2971.

Couvreur, V., Vanderborght, J., Beff, L., and Javaux, M. (2014), Horizontal soil water potential heterogeneity: simplifying approaches for crop water dynamics models. *Hydrol. Earth Syst. Sci.*, 18, 1723-1743.

Dawson, T. E., and Pate, J. S. (1996), Seasonal water uptake and movement in root systems of Australian phraeatophytic plants of dimorphic root morphology: a stable isotope investigation. *Oecologia*, 107, 13–20.

da Silva, E. V., Bouillet, J.-P., de Moraes Gonçalves, J. L., Abreu Junior, C. H., Trivelin, P. C. O., Hinsinger, P., Joudan, C., Nouvellon, Y., Stape, J. L., and Laclau, J.-P. (2011), Functional specialization of Eucalyptus fine roots: contrasting potential uptake rates for nitrogen, potassium and calcium tracers at varying soil depths. *Functional Ecology*, 25, 996-1006.

De Kauwe, M. G., Zhou, S.-X., Medlyn, B. R., Pitman, A. J., Wang, Y.-P. Duursma, R. A., and Prentice, I. C. (2015), Do land surface models need to include differential plant species responses to drought? Examining model predictions across a mesic-xeric gradient in Europe. *Biogeosciences*, 12, 7503-7518.

de Kroon, H., and Mommer, L. (2006), Root foraging theory put to the test. *TRENDS in Ecology and Evolution*, 21(3), 113-116.

Drewniak, B., Song, J., Prell, J., Kotamarthi, V. R., and Jacob, R. (2013), Modeling agriculture in the Community Land Model. *Geosci. Model Dev.*, 6, 495–515. doi:10.5194/gmd-6-495-2013.

El Masri, B., Shu, S., and Jain, A. K. (2015), Implementation of a dynamic rooting depth and phenology into a land surface model: Evaluation of carbon, water, and energy fluxes in the high latitude ecosystems. *Agriculture and Forest Meteorology*, 211–212, 85–99.

Fan, Y., Minguez-Macho, G., Jobbágy, E. G., Jackson, R. B., and Otero-Casal, C. (2017), Hydrologic regulation of plant rooting depth. Proceedings of the National Academy of Sciences, 144(40), 10572–10577.

Finzi, A., C., Norby, R. J, Calfapietra, C., Gallet-Budynek, A., Gielen, B., Holmes, W. E., Hoosbeek, M. R., Iversen, C. M., Jackson, R. B, Kubiske, M. E., Ledford, J., Liberloo, M., Oren, R., Polle, A., Pritchard, S., Zak, D. R., Schlesinger, W. H., and Ceulemans, R. (2007), Increases in nitrogen uptake rather than nitrogen-use efficiency support higher rates of temperate forest productivity under elevated CO2. *Proceedings of the National Academy of Sciences*, 104, 14014-14019.

Fisher, J. B., Sitch, S., Malhi, Y., Fisher, R. A., Huntingford, C., and Tan, S.-Y. (2010), Carbon cost of plant nitrogen acquisition: A mechanistic, globally applicable model of plant nitrogen uptake, retranslocation, and fixation. *Global Biogeochemical Cycles*, 24(GB1014). doi:10.1029/GB003621.

Gale, M. R., and Grigal, D. F. (1987), Vertical root distribution of northern tree species in relation to successional status. *Canadian Journal of Forest Research*, 17, 829-834.

Grossiord, C., Sevanto, S., Dawson, T. E., Adams, H. D., Collins, A. D., Dickman, L. T., Newman, B. D., Stockton, E. A., and McDowell, N. G. (2017), Warming combined with more extreme precipitation regimes modifies the water sources used by trees. *New Phytologist*, 213, 584–596.

Grossman, J. D., and Rice, K. J. (2012), Evolution of root plasticity responses to variation in soil nutrient distribution and concentration. *Evolutional Applications*, 5, 850-857.

Hermans, C., Hammond, J. P., White, P. J., and Verbruggen, N. (2006), How do plants respond to nutrient shortage by biomass allocation? *TRENDS in Plant Science*, 11(12),610-617.

Hodge, A. (2004), The plastic plant: root responses to heterogeneous supplies of nutrients. *New Phytologist*, 162(1), 9–24. doi:10.1111/j.1469-8137.2004.01015.x.

Huang, J., Li, Y., Fu, C., Chen, F., Fu, Q., Dai, A., Shinoda, M., Ma, Z., Guo, W., Li, Z., Zhang, L., Liu, Y., Yu, H., He, Y., Xie, Y., Guan, X., Ji, M., Lin, L., Wang, S., Yan, H., and Wang, G. (2017), Dryland climate change: Recent progress and challenges. *Reviews of Geophysics*, 55(3), 719–778. doi:10.1002/2016RG000550.

Iversen, C. (2010), Digging deeper: fine-root responses to rising atmospheric CO2 concentration in forested ecosystems. *New Phytologist*, 186(2), 346–357. doi:10.1111/j.1469-8137.2009.03122.x.

Iversen, C., M., Hooker, T. D., Classen, A. T., and Norby, R. J. (2011), Net mineralization of N at deeper soil depths as a potential mechanism for sustained forest production under elevated CO2. *Global Change Biology*, 17, 1130-1139.

Jackson, R. B., Canadell, J., Ehleringer, J. R., Mooney, H. A., Sala, O. E., and Schulze, E. D. (1996), A global analysis of root distributions for terrestrial biomes. *Oecologia*, 108, 389–411.

Jackson, R. B., Mooney, H. A., and Schulze, E.-D. (1997), A global budget for fine root biomass, surface area, and nutrient contents. *Proc. Natl. Acad. Sci. USA*, 94, 7362-7366.

Jobbágy, E. G., and Jackson, R. B. (2001), The distribution of soil nutrients with depth: Global patterns and the imprint of plants. *Biogeochemistry*, 53, 51–77.

Juárez, R. I. N., Hodnett, M. G., Fu, R., Goulden, M. L., and von Randow, C. (2007), Control of dry season evapotranspiration over the Amazonian forest as inferred from observations at a southern Amazon forest site. *Journal of Climate*, 20, 2827–2839. doi:10.1175/JCLI4184.1.

Karam, H. N., and Bras, R. L. (2008), Climatological basin-scale Amazonian evapotranspiration estimated through a water budget analysis, *Journal of Hydrometeorology*, 9, 1048–1059. doi:10.1175/2008JHM888.1.

Knight, J. H. (1999), Root distributions and water uptake patterns in Eucalyptus and other species. In: Landsberg, J (ed) The ways trees use water. Water and salinity issues in agroforestry no. 5 (pp. 55-85). Barton, ACT: RIRDC publication 99/37.

Koven, C. D., Riley, W. J., Subin, Z. M., Tang, J. Y., Torn, M. S., Collins, W. D., Bonan, G. B., Lawrence, D. M., and Swenson, S. C. (2013), The effect of vertically resolved soil biogeochemistry and alternate soil C and N models on C dynamics of CLM4. *Biogeosciences*, 10, 7109–7131. doi:10.5194/bg-10-7109-2013.

Kurz-Besson, C., Otieno, D., Lobo do Vale, R., Siegwolf, R., Schmidt, M., Herd, A., Nogueira, Ca., David, T. S., David, J. S., Tenhunen, J., Pereira, J. S., and Chaves, M. (2006), Hydraulic lift in cork oak trees in a savannah-type Mediterranean ecosystem and its contribution to the local water balance. *Plant and Soil*, 282, 361–378.

Lai, C.-T., and Katul, G. (2000), The dynamic role of root-water uptake in coupling potential to actual transpiration. *Advances in Water Resources*, 23, 427-439.

Lee, E., Kumar, P., Barron-Gafford, G. A., Hendryx, S. M., Sanchez-Cañete, E. P., Minor, R. L., Colella, T., and Scott, R. L. (2018), Impact of hydraulic redistribution on multispecies vegetation water use in a semiarid savanna ecosystem: An experimental and modeling synthesis. *Water Resources Research*, 54. doi:10.1029/2017WR021006.

Lee, M., Nakane, K., Nakatsubo, T., and Koizumi, H. (2005), The importance of root respiration in annual soil carbon fluxes in a cool-temperate deciduous forest. *Agricultural and Forest Meteorology,* 134, 95–101. doi:10.1016/j.agrformet.2005.08.011.

Ludwig, F., Dawson, T. E., Kroon, H., Berendse, F., and Prins, H. H. T. (2003), Hydraulic lift in Acacia tortilis trees on an East African savanna. *Oecologia*, 134, 293–300.

Maeght, J.-L., Rewald, B., Pierret, A. (2013), How to study deep roots – and why it matters. *Frontiers in Plant Science*, 4(299), 1–14. doi:10.3389/fpls.2013.00299.

Matamala, R., and Stover, D. B. (2013), Introduction: modeling the hidden half – the root of our problem. *New Phytologist*, 200, 939–942.

Mayaki, W. C., Reare, I. D., and Stone L. R. (1976), Top and root growth of irrigated and non-irrigated soybean. *Crop Sci.*, 16, 92–94.

McMurtrie, R. E., Iversen, C. M., Dewar, R. C., Medlyn, B. E., Näsholm, T., Pepper, D. A., and Norby, R. J. (2012), Plant root distributions and nitrogen uptake predicted by a hypothesis of optimal root foraging. *Ecology and Evolution*, 2(6), 1235–1250. doi:10.1002/ece3.266.

Nepstad, D. C., de Carvalho, C. R., Davidson, E. A., Jipp, P. H., Lefebvre, P. A., Negreiros, G. H., da Silva, E. D., Stone, T. A., Trumbore, S. E., and Vieira, S. (1994), The role of deep roots in the hydrological and carbon cycles of Amazonian forests and pastures. *Nature*, 372, 666–669.

Neumann, R. B., and Cardon, Z. G. (2012), The magnitude of hydraulic redistribution by plant roots: a review and synthesis of empirical and modeling studies. *New Phytologist*, 194, 337–352.

O'Grady, A. P., Eamus, D., and Hutley, L. B. (1999), Transpiration increases during the dry season: patterns of tree water use in eucalypt open-forests of northern Australia. *Tree Physiology*, 19, 591–597.

Oleson, K. W., Lawrence, D. M., Bonan, G. B., Drewniak, B., Huang, M., Koven, C. D., Levis, S., Li, F., Riley, W. J., Subin, Z. M., Swenson, S. C., Thornton, P. E., Bozbiyik, A., Fisher, R., Heald, C. L., Kluzek, E., Lamarque, J.-F., Lawrence, P. J., Leung, L. R., Lipscomb, W., Muszala, S., Ricciuto, D. M., Sacks, W., Sun, Y., Tang J., and Yang Z.-L. (2013), Technical Description of version 4.5 of the Community Land Model (CLM). Boulder, Colorado.: NCAR.

Oliveira, R. S., Dawson, T. E., Burgess, S. S. O., and Nepstad, D. C. (2005), Hydraulic redistribution in three Amazonian trees. *Oecologia*, doi:10.1007/s00442-005-0108-2.

Padilla, F. M., Miranda, J. D., Jorquera, M. J., and Pugnaire, F. I. (2009), Variability in amount and frequency of water supply affects roots but not growth of arid shrubs. *Plant Ecology*, 204, 261–270.

Padilla, F. M., Miranda, J. d. D., Armas, C., and Pugnaire, F. I. (2015), Effects of changes in rainfall amount and pattern on root dynamics in an arid shrubland. *Journal of Arid Environments*, 114, 49–53.

Peek, M. S., Leffler, A. J., Hipps, L., Ivans, S., Ryel, R. J., and Caldwell, M. M. (2006), Root turnover and relocation in the soil profile in response to seasonal soil water variation in a natural stand of Utah juniper (Juniperus osteosperma). *Tree Physiology*, 26, 1496–1476.

Prieto, I., Armas, C., and Pugnaire, F. I. (2012), Water release through plant roots: new insights into its consequences at the plant and ecosystem level. *New Phytologist*, 193, 830–841.

Qian, T., Dai, A., Trenberth, K. E., and Oleson, K.W. (2006), Simulation of global land surface conditions from 1948 to 2004: Part I: Forcing data and evaluations. *J. Hydrometeor.*, 7, 953–975.

Raich, J. W., and Schlesinger, W. H. (1992), The global carbon dioxide flux in soil respiration and its relationship to vegetation and climate. *Tellus*, 44B, 81–99.

Reubins, B., Poeson, J., Danjon, F., Geudens, G., and Muys, B. (2007), The role of fine and coarse roots in shallow slope stability and soil erosion control with a focus ion root system architecture: a review. *Trees*, 21, 385-402.

Schenk, H. J., and Jackson, R. B. (2002a), The global biogeography of roots. *Ecological Monographs*, 72(3), 311–328.

Schenk, H. J., and Jackson, R. B. (2002b), Rooting depths, lateral root spreads and below-ground/above-ground allometries of plants in water-limited ecosystems. *Journal of Ecology*, 90, 480–494.

Schultz, N., M., Lee, X., Lawrence, P. J., Lawrence, D. M., and Zhao, L. (2016), Assessing the use of subgrid land model output to study impacts of land cover change. *Journal of Geophysical Research: Atmospheres*, 121, 6133-6147.

Sivandran, G., and Bras, R. L. (2013), Dynamic root distributions in ecohydrological modeling: A case study at Walnut Gulch Experimental Watershed. *Water Resources Research*, 49, 3292–3305. doi:10.1002/wrcr.20245.

Song, Y., Jain, A. K., and McIsaac, G. F. (2013), Implementation of dynamic crop growth processes into a land surface model: evaluation of energy, water and carbon fluxes under corn and soybean rotation. *Biogeosci. Discuss*., 10, 9897–9945.

Swenson, S. C., and Lawrence, D. M. (2014), Assessing a dry surface layer-based soil resistance parameterization for the Community Land Model using GRACE and FLUXNET-MTE data. *Journal of Geophysical Research: Atmospheres*, 119, 10,299-10,312.

Tang, J., Riley, W., and Niu, J. (2015), Incorporating root hydraulic redistribution in CLM4.5: Effects on predicted site and global evapotranspiration, soil moisture and water storage. *Journal of Advances in Modeling Earth Systems*, 7, 1828-1848.

Tobin, B., Čermák, J., Chiatante, D., Danjon, F., Di lorio, A., Dupuy, L., Eshel, A., Jourdan, C., Kalliokoski, T., Laiho, R., Nadezhdina, N., Nicoll, B., Pagès, L., Silva, J., and Spanos, I. (2007), Towards developmental modelling of tree root systems. *Plant Biosystems*, 141(3),481-501.

Wang, J., Fu, B., Lu, N., and Zhang, L. (2017), Seasonal variation in water uptake patterns of three plant species based on stable isotopes in the semi-arid Loess Plateau. *Science of the Total Environment*, 609, 27–37.

Warren, J. M., Hanson, P. J., Iversen, C. M., Kumar, J., Walker, A. P., and Wullschleger, S. D. (2015), Root structural and functional dynamics in terrestrial biosphere models – evaluation and recommendations. *New Phytologist*, 205(1), 59–78. doi:10.1111/nph.13034.

Warren, J. M., Meinzer, F. C., Brooks, J. R., and Domec, J. C. (2005), Vertical stratification of soil water storage and release dynamics in Pacific Northwest coniferous forests. *Agricultural and Forest Meteorology*, 130 (1-2), 39-58.

Wilcox, C. S., Ferguson, J. W., Fernandez, G. C. J., and Nowak, R. S. (2004), Fine root growth dynamics of four Mojave Desert shrubs as related to soil moisture and microsite. *Journal of Arid Environments,* 56, 129-148.

Yang, B., Wen, X., and Sun, X. (2015), Seasonal variations in depth of water uptake for a subtropical coniferous plantation subjected to drought in an East Asian monsoon region. *Agricultural and Forest Meteorology*, 201, 218–228.

Yang, Y., Donohue, R. J., and McVicar, T. R. (2016), Global estimation of effective plant rooting depth: Implications for hydrological modeling. *Water Resources Research*, 52, 8260–8276. doi:10.1002/2016WR19392.

Yuan, Z. Y., and Chen, H. Y. H. (2012), A global analysis of fine root production as affected by soil nitrogen and phosphorus. *Proceedings of the Royal Society B*, 279, 3796-3802.

Zencich, S. J., Froend, R. H., Turner, J. V., and Gailitis, V. (2002), Influence of groundwater depth on the seasonal sources of water accessed by Banksia tree species on a shallow sandy coastal aquifer. *Oecologia*, 131: 8-19.

Zeng, X. (2001), Global vegetation root distribution for land modeling. *Journal of Hydrometeorology*, 2, 525–530.

Zhao, Q. M. and Running, S. W. (2010), Drought induced reduction in global terrestrial net primary production from 2000 through 2009. *Science*, 329-943.

Zhao, Q. M. Kimball, J. S., McDowell, N. G., and Running, S. W. (2013), A remotely sensed global terrestrial drought severity index Mu. *Bulletin of the American Meteorological Society*. 94(1), 83-98.

Zhu, S., Chen, H., Zhang, X., Wei, N., Shangguan, W., Yuan, H., Zhang, S., Wang, L., Zhou, L., and Dai, Y. (2017), Incorporating root hydraulic redistribution and compensatory water uptake in the Common Land Model: Effects on site level and global land modeling. *Journal of Geophysical Research: Atmospheres*, 122, 7308–7322. doi:10.1002/2016JD025744.

Zhu, Y., Wang, G., and Li, R. (2016), Seasonal dynamics of water use strategy of two salix shrubs in alpine sandy land, Tibetan Plateau. *PLOS One*, DOI:10.1371/journal.pone.0156586.

4 AN OPTIMIZATION APPROACH FOR DYNAMIC CARBON ALLOCATION IN THE E3SM LAND MODEL

4.1 Introduction

Terrestrial photosynthesis (gross primary productivity; GPP) is responsible for taking up 150-175 gigatons of CO_2 from the atmosphere every year (Welp et al., 2011) with rates of GPP varying widely among ecosystem types (Beer et al., 2010). As rates of GPP may have increased about 31% over the last century (Campbell et al., 2017), there is large potential for feedbacks from plant physiological response to influence future climate (Cao et al., 2009). Furthermore, the response of plants to environmental change can have implications on the carbon cycle, if the reported increases in GPP result in increases in net primary productivity (NPP; Nemani et al., 2003) and biomass or soil carbon (C) storage (Ise et al., 2010; Matamala et al., 2003; Schmidt et al., 2011). Therefore, in order to understand the impact of future changes in GPP on climate, it is imperative to predict the partitioning of GPP into not only NPP and respiration (Delucia et al., 2007; Hopkins et al., 2013) but also into plant biomass components (McNickle et al., 2016; Song et al., 2016). Currently, most Earth system models (ESMs) used to predict biosphere-atmosphere feedbacks do not allow for dynamic allocation of GPP into biomass for different plant tissues.

Earth system models use simplistic rule-based allocation to partition plant biomass between leaves, stems, and roots. However, studies show that actual partitioning of biomass is not so simple. Plants respond to resource availability with physiological plasticity. According to Optimal Partitioning Theory, plants allocate biomass to maximize the uptake of the most limiting resource (Bloom et al., 1985). For example, trees in the Amazon shifted investment away from

maintenance to prioritize growth during drought (Doughty et al., 2015). In fact, changes in seasonal growth rate in the tropics are likely caused by shifts in allocation, rather than productivity (Doughty et al., 2014). Chen et al. (2013) found forests traded NPP allocated to roots for stem when nitrogen availability increased. But, when nitrogen stressed, plants will increase allocation to roots (Hermans, 2006). Kobe et al. (2010) also found increased allocation to roots when nitrogen was limiting, but suggested that additional resources were moving into non-structural carbon storage as well. This behavior suggests plants that have plasticity can optimize growth such that they maximize uptake of limiting resources. As such, the use of fixed allocation rules can lead to an overestimation in stem carbon, biomass and residence time, while underestimating leaf carbon and NPP (Song et al., 2016). This can have serious consequences for the carbon cycle, however, methods have been applied to dynamically allocate carbon in models to improve ESM models and their predictions.

For example, Xia et al. (2017) used the approach from Friedlingstein et al. (1999), to dynamically allocate biomass based on water, nitrogen and light limitation. Xia et al. (2017) showed that including dynamic allocation of C not only enhanced the carbon sink of the Community Atmosphere Biosphere Land Exchange (CABLE) model, but a long-term trend of increasing carbon sink was discovered. Another study by Montané et al. (2017) tested a dynamic allocation scheme that varied the ratio of coarse root:stem and stem:leaf carbon based on the annual NPP suggested by Litton et al (2007) in Community Land Model (CLM4.5). They noted that this method improved the leaf:stem ratio and reduced the overestimation of above-ground biomass (Montané et al., 2017). Alternatively, Gim et al. (2017) introduced a new allocation scaling scheme (based on Dickinson et al., 1998) in the Noah-MP model that increased the

allocation to leaves in the early growing season as a function of NPP. Although the model did improve GPP and ecosystem respiration (ER), the model did not include allocation response to the environment (Gim et al., 2017). The difficulty in adding a dynamic allocation of C to plant parts resides in the difficulty to parameterize models and the paucity of data to validate them.

Recently, a novel method for dynamic allocation was proposed by Lynch, 2015 using the Cobb-Douglas production function. The Cobb-Douglas production function is an economic approach of cost-benefit analysis to maximize production with multiple inputs (Cobb and Douglas, 1928). The method relies on the similarities between ecosystems and economics (Bloom et al., 1985). Economic frameworks have been used in ecological applications for root distribution (Lynch, 2015), storage (Chapin et al., 1990), and animal foraging behavior (Jorge et al., 2012), to name a few. In our model, carbon and nitrogen are analogous to the inputs, whereas the production output is plant biomass or net primary productivity (NPP).

We propose to incorporate this new method of dynamic allocation that uses a Cobb-Douglas type production function to maximize NPP based on the benefit of carbon and nitrogen uptake against the cost of producing and maintaining biomass. The approach has been used to predict productivity, biome distribution, and plant response to resource limitations (McNickle et al., 2016). We anticipate that by allowing plants to dynamically allocate carbon, ESMs will improve plant response to resources, thereby allowing the model to more accurately capture GPP, NPP and thus, the carbon cycle. Our method is designed as a proof-of-concept to test the feasibility of such an approach in a state-of-the-art ESM. As such, we will consider two plant component pools (leaves and fine roots) and evaluate how the model distributes carbon across a

variety of ecosystems with different plant functional types (PFTs). We will compare the simulated GPP with observations to validate the results. Finally, we will conclude with suggestions for expanding the pilot study to a fully dynamic allocation scheme.

4.2 Methods

The Energy Exascale Earth System Model (E3SM) is a fully coupled atmosphere, ocean, and land ESM developed by the U.S. Department of Energy (DOE). The E3SM is a branch from the Community Earth System Model (CESM) v1.2, and the land model of the E3SM (ELM) v0 is similar to the Community Land Model v4.5 (CLM4.5). The ELM v1 is used in this study and has additional model developments, particularly in the biogeochemistry component of the model and also has a recently added dynamic root module (Drewniak et al., 2019).

In brief, ELM uses fixed carbon allocation ratios to assign new growth to different vegetation tissue components. These fixed allocation ratios are defined as new growth to: fine roots:leaf, coarse root:stem, stem:leaf and live wood:total wood. Although these tissue component ratios are fixed, they vary with plant functional type (PFT), with an exception of the stem component. In ELM, the stem:leaf ratio is a function of NPP such that allocation to stem increases under favorable growth environments (Oleson et al., 2013). For all woody plants PFTs represented in ELM, the fine root:leaf ratio is 1, whereas for the grasses fine roots:leaf ratio has a value of 2.

The dynamic C allocation model incorporated here estimates the optimal fine root:leaf ratio using principles from the Cobb-Douglas production function as proposed in Lynch (2015). Instead of considering the whole plant, consisting of root (below ground) vs shoot (above ground), as in Lynch (2015) and Ågren and Franklin (2002), here we focus solely on the ephemeral tissues consisting of leaves and fine roots. We considered introducing dynamic allocation to these two tissue types because 1) leaves and roots are the two plant components in ELM fully responsible for taking up the C and nitrogen (N) resources, 2) we are introducing the Cobb-Douglas production function in ELM as a proof of concept, and 3) varying all the allometric ratios at once could result in non-convergence of the formula and/or result in difficult to explain model behavior. Here, we center modeling efforts on C and N resources, and do not separate the N species, nor do we consider phosphorus uptake differently in this model. We apply the same equations from Lynch (2015), but substituting the parameters from model output as detailed below. When parameters and processes were not included in the model, they were assumed from the Lynch (2015) study.

For the Cobb-Douglas production function, we assume that vegetation is maximizing productivity (NPP in this case). The function introduced recognizes that C acquisition requires N investment in leaves, and that N acquisition requires investment of C in roots. Therefore, we need to determine some optimum allocation of biomass such that the uptake of resources (i.e., C and N) are maximized given the costs associated with growth of plant tissues. Writing the uptake of C as π_C and the uptake of N as π_N, the Cobb-Douglas equation for productivity as a function of leaf (u_l) and root biomass (u_r) can be written as:

$$P(u_l, u_r) = \pi_C{}^{\alpha} \pi_N{}^{\beta} \quad (1)$$

The exponents α and β represent the relative demand of C and N, respectively. The relative demand α and β symbolize the plant stoichiometric ratio of C and N, and therefore, sum to one. Although observations suggest α and β can vary over time and space, we will consider them fixed in ELM. This is because the C:N ratios for the plant components are held fixed in ELM, although they do vary with PFT and with plant component (i.e., leaves, roots, stems, etc.). The uptake of C can be written as (harvest functions):

$$\pi_C = H_C(u_l) - c_C(u_l) - c_C(u_r) \quad (2)$$

and for N

$$\pi_N = H_N(u_r) - c_N(u_l) - c_N(u_r) \quad (3)$$

where H_C and H_N stand for the uptake of carbon and nitrogen and c_C and c_N are the carbon and nitrogen cost associated with growing and maintaining above and below ground biomass, as a function of the leaf biomass (u_l) and root biomass (u_r). In order to keep the equation simple, and to ensure the law of diminishing returns is met, we assume the C and N uptake are of the form:

$$H_C = GPP_{pot} * \left(1 - e^{-(u_l + u_l * stem\_leaf)}\right) \quad (4)$$

and

$$H_C = Nalloc_{pot} * (1 - e^{-u_r}) \quad (5)$$

where GPP_{pot} is the annual potential GPP (i.e., the GPP without N limitation) and $Nalloc_{pot}$ is the potential N uptake (i.e., without any N competition from decomposition). Therefore, the uptake equations represent the maximum uptake without any constraints and are considered potential uptake rates. The C uptake in equation (4) also includes the stem component (for woody vegetation) as a function of leaf C (i.e., via the stem:leaf ratio (stem_leaf)).

The cost functions (c_C and c_N) represent the maintenance costs and new growth costs of tissue for both C and N. They are written as:

$$c_c(l) = u_l * (mr + gr) * (1 + stem\_leaf) \quad (6)$$

and

$$c_c(r) = u_r * (mr + gr) + u_l(mr + gr) * stem\_leaf * croot\_stem \quad (7)$$

Similar to the harvest functions, cost functions include the C and N costs of the above- and below-ground plant components, specifically the stem and coarse roots for woody vegetation. They are written as a function of the leaf C in order to maintain only two unknown variables in the algorithm. Even though ELM only considers carbon costs of new tissue (i.e., c_N=0), we include nitrogen costs in this study. The N costs are assumed to be the same as the C costs weighted by the C:N ratio of the components already provided for each PFT in ELM.

This allows us to solve two equations with two unknowns, while still considering the whole plant (PFT) for the optimization. The first step of the optimization is done by taking the derivative of equation (1) with respect to leaf biomass and root biomass separately. Finally, they should satisfy:

$$\frac{\partial P_{(u_l,u_r)}}{\partial u_l} = \frac{\partial P_{(u_l,u_r)}}{\partial u_r} = 0 \quad (8)$$

The optimization is solved using the Newton-Raphson method with a finite difference approximation for the derivatives. The allocation parameters for fine root:leaf ratio is updated annually.

The impacts of this dynamic C allocation algorithm are shown in Figure 4.1. When the fine root:leaf ratio decreases, more carbon is allocated to leaves and less to roots. This has a

direct effect on photosynthesis by increasing the leaf area index (LAI). Increased LAI affects the stomatal conductance and the maximum rate of carboxylation (Vcmax), so overall photosynthesis and therefore GPP can be increased. Increases to stomatal conductance and Vcmax can also increase evapotranspiration (ET) decreasing soil moisture. Decreases in soil moisture content that lead to soil moisture stress, may lower stomatal conductance, Vcmax, and potentially the nitrogen available for uptake, all factors that can result in decreased GPP. When fine root:leaf ratio increases, more carbon is allocated to roots than leaves. The resulting lower LAI reduces GPP. The new dynamic root model, introduced by Drewniak (2019) allows roots to shift distribution such that water and nitrogen uptake can be optimized, but gives priority to plant water demands. This plasticity of rooting depth distribution under non-uniform profiles of water and nitrogen can help plants increase nutrient uptake by resolving the vertical structure of roots over time. Despite the new dynamic root allocation, N uptake is not generally increased because uptake is based on plant demand and not biomass. However, since root C:N ratios are less than leaves, the N demand can decrease, thereby lowering N limitation. It should be noted that since PFTs in ELM are modeled using the big-leaf approach, the optimization will be a team optimum, rather than an individual. Therefore, competition within a PFT is not considered, and the result is more representative of a monoculture, similar to a cropland. Future versions of the model should take this into account and include such competition.

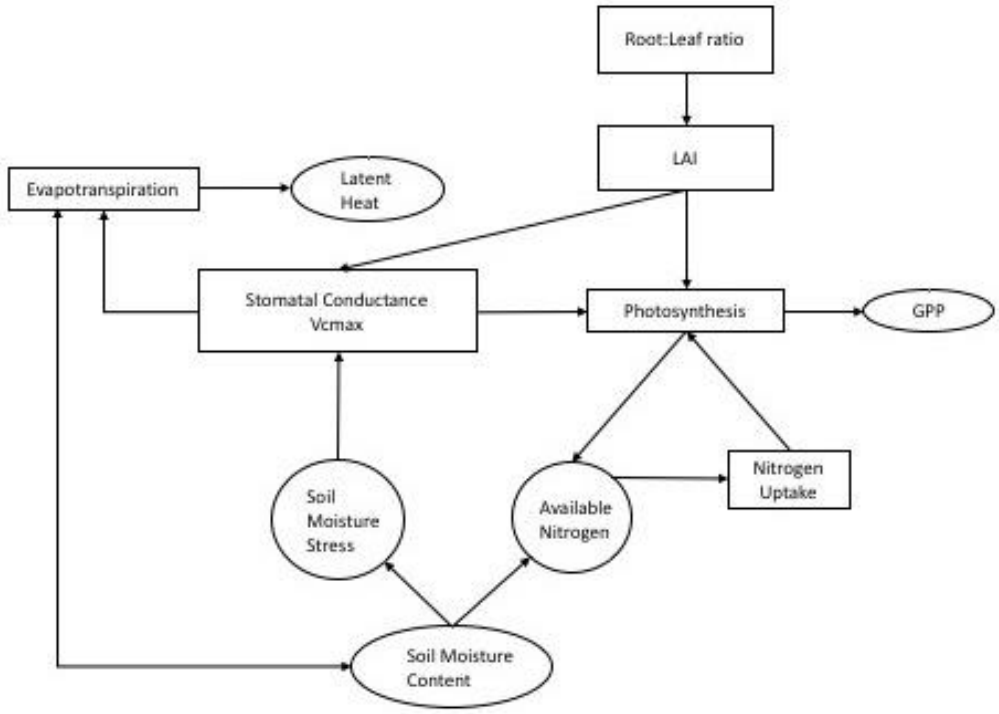

Figure 4.1. Schematic of the interactions of changing the fine root:leaf ratio.

For our simulations, ELM was run offline in point mode at 31 FLUXNET2015 (Fluxnet, 2016) sites (Table IX). Each site was run two times: once with the default model setup with fixed C allocation (CONTROL) and once with the Cobb-Douglas production function representing the dynamic C (and N) allocation (DCA). These sites encompass 12 of the 16 PFTs in ELM and cover a range of temperature and precipitation environments across 13 countries. From these, over one-third represent evergreen vegetation, over one-third are seasonal deciduous forests and the remaining six are stress deciduous phenology vegetation types. Many sites include multiple PFTs, indicated as MIX in Table IX, and for these cases the most dominant PFT types are shown. Each site is run independently using with atmospheric forcing local to that site as

provided by the Oak Ridge National Laboratory (D. Ricciuto, personal communication, February 2, 2016; see Table IX). Therefore, the years simulated in the model will vary with site. Regardless, for each site the atmospheric forcing data was cycled to get a minimum of 250 years accelerated spin-up and then for a minimum of 200 years during the post spin-up to ensure each site was at equilibrium following the spin-up procedure as suggested by Koven et al. (2013) and D. Ricciuto (personal communication, February 2, 2016). Finally, each site was run from 1850 until the end of the observation period (see Table IX) with transient land cover turned off and transient CO_2 turned on. Phosphorus was also active in the model; however, phosphorus limitation only occurred at five sites (AU-Tum, BR-Sa1, RU-Cok, RU-Sam, and US-UMB) and the phosphorus limitation did not exceed N limitation at any site. The DCA model reached steady state in fine root:leaf ratio early in the simulations for all sites except for three grassland sites US-Tom, US-Var, and US-Wkg, where the fine root:leaf ratio continued to vary throughout the simulation. All analyses were done on the last years of the simulation that match those of the observed years in Table IX.

Table IX. List of sites included in the simulations

Site	Longitude	Latitude	Elevation (m)	Primary PFT*	Years	MAT (°C)	MAP (mm)	Fine Root: Leaf ratio
Evergreen Phenology								
BE-Bra	4.5206	51.3092	16	ENFT (1)	1996-2013	9.8	750	0.60
BE-Vie	5.9968	50.3055	450	ENFT (1)	1996-2014	7.8	1062	0.50
CA-Gro	-82.1556	48.2167	300	MIX (1/7)	2003-2014	1.3	831	0.79
CZ-BK1	18.5384	49.5026	908	ENFT (1)	2000-2012	6.7	1316	0.56
DE-Tha	13.5669	50.9636	380	ENFT (1)	1996-2014	8.2	843	0.51
NL-Loo	5.744	52.1679	25	ENFT (1)	1996-2014	9.8	786	0.59
US-Blo	-120.6328	38.3953	1315	ENFT (1)	1997-2007	11.09	1226	1.13
US-Syv	-89.3477	46.242	540	MIX (1/7)	2001-2014	3.81	826	0.97
FI-Hyy	24.2848	61.8474	181	ENFB (2)	1996-2014	3.8	709	1.78
IT-Lav	11.2812	45.9553	1370	ENFB (2)	2003-2012	7.8	1291	2.18
IT-Ren	11.4347	46.5878	1747	ENFB (2)	1998-2013	4.7	809	1.04
BR-Sa1	-54.9589	-2.8567	88	MIX (4/6)	2002-2011	26.13	2075	0.98
AU-Tum	148.152	-35.6557	1200	EBFT (5)	2001-2013	9.5	963	0.81
Seasonal Deciduous Phenology								
DK-Sor	11.6458	55.4869	40	DBFT (7)	1996-2012	8.2	660	0.48
FR-Pue	3.5958	43.7414	270	MIX (1/7)	2000-2013	13.5	3041	0.25
IT-Ro2	11.9209	42.3903	224	DBFT (7)	2002-2012	15.15	876	0.55
US-Ha1	-72.1715	42.5378	303	MIX (1/7)	1991-2012	6.62	1071	0.48
US-Oho	-83.8438	41.5545	230	DBFT (7)	2004-2013	10	849	0.21
US-PFa	-90.2723	45.9459	470	MIX (1/7)	1995-2014	4.33	823	0.35
US-UMB	-84.7138	45.5598	234	DBFT (7)	2000-2014	5.83	803	0.16
US-Wcr	-90.0799	45.8059	520	DBFT (7)	1999-2014	4.02	787	0.41
DK-ZaH	-20.5503	74.4732	38	BDST (11)	2000-2009	-9	211	0.48
RU-Cok	147.883	70.6167	30	BDST (11)	2003-2013	-14.3	232	0.35

Site	Longitude	Latitude	Elevation (m)	Primary PFT*	Years	MAT (°C)	MAP (mm)	Fine Root: Leaf ratio
AT-Neu	11.3175	47.1167	970	C3GA (12)	2002-2012	6.3	852	0.33
RU-Sam	126.4958	72.3738	0	C3GA (12)	2002-2014	-11.9	101	0.32
Stress Deciduous Phenology								
US-Los	-89.9792	46.0826	480	BDSB (10)	2000-2014	4.08	828	0.51
DE-Hai	10.452	51.0793	430	MIX (13/15)	2000-2012	8.3	720	0.35
US-Ton	-120.966	38.1159	-9	C3G (13)	2001-2014	15.8	559	0.34†
US-Var	-120.9507	38.4067	129	C3G (13)	2000-2014	15.8	559	0.44†
US-Wkg	-109.9419	31.7365	1531	C4G (14)	2004-2014	15.64	407	0.40†
BE-Lon	4.7445	50.5522	165	CRO (15)	2004-2014	10	800	0.41

* ENFT = Evergreen Needleleaf Temperate Forest, ENFB = Evergreen Needleleaf Boreal Forest, EBFT = Evergreen Broadleaf Temperate Forest, DBFT = Deciduous Broadleaf Temperate Forest, BDST = Broadleaf Deciduous Temperate Shrub, C3GA = C3 Arctic Grass, BDSB = Broadleaf Deciduous Boreal Shrub, C3G = C3 Grass, C4G = C4 Grass, CRO = C3 Cropland (grass), Mix = a mixture of PFTs

† indicates the average fine root:leaf ratio is reported

4.3 Results

4.3.1 Fine Root:Leaf Ratio

The root:leaf ratio is mostly correlated with PFT (and by extension, phenology type). For most sites, more biomass was allocated to leaves than roots, therefore keeping the fine root:leaf ratios below 1 (Table IX). Across all sites, the average root:leaf ratio was 0.62.

The highest simulated fine root:leaf ratio occurred for evergreen phenology PFTs, with an average of 0.96. Four sites had a fine root:leaf ratio greater than one. Of those, three sites (FI-Hyy, IT-Lav, and IT-Ren) are needleleaf evergreen boreal forests. The other site, US-Blo is a needleleaf evergreen temperate forest. The site IT-Lav had the highest root:leaf ratio of 2.17.

By comparison, the lowest fine root:leaf ratios occurred for seasonal deciduous phenology PFTs, averaging 0.37. The minimum root:leaf ratio was 0.17 at the US-UMB site, a deciduous broadleaf temperate forest. Three of the lowest root:leaf ratios occurred at deciduous broadleaf temperate forest sites.

Finally, stress deciduous PFTs had an average fine root:leaf ratio of 0.41. Three of the grassland sites had a variable fine root:leaf ratio. The range over one atmospheric cycle was small, from 0.33-0.36, 0.41-0.48, 0.34-0.46 at the US-Tom, US-Var, and US-Wkg, respectively.

4.3.2 Gross Primary Productivity (GPP)

The DCA model increased GPP in most ecosystems (Figure 4.2), compared to CONTROL (i.e. fixed allocation), particularly in those with root:leaf ratios less than one. The largest increases in GPP occurred in the evergreen needleleaf temperate PFTs and the C3 grasslands. However, reductions in GPP occurred in evergreen needleleaf boreal and evergreen broadleaf tropical PFTs. The largest increase in GPP did not correlate with the lowest root:leaf ratios as more biomass allocated to leaves did not always result in proportional increases in GPP.

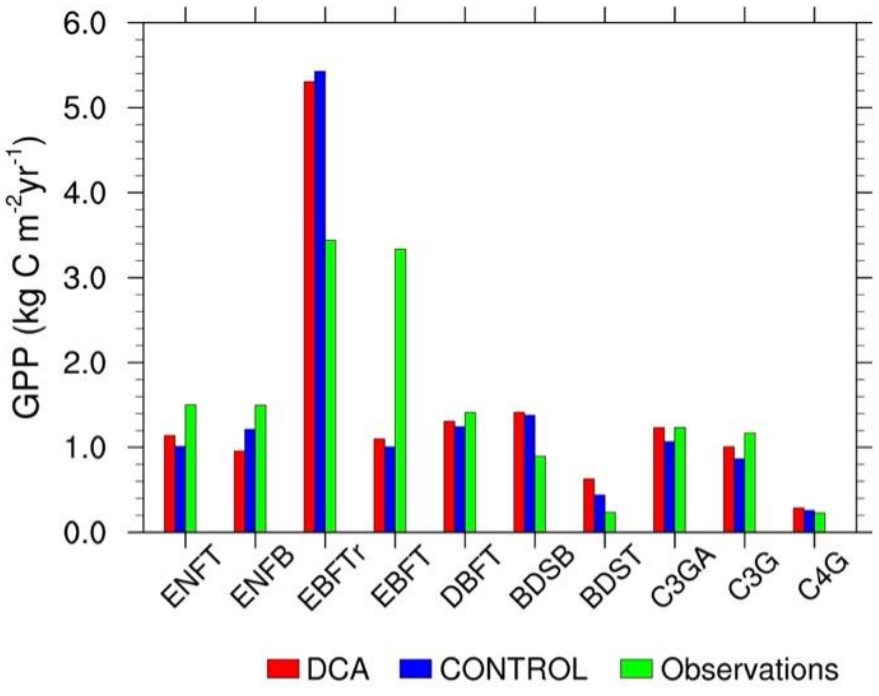

Figure 4.2. Simulated and observed mean annual GPP (kg C m^{-2} yr^{-1}) for different PFTs. ENFT: Evergreen Needleleaf Forest (Temperate), ENFB: Evergreen Needleleaf Forest (Boreal), ENFTr: Evergreen Needleleaf Forest (Tropical), EBFT: Evergreen Broadleaf Forest (Temperate), DBFT: Deciduous Broadleaf Forest (Temperate), BDSB: Broadleaf Deciduous Shrub (Boreal), BDST: Broadleaf Deciduous Shrub (Temperate), C3GA: C3 Arctic Grass, C3G: C3 Grass, C4G: C4 Grass.

Model performance at evergreen sites was mixed, with some sites simulating increases in GPP from the DCA model and others simulating decreases compared with CONTROL. At eight of the evergreen phenology sites, the model simulated increased GPP compared with CONTROL (Figure 4.3, Figure 4.4-Figure 4.8, Appendix C, Figure 4.9, Appendix C, and Figure 4.10, Appendix C): BE-Bra, BE-Vie, CA-Gro, CZ-BK1, DE-Tha, NL-Loo, IT-Ren, and AU-Tum. These evergreen sites had fine root:leaf ratios less than one and are located in temperate zones, except for IT-Ren. IT-Ren had a fine root:leaf ratio of slightly greater than one (1.04) and is classified as a boreal forest site. The modeled increase in GPP between DCA and CONTROL ranged from 2.9% up to 23.9%. In general, the lower the fine root:leaf ratio, the higher the simulated increase in GPP. Also at these sites, with the exception of IT-Ren, the CONTROL model underestimated GPP compared with observations more so than the DCA model, so all changes in the fine root:leaf ratio from the DCA model resulted in improved model agreement with observations.

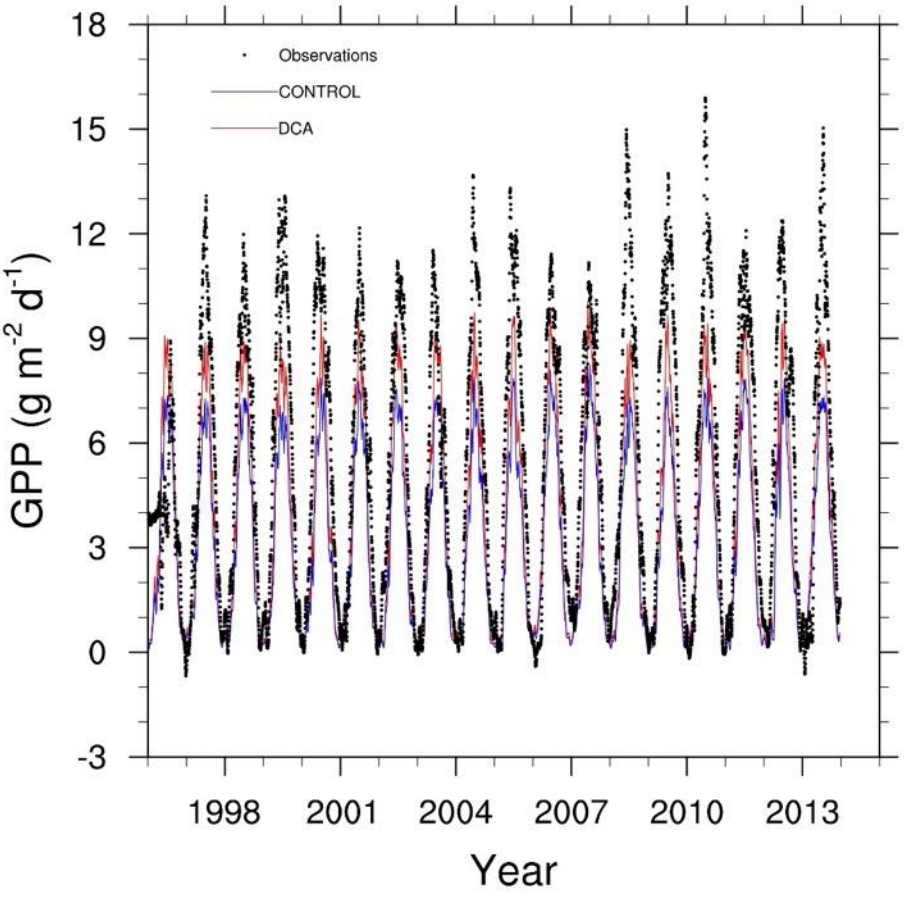

Figure 4.3. GPP of DCA (red line), CONTROL (blue line), and observations (black dots) at the De-Tha (evergreen needleleaf phenology) site.

Five of the evergreen sites simulated decreased GPP with the DCA model compared with CONTROL. Three of the five sites had root:leaf ratios greater than one, although the other two evergreen sites that had root:leaf less than 1 had mixed vegetation, US-Syv (Figure 4.11, Appendix C) and BR-Sa1 (Figure 4.12, Appendix C). At these sites, one of the PFTs had a root:leaf ratio of less than one and one had a root:leaf ratio greater than one, resulting in the average root:leaf greater than 1. Therefore, at evergreen phenology sites, the decrease in GPP

coincides with root:leaf ratios greater than one. The strongest decrease was at IT-Lav (Figure 4.13) and FI-Hyy (Figure 4.14, Appendix C) which coincided with the highest root:leaf ratios. The DCA simulated decreases in GPP were 41% and 27% greater than CONTROL at IT-Lav and FY-Hyy, respectively. The remaining three sites had small simulated decreases in GPP compared with CONTROL, ranging between 2.2% and 6.9%. At four of the sites where GPP is decreased in DCA, the model underestimates GPP compared with observations (Figure 4.11, Appendix C, Figure 4.13, and Figure 4.14-Figure 4.15, Appendix C), making DCA agreement with observations worse than CONTROL. At one site (BR-Sa1, Figure 4.12, Appendix C), the DCA and CONTROL model overestimates GPP.

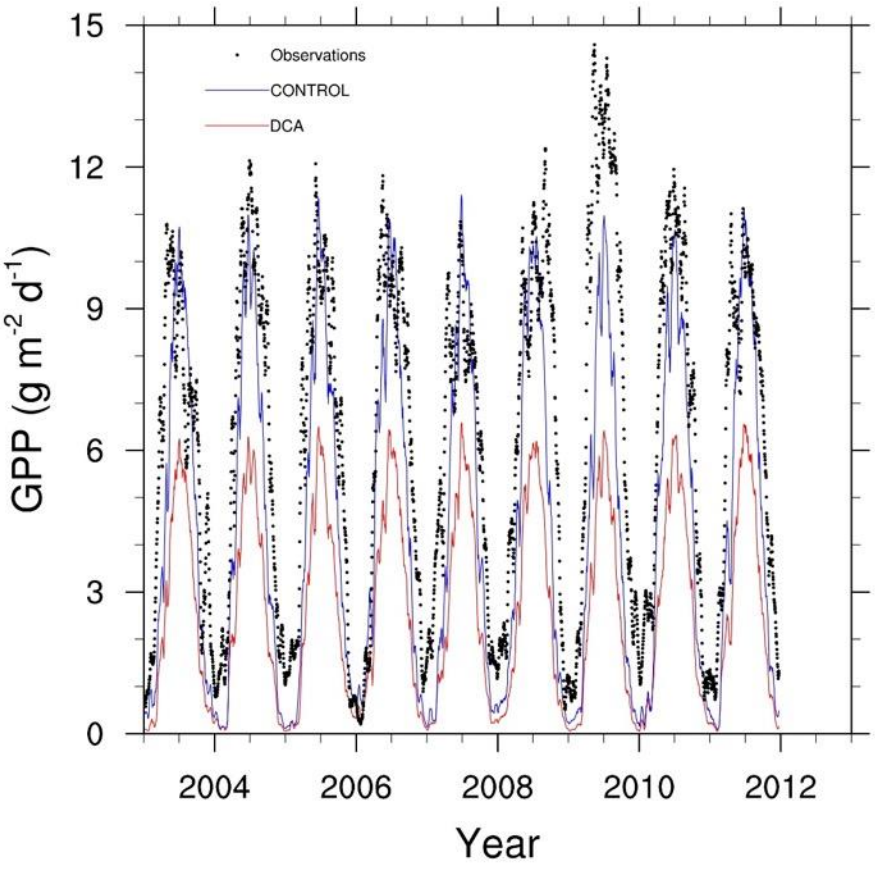

Figure 4.13. GPP of DCA (red line), CONTROL (blue line), and observations (black dots) at the IT-Lav (evergreen needleleaf phenology) site.

Most of the seasonal deciduous sites simulated increases in GPP estimates. However, the smallest modeled increases in GPP occurred at sites with broadleaf deciduous temperate vegetation types, despite having some of the lowest root:leaf ratios (Figure 4.16 and Figure 4.17-Figure 4.26, Appendix C). All of the broadleaf deciduous forest sites had simulated increases in GPP ranging between 3.8%-9.7%, most were close to 5%. Many of these sites have improved agreement with observations since CONTROL underestimates GPP more so than the DCA model (i.e., sites DK-Sor, US-Ha1, US-Oho, US-FPa, US-UMB, US-WCr, AT-Nue), and therefore the DCA model performed better than the CONTROL. However, there are a few sites

where both the CONTROL and the DCA model overestimate GPP (i.e., FR-Pue, DK-Zah, RU-Cok, and RU-Sam). The strongest increase in GPP was at sites RU-Cok and RU-Sam, a deciduous shrub and arctic grassland in boreal regions. However, these sites overestimated GPP compared with observations (Figure 4.24 and Figure 4.26, Appendix C, respectively) so GPP estimates were worse than CONTROL by about 60%.

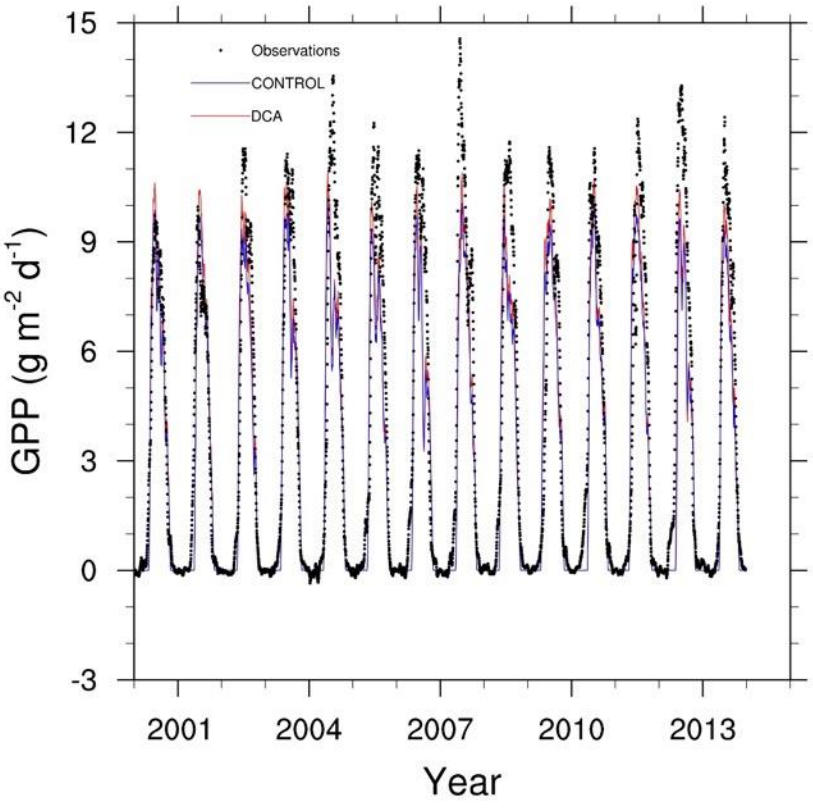

Figure 4.16. GPP of DCA (red line), CONTROL (blue line), and observations (black dots) at the US-UMB (seasonal deciduous phenology) site.

One seasonal deciduous site had a decrease in GPP, a deciduous broadleaf temperate forest. This site (IT-Ro2) had a root:leaf ratio less than one (Figure 4.27), and an increased allocation to leaves resulted in GPP estimates lower than that of the CONTROL. Here the DCA model compared slightly worse than CONTROL in simulated GPP versus observed GPP.

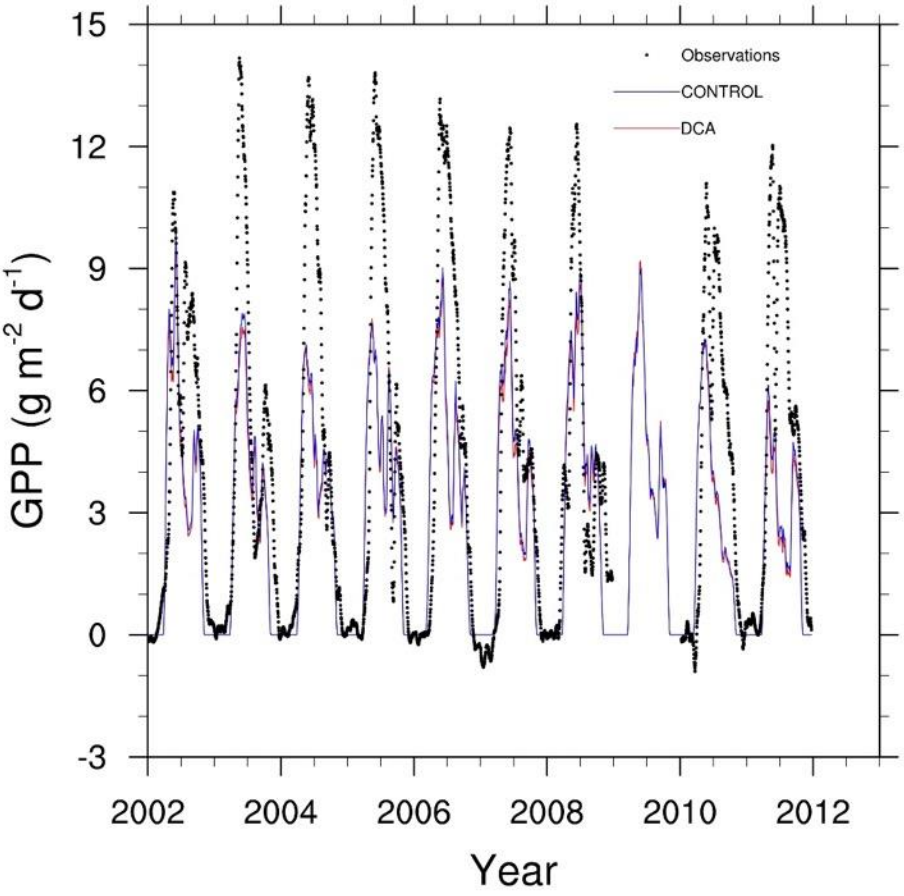

Figure 4.27. GPP of DCA (red line), CONTROL (blue line), and observations (black dots) at the IT-Ro2 (broadleaf deciduous phenology) site.

The stress deciduous sites all had an overall increase in GPP (Figure 4.28 and Figure 4.29-Figure 4.33, Appendix C). However, in two of the grassland sites (US-Var and US-Wkg), the GPP did not increase compared with CONTROL for all years. Some years, the DCA model simulated increases in GPP compared with CONTROL, and other years a decrease was simulated. Figure 4.28 shows an example of the variability at the US-Var site. In US-Wkg (Figure 4.32, Appendix C), the GPP seems anticorrelated with observations and the CONTROL model performed better. Over all sites, simulated increases in GPP ranged between 11-27%. The stress deciduous shrub at site US-Los had an increase in GPP, but since the model tends to overestimate GPP at this site (Figure 4.29, Appendix C), overall performance was degraded by the DCA model.

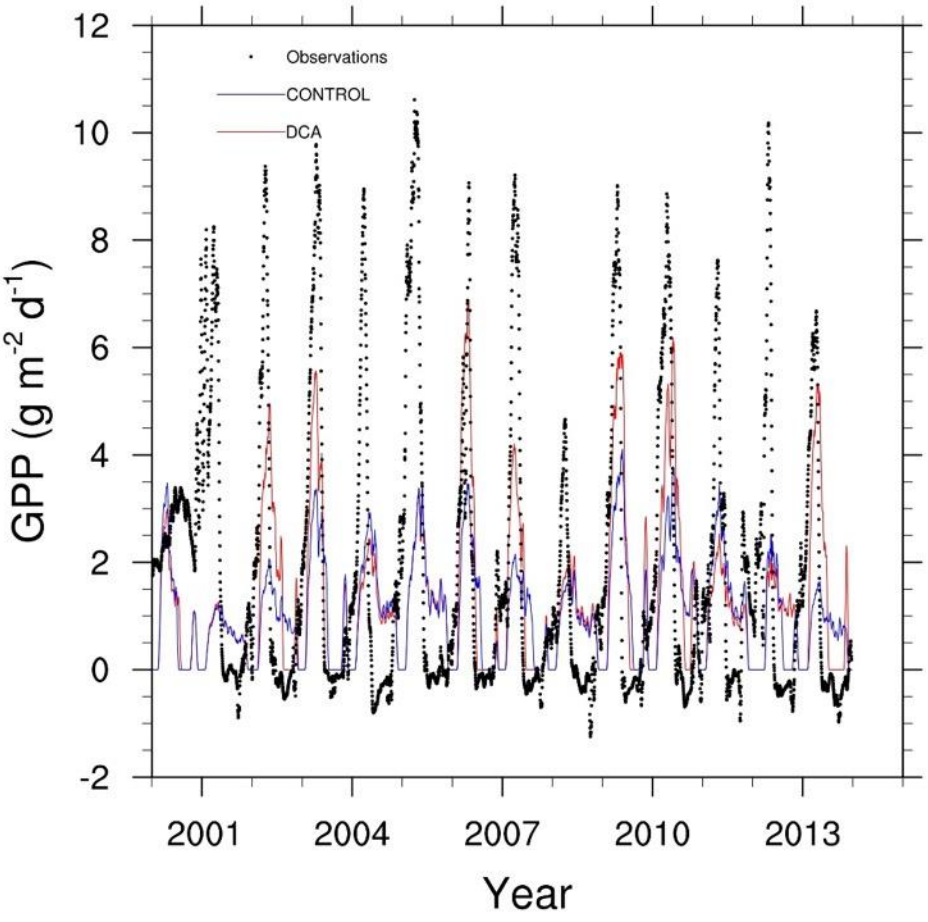

Figure 4.28. GPP of DCA (red line), CONTROL (blue line), and observations (black dots) at the US-Var (stress deciduous phenology) site.

4.3.3 Model Agreement with Observations

4.3.3.1 Gross Primary Productivity

The largest model improvement was for the standard deviation (SD) (Figure 4.34), as the DCA model matches observed variability more closely than the CONTROL model. The evergreen sites showed the largest improvements in SD. In particular, evergreen sites that had

fine root:leaf ratios of less than 1 and modeled increases in GPP also have improved SD with observations compared with CONTROL (i.e., BE-Bra, Be-Vie, CA-Gro, CZ-BK1, DE-Tha, NL-Loo, and AU-Tum). However, the correlation with observations was worse for the DCA model than CONTROL for these sites. The remaining evergreen sites in the DCA had worse SD agreement with observations than the CONTROL (i.e., US-Blo, US-Syv, FI-Hyy, IT-Lav, IT-Ren, and BR-Sa1). These sites also had simulated fine root:leaf ratios of greater than one and where DCA simulated GPP generally decreased. Most of the difference was small, with the exception of two sites, FI-Hyy and IT-Lav, where the highest fine root:leaf ratios occurred and where the largest decrease in GPP occurred in DCA. However, a few sites did increase correlation with observations compared with control (US-Blo, FI-Hyy, IT-Lav, and BR-Sa1).

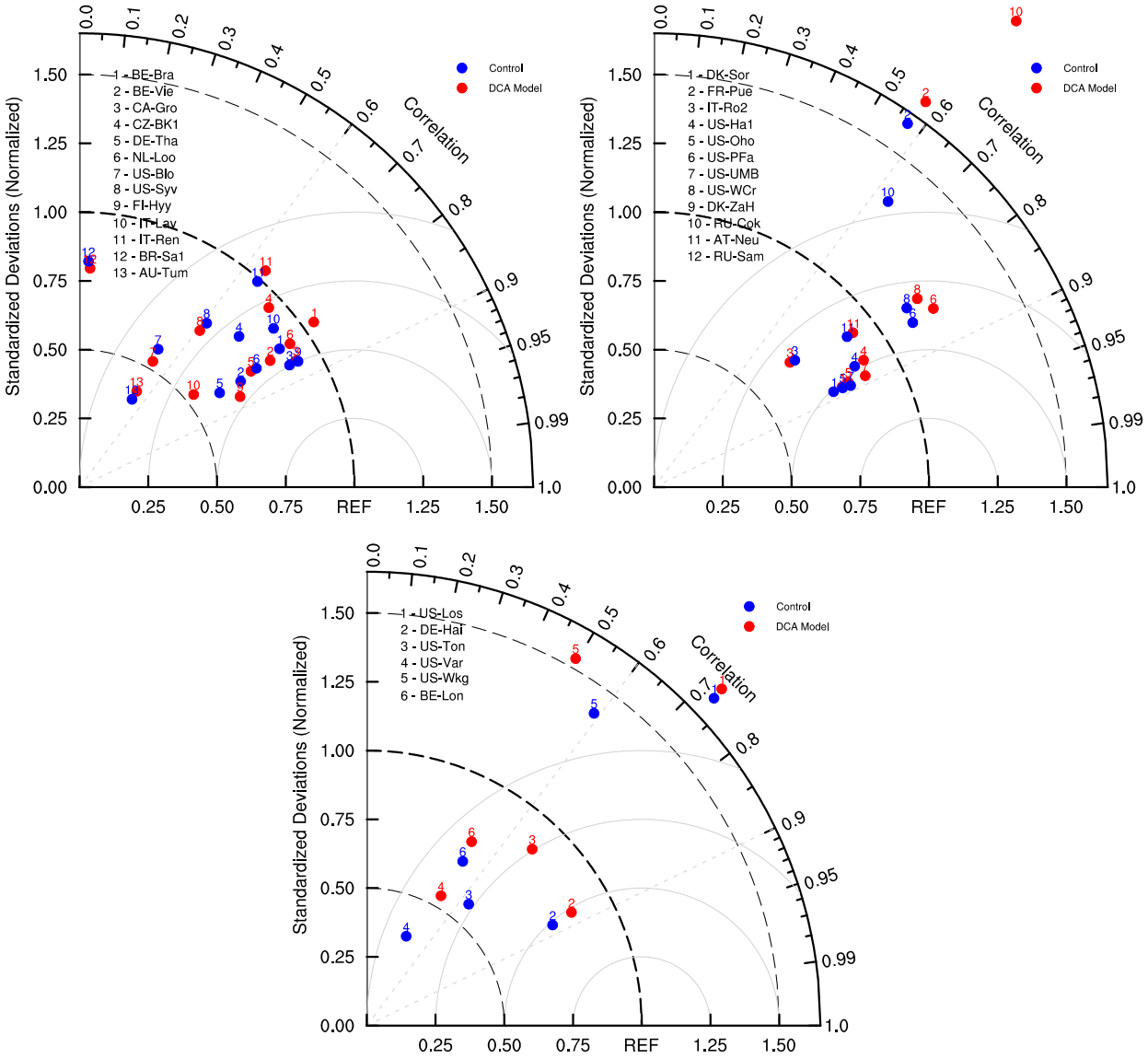

Figure 4.34. Taylor diagram for GPP, broken down by phenology. Top left shows evergreen sites, top right shows seasonal deciduous sites, and bottom shows stress deciduous sites. Sites that do not appear on the plot indicate the variance is very large.

Some of the seasonal deciduous sites experienced improvements in SD agreement with observations (Figure 4.34; i.e., DK-Sor, US-Ha1, US-Oho, US-UMB, and AT-Nue). Most of the improvements were small. The remaining sites had worse SD agreement with observations with DCA compared with CONTROL (FR-Pue, IT-Ro2, US-PFa, US-Wcr, DK-Zah, RU-Cok, and RU-Sam). The largest change in SD occurs at sites RU-Cok, and RU-Sam. Not surprisingly, these are also sites where the largest overestimation of GPP occurs for the DCA model compared with observations (Figure 4.24 and Figure 4.26, Appendix C). Only three sites had improved correlation with the DCA model, FR-Pue, AT-Neu, and RU-Sam. All changes in correlation were small, regardless of sign.

The stress deciduous sites also saw mostly improved variance agreement (Figure 4.34), with the exception of the C4 site (US-Wkg) and the broadleaf shrub site (US-Los). The largest improvements in SD were for US-Ton and US-Var. Only two sites also saw improvements in correlation with the DCA model compared with CONTROL, US-Ton, and US-Var, but these were also small.

4.3.1.2 Net Ecosystem Exchange

Given the tight coupling of the carbon and nitrogen cycling in the model, we expect that the changes in NEE would match the changes in GPP, and indeed, the patterns are quite similar. The largest model improvement was for the standard deviation (SD) (Figure 4.35).

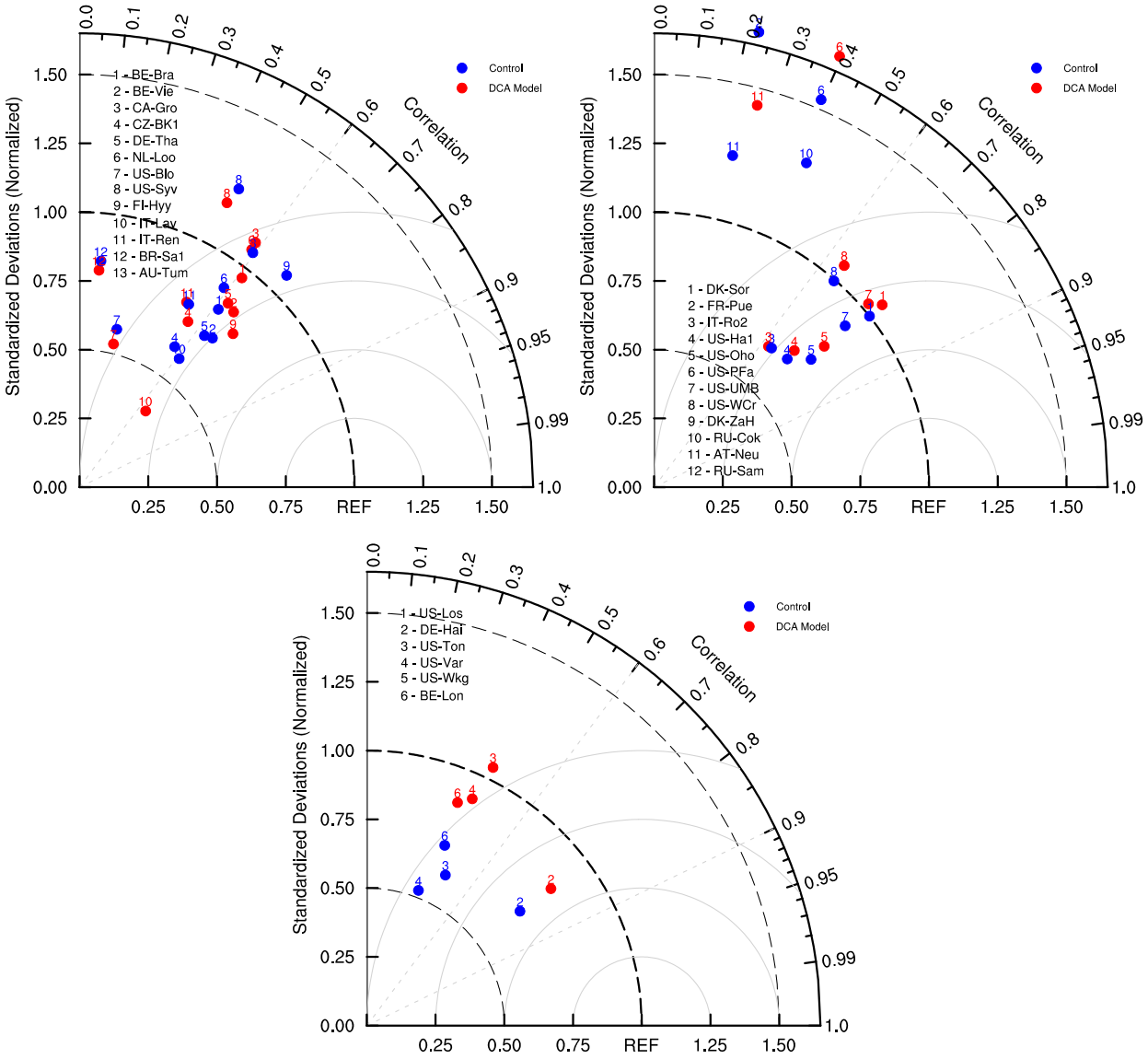

Figure 4.35. Taylor diagram for NEE, broken down by phenology. Top left shows evergreen sites, top right shows seasonal deciduous sites, and bottom shows stress deciduous sites. Sites that do not appear on the plot indicate the variance is very large.

Most of the largest improvements to SD between DCA and observations compared with CONTROL were at evergreen sites (BE-Bra, BE-Vie, CZ-BK1, DE-Tha, NL-Loo, IT-Ren, and

AU-Tum). The site NL-Loo also had improved correlation with observations with the DCA compared with CONTROL. There were several evergreen sites where DCA SD was worse compared with CONTROL (i.e., CA-Gro, US-Blo, US-Syv, FI-Hyy, IT-Lav, and BR-Sa1). However, three of those sites (US-Blo, FI-Hyy, and IT-Lav) had improved correlations.

A few of the seasonal deciduous sites did see improvement with SD agreement with observations, (US-Ha1, US-Oho, and US-UMB), but the remaining sites had worse agreement (Figure 4.35). These changes in SD agreement were smallest compared with other phenology sites, except for the shrub and arctic grasslands, which have some of the largest changes in SD between DCA and CONTROL. Only two sites also saw increases in correlation, FR-Pue and AT-Neu.

The stress deciduous sites in general have better SD agreement with observations with DCA than CONTROL. The largest improvements were at the C3 grass sites (US-Ton and US-Var). However, the C4 site (US-Wkg) and the broadleaf shrub site (US-Los) showed worse SD agreement with observations using the DCA model compared with CONTROL. Two sites also had improved correlation with observations using the DCA model, DE-Hai, and US-Var.

4.4 Discussion

Allowing plants to dynamically allocate C and N based on resource growth demands in ELM has resulted in fine root:leaf ratios that vary with site (Table IX). The resulting shift in plant biomass is reflected in changes in LAI (Table IX), and has implications for the ecosystem

C cycle. The response of vegetation is dependent on the phenology of the PFT(s). DCA improved agreement with observations at some sites when compared to the current model, but not everywhere. The resulting root:leaf ratios of the DCA simulation indicate vegetation are responding to resource limitations in order to maximize NPP. The success of this proof of concept demonstrates the importance of dynamic carbon allocation and highlights additional nutrient and water uptake processes that would benefit both the ELM and the dynamic carbon allocation model.

The patterns of fine root:leaf ratio simulated by DCA show a clear relationship with phenology type. The highest fine root:leaf ratios are simulated at the evergreen phenology sites. Since the dynamic allocation model is driven by the most limiting resource, high fine root:leaf ratios indicate the limiting resource is N, because more C is directed to fine roots. In ELM, evergreen phenology has the slowest nutrient cycling, which could result in less N availability. For example, the leaf and root turnover (i.e., the lifetime of a leaf or root) is highest (3.5 years) at the needleleaf evergreen boreal forests and second highest (1.5 years) at the needleleaf evergreen temperate forests. In addition, in ELM, the stoichiometry requirements of C:N in evergreen leaves is higher than other PFTs, requiring less N. The slowness of the biomass (i.e. leaves and roots) entering the litter pool and the lower N inputs from the higher C:N ratios could result in an N limited environment for plant growth. Therefore, lower N availability drives higher fine root:leaf ratios in evergreen PFTs.

On the contrary, seasonal deciduous sites have much lower fine root:leaf ratios, suggesting a C limited environment. Seasonal deciduous vegetation in ELM has a faster nutrient

cycle than evergreen plants. For example, the active growing season is limited by day length and thus leaf turnover is short (1 year). In addition, the stoichiometry of deciduous leaves has a lower C:N ratio requirement, requiring more N. The faster rate of inputs with higher N amounts could result in higher N availability at seasonal deciduous sites. Therefore, C would be the stronger limiting nutrient at these sites and result in lower fine root:leaf ratios.

Finally, stress deciduous sites also have low fine root:leaf ratios, suggesting a C limited environment. Grasses have the fastest nutrient cycle of all PFTs in ELM, especially since grasses don't have a woody component. Woody material decomposes slowly due to its high C:N ratio. Therefore, decomposing stem and coarse roots immobilizes some nitrogen in the decomposition process for trees and shrubs. Strong variability in the soil nitrogen mineralization pool (not shown) is evidence of the high turnover at grass sites. When available nitrogen is highest, DCA responds with lower root:leaf ratios, when available nitrogen drops, the root:leaf ratio increases. The differences in nutrient turnover drive the patterns of root:leaf ratio produced by the DCA model.

Despite the importance of nutrient turnover on biomass allocation in the model, tissue turnover rate in models is largely inconsistent (De Kauwe et al, 2014). Studies of root turnover found that different orders of roots had residence times of months to years (Lynch et al., 2013; Liu et al., 2015). Others showed that root turnover, even in elevated CO_2 environments, had root turnover of years to decades (Matamala et al., 2003). De Kauwe et al. (2014) found that wood turnover did increase in elevated CO_2. The process of root and biomass turnover times should be

addressed in future model development since it will have an important role in how carbon is allocated and stored in ESMs.

Nearly all the sites (evergreen, seasonal deciduous and stress deciduous) that had a root:leaf ratio less than one had simulated increases in GPP. The increased LAI caused by increased allocation to the leaf compartment in the DCA simulation resulted in increased GPP (Figure 4.1 and Figure 4.2). The increased GPP in the dynamic carbon allocation model shows that the default configuration in ELM does not optimize GPP, but has the potential to increase GPP by replacing the strict C allometric rules with a more flexible C partitioning method. Our test of the method on a small set of grid cells was sufficient to determine trends from the different PFTs, and shows promise that this method of dynamic carbon allocation can be applied to an ESM. Furthermore, the vegetation plasticity response in the dynamic carbon allocation model shows that ELM can increase the terrestrial carbon sink capacity.

Sites with the lowest root:leaf ratios did not necessarily have large increases in GPP. The largest annual increase in GPP (not shown) compared with CONTROL occurred at evergreen sites, despite having the lowest fine leaf:root ratios in DCA. In fact, increases in GPP at deciduous sites were half to one-quarter of those simulated in evergreen sites. The difference in GPP response can be attributed to several factors. First, evergreen PFTs have a longer growing season, so they can continue to accumulate GPP when seasonal deciduous trees are dormant. In addition, evergreen PFTs have a higher Vcmax parameter in ELM than broadleaf PFTs, which, along with increases in LAI, can increase photosynthesis (Figure 4.1). Finally, it is possible that the deciduous vegetation are self-shading, resulting in smaller increases in GPP as the

diminishing return is approached for increases in LAI. Therefore, smaller changes in fine root:leaf ratio will have a stronger impact on evergreen than deciduous PFTs.

Evergreen sites that had root:leaf ratios greater than one had simulated decreases in GPP compared with CONTROL. Decreased LAI from decreased leaf allocation resulted in decreased GPP. To understand this behavior, one must consider how nitrogen uptake is simulated by ELM. Increases in root biomass do not translate to increases in nitrogen uptake, since nitrogen uptake is simulated based on its availability and not root biomass or area. Future versions of the model should correct this behavior such that nutrient uptake is increased as root biomass/area increases. The lower LAI, therefore, plays a stronger role driving a decrease in GPP. Therefore, at nitrogen limited sites, when more carbon is allocated to the root than the leaf, GPP is not optimized by the DCA model.

There is one site with low root:leaf ratios but had a decrease in GPP, IT-Ro2. Despite having a root:leaf ratio less than one, GPP decreased. This site is located in a Mediterranean climate with high temperature and low, seasonal rainfall. The simulated increase to LAI can increase transpiration, reducing soil moisture and causing water stress (see Figure 4.1). The resulting decrease in water use efficiency downregulated GPP. This is a known problem in modeling seasonally dry ecosystems (Drewniak et al., 2019). One solution would be to shift the water uptake to be a weighted function of water availability such that shallow roots can extract water during the wet season and deep roots will continue to function during the dry season (De Kauwe et al., 2015). Other studies have suggested using hydraulic redistribution to improve water uptake (Tang et al., 2015). Finally, improvements to the root parameterizations and

stomatal conductance model could help improve the soil water extracted from different depths (Bouda and Saiers, 2017). Soil moisture plays a strong role mediating GPP in dry season sites, but increasing water availability should improve the performance of the dynamic carbon allocation model.

While the DCA improves the standard deviation of GPP and NEE compared with observations (Figure 4.34 and Figure 4.35), other metrics such as correlation with observations were largely unchanged. This could be an indicator that the model misses the timing of onset and offset of the active growing period. The lack of correlation could also be an artifact of noise in the data (both observed and modeled). In fact, the simulated GPP at most sites is underestimated by the model, even with the new DCA model. However, the DCA model seems to have a stronger peak in GPP, which would contribute more to improve the variance than the correlation of the existing CONTROL model. Further testing is warranted with a full Cobb-Douglas dynamic carbon allocation model and at sites with biomass partitioning data for comparison.

The DCA model optimizes NPP by altering only one variable, the fine root:leaf ratio. However, we did not include in the production function the other components of biomass, including live wood and coarse roots, or storage, which are fixed. These long-lived biomass pools do not provide additional carbon or nitrogen uptake benefit in the model, but, they do provide structural support and contribute to the overall carbon storage, growth and maintenance respiration (costs) of the plant. Furthermore, it was argued by Wolf et al. (2011) that the wood component of the stem is more important than the foliage for allocation dynamics. In fact, under elevated CO_2, allocation to stem increased in ecosystems (De Kauwe et al., 2014), which could

have serious consequences for the carbon storage capacity of forests given the longer lifetimes of stem compared with leaves and roots. However, longer growing seasons and fertilization reduce the density of wood (Petzsch et al., 2018), which may counter some of the effect on carbon sequestration. Regardless, dynamic allocation will have a stronger impact on long term carbon fluxes than short term carbon fluxes (Montane et al., 2017). The dynamic carbon allocation model should be expanded to include all parts of the plant, not just those that are responsible for carbon and nitrogen uptake. In addition, other nutrients should be considered by the dynamic carbon allocation model. ELM has both nitrate and ammonium species of nitrogen and phosphorus. The dynamic carbon allocation model is flexible enough to include these additional species and should be expanded.

4.5 Conclusion

The Cobb-Douglas dynamic carbon allocation model shows promise for including a dynamic approach to carbon partitioning in ESMs. DCA simulated fine root:leaf ratios are correlated with nutrient cycling. At most sites tested, the DCA model increased GPP. The DCA method was not as effective increasing GPP in evergreen ecosystems when nitrogen was the limiting resource or in dry season deciduous ecosystems which can suffer from decreased WUE. This failure was largely the result of missing processes in the model, such as nitrogen uptake based on root biomass. The effect of DCA was mixed in grasslands. In the future, the Cobb-Douglas algorithm should consider woody tissue (stem and coarse roots) and grain (for crops). In addition, phosphorus nutrients and distinguishing the nitrogen species of nitrate and ammonium should be included the Cobb-Douglas equation.

4.6 References

Ågren, G.I., and Franklin, O. (2003), Root: shoot ratios, optimization and nitrogen productivity. *Annals of Botany*, 92, 795-800.

Beer, C., Reichstein, M., Tomelleri, E., Ciais, P., Jung, M., Carvalhais, N., Rödenbeck, C., Arain, M.A., Baldocchi, D., Bonan, G.B. and Bondeau, A. (2010), Terrestrial gross carbon dioxide uptake: global distribution and covariation with climate. *Science*, p.1184984.

Bloom, A. J., Chapin, F. S., and Mooney, H. A. (1985), Resource limitation in plants – an economic analogy. *Annu. Rev. Ecol. Syst.*, 16, 363-392.

Bouda, M., and Saiers, J. E. (2017), Dynamic effects of root system architecture improve root water uptake in 1-D process-based soil-root hydrodynamics. *Advances in Water Resources*, 110, 319-334.

Campbell, J. E., Berry, J. A., Seibt, U., Smith, S. J., Montzka, S. A., Launois, T., Belviso, S., Bopp, L., and Laine, M. (2017), Large historical growth in global terrestrial gross primary productivity. *Nature*, 544, 84-87.

Cao, L., Bala, G., Caldeira, K., Nemani, R., and Ban-Weiss, G. (2010), Importance of carbon dioxide physiological forcing to future climate change. *Proceedings of the National Academy of Sciences*, 107(21), 9513-9518.

Chapin, F.S., Matson, P.A., Mooney, H.A. (2002), Principles of Terrestrial Ecosystem Ecology. New York: Springer, print.

Chen, G., Yang, Y., and Robinson, D. (2013), Allocation of gross primary production in forest ecosystems: allometric constraints and environmental responses. *New Phytologist*, 200, 1176-1186.

Cobb, C.W., and Douglas, P.H. (1928), A Theory of Production. *American Economic Review*, 18 (Supplement), 139–165.

De Kauwe, M.G.; Medlyn, B.E.; Zaehle, S.; Walker, A.P.; Dietze, M.C.; Wang, Y.P.; Luo, Y.; Jain, A.K.; El-Masri, B.; Hickler, T., Wårlind, D., Wang, E., Parton, W. J., Thornton, P. E. Wang, S., Prentice, I. P., Asao, S., Smith, B., McCarthy, H. R., Iversen, C. M., Hanson, P. J., Warren, J. M., Oren, R., and Norby, R. J. (2014), Where does the carbon go? A model-data intercomparison of vegetation carbon allocation and turnover processes at two temperate forest free-air CO2 enrichment sites. *New Phytol.*, 203, 883–899.

De Kauwe, M.G.; Zhou, S.X.; Medlyn, B.E.; Pitman, A.J.; Wang, Y.P.; Duursma, R.A.; Prentice, I.C. (2015), Do land surface models need to include differential plant species responses to drought? Examining model predictions across a mesic-xeric gradient in Europe. *Biogeosciences*, 12, 7503–7518.

Delucia, E. H., Drake, J. E., Thomas, R. B., and Gonzalez-Meler, M. (2007), Forest carbon use efficiency: is respiration a constant fraction of gross primary production? *Global Change Biology*, 13, 1157-1167.

Dickinson, R., Sahaikh, M., Bryant, R., and Graumlich, L. (1998), Interactive canopies for a climate model. *Journal of Climate*, 11, 2823-2836.

Doughty, C. E., Malhi, Y., Araujo-Murakami, A., Metcalfe, D. B., Silva-Espejo, J. E., Arroyo, L., Heredia, J. P., Pardo-Toledo, E., Mendizabal, L. M., Rojas-Landivar, V. D., Vega-Martinez, M., Flores-Balencia, M., Sibler-Rivero, R., Moreno-Vare, L., Viscarra, L. J., Chuviru-Castro, T., Osinaga-Becerra, M., and Ledezma, R. (2014), Allocation trade-offs dominate the response of tropical forest growth to seasonal and interannual drought. *Ecology*, 95(8), 2192-2201.

Doughty, C. E., Metcalfe, D. B., Girardin, C. A. J., Amézquita, F. F., Cabrera, D. G., Huasco, W. H., Silva-Espejo, J. E., Araujo-Murakami, A. da Costa, M. C., Rocha, W., Feldpausch, T. R., Mendoza, A. L. M., da Costa, A. C. L., Meir, P., Phillips, O. L., and Malhi, Y. (2015), Drought impact on forest carbon dynamics and fluxes in Amazonia. *Nature*, 519, 78-82.

Drewniak, B. A. (2019), Simulating dynamic roots in the Energy Exascale Earth System Land Model. *Journal of Advances in Modeling Earth Systems*, 11, https://doi.org/10.1029/2018MS001334.

Friedlingstein, P.; Joel, G.; Field, C.B.; Fung, I.Y. (1999), Toward an allocation scheme for global terrestrial carbon models. *Glob. Chang. Biol.*, 5, 755–770.

Gim, H.-J., Park, S. K., Kang, M., Thakuri, B. M., Kim, J., and Ho, C.-H. (2017), An improved parameterization of the allocation of assimilated carbon to plant parts in vegetation dynamics for Noah-MP. *Journal of Advances in Modeling Earth Systems*, 9, 1776-1794.

Hermans, C., Hammond, J. P., White, P. J., and Verbruggen, N. (2006), How do plants respond to nutrient shortage by biomass allocation? *TRENDS in Plant Science*, 11(12),610-617.

Hopkins, F., Gonzalez-Meler, M. A., Flower, C. E., Lynch, D. J., Czimczik, C., Tang, J., and Subke, J.-A. (2013), Ecosystem-level controls on root-rhizosphere respiration. *New Phytologist*, 199(2), 339-351.

Ise, T., Litton, C. M., Giardina, C. P., and Ito, A. (2010), Comparison of modeling approaches for carbon partitioning: Impact on estimates of global net primary production and equilibrium biomass of woody vegetation from MODIS GPP. *Journal of Geophysical Research*, 115, G04025, doi:10.1029/2010JG001326.

Jorge, M.L., Brown, J.S., and van der Merwe, M. (2012), Handling time and the evolution of caching behavior. *Behavioral Ecology*, 23: 410-417.

Kobe, R. K., Iyer, M., and Walters, M. B. (2010), Optimal partitioning theory revisited: Nonstructural carbohydrates dominate root mass responses to nitrogen. *Ecology*, 91(1), 166-179.

Litton, C. M., Raich, J. W., and Ryan, M. G. (2007), Carbon allocation in forest ecosystems. *Global Change Biology*, 13, 2089-2109.

Liu, B. He, J., Zeng, F., Lei, J., and Arndt, S. K. (2016), Life span and structure of ephemeral root modules of different functional groups in a desert system. *New Phytologist*, doi: 10/1111/nph.13880.

Lynch, D. J., Matamala, R., Iversen, C. M., Norby, R. J., and Gonzalez-Meler, M. A. (2013), Stored carbon partly fuels fine-root respiration but is not used for production of new fine roots. *New Phytologist*, 199(2), 420-430.

Lynch, D.J. (2015), Impacts of Fine-Roots on Terrestrial Net Primary Productivity and Soil Nutrient Cycling (Ph.D. Thesis), University of Illinois at Chicago, Chicago, IL, USA.

Matamala, R., Gonzalez-Meler, M.A., Jastrow, J.D., Norby, R.J. and Schlesinger, W.H. (2003), Impacts of fine root turnover on forest NPP and soil C sequestration potential. *Science*, 302(5649), pp.1385-1387.

McNickle, G. G., Gonzalez-Meler, M. A., Lynch, D. J., Baltzer, J. L., and Brown, J. S. (2016), The world's biomes and primary production as a triple tragedy of the commons foraging game played among plants. *Proc. R. Soc. B*, 283, 20161993.

Montane, F., Fox, A. M., Arellano, A. F., MacBean, N., Alexander, M. R., Dye, A., Bishop, D. A., Trouet, V., Babst, F, Hessl, A. E., Pederson N., Blanken, P. F., Bohrer, G., Gough, C. M., Litvak, M. E., Novick, K. A., Phillips, R. P., Wood, J. D., and Moore, D. J. P. (2017), Evaluating the effect of alternative carbon allocation schemes in a land surface model (CLM4.5) on carbon fluxes, pools, and turnover in temperate forests. *Geoscientific Model Development*, 10, 3499-3517.

Nemani, R.R., Keeling, C.D., Hashimoto, H., Jolly, W.M., Piper, S.C., Tucker, C.J., Myneni, R.B. and Running, S.W. (2003), Climate-driven increases in global terrestrial net primary production from 1982 to 1999. *Science*, *300*(5625), pp.1560-1563.

Pretzsch, H., Biber, P., Schütze, G., Kemmerer, J., Uhl, E. (2018), Wood density reduced while wood volume growth accelerated in Central European forests since 1870. *Forest Ecology and Management*, 429, 589-616.

Oleson, K. W., Lawrence, D. M., Bonan, G. B., Drewniak, B., Huang, M., Koven, C. D., Levis, S., Li, F., Riley, W. J., Subin, Z. M., Swenson, S. C., Thornton, P. E., Bozbiyik, A., Fisher, R., Heald, C. L., Kluzek, E., Lamarque, J.-F., Lawrence, P. J., Leung, L. R., Lipscomb, W., Muszala, S., Ricciuto, D. M., Sacks, W., Sun, Y., Tang J., and Yang Z.-L. (2013), Technical Description of version 4.5 of the Community Land Model (CLM). Boulder, Colorado.: NCAR.

Schmidt, M.W., Torn, M.S., Abiven, S., Dittmar, T., Guggenberger, G., Janssens, I.A., Kleber, M., Kögel-Knabner, I., Lehmann, J., Manning, D.A. and Nannipieri, P. (2011), Persistence of soil organic matter as an ecosystem property. *Nature*, *478*(7367), p.49.

Song, X., Zeng. X.-D., and Li, F. (2016), Evaluation of the individual allocation scheme and its impacts in a dynamic global vegetation model. *Atmospheric and Oceanic Science Letters*, 9:1, 38-44.

Tang, J., Riley, W., and Niu, J. (2015), Incorporating root hydraulic redistribution in CLM4.5: Effects on predicted site and global evapotranspiration, soil moisture and water storage. *Journal of Advances in Modeling Earth Systems*, 7, 1828-1848.

Welp, L.R., Keeling, R.F., Meijer, H.A., Bollenbacher, A.F., Piper, S.C., Yoshimura, K., Francey, R.J., Allison, C.E. and Wahlen, M. (2011), Interannual variability in the oxygen isotopes of atmospheric CO 2 driven by El Niño. *Nature*, *477*(7366), p.579.

Wolf, A., Field, C. B., and Berry, J. A. (2011), Allometric growth and allocation in forests: a perspective from FLUXNET. *Ecological Applications*, 21(5), 1546-1556.

Xia, J., Yuan, W., Wang, Y.-P. and Zhang, Q. (2017), Adaptive carbon allocation by plants enhances the terrestrial carbon sink. *Scientific Reports*, 7(3341), doi:10/1038/s41598-017-03574-3.

5 MODELING THE IMPACT OF AGRICULTURAL LAND USE AND MANAGEMENT ON U.S. CARBON BUDGETS

This chapter was previously published as Drewniak, B. A., Mishra, U., Song, J., Prell, J., and Kotamarthi, V. R. 2015. Modeling the impact of agricultural land use and management on US carbon budgets. *Biogeosciences*, 12, 2119-2129, https://doi.org/10.5194/bg-12-2119-2015.

5.1 Introduction

Bioenergy crops are promoted as a renewable energy source capable of improving energy security and mitigating greenhouse gas (GHG) emissions from fossil fuels. These crops are considered environmentally friendly and economically competitive, because CO_2 emitted by biofuel combustion is partially balanced by atmospheric uptake through photosynthesis (Hughes et al., 2010). The Renewable Fuel Standard of the U.S. Energy Independence and Security Act (EISA 2007) sets a national target of producing 136 billion liters of renewable fuels by 2022. Of this, at least 61 billion liters is expected to come from cellulosic ethanol (U.S. Environmental Protection Agency, 2010). Though maize grain and sugarcane are currently the major global sources for bioethanol production, maize production in the United States is not sufficient to meet the renewable fuel targets. Furthermore, recent studies suggest that production of ethanol from maize grain might in fact increase GHG emissions because of changes in land use (Searchinger et al., 2008; Kim et al., 2009; Melillo et al., 2009). For these reasons, cellulosic biofuels produced from cellulose and hemicellulose plant biomass are considered a viable alternative to conventional crop-based biofuels.

Cellulosic biofuels can be made from perennial feedstocks or from residues of annual cropping and forestry activities, thereby reducing or eliminating the need for additional agricultural land. The use of crop residues for bioethanol production shows promise for fulfilling U.S. renewable fuel goals, but more research is needed on the effects on soil organic carbon (SOC) of crop residue removal from croplands (Mishra et al., 2013) and net GHG balance (McKone et al., 2011). Furthermore, crop residues play a crucial role in sustainability and resilience of agroecosystems (Karlen et al., 2009). Therefore, to understand the environmental consequences of using crop residues for bioenergy production on large spatial scales, it is essential to know the impacts on the SOC pool of differential rates of crop residue removal and nitrogenous fertilizer applications.

Crop residue is responsible for maintaining soil moisture, returning carbon and other nutrients to soil, and erosion mitigation; in general, it provides a sustainable environment for cultivation activities (Lal, 2009). Without residue cover, wind and water erosion will increase (Van Pelt et al., 2013). Long-term residue harvest results in loss of yields and productivity by decreasing the nutrient content of soils (Blanco-Canqui and Lal, 2009a). These arguments demonstrate that using crop residues as a bioenergy fuel resource could have detrimental impacts on agroecosystems (Blanco-Canqui and Lal, 2009a).

Globally, soils store more carbon than the atmosphere and biosphere combined, acting both as a source and sink of atmospheric CO_2 (IPCC, 2013). However, cultivation loss of SOC ranges from 50% to70% (Lal and Bruce, 1999). Over the U.S. Midwest, land conversion led to a 25-50% reduction of soil carbon (Houghton et al., 1999; Lal, 2002). The result is large carbon

payback times, ranging from a few years to several centuries (Fargione et al., 2008; Gibbs et al., 2008; Searchinger et al., 2008). On the other hand, conversion from cultivation to native grasslands, such as through enrollment in the Conservation Reserve Program, resulted in increased soil carbon (Anderson-Teixeira et al., 2009; Pineiro et al., 2009). Therefore, it is critical to evaluate the impact of agricultural land use and management on regional carbon budgets.

The influence of agriculture on the carbon cycle is complex; carbon capture and storage in croplands are dependent on management practices, including tillage, fertilizer applications, residue management, and crop sequence (West and Post, 2002; Hooker et al., 2005; Dou and Hons, 2006; Huggins et al., 2007; Khan et al., 2007; Kim et al., 2009). SOC stocks and fluxes at a particular location are soil and site specific and reflect the long-term balance between organic matter inputs from vegetation and losses due to decomposition, erosion, and leaching. Some studies have attempted to quantify carbon sequestration from mitigation strategies such as no-till or conservation tillage practices, residue management, use of cover crops, and restoration and reserve actions (Conant et al., 2001; West and Post, 2002). These studies showed that as farming techniques are improved to maximize yield and minimize disturbance, SOC can be maintained and perhaps even increased over time.

However, the effect of altered management on agricultural soil's ability to store or emit carbon is unresolved, largely as a result of conflicting evidence. For example, some studies on the effects of nitrogen fertilizer indicated a decrease in SOC caused by increased decomposition (Khan et al., 2007; Russell et al., 2009), while others reported an increase in SOC from increased

biomass returned to the soil after harvest (Jung and Lal, 2011; Halvorson et al., 1999; Wilts et al., 2004). SOC increases when crop residue is returned to the land (Buyanovsky and Wagner, 1998; Wilhelm et al, 2004; van Groenigen et al., 2011), but residue can also increase decomposition in warm, moist areas (Johnson et al., 2005). Perhaps the disagreement is the result of the large variability and uncertainty of field measurements, which make developing conclusions difficult (Karlen et al., 2011). For example, Smith et al. (2012) found no differences between the residue-returned and residue-harvested treatments, and in some cases the residue-harvested sites had increased SOC. Thorburn et al. (2012) also found no consensus regarding residue harvest and SOC response. Nonetheless, most studies found a loss of SOC with residue harvesting. Although the variability of SOC measurements can be attributed to any number of effects — including topography (Senthilkumar et al., 2009b), SOC baseline (Senthilkumar et al., 2009a), aggregate protection (Ananyeva et al., 2013), and even depth (Kravchenko and Robertson, 2011; Syswerda et al., 2011) — it is generally agreed that if crop residue is used as feedstock for biofuels, additional carbon losses can occur (Karlen et al., 2011).

Soil organic carbon losses can be mitigated through recommended management practices, but studies disagree on the limits of harvestable crop residue to maintain SOC levels in soils. Estimates of harvestable non-grain biomass range from 13% (Tan et al., 2012) to 50% (Blanco-Canqui and Lal, 2009a), with an average of about 25%, although that might require stabilization of SOC (Tan et al., 2012). These estimates consider erosion, soil productivity, maintaining SOC, surface crusting, porosity, aggregate breakdown, compaction, and soil temperature, but the wide range in estimated biomass available for harvest leaves questions regarding the sustainability of cellulosic ethanol. However, because the rate of SOC loss tends to

increase with increased biomass harvest (Lemke et al., 2010), harvesting small amounts of residue for biofuel might be feasible.

Modeling studies can supplement observational data and explore possible differences in SOC by investigating idealized cases. A benefit is that the wide study area can be extended to regional or global scales without resorting to geospatial methods of interpolating sparse data. In this study, we evaluated the influence of cultivation on SOC by using the agriculture version of the Community Land Model (CLM), CLM-Crop (Drewniak et al., 2013). Our analysis includes impacts of changes in land use and also in management practices, such as crop residue harvesting and fertilizer application. A description of the model and the simulations performed is presented in Sect. 2, followed by results and a discussion in Sect. 3 and Sect. 4, respectively.

5.2 Methods

5.2.1 CLM-Crop model description

CLM-Crop, the agriculture version of CLM, includes representations of maize, spring wheat, and soybean crop types with fully coupled carbon-nitrogen cycling (Drewniak et al., 2013). The variation of carbon and nitrogen allocation to plant components with the growth phase of crop development is based on the dynamic vegetation model Agro-IBIS (Kucharik and Brye, 2003). The growth phases are defined as planting, emergence, grain fill, and harvest. Plant date and growth period are determined from the Crop Calendar Dataset (Sacks et al., 2010), and

each phase is reached according to a phenological heat unit (PHU) method (see Drewniak et al., 2013).

Several processes governing nitrogen cycling are included in CLM-Crop to represent nitrogen retranslocation, fertilization, and nitrogen fixation in soybean. Nitrogen retranslocation occurs during the grain fill growth phase, when nitrogen in the leaves and stem are mobilized to meet organ demands. Fertilizer is applied during the emergence phase for 20 days at constant rates of 150 kg/ha for maize, 80 kg/ha for spring wheat, and 25 kg/ha for soybean. The 20-day fertilization period is designed to optimize nitrogen usage and reduce loss of excess nitrogen through denitrification. Soybean nitrogen fixation allows soybean crops to behave as legumes fixing additional nitrogen through roots — a treatment similar to that of the SWAT model (Neitsch et al., 2005).

Harvest occurs as soon as maturity is reached. Grain is removed from the system to represent the consumption of that plant component. The remaining stems and leaves are considered residue and are split into litter and product pools. Litter is returned to the soil through the decomposition process, while product is removed with the grain for uses such as biofuels, animal bedding, etc. The amount of residue returned as litter can be varied for different scenarios. High returns represent sustainable agriculture practices to maintain soil fertility, and low returns are indicative of high cellulosic biofuel usage.

5.2.2 Input data

CLM-Crop requires two types of input: climate data and surface data. The climate data from the National Center for Environmental Protection reanalysis for 1948-2004 (Kalnay et al., 1996) include temperature, wind speed, humidity, precipitation, solar radiation, and surface pressure at 3-hr intervals. Because the spin-up of the model requires over 600 yr of simulation, we cycled through the reanalysis data to reach a steady state (Thornton and Rosenbloom, 2005).

Surface data sets assign the proportion of each land type and plant functional type in a grid cell; crops are grown separately from natural vegetation to eliminate competition for resources. Natural vegetation prescribed from Bonan et al. (2002) includes a generic crop area. Crop distribution for 1992 from Leff et al. (2004) is used to construct maize, wheat, and soybean coverage from the total generic crop area. Because the wheat coverage includes both spring and winter wheat, we model winter wheat as spring wheat in CLM-Crop. Some crop areas overestimated as double cropping in the data set might result in a crop area being counted twice.

In addition to land use, the surface data include the planting dates and growth period of each crop type from the Crop Calendar Dataset (Sacks et al., 2010). Planting date is the average day of year when planting occurs, aggregated from 0.5° resolution to 2.8° for CLM-Crop. In regions where data are not available, Sacks et al. (2010) used nearest-neighbor extrapolation to infer planting date. Growth period is calculated in Sacks et al. (2010) as the average number of PHUs between the average planting date and the average harvest date for the 30-yr Climatic Research Unit data set (New et al., 1999).

5.2.3 Simulations

CLM-Crop was run at a resolution of 2.8° × 2.8° by using the spin-up procedure in Thornton and Rosenbloom (2005). During spin-up, only natural vegetation was active, and croplands were simulated as grass until a steady SOC state was reached. At the end of the spin-up, the land use was converted to include agriculture, representative of the early 1990's land use maps from Leff et al. (2004). CLM does not have a dynamic vegetation capability when crops are active, so land use/land cover is held constant for the remaining simulations. Several case studies were designed and run to evaluate the influence of management practices on SOC (Table X). Each case study was run for a total of 171 years (three complete cycles of the 1948-2004 data) at an hourly time step to represent the most intense cultivation period in North America (Ramankutty and Foley, 1999). However, we consider only the last 57 yr of simulation for analysis with averaged data. The control simulation, representing current fertilizer and management practices over North America, is compared to an extension of the spin-up, with crops represented as grass. Additional experiments compared the impact on soil carbon from four agricultural practices (high, medium, and low residue levels and zero fertilizer) with our control simulation.

Table X. CLM-Crop simulations performed.

Run name	Land use	Fertilizer	Residue
Control	Leff et al., 2004	Yes	70% — all crops
High residue	Leff et al., 2004	Yes	90% — all crops
Medium residue	Leff et al., 2004	Yes	30% — maize 30% — wheat 40% — soybean
Low residue	Leff et al., 2004	Yes	10% — all crops
No fertilizer	Leff et al., 2004	No	70% — all crops
Grass	Bonan et al., 2002	Not applicable	Not applicable

To investigate the effects of land use changes on SOC, different residue management practices, and varied fertilizer application, the results from six scenarios were analyzed (Table X). First, conventional crop management (control run, 70% residue) is compared with crops simulated as grass (grass run). Second, effects of high (90%), medium (30-40%), and low (10%) residue are compared with values for the control run. Third, the effect of no fertilizer application (with 70% residue) is evaluated by comparison with the control run.

5.3 Results

5.3.1 Soil organic carbon

Simulated SOC values from the control run range from < 2 kg C m^{-2} in the Southwest to > 20 kg C m^{-2} in the northern United States (Figure 5.1). Average SOC values are lower in crop ecosystems than in natural vegetation systems because of biomass removal and other land management. The total stored SOC over all land surface types in the United States, as calculated

by CLM-Crop, is 84 Pg C, which falls within the range of previous estimates of 78-85 Pg C (Kern, 1994). CLM-Crop-simulated SOC for agriculture sites over the contiguous United States (CONUS) has a pattern similar to that of total SOC, with higher SOC in the northern part of the country and lower SOC in the southern regions.

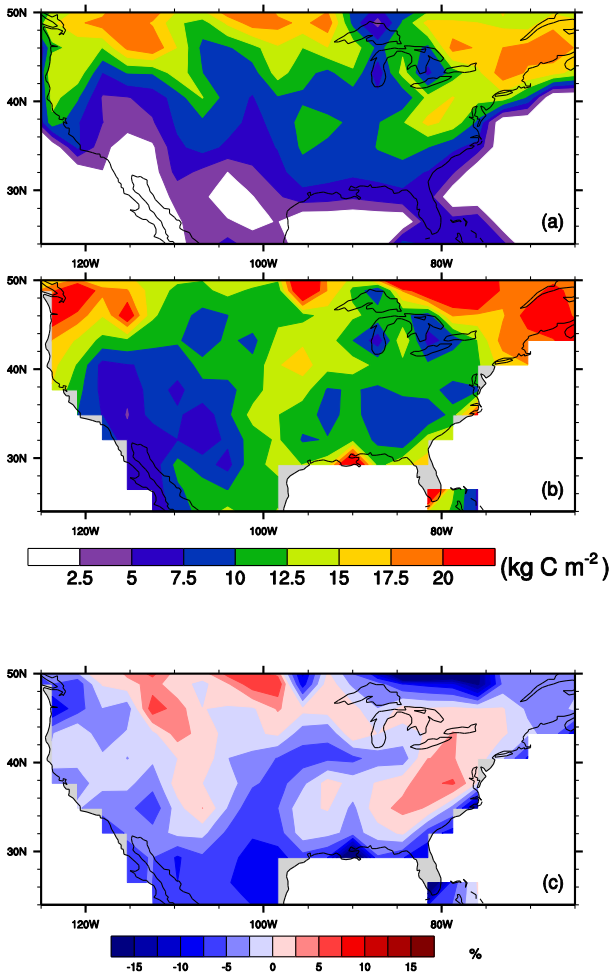

Figure 5.1. (a) Total SOC (kg C m^{-2}) simulated by CLM-Crop over the contiguous United States. (b) Total SOC from the IGBP over the same domain as in (a). (c) Percent difference between (a) and (b).

The general spatial pattern of the model-calculated SOC over CONUS is evaluated by using available spatially gridded data sets of SOC. The data developed by the global soil carbon International Geosphere-Biosphere Program (IGBP; Global Soil Data Task Group, 2000) for CONUS are summarized in Figure 5.1b. The SOC pattern and magnitude are similar to the model-calculated values (Figure 5.1a). The differences between the model-calculated SOC and the IGBP data set are shown in Figure 5.1c. In most regions, the percent difference between the data set and the model simulation is < 5%. Areas with higher percent differences are in boreal regions, where CLM tends to underestimate soil carbon (Koven et al., 2013).

Figure 5.1 includes both managed and natural lands. To evaluate the model-simulated SOC over agricultural lands, we selected self-identified measurements of SOC from agricultural lands available from the International Soil Carbon Network (ISCN; 2014). This data set has over 4,000 unique SOC measurements to 1-m depth from croplands over CONUS. Although CLM soil depth (3.8 m) is deeper than the observations (1 m), since nearly two-thirds of SOC is found within the top 1 m (Jobbagy and Jackson, 2000), the bulk of the soil carbon is still captured in the observations. Because the ISCN data were collected over a wide variety of soils, at different points in the crop cycle and different times since the change in land used, variability is large, and the number of outliers from the median of the sample is significant. The plot in Figure 5.2 shows the range of values with significant occurrences in the upper quartile and above the 90th percentile of the distribution. We filtered out outliers with SOC measurements > 50 kg C m^{-2} in this figure only to improve readability of the graph, since only a small portion (2.5%) of the measured values were higher than 50 kg C m^{-2} and SOC in agriculture lands is typically less than 50 kg C (Kern et al., 1994; Mishra et al., 2010). The model results for the grid cells identified as

cropland are included in Figure 5.2. The model results have a smaller range than the ISCN data, as would be expected for SOC values extracted at the end of the simulation period and post-harvest. In addition, the SOC in the model is less variable because of the larger grid cells with uniform soil type. Nevertheless, the median SOC values simulated by CLM-Crop fall within range of the middle 50% of the ISCN measurements (Figure 5.2), and thus the simulated values are comparable, on average, with the observations. In order to compensate for the mismatch of soil depth, we added an additional 36% of SOC to the observed stocks (to account for the ~1/3 carbon between 2-3 m soil depth; Jobbagy and Jackson, 2000). The resulting increase in observed SOC (not shown) caused median CLM-Crop SOC stocks to fall outside the 50 percentile of the observations, but the top 75 percentile of CLM SOC still fall within the observed range.

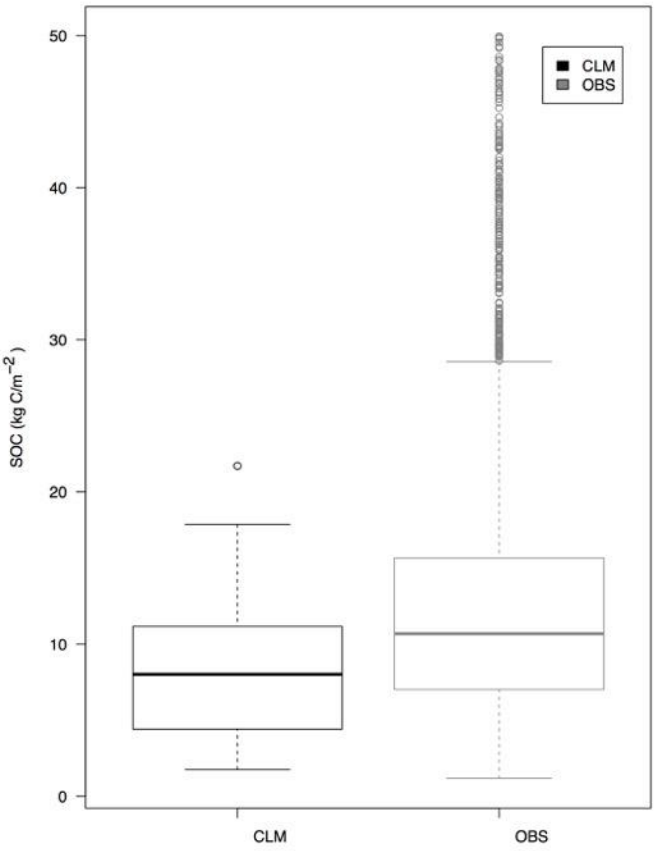

Figure 5.2. Box plot of the weighted average total SOC over croplands, as simulated in CLM-Crop and in observations from the ISCN. Observations reporting > 50 kg C m^{-2} were removed from the analysis.

In a further evaluation of the model's performance over agricultural lands, we completed a site-by-site comparison of modeled SOC to observed SOC. We applied a filter to separate soil over the modeling domain into three types (clay, sand, and silt), to examine the model behavior against the different textures. Figure 5.3 plots simulation results versus observations of SOC for values selected as described above. Each point indicates the mean observational SOC stock at the

model grid scale with the standard deviation. The plot indicates that although the model does tend to underestimate soil carbon over croplands, CLM does reasonably well at catching a wide range of SOC values at agricultural sites for all soil textures. The model does not capture the individual site observations well (RMSE = 13.1 kg C m^{-2}; R^2 = 0.016), due to the high spatial variability. CLM tends to simulate high SOC in sandy soils, low SOC for silt soils, and clay SOC in between, however the soil texture is determined from the model data and therefore may not accurately represent the soil texture of the observations. This result is encouraging, in view of difficulties in comparing CLM-Crop-simulated SOC with observations at agriculture sites. First, the large grid size used in the model simulation cannot resolve the small-scale variability between farm-scale measurements, which are apparent from the large standard deviation in observations. Second, the model is run with static management for long time periods and cannot capture changes in management or land use over long temporal and large spatial resolutions while observations are taken over various time frames with vastly different land use history. Finally, measurements are 1 m depth, and CLM-Crop estimates SOC for the total soil column (> 300 cm). When we attempt to adjust the observed SOC to include carbon at deeper soil layers (by adding ~1/3 more carbon as in Figure 5.2), RMSE increases to 18.8 kg C m^{-2}, although R^2 did not change. Despite these challenges, CLM can capture the range of SOC present at many agriculture sites and in many cases CLM SOC estimates fall within the standard deviation of the observations.

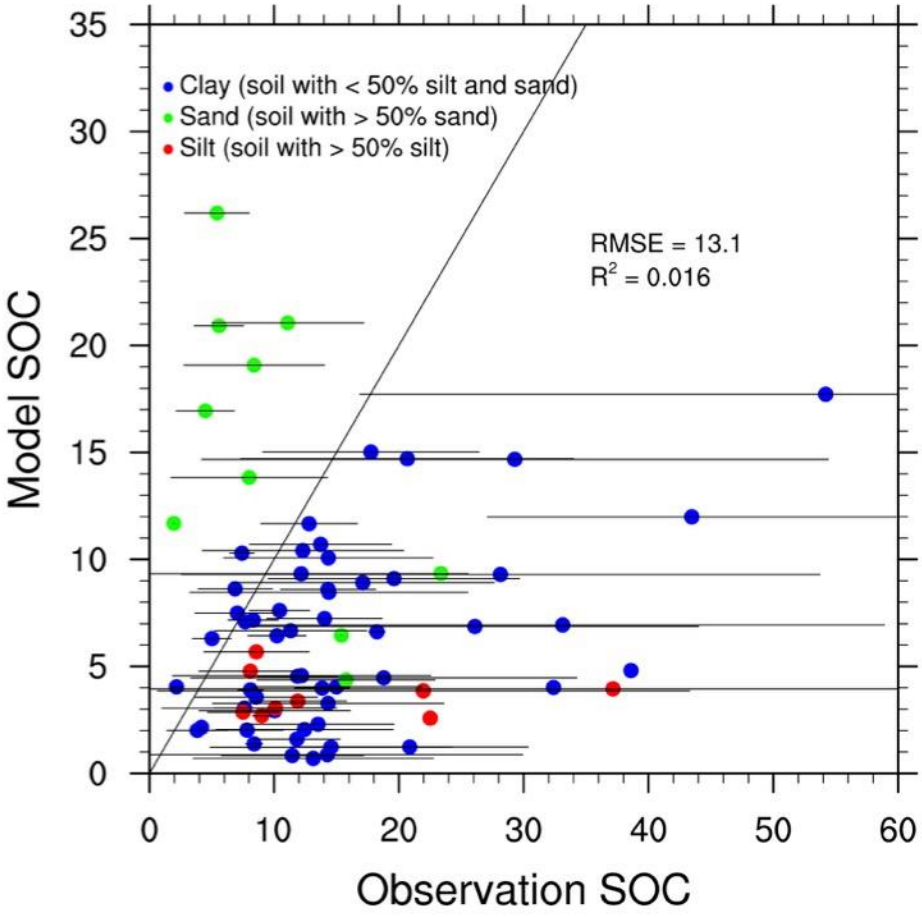

Figure 5.3. CLM-modeled SOC (kg C m^{-2}) versus ISCN observations for model derived soil texture types clay, sand, and silt. Each point represents the mean observed SOC value in the grid cell; error bars show the standard deviation. The black line represents the 1:1 ratio.

In order to explore the model performance further, we examined the effect of climate variability on SOC stocks. CLM SOC stocks decrease with increasing mean annual temperature and total annual precipitation (Figure 5.4), which is also supported by observations. Higher temperatures and soil moisture generally result in higher below ground activity and therefore faster turnover of soil carbon (Wei et al., 2014). Natural vegetation follows the same temperature

trends, but regions with higher annual precipitation indicate higher SOC stock. This is possibly the result of increased productivity when precipitation is high, however the variability in natural vegetation is quite large making conclusions difficult.

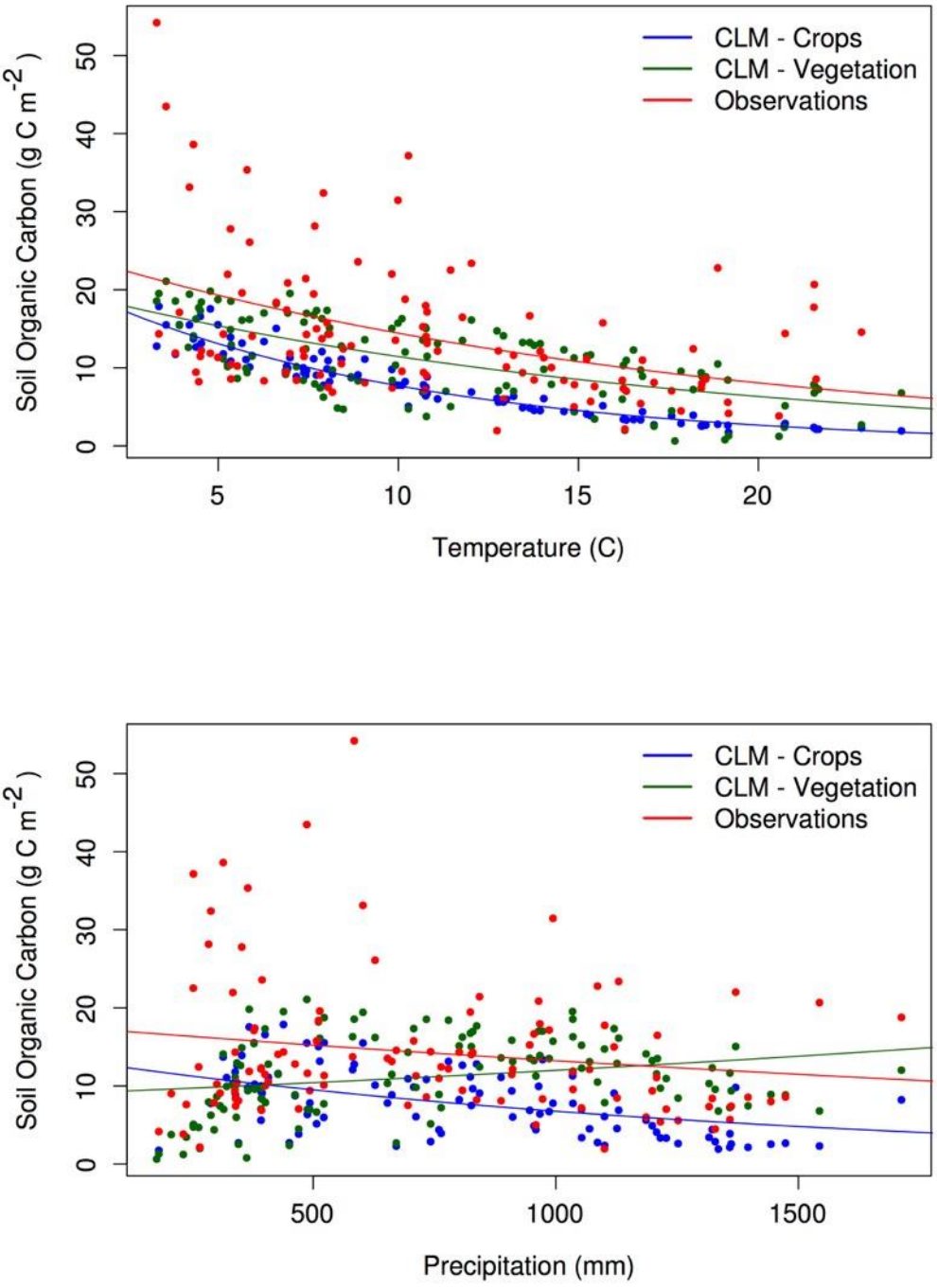

Figure 5.4. The effects of temperature (top) and precipitation (bottom) on SOC stock from CLM crops (blue) and natural vegetation (green) and ISCN observations (red).

Finally, we also consider the ability of the model to capture temporal changes in SOC from land use conversion. Percent SOC loss since conversion from forest to agriculture, as summarized in Wei et al. (2014), is plotted in Figure 5.5 over temporal periods ranging from 1-207 years with a subset (500 points) of CLM SOC percent loss taken from random grids and time periods. Although CLM does not simulate the rapid loss of SOC that occurs in some field observations, by the end of the simulation, CLM does capture the range of SOC loss as seen in observations. Initial lower SOC stocks likely cause the initial modest decline in SOC simulated by the model, since SOC loss increases with increasing initial SOC concentration (Wei et al., 2014). This result highlights CLMs ability to capture changes in SOC over long time periods.

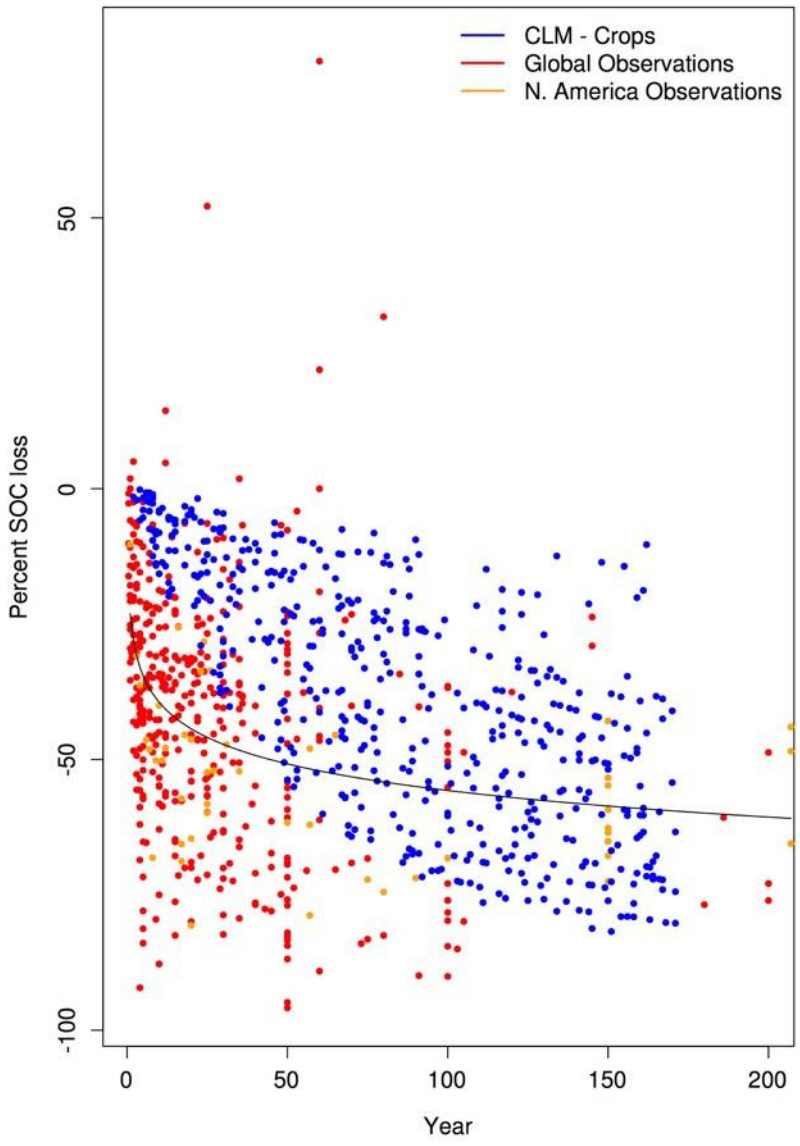

Figure 5.5. Percent decrease of SOC after conversion from natural vegetation to cropland. Percent decrease data from Wei et al. (2014) are in red (US points are orange) and CLM percent loss is blue.

5.3.2 CLM-Crop-simulated changes in soil carbon

Most grid cells lost between 3% and 45% of total SOC, averaged across the grid cell. The amount of SOC lost was correlated with the size of the agriculture land base; higher agriculture land use resulted in larger SOC loss. Individual crop soil columns indicate high losses of SOC, up to a maximum of 75% of total SOC, although average soil loss is 33-51%. Total loss also varied with crop type; maize and wheat lost about 10% less SOC than soybean. This is understandable, given the low residue of soybean crops, although this result varied with location. For example, total simulated SOC loss over maize and soybean soil columns at the Bondville site in Illinois was 48%. At the Mead, Nebraska, site, losses of SOC for maize and soybean columns were approximately 44% and 52%, respectively.

While these site-level SOC losses are comparable with observations (Lal, 2004), comparison with the SOC values in the control simulation might be exaggerated as a result of the subgrid hierarchy, because the accumulated SOC estimated by the grass simulation was influenced by all vegetation types in the soil column, while the soil column in the control simulation only included one crop type. In addition, Ramankutty and Foley (1999) showed that most early croplands from the late 1800s were formed through deforestation and later prairie removal. This implies that our estimation might be exaggerated, because grassland ecosystems can hold more carbon than forests (Schlesinger, 1997). Overall, a 10% loss in total SOC over the United States between the control run and the grass run accounts for a nationwide carbon loss of more than 8 Pg (Figure 5.6).

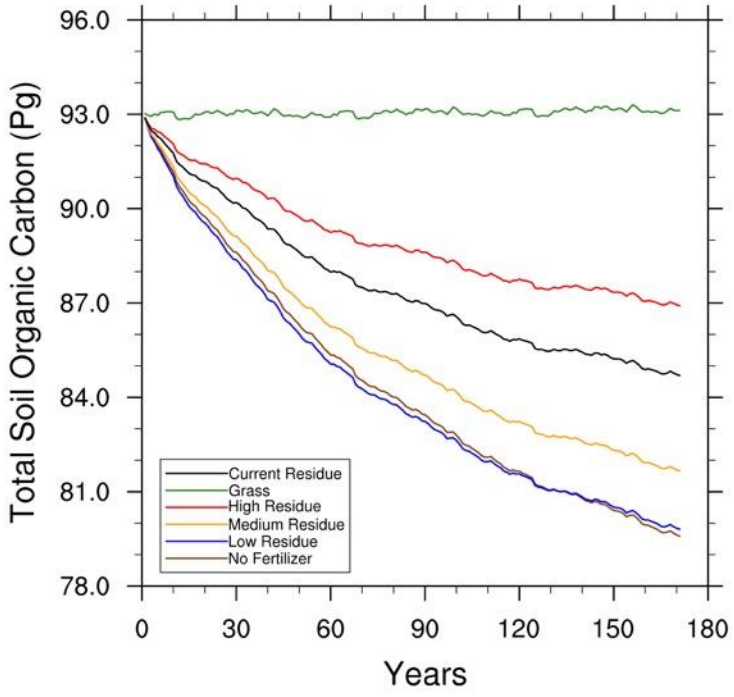

Figure 5.6. Simulated change in total U.S. SOC (Pg C) due to agricultural land management for all scenarios.

Residue management can have the largest impact on soil carbon. Increasing the residue left on the field to 90% results in a 2.6% increase of SOC, but allowing a 10% residue amount (as a potential result of increased cellulosic biofuel demand) leaves an SOC decrease of over 5.7%. The difference between these two scenarios is over 7 Pg C, almost the same amount as the total carbon loss due to agricultural land use. Interestingly, we found no notable differences between crop responses. Even a more modest decrease in the residue returned to the field (30-40%) results in a 3.5% loss of SOC compared to the control simulation. Increasing the residue

harvest will increase the amount of SOC loss (Anderson-Teixeira et al., 2009; Blanco-Canqui and Lal, 2009b). Harvesting residue results in the loss of not only soil carbon, but also soil fertility, indicated by declining yields (Figure 5.7). This implies that increased residue harvest for cellulose might result in expansion of croplands to counter yield declines.

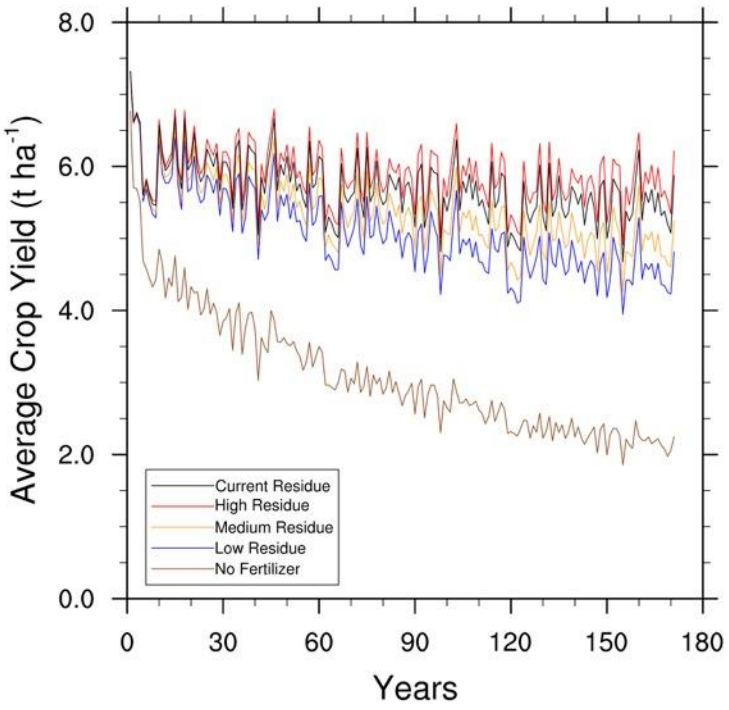

Figure 5.7. The effect of agricultural land management change on crop annual average nitrogen uptake.

Eliminating fertilizer use showed the biggest impact on yields and SOC, simulating over 6% loss (Figure 5.6). Globally, decreases in yields of roughly 60-70% occurred for maize and wheat, but soybeans, relying less on fertilizer inputs, suffered a 22% decrease in yields. The different response between plant types was large: individual maize and wheat soil columns lost an average of 63% SOC, whereas soybean only lost 11%. Despite low yields, leaving 70% residue allowed carbon inputs to maintain nearly the same SOC level as in the run with low residue return. This indicates a critical role for fertilization in soil carbon storage, without which an additional 5 Pg C might be lost due to cultivation. The observed result is not surprising, as fertilizer contributes to the total biomass accumulated during crop development, and increased biomass returned as residue will allow the soil to retain some of the nutrients taken up during crop growth, improving the soil fertility.

5.4 Discussion

CLM-Crop has proven to be a valuable tool for evaluating changes in soil carbon under various management practices. Our results indicate that the SOC for agricultural sites will be reduced through any management practice while disturbance continues, with the total amount lost depending on the management practice. Model-estimated U.S. losses of SOC due to current cultivation practices are around 10%, with a potential for greater loss as the amount of harvested residue increases.

The amount of biomass residue left on the field after grain harvest has the most significant effect on SOC. Cellulosic biofuels rely on harvesting the stems and leaves of crops,

resulting in an additional 5% loss of carbon within the soil system. Currently, model subgrids growing a single crop type on an independent soil column typically lose 33-51% of SOC, and that loss increases to nearly 90% when residue is harvested. Over long time scales, this effect can degrade the sustainability of the soil for crop growth and can negatively affect yield. For example, plant nitrogen uptake (Figure 5.8) decreased linearly with increasing residue harvest. The high residue returns uptake 7.4% more N than the current residue runs, whereas medium and low residue returns have 6.6% and 15.6% lower N uptake, respectively. When fertilizer is not included, the resulting N uptake is 57% lower. This impact is transferred to yields (Figure 5.7) resulting in 9% and 17% lower yields for the medium and low residue returns, respectively. Thus, the effects of residue management on SOC are very important, and increasing the amount of residue used for cellulosic ethanol production could have a significant impact on soil carbon storage and ultimately plant productivity. Leaving plant residue from crop production in the soil decreases the amount of carbon lost to the atmosphere. However, meeting cellulosic biofuel demand through cultivation of managed grasses such as switchgrass and Miscanthus has been shown to increase soil carbon storage over time (Anderson-Teixeira et al., 2009), most likely because nutrient demands and management practices are different for these types of biofuel crops.

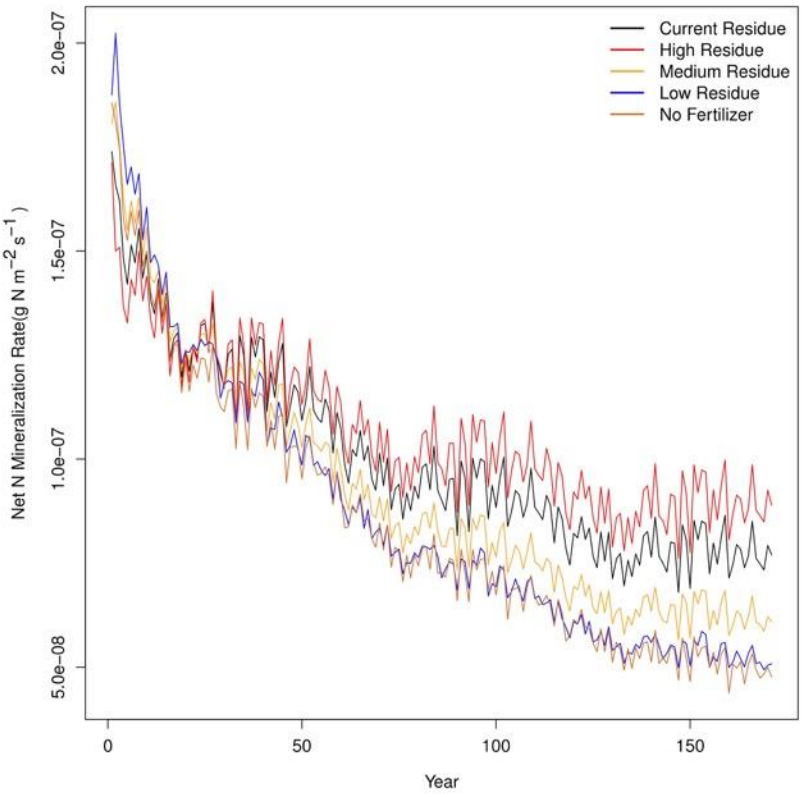

Figure 5.8. The effect of agricultural land management change on annual crop yield.

Disagreement between studies about the possible effect of fertilizer on SOC leaves this management practice open for further research. Our findings suggest that fertilizer use might improve yield and increase the amount of carbon returned to the soil in crop residue; however, increased residue removal for biofuels could reduce this effect. As fertilizers improve and are applied to maximize plant uptake while minimizing loss to leaching and denitrification, fertilizer might provide an important tool for farmers to mitigate the soil carbon loss due to increasing residue harvest for biofuel use. However, care must be taken to ensure that fertilizer inputs do

not exceed plant uptake, which could result in increased nitrogen leached into the groundwater and increased greenhouse gas emission of N_2O via nitrification and denitrification pathways. The effect of increased decomposition when fertilizer is used also needs to be explored.

Expanding the model to incorporate other management practices (rotation, tillage, irrigation, etc.) is important activity for future model development. Erosion, for example, is expected to increase as a result of crop residue harvest (Lal and Pimentel, 2007). This secondary effect of residue harvest can have multiple consequences. First, soil fertility will decline with the loss or transport of soil organic matter. Second, erosion processes result in the breakdown of soil aggregates promoting oxidation of SOC. Both effects will reduce nutrient and water holding capacities of the soil (Lal and Pimentel 2008). Finally, the loss of nutrients will result in a decline of crop productivity, further enhancing SOC loss. As such, our result should be considered a lower bound estimate of SOC loss from residue harvest. Including these effects and expanding agricultural models to a global scale should be a priority for future model development. Given the challenges comparing with observations, focusing on model developments that capture cropland SOC dynamics is equally important as developing datasets that can be used for climate model validation, especially considering the increasing complexity of ESMs that include cropland representation. Although the crop representation in CLM-Crop is flexible enough for expansion to a global scale, rigorous testing is needed to ensure that crop behavior is consistent with regional observations.

There are some limitations to our modeling approach that lead to uncertainties in the model prediction of SOC. For example, changes in land use and land cover are not included in

CLM. Historical changes in land use indicate a steady increase in cultivated land which peaked in the 1940's and declined thereafter (Waisanen and Bliss, 2002). Using a modern land use cover over the historical period may result in an over prediction of SOC loss, because the model will overestimate the agricultural land base in some (early) years and the model won't capture increases in SOC when agriculture land is abandoned. This also limits the influence of beneficial agriculture practices such as crop rotation and fallowing. Historical changes in land management are also not represented in the model, such as changes in residue harvest over time or organic matter additions. For example, Lal et al. (1999) suggest early cultivation removed residue following harvest until after 1940 when residue was returned to the field. The high spatial variability and difficulty finding these types of historical data is a major challenge for trying to add these features to CLM.

Finally, further research is needed for full evaluation of the importance of agro-ecosystem impacts on soil carbon. We have shown here that SOC loss can vary greatly, depending on management practices. Practices such as residue management can have significant impact on SOC retained in agricultural soils, with higher residue removal from soil leading to higher SOC losses. Use of fertilizer can compensate for some of the loss, but the benefit is limited. Further modeling studies are important for simulating these competing effects on carbon storage. Our study suggests that considerable care is needed in designing appropriate management practices to realize the full carbon mitigation benefits of using biofuels from cellulosic ethanol.

5.5 References

Ananyeva, K., Wang, W., Smucker, A. J. M., Rivers, M. L., and Kravchenko, A. N. (2013), Can intra-aggregate pore structures affect the aggregate's effectiveness in protecting carbon? *Soil Biology and Biogeochemistry*, 57, 868-875.

Anderson-Teixiera, K., Davis, S. C., Masters, M. D., and Delucia, E. H. (2009), Changes in soil organic carbon under biofuel crops. *Global Change Biology Bioenergy*, 1, 75-96.

Blanco-Canqui, H., and Lal, R. (2009a), Crop residue removal impacts on soil productivity and environmental quality. *Plant Sciences*, 28(3), 139-163.

Blanco-Canqui, H., and Lal R. (2009b), Corn stover removal for expanded uses reduces soil fertility and structural stability. *Soil Sci. Soc. Am. J.*, 73, 418-426.

Bonan, G. B., Levis, S., Kergoat, L., and Oleson, K. W. (2002), Landscapes as patches of plant functional types: An integrating concept for climate and ecosystem models. *Global Biogeochem. Cy.*, 16, 1021, doi:10.1029/2000GB001360.

Buyanovsky, G. A., Wagner, G. H. (1998), Changing role of cultivated land in the global carbon cycle. *Biol. Fertil. Soils*, 27, 242-245.

Conant, R. T., Paustian, K., and Elliott, E. T. (2001), Grassland management and conservation into grassland: Effects on soil carbon, *Ecological Applications*, 11, 343-355.

Dou, F., and Hons, F. M. (2006), Tillage and nitrogen effects on soil organic matter fractions in wheat-based systems. *Soil Sci. Soc. Am. J.*, 70, 1896-1905.

Drewniak, B., Song, J., Prell, J., Kotamarthi, V. R., and Jacob, R. (2013), Modeling agriculture in the Community Land Model. *Geoscientific Model Development*, 6, 495-515, doi:10.5194/gmd-6-495-2013.

EISA, Energy Independence and Security Act of 2007, H.R. 6, 110th Cong (2007). Retrieved from GPO Access database: http://frwebgate.access.gpo.gov/cgi-bin/getdoc.cgi?dbname=110_cong_bills&docid=f:h6enr.txt.pdf.

Fargione, J., Hill, J. Tilman, D. Polasky, S., and Hawthorne, P. (2008), Land clearing and the biofuel carbon debt. *Science*, 319, 1235-1238.

Gibbs, H. K., Johnston, M., Foley, J. A., Holloway, T., Monfreda, C., Ramankutty, N., and Zaks, D. (2008), Carbon payback times for crop-based biofuel expansion in the tropics: The effects of changing yield and technology. *Environ. Res. Let.*, 3, 034001, doi:10.1088/1748-9326/3/3/034001.

Global Soil Data Task Group. (2009). Global Gridded Surfaces of Selected Soil Characteristics (IGBP-DIS), International Geosphere-Biosphere Programme - Data and Information System, retrieved from http://www.daac.ornl.gov, doi:10.3334/ORNLDAAC/569.

Halvorson, A. D., Reule, C. A., and Follett, R. F. (1999), Nitrogen fertilization effects on soil carbon and nitrogen in a dryland cropping system. *Soil Sci. Soc. Am. J.*, 63, 912-917.

Hooker, B. A., Morris, T. F., Peters, R., and Cardon, Z. G.: Long-term effects of tillage and corn stalk return on soil carbon dynamics, *Soil Sci. Soc. Am. J.*, 69, 188-196, 2005.

Houghton, R. A., Hackler, J. L., and Lawrence, K. T. (1999), The U.S. carbon budget: Contributions from land-use change. *Science*, 285, 574-578.

Huggins, D. R., Allmaras, R. R., Clapp, C. E., Lamb, J. A., and Randall, G. W. (2007), Corn-soybean sequence and tillage effects on soil carbon dynamics and storage. *Soil Sci. Soc. Am. J.*, 71, 145-154.

Hughes, J. K., Lloyd, A. J., Huntingford, C., Finch, J. W., Harding, R. J.: The impact of extensive planting of Miscanthus as an energy crop on future CO_2 atmospheric concentrations. *GCB Bioenergy*, 2, 79–88, 2010.

International Soil Carbon Network, (2014). International soil carbon database, retrieved from http://www.fluxdata.org/nscn/SitePages/ISCN.aspx.

IPCC, (2013). Climate Change 2013: The Physical Science Basis. Contribution of Working Group I to the Fifth Assessment Report of the Intergovernmental Panel on Climate Change, edited by Stocker, T. F., Qin, D., Plattner, G.-K., Tignor, M., Allen, S. K., Boschung, J., Nauels, A., Xia, Y., Bex V., and Midgley, P. M. (Eds.). Cambridge, United Kingdom and New York, NY, USA: Cambridge University Press.

Jobbagy, E. G., and Jackson, R. B. (2000), The vertical distribution of soil organic carbon and its relation to climate and vegetation. *Ecological Applications*, 10(2), 423-436.

Johnson, J. M. F., Reicosky, D. C., Allmaras, R. R., Sauer, T. J., Venterea, R. T., and Dell, C. J. (2005), Greenhouse gas contributions and mitigation potential of agriculture in the central USA. *Soil and Tillage Research*, 83, 73-94.

Jung, J. Y., and Lal, R. (2011), Impacts of nitrogen fertilization on biomass production of switchgrass (Panicum virgatum L.) and changes in soil organic carbon in Ohio. *Geoderma*, 166, 145-152.

Karlen, D. L., Lal, R., Follett, R. F., Kimble, J. M., Miranowski, J. M., Cambardella, C. A., Manale, A., Anex, R. P., and Rice, C. W. (2009), Crop residues: the rest of the story. *Environ. Sci. Technol.*, 43, 8011–8015.

Karlen, D. L., Varvel, G. E., Johnson, J. M. F., Baker, J. M., Osborne, S. L., Novak, J. M., Adler, P. R., Roth, G. W., and Birrell, S. J. (2011), Monitoring soil quality to assess the sustainability of harvesting corn stover. *Agronomy Journal*, 103, 288-295.

Kalnay, E., M. Kanamitsu, R. Kistler, W. Collins, D. Deaven, L. Gandin, M. Iredell, S. Saha, G. White, J. Woollen, Y. Zhu, M. Chelliah, W. Ebisuzaki, W. Higgins, J. Janowiak, K., Mo, C., Ropelewski, C., Wang, J., Leetmaa, A., Reynolds, R., Jenne, R., and Joseph, D.

(1996), The NCEP/NCAR 40-year reanalysis project. *Bull. Amer. Meteor. Soc.*, 77, 437-470.

Kern, J. S. (1994), Spatial patterns of soil organic carbon in the contiguous United States. *Soil Sci. Soc. Am. J.*, 58, 439-455.

Khan, S. A., Mulvaney, R. L., Ellsworth, T. R., and Boast, C. W. (2007), The myth of nitrogen fertilization for soil carbon sequestration. *J. Environ. Qual*, 36, 1821-1832.

Kim, H., Kim, S., and Dale, B. E. (2009), Biofuels, land use change, and greenhouse gas emissions: Some unexplored variables. *Environ. Sci. Technol.*, 43, 961-967.

Koven, C. D., Riley, W. J., Subin, Z. M., Tang, J. Y., Torn, M. S., Collins, W. D., Bonan, G. B., Lawrence, D. M., and Swenson, S. C. (2013), The effect of vertically resolved soil biogeochemistry and alternate soil C and N models on C dynamics of CLM4. *Biogeosciences*, 10, 7109-7131.

Kravchenko, A. N. and Robertson, G. P. (2011), Whole-profile soil carbon stocks: The danger of assuming too much from analysis of too little. *Soil Sci. Soc. Am. J.*, 75, 235-240.

Kucharik, C. J., and Brye, K. R. (2003), Integrated BIosphere Simulator (IBIS) yield and nitrate loss predictions for Wisconsin maize receiving varied amounts of nitrogen fertilizer. *J. Environ. Qual.*, 32, 247–268.

Lal, R. (2002), Soil carbon dynamics in cropland and rangeland. *Environmental Pollution*, 116, 353-352.

Lal, R. (2004), Soil carbon sequestration impacts on global climate change and food security. *Science*, 304, 1623-1627.

Lal, R. (2009), Soil quality impacts of residue removal for bioethanol production. *Soil and Tillage Research*, 102, 233-241.

Lal, R., and Bruce, J. P. (1999), The potential of world cropland soils to sequester C and mitigate the greenhouse effect. *Environmental Science and Policy*, 2, 177-185.

Lal, R., and Pimentel, D. Biofuels from crop residues. *Soil and Tillage Research*, 93, 237-238, 2007.

Lal, R., and Pimentel, D. Soil Erosion: A carbon sink or source? *Science*, 319, 1040-1042, 2008.

Lal, R., Kimble, J. M., Follett, R. F., and Cole, C. V. (1999) The potential of U.S cropland to sequester carbon and mitigate the greenhouse effect. Chelsea, MI: Ann Arbor Press.

Leff, B., Ramankutty, N., and Foley, J. A. (2004), Geographic distribution of major crops across the world. *Global Biogeochem. Cy.*, 18, GB1009, doi:10.1029/2003GB002108.

Lemke, R. L., VandenBygaart, A. J., Campbell, C. A., Lafond, G. P., and Grant, B. (2010), Crop residue removal and fertilizer N: Effects on soil organic carbon in a long-term crop rotation experiment on a Udic Boroll. *Agriculture, Ecosystems and Environment*, 135, 42-51.

Mellio, J. M., Reilly, J. M., Kicklighter, D. W., Gurgel, A. C., Cronin, T. W., Paltsev, S., Felzer, B. S., Wang, X., Sokolov, A. P., and Schlosser, C. A. (2009), Indirect emissions from biofuels: How important? *Science*, 326, 1397-1399.

Mishra U., Lal, R., Liu, D., and Van Meirvenne, M. (2010), Predicting the spatial variation of soil organic carbon pool at a regional scale. *Soil Science Society of America Journal*, 74: 906-914.

Mishra, U., Torn, M. S., and Fingerman, K. (2013), Miscanthus biomass productivity within U.S. croplands and its potential impact on soil organic carbon. *Global Change Biology Bioenergy*, 5:391-399. doi: 10.1111/j.1757-1707.2012.01201.x.

McKone, T.E., Nazaroff W.W., Berck P., Auffhammer, M., Lipman, T., Torn, M.S., Masanet, E., Lobscheid, A., Santero, N., Mishra, U., Barrett, A., Bomberg, M., Fingerman, K., Scown, C., Stogen, B., and Horvath, A. (2011), Grand Challenges for life-cycle assessment of biofuels. *Environ. Sci. Technol.*, 45, 1751–1756.

Neitsch, S. L., Arnold, J. G., Kiniry, J. R., and Williams J. R. (2005). Soil and Water Assessment Tool, Theoretical Documentation: Version 2005, Temple, TX: USDA Agricultural Research Service and Texas A&M Blackland Research Center.

New, M., Hulme, M., and Jones, P. D. (1999), Representing twentieth-century space-time climate variability. Part I: Development of a 1961-90 mean monthly terrestrial climatology. *J. Climate*, 12, 829-856.

Pineiro, G., Jobbagy, E. G., Baker, J., Murray, B. C., and Jackson, R. B. (2009), Set-asides can be better climate investment than corn ethanol. *Ecological Applications*, 19, 277-282.

Ramankutty, N. and Foley, J. A. (1999), Estimating historical changes in global land cover: Croplands from 1700 to 1992. *Global Biogeochem. Cy.*, 13, 997-1027.

Russell, A. E., Cambardella, C. A., Laird, D. A., Jaynes, D. B., and Meek, D. W. (2009), Nitrogen fertilizer effects on soil carbon balances in midwestern U.S. agricultural systems, *Ecological Applications*, 19, 1102-1113.

Sacks, W. J., Deryng, D., Foley, J. A., and Ramankutty, N. (2010), Crop planting dates: An analysis of global patterns. *Global Ecology and Biogeography*, doi: 10.1111/j.1466-8238.2010.00551.x.

Schlesinger, W. H. (1997), Biogeochemistry: An Analysis of Global Change, San Diego, CA: Academic Press.

Searchinger, T., Heimlick, R., Houghton, R. A., Dong, F., Elobeid, A., Fabiosa, J., Tokgoz, S., Hayes, D., and Yu, T.-H. (2008), Use of U.S. croplands for biofuels increases greenhouse gases through emissions from land use change. *Science*, 319, 1238 -1240.

Senthilkumar, S., Basso, B., Kravchenko, A. N., and Robertson, G. P. (2009a), Contemporary evidence of soil carbon loss in the U.S. corn belt. *Soil Sci. Soc. Am. J.*, 73, 2078-2086.

Senthilkumar, S., Kravchenko, A. N., and Robertson, G. P. (2009b), Topography influences management system effects on total soil carbon and nitrogen. *Soil Sci. Soc. Am. J.*, 73, 2059-2067.

Smith, W. N., Grant, B. B., Campbell, C. A., McConkey, B. G., Desjardins, R. L., Krobel, R., and Malhi, S. S. (2012), Crop residue removal effects on soil carbon: Measured and inter-model comparisons. *Agriculture, Ecosystems and Environment*, 161, 27-38.

Syswerda, S. P., Corbin, A. T., Mokma, D. L., Kravchenko, A. N., and Robertson, G. P. (2011), Agricultural management and soil carbon storage in surface vs. deep layers. *Soil Sci. Soc. Am. J.*, 75, doi:10.2136/sssaj2009.0414.

Tan, Z., Liu, S., Bliss, N., and Tieszen, L. L. (2012), Current and potential sustainable corn stover feedstock for biofuel production in the United States. *Biomass and Bioenergy*, 47, 372-386.

Thornton, P. E. and Rosenbloom, N. (2005), Ecosystem model spin-up: Estimating steady state conditions in a coupled terrestrial carbon and nitrogen cycle model. *Ecological Modeling*, 189, 25-48.

Thorburn, P. J., Meier, E. A., Collins, K., and Robertson, F. A. (2012), Changes in soil carbon sequestration, fractionation and soil fertility in response to sugarcane residue retention are site-specific. *Soil and Tillage Research*, 120, 99-111.

U.S. Environmental Protection Agency. (2010). Regulation of Fuels and Fuel Additives: Changes to Renewable Fuel Standard Program; Final Rule. Federal Register, 5, 14670-14904.

van Groenigen, K. J., Hastings, A., Forristal, D., Roth, B., Jones, M., and Smith, P. (2011), Soil C storage as affected by tillage and straw management: An assessment using field measurements and model predictions. *Agriculture, Ecosystems and Environment*, 140, 218-225.

Van Pelt, R. S., Baddock, M. C., Zobeck, T. M., Schlegel, A. J., Vigil, M. F., and Acosta-Martinez, V. (2013), Field wind tunnel testing of two silt loam soils on the North American central high plains. *Aeolian Research*, 10, 53-59.

Waisanen, P. J. and Bliss, N. B. (2002), Changes in population and agricultural land in conterminous United States counties, 1790-1997. *Global Biogeochemical Cycles*, 16 (4), doi:10.1029/2001/GB001843.

Wei, X., Shao, M., Gale, W., and Li, L. (2014), Global pattern of soil carbon losses due to the conversion of forests to agricultural land. *Nature*, DOI:10.1038/srep04062.

West, T. O. and Post, W. M. (2002), Soil organic carbon sequestration rates by tillage and crop rotation: A global data analysis. *Soil Sci. Soc. Am. J.*, 66, 1930-1946.

Wilhelm, W., Johnson, J. M. F., Hatfield, J. L., Voorhees, W. B., and Linden, D. R. (2004), Crop and soil productivity response to corn residue removal: A literature review. *Agronomy Journal*, 96, 1-17.

Wilts, A. R., Reicosky, D. C., Allmaras, R. R., and Clapp, C. E. (2004), Long-term corn residue effects: Harvest alternatives, soil carbon turnover, and root-derived carbon. *Soil Sci. Soc. Am. J.*, 68, 1342-1351.

6 CONCLUSION

Climate change is expected to have a significant influence on temperature, the hydrology cycle, extreme events, and sea level rise. The primary driver behind the evolution of land surface models (LSMs) is to capture the interactions between the land and the atmosphere, but LSMs also need to predict changes in vegetation dynamics as a response to climate change. These feedbacks are drivers of climate and are the target of much of the model development work being done today. In order to estimate the full influence of climate on the earth and energy systems, we must include the appropriate ecosystem responses that have significant feedbacks to the energy and carbon cycle. This premise of this thesis is land representation in earth system models falls short of being able to accurately predict Earth's future under climate change. To that extent, I have identified a limited set of areas that can be targets for improvement, all of which influence the carbon cycle. Some of these improvements have been tested in two Earth System Land Models, the Energy Exascale Earth System Land Model (ELM), the newest of climate models available to the community, and the Community Earth System Land Model (CLM). The work to update the LSMs is the first step to a stronger understanding of the biosphere-climate system and will enhance our ability to predict future climate impacts.

I identified in Chapter 2 several processes that are missing in LSMs that are necessary to capture ecosystem response to multiple co-occurring stressors. Some of the model development can be thought of as near-term targets such as a more flexible framework for representing the allocation and storage of vegetation carbon through better carbon-nitrogen coupling, dynamic allocation, and dynamic roots. Other development suggestions can be considered long-term work such as succession, competition, and trait-based modeling. Regardless, all the activities will

impact how vegetation grow and respond to environmental factors with potential for influencing the carbon storage capacity of the land surface.

Addressing two of the suggested developments, dynamic roots and dynamic allocation revealed additional work to be done. Although the changes did impact the productivity of vegetation in the model, the changes were incremental, and the response indicated that the water and nitrogen uptake are still areas of model development that need attention. Particularly, allowing variable water and nitrogen uptake (this could include phosphorus too), with depth and time, could benefit the model greatly and improve performance in those tricky spots (for example the dry season Amazon). These studies also highlighted the importance of integrating water and biogeochemistry. Despite the tight coupling of water and biogeochemistry, current research seems to be considering each independently. They need to be addressed together to really impact model performance and improve predictability.

The most significant impact came from adding agricultural land management to the model. This is not surprising, but it should be alarming in the sense that we are modifying the land without any regard for the consequences. Even more important is the role that humans have played to modify the land through management, land use and land cover change, and the subsequent effects on carbon storage and turnover of those activities. Humans have turned lush forests and prairies into farmland, covered wetlands with impervious asphalt and concrete, withdrawn freshwater for irrigation and drinking, changed the course of rivers, created and destroyed lakes, and fragmented ecosystems through logging, farming, and urban buildup. All these activities have an influence on the carbon cycle, which was highlighted in Chapter 5 in the

change in SOC from agriculture alone, reinforcing the notion that land matters. Our decisions and actions are the biggest player of uncertainty and they are not being accounted for in most ESMs.

One major limitation of this work is the coupling between the atmosphere and land is not addressed. I began in the introduction describing the importance of the land in the climate system and yet, I have not turned on the atmosphere in any of the results presented in this thesis. One argument for this is that the model needs to be tested offline before coupling to the atmosphere as a test of validity. Another argument is the results are revealing in how they stand without coupling the atmosphere. Both of these arguments are compelling, but, the feedbacks between the land and atmosphere are critical to test before the results are to be believed. It is unlikely that the dynamic roots and carbon allocation would change significantly when coupled to the atmosphere. But human land management is likely to have strong interactions with the atmosphere.

Adding to the complexity of this work is the issue of scale. Land processes occur across a variety of spatial and temporal scales. At the resolution of the current ESMs, only some processes can be represented. Others are included empirically or not at all, either because they are believed to be less important to model at the coarse ESM resolution or because they are difficult to observe or impossible to parameterize. Our efforts to bridge across scales are limited. One solution is to couple models of different resolutions (i.e. site model with a regional or global model). But these couplings are generally problematic, as they require models of different languages to communicate effectively. This can lead to a loss of information along the way.

Another method is to scale up point or regional models to global resolutions (or vice versa by scaling down global models to field scale). In the former, additional data is required that is often not available or difficult to validate across large areas. In the latter, models are still missing processes that are important to capture small scale or temporal events. As such, there is a push in the modeling community to develop scale-aware parameterizations that adjust according to resolution. In the meantime, models are tuned separately for coarse and fine resolutions. Observations play a key role in this effort, by highlighting not only the processes that are important, but at which scales they become so.

One final thought is while this thesis has added a few important model processes into LSMs, there are many more, several identified in the results of the studies included here. However, one question remains: are these model improvements significant enough to justify increasing complexity at the expense of a parsimonious model? Each addition comes with more degrees of freedom, extra parameters to tune, increased likelihood of non-convergence, and the possibility of the model becoming unwieldy both to understand and to untangle. On the other hand, each new process added to ESMs give users an opportunity to explore interactions that might not be possible in a lab or in a field. We increase the resolution of the model and begin to resolve finer scale processes. Should all these new processes be added permanently to ESMs – certainly not. But the advances in supercomputing allow modelers to be more bold and adventurous in exploring the earth system. The experiences also provide a chance for modelers and empiricists to share experiences so models and observations can inform each other. The importance of data to drive the design of model development, as well as provide a means to verify and validate model results, cannot be understated.

In short, the brief presence of modern humans on the earth has had significant consequences. We need to understand how our actions have shaped the climate and perhaps minimize our impact as we shape the next phase of the Earth's life cycle. Earth system models are one tool we have to further that understanding. These models will continue to evolve as we learn more from observations with the hope that they will help inform our decisions. After all, our actions related to land matters demonstrate how much land matters.

7 APPENDICES

A. Supplementary Material for Chapter 2

Table I. Summary of previous studies that have investigated nitrogen deposition, drought, and the interactions of ecosystems.

Nitrogen Deposition						
Ecosystem	**PFT**	**Region**	**Study Type**	**Nitrogen Treatment**	**Finding**	**Reference**
NA	NA	Global	Overview	NA	N limited ecosystems have stronger growth responses to N deposition, and N mineralization and leaching rates increase. Diversity changes usually result from N deposition.	Matson et al., 2002
Acer saccharum	BDT	Michigan, USA	N fertilization study	30 kg NO_3^- ha^{-1} yr^{-1}	Observed increases in photosynthesis, woody carbon, and soil carbon; no change in leaf mass or area was found.	Pregitzer et al., 2008
Acer saccharum, *Fagus grandifolia*, and *Picea rubens*	BDT	Maine, USA	N fertilization study	25.2 kg NH_4 ha^{-1} yr^{-1}	Foliar N increased with increasing N deposition.	Elvir et al., 2005
Fagus grandifolia, *Acer saccharum*, and *Betula alleghaniensis*	BDT	North Carolina and Virginia, USA	N deposition gradient study	9–15 kg N ha^{-1} yr^{-1}	N deposition caused increase in foliar N in all species and an increase in basal area in sugar maple.	Boggs et al., 2005
Calluna vulgaris		Europe	N deposition gradient study	1–15 kg N ha^{-1} yr^{-1}	Foliar N increased with increasing N deposition.	Pitcairn et al., 2001
73 forest sites including evergreen needleleaf, evergreen broadleaf, deciduous broadleaf, and mixed forest	NET, BET, BDT	Global (mainly focused on N. America, Europe, and some S. America)	Statistical analysis of FLUXNET data paired with estimates of N deposition	0.5–30 kg N ha^{-1} yr^{-1}	In general, the maximum rate of photosynthesis has a positive nonlinear correlation with N deposition for evergreen needleleaf forests, but no relationship in deciduous forests. A positive relationship between N deposition and foliar N exists, but not for all forests. Separating climate effects on carbon cycle is difficult.	Fleischer et al., 2013

Nitrogen Deposition						
Ecosystem	**PFT**	**Region**	**Study Type**	**Nitrogen Treatment**	**Finding**	**Reference**
Acer saccharum	BDT	Michigan, USA	N deposition gradient study	6.8–11.8 kg N ha^{-1} yr^{-1} (mostly NO_3^-)	N fertilization increased foliar N, but did not stimulate photosynthesis, but nutrient deficiencies may have been present. Nitrogen Use Efficiency (NUE) alsodecreased at treated sites.	Talhelm et al., 2011
Miscanthus	C4 Grass	Illinois	N fertilization study	0 and 224 kg N ha^{-1} (form of urea)	Productivity and yield increased as a result of higher canopy leaf area, but no effect on photosynthesis or photosynthetic capacity.	Wang et al., 2012a
24 most common species in temperate forests	NET, BET, BDT	North-Central USA	Forest inventory analysis	3–11 kg N ha^{-1} yr^{-1}	Nitrogen deposition caused enhanced growth in most species with mycorrhizal associations. Some had no response and a few had negative growth response. Species with ectomycorrhizal associations showed decreased survivorship.	Thomas et al., 2010
Needleleaf, deciduous broadleaf, evergreen boradleaf	NET, BET, BDT	Boreal, temperate, and tropical	Statistical analysis	NA	N addition leads to increased carbon uptake in wood.	de Vries et al., 2014
All	NA	Global	Meta-analysis	low (<100 kg N ha^{-1}) and high (>100 kg N ha^{-1})	N enrichment resulted in increases in foliar N and biomass, more for herbaceous than woody species. The biomass increase effect decreased with increasing latitude and with decreasing precipitation.	Xi and Wan, 2008
Acer saccharum	BDT	Great Lakes region	N fertilization study	30 kg NO_3^- ha^{-1} yr^{-1}	N deposition resulted in increased biomass in stems, increased maximum tree height, and increased growth rate and mortality of small individuals.	Ibanez et al., 2015
Needleleaf boreal	NET	Northeast China	3-year N enrichment experiment in an old growth forest	low (20 kg N ha^{-1} yr^{-1}) medium (50 kg N ha^{-1} yr^{-1}) high (100 kg N ha^{-1} yr^{-1})	Foliar N increased, woody biomass increased, and NPP increased.	Du and Fang, 2014

Nitrogen Deposition						
Ecosystem	**PFT**	**Region**	**Study Type**	**Nitrogen Treatment**	**Finding**	**Reference**
Herbaceous (grasslands)	C3 and C4 grass	India	N fertilization study	60 kg N ha^{-1} yr^{-1} and 120 kg N ha^{-1} yr^{-1} (form of urea)	N deposition caused an increase in biomass and trait shifts leading to a reduction in N-fixing species.	Verma et al., 2014
Temperate mixed forest	NET, BET, BDT	New York, USA	Survey	5-10 kg N ha^{-1} yr^{-1}	Foliar N increased with increasing N deposition.	McNeil et al., 2007
Drought						
Ecosystem	**PFT**	**Region**	**Study Type**	**Water Treatment**	**Finding**	**Reference**
Temperate forests	NET, BET, BDT	United States	Review	NA	Forest response to drought will likely include: reduction in NPP and water use, increase in mortality of small plants, and buildup of undecomposed material on forest floor. Deep-rooted plants and those with substantial carbon reserves have higher chance of survival.	Hanson and Weltzin et al., 2000
Rainforest	NET, BET, BDT	Amazon	Synthesis	NA	Amazon forests are suceptable to water stress through carbon loss.	Phillips et al., 2009
All	All	Global	Review	NA	Drought reduces productivity and weakens carbon uptake, increases vulnerability to wildfire and mortality from both indirect and direct effects.	He et al., 2014
Grasslands	C3 and C4 grass	Europe	Greenhouse experiment with 9 species	Watered to field capacity and watered only when leaves withered.	Drought reduced biomass production and alloction to roots. Drought did not impact Specific Leaf Area (SLA). The impacts of droght varied with provenance.	WeiBhuhn et al., 2011
Pinus halepensis	NET	NA (seed source Mount Carmel, Isreal)	Greenhouse experiment	4 water treatments: 100% (350 mL/week/pot) and 75%, 50%, and 25%	Tree growth most sensitive to high drought, with increased biomass to roots and decreased biomass to stems.	Klein et al., 2011
Quercus ilex	NET	Mediterranean	Precipitation gradient and throughfall exclusion experiment	Along gradient, precipitation increased twofold. Throughfall exclusion experiment experienced ambient and 28% of annual precipitation.	Leaf production and litterfall decreased with decreasing precipitation. Although root production also decreased, the ratio of root to leaf increased with lower water availability. An increasing stem area to leaf area ratio was found with decreasing precipitation, which disapeared after many years and suggests a long-term acclimation process.	Martin-St. Paul et al., 2013
Drought						

Ecosystem	PFT	Region	Study Type	Water Treatment	Finding	Reference
Populus	BDT	Belgium	Study over a dry season	Dry spring resulted in 15–25% less precipitation	Dry season resulted in lower GPP and leaf growth. Increased WUE and root allocation during stomatal closure.	Broeckx et al., 2014
C4 grasses Napier grass and Mulato II	C4 Grass	Palmira, Columbia	Greenhouse experiment	Well watered and progressive drying over 21 days	Drought resulted in a 35% reduction in shoot mass for both grasses and a 20–50% reduction in root biomass. Napier grass sustained carbon assimilation longer, while Mulato conserved water with early stomatal closure.	Cardoso et al., 2015
Tropical forest	BET, BDT	Eastern Amazon	Throughfall exclusion experiment	Two treatments: ambient and 50% reduction in precipitation	No eveidnce found to support changes in carbon allocation or growth rate from drought, no depletion in carbon stores occured. Suggest hydraulics are the cause of mortality.	Rowland et al., 2015
Fagus sylvatica forest	BDT	Germany	Precipitation gradient	540–820 mm/yr	Fine root biomass increases with decreasing precipitation, support optimal partitioning theory.	Hertel et al., 2013
Aspalathus linearis (rooibos)	BDS	South Africa	Greenhouse experiment	Two treatments: weekly watering 100 ml distilled water and no water for 6 weeks.	Decrease in maximum photosynthetic rate and energy storage. Relative growth rate decreased, roots not affected but decline in shoot production. WUE and C/N increased.	Lotter et al., 2014
Fagus sylvatica forest	BDT	Germany	Precipitation gradient and contrasting precipitation years	520–970 mm/yr; one year had 20% less precipitation and one year had 20% more precipitation than average	Decrease in root biomass with decreasing precipitation. Carbon partitioning between root:leaf increased with increasing moisture. Suggest optimal partitioning is relative and not absolute, root turnover should be considered.	Meier et al., 2008
Mediterranean shrubs	BDS, BES	Spain	Greenhouse experiment	Two water amounts: ambient (typical precipitation amounts) and 30% reduction.	More biomass was allocted to roots in water stressed plants. Frequency of water supply did not affect biomass allocation. Biomass was not affected by water supply or frequency.	Pradilla et al., 2009
				N and Drought		
Ecosystem	**PFT**	**Region**	**Study Type**	**Water Treatment**	**Finding**	**Reference**
Perennial grass (*Molinia caerulea*)	C3 Grass	Germany	Fertilization/ drought greenhouse study	N: 0 and 48 kg NH_4NO_3 ha^{-1} yr^{-1} W: 18% less water treatment	N deposition caused increased evaporative demands and increased drought susceptibility. Grasses were unable to control N allocation during senescence.	Friedrich et al., 2012

N and Drought						
Ecosystem	**PFT**	**Region**	**Study Type**	**Water Treatment**	**Finding**	**Reference**
Shrub (*Calluna vulgaris*)	BDS	NA	Fertilization/ drought greenhouse study	N: 0 and 48 kg NH_4NO_3 ha^{-1} yr^{-1} W: 12% less water treatment (30% less soil water content)	N and drought treatment resulted in an increased biomass production, increased shoot:root ratios, and N content in biomass. Drought weakened the growth stimulation from the N treatment.	Meyer-Grünefeldt et al., 2013
Shrub (*Calluna vulgaris*)	BDS	Germany	Fertilization/drought greenhouse and field study	N: 0, 35 kg NH_4NO_3 ha^{-1} yr^{-1} W: 25% reduction in growing season precipitation (35% less soil water content)	Significant nitrogen drought interactions resulted in lower shoot-to-root ratios than expected from individual treatment. Drought susceptibility is dependent on plant age, since investement in above ground biomass is a priority during early development.	Meyer-Grünefeldt et al., 2015
Deciduous woody tree (*R. pseudoacacia*)	BDT	NA	Pot manipulation experiment with three water treatments and two N treatments.	N: 0, 154 mg NH_4NO_3 kg^{-1} dw soil W: water content of 70-75%, 50-55%, and 30-35% of field capacity	Positive effects (i.e., biomass accumulation leaf WUE) from N fertilization were reduced under severe drought, but did result in reduced transpiration water loss.	Liu et al., 2013
Ash (temperate forest)	BDT	Northeast China	Manipulation experiment looking at three water and nitrogen regimes	N: 0, 100 kg NH_4NO_3 ha^{-1} yr^{-1} W: low (33% less), ambient, and high (33% increase) in precipitation	Rubisco increased in leaves under low water and high N treatment, but had no impact on photosynthesis. However, N treatment weakened the reduced growth response caused by low water treatment.	Wang et al., 2012
Picea abies	NET	Czech Republic	N and drought experiment in two 12-year-old stands	N: 0, 100 kg NH4 ha^{-1} yr^{-1} W: 60% precipitation reduction	N and drought resulted in reduced stem biomass, needle length, and fine root biomass. The distribution of roots also occurred with fine roots in deeper soil layers.	Palatova, 2004

N and Drought						
Ecosystem	**PFT**	**Region**	**Study Type**	**Water Treatment**	**Finding**	**Reference**
Desert plants Brassicaceae and Chenopodiaceae (*Malcolmia africana* and *Brassia hyssopifolia*)	C3 Grass or BDS	China	Nitrogen and drought pot experiment, 3 levels of N treatment and 3 levels of water treatment	N: 0, 94, 370 kg N ha^{-1} yr^{-1} W: 60–70%, 30–40%, and 10–20% field capacity	N increased root weight, leaf area, and total biomass, but less so in the drought treatment. Net photosynthetic rate and shoot:root ratio also increased. N deposition in this ecosystem may alleviate some water stress.	Zhou et al., 2011
Pinus sylvestris	NET	Czech Republic	Pot and 12-year-old stand N and drought experiment	N: 0 and 100 kg N ha^{-1} yr^{-1} as NH_4 W: 60% of precipitation	The combined N and drought effect was a reduced aboveground and root biomass in both the stand and pots. Mycorrhizal infection was also reduced.	Palatova, 2002
Mongolian grassland	C3 and C4 Grass	Mongolia	N fertilization study during drought and non-drought years in grazed and non-grazed plots.	N: 0, 3 kg N ha-1 yr-1, 15 kg N ha-1 yr-1 as NH4NO3 W: about 50% of precipitation during drought years	Drought reduced above ground biomass dispite N addition. During non-drought years, high N addition significantly increased biomass. N addition increased recovery after drought.	Kinugasa et al., 2012
Jatropha curcas	BES	Brazil	Greenhouse experiment with 4 N treatments and 4 water treatments	N: 0, 0.8, 1.7, and 2.5 g/plant as NH_4 W: 40%, 60%, 80%, 100% of plant available water	Drought reduced the effects of N (i.e., increased stem basal area and plant height and leaf area growth).	Albuquerque et al., 2013
Larrea tridentata	BES	Desert ecosystem	Two treatments of N and soil moisture	N: 0 and 40 kg N ha^{-1} yr^{-1} W: 7% (w/w) and 15% (w/w) moisture content	Leaf biomass was lower under water stress, but water content did not affect root-to-shoot ratio. N availability did not seem to have an impact on C uptake.	Verburg et al., 2014

B. Supplementary Material for Chapter 3

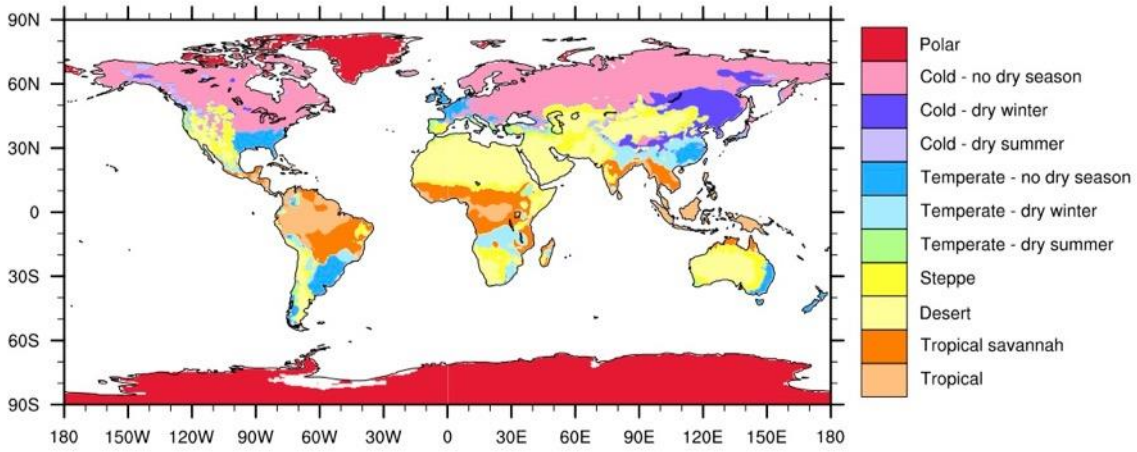

Figure 3.5. Global map of condensed Köppen-Geiger Climate Classification zones based on Peel et al. (2007). Original data downloaded from ORNL DAAC (2017).

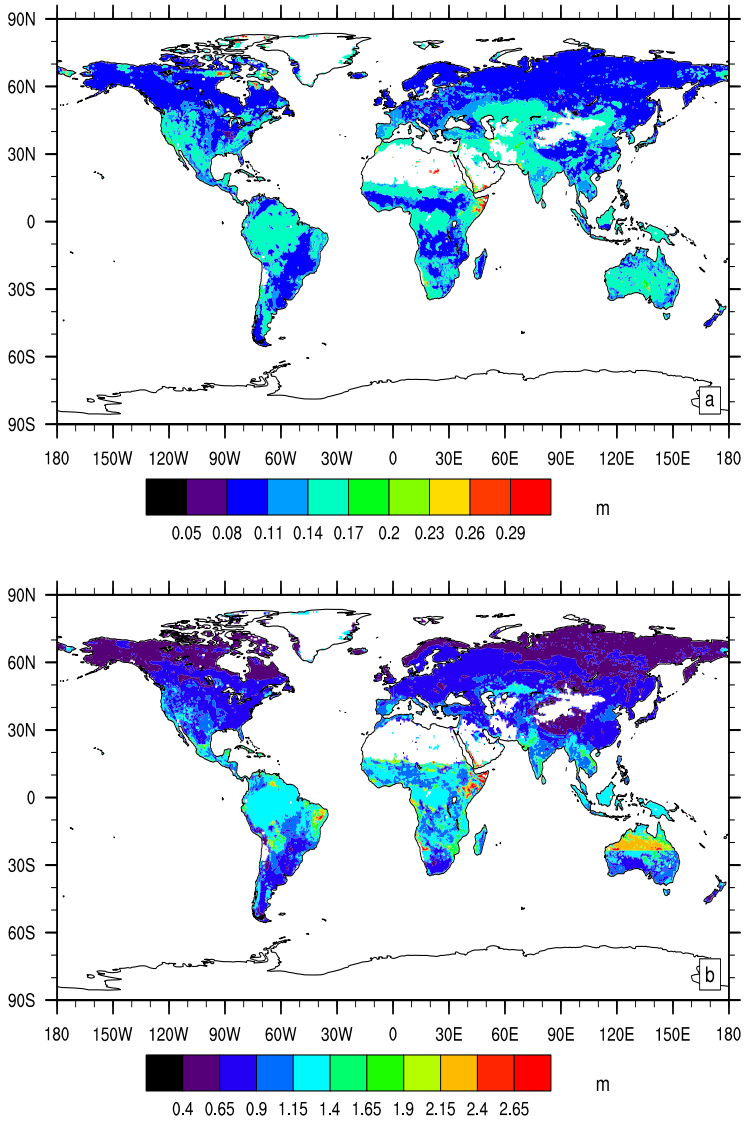

Figure 3.6. Soil layer depth (m) above which (a) 50% and (b) 95% of root biomass exist for the DYNROOT simulation.

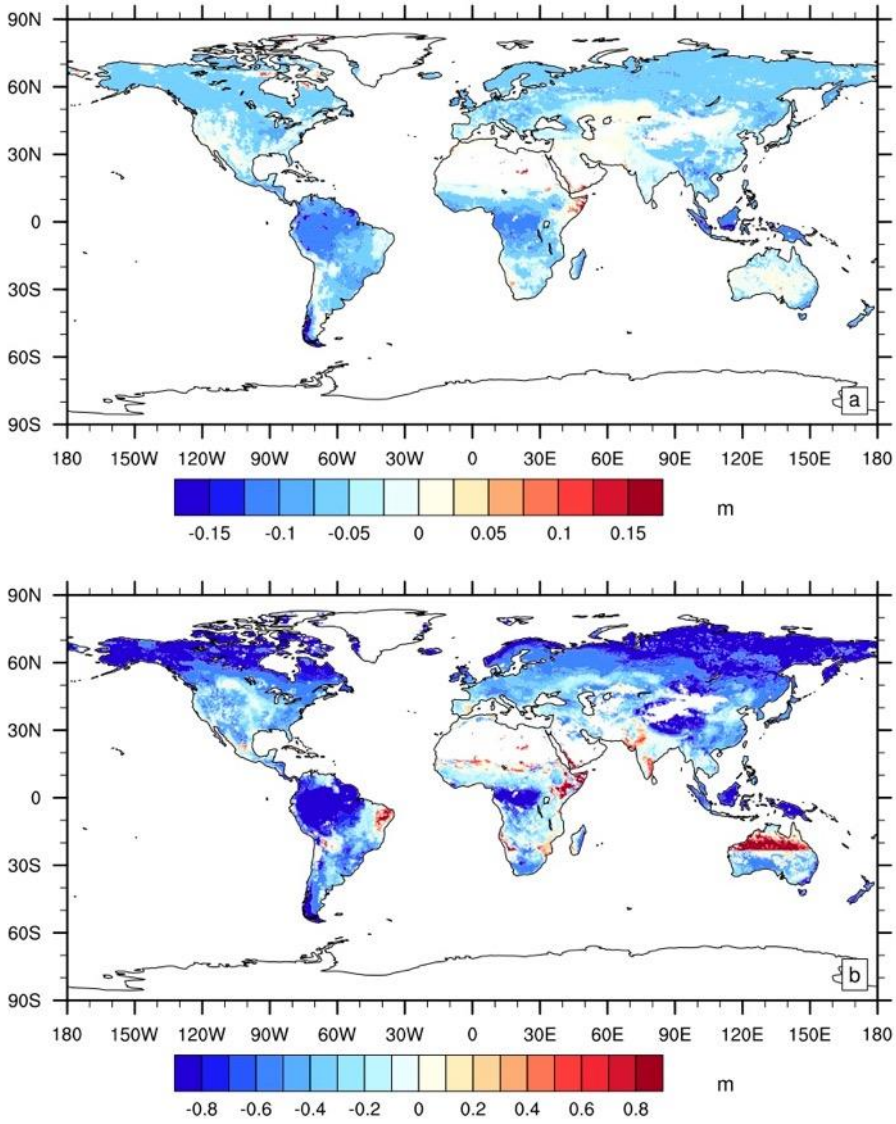

Figure 3.7. Difference in soil layer depth (m) above which (a) 50% and (b) 95% of root biomass exist between DYNROOT and CONTROL (shown as DYNROOT – CONTROL).

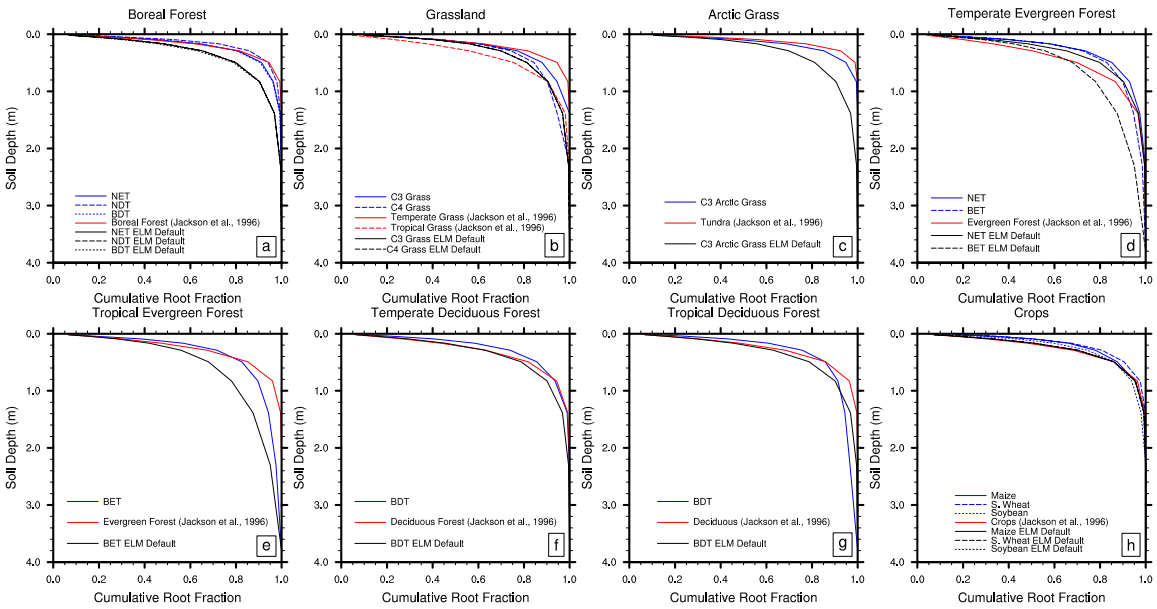

Figure 3.10. Cumulative root fraction averaged different vegetation types in ELM for DYNROOT (blue line), CONTROL (black line), and Jackson et al., 1996 (red line). The vegetation types included are (a) Boreal forest; (b) grassland; (c) arctic grass; (d) temperature evergreen forest; (e) tropical evergreen forest; (f) temperate deciduous forest; (g) tropical deciduous forest; and (h) crops. The PFT(s) in each ecosystem are denoted by a letter combination which represent: NET: needleleaf evergreen tree; NDT: needleleaf deciduous tree, BDT: broadleaf deciduous tree; BET: broadleaf evergreen tree.

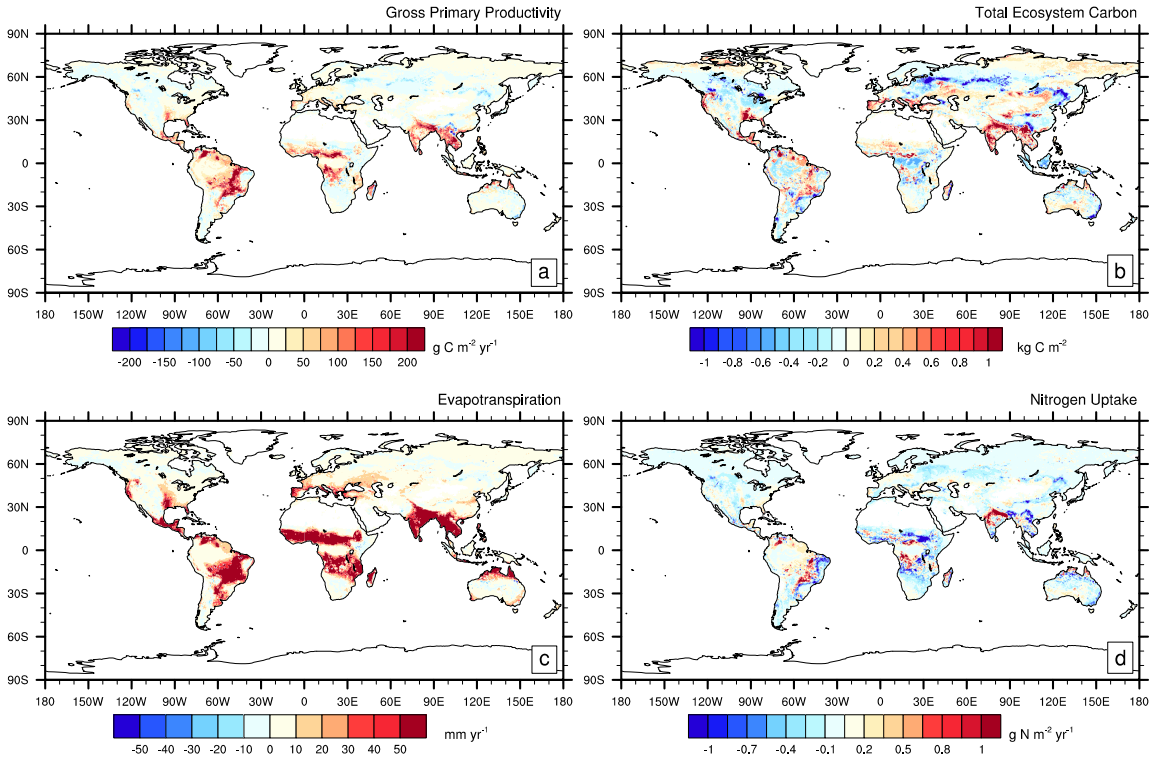

Figure 3.14. Difference between DYNROOT-50W and CONTROL of (a) gross primary productivity (g C m^{-2} $year^{-1}$); (b) total ecosystem carbon (kg C/m^2); (c) transpiration (mm/year); and (d) nitrogen uptake (g N m^{-2} $year^{-1}$).

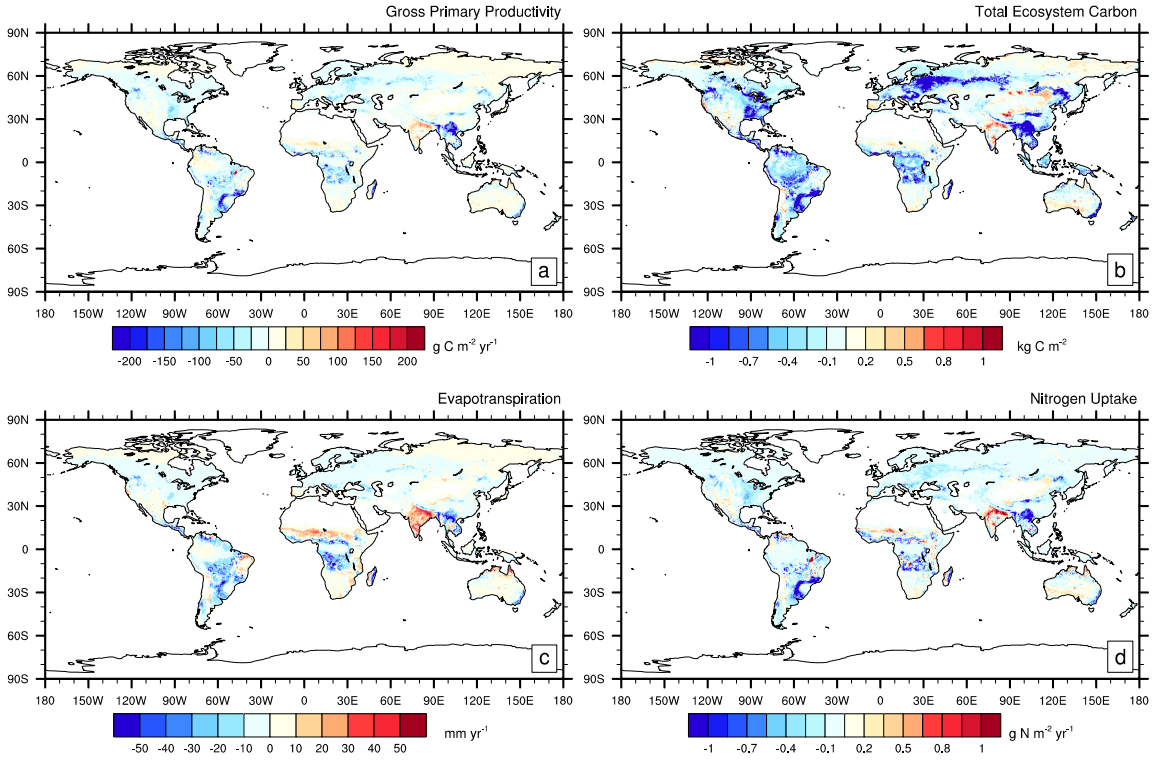

Figure 3.15. Difference between DYNROOT-90W and CONTROL of (a) gross primary productivity (g C m^{-2} $year^{-1}$); (b) total ecosystem carbon (kg C/m^2); (c) transpiration (mm/year); and (d) nitrogen uptake (g N m^{-2} $year^{-1}$).

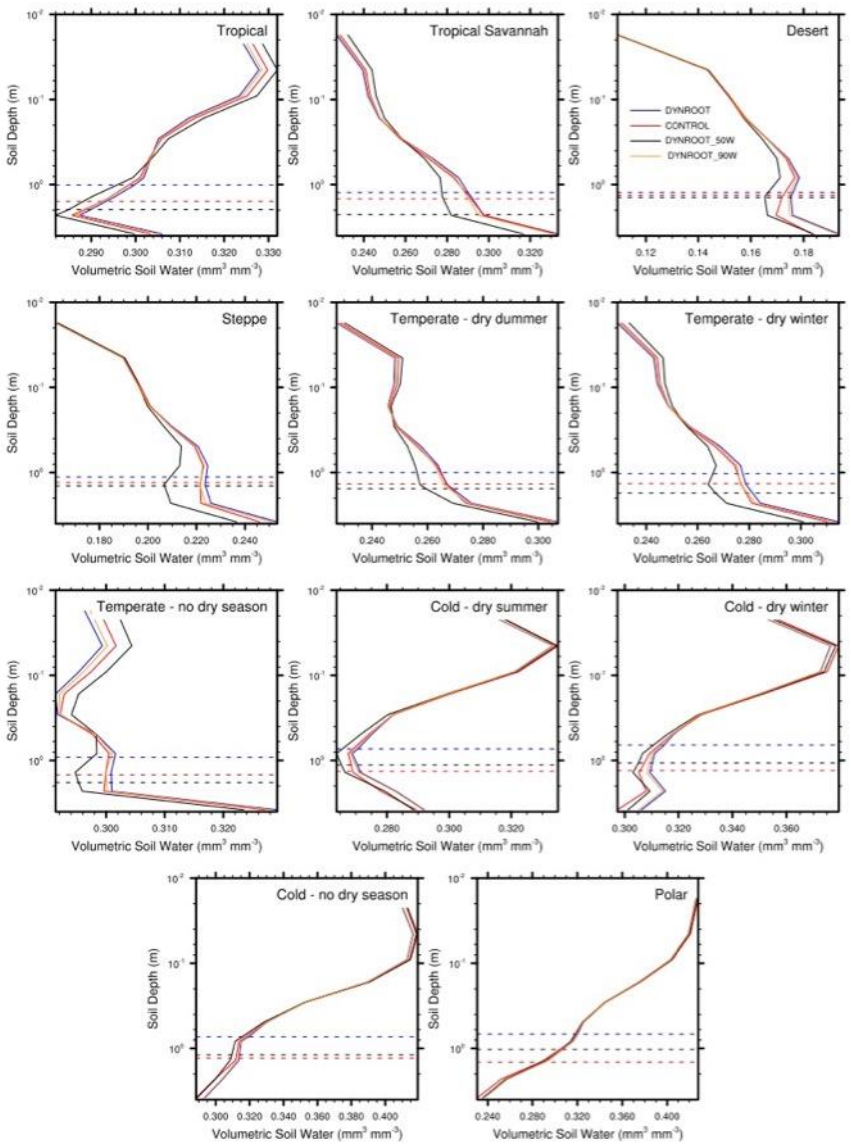

Figure 3.18. Climate zone averaged volumetric soil water (mm^3 mm^{-3}) with soil depth for DYNROOT (blue line), CONTROL (red line), DYNROOT_50W (black line) and DYNROOT_90W (orange line). Average D95 for each climate zone is shown in dashed lines for DYNROOT (blue dashed line), CONTROL (red dashed line) and DYNROOT_50W (black dashed line).

C. Supplementary Material for Chapter 4

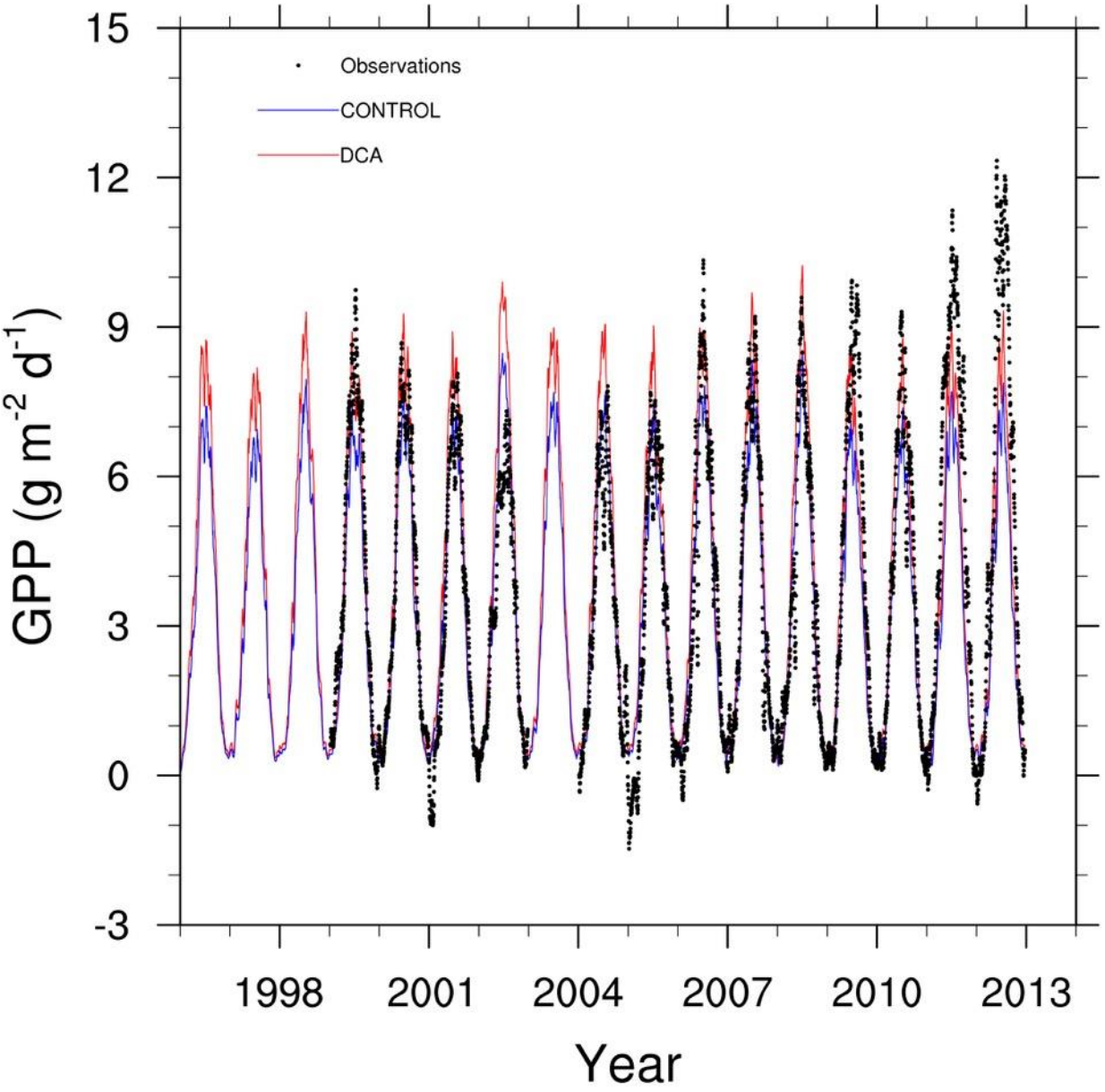

Figure 4.4. GPP of DCA (red line), CONTROL (blue line), and observations (black dots) at the BE-Bra site.

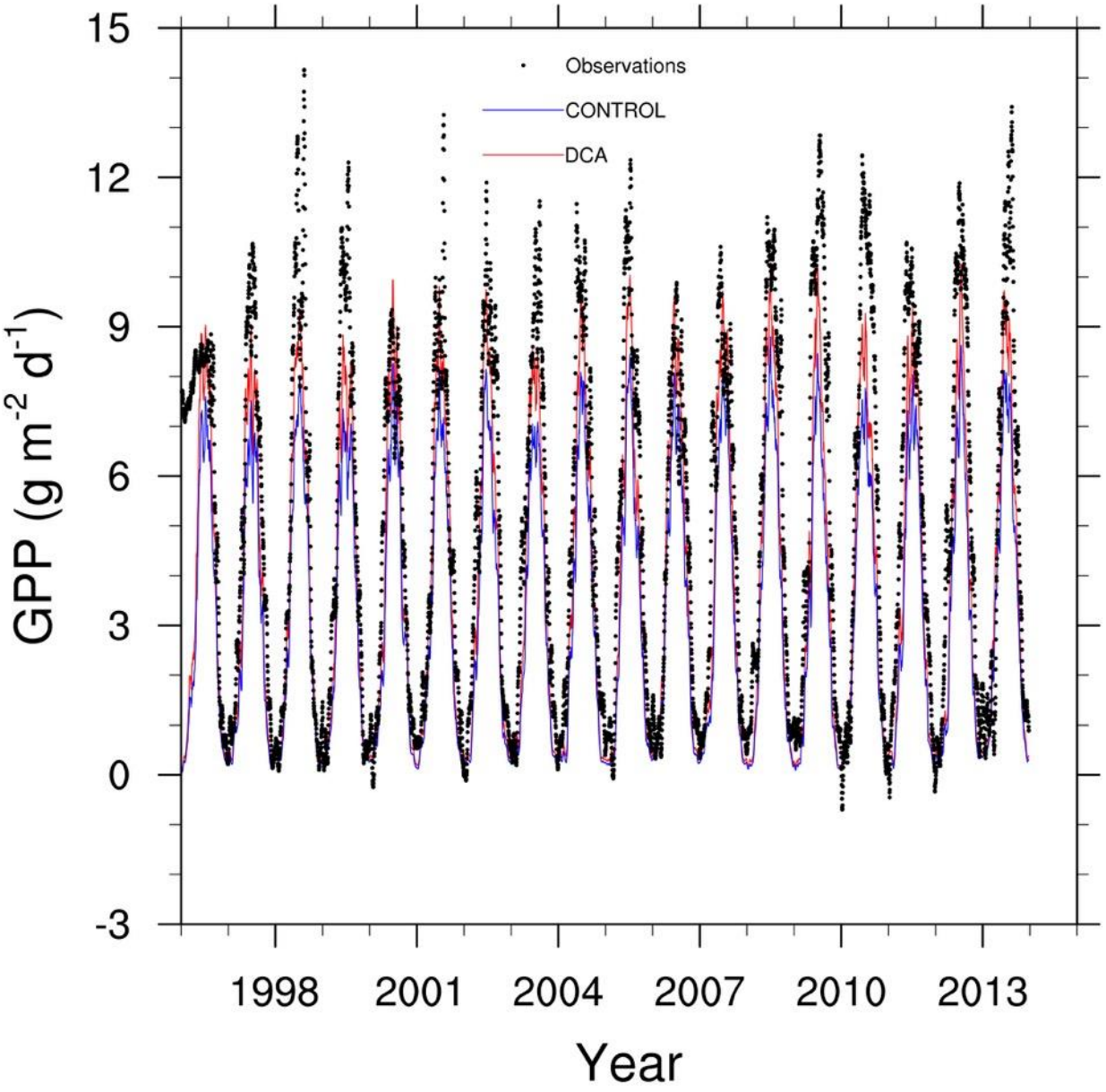

Figure 4.5. GPP of DCA (red line), CONTROL (blue line), and observations (black dots) at the BE-Vie site.

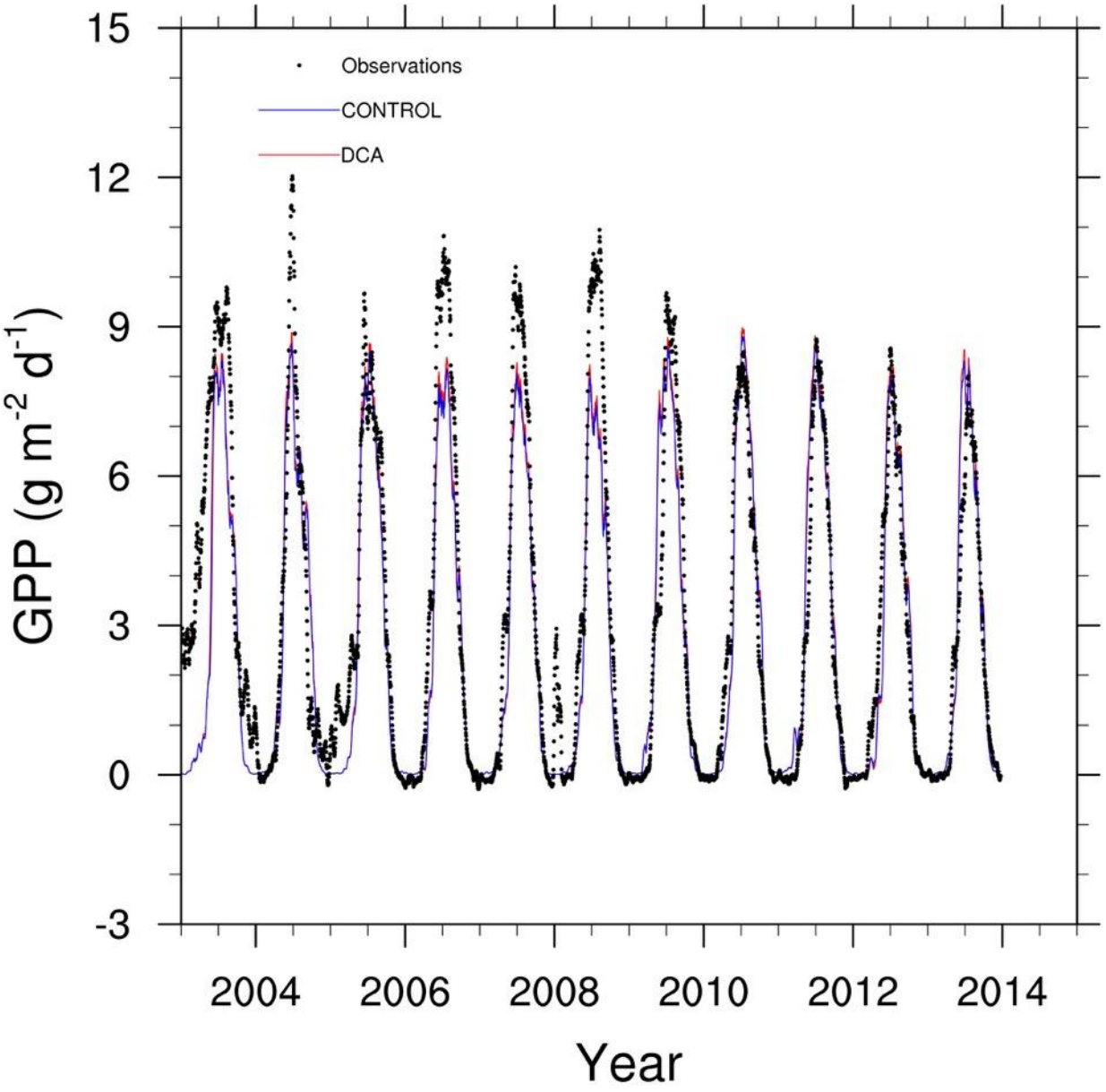

Figure 4.6. GPP of DCA (red line), CONTROL (blue line), and observations (black dots) at the CA-Gro site.

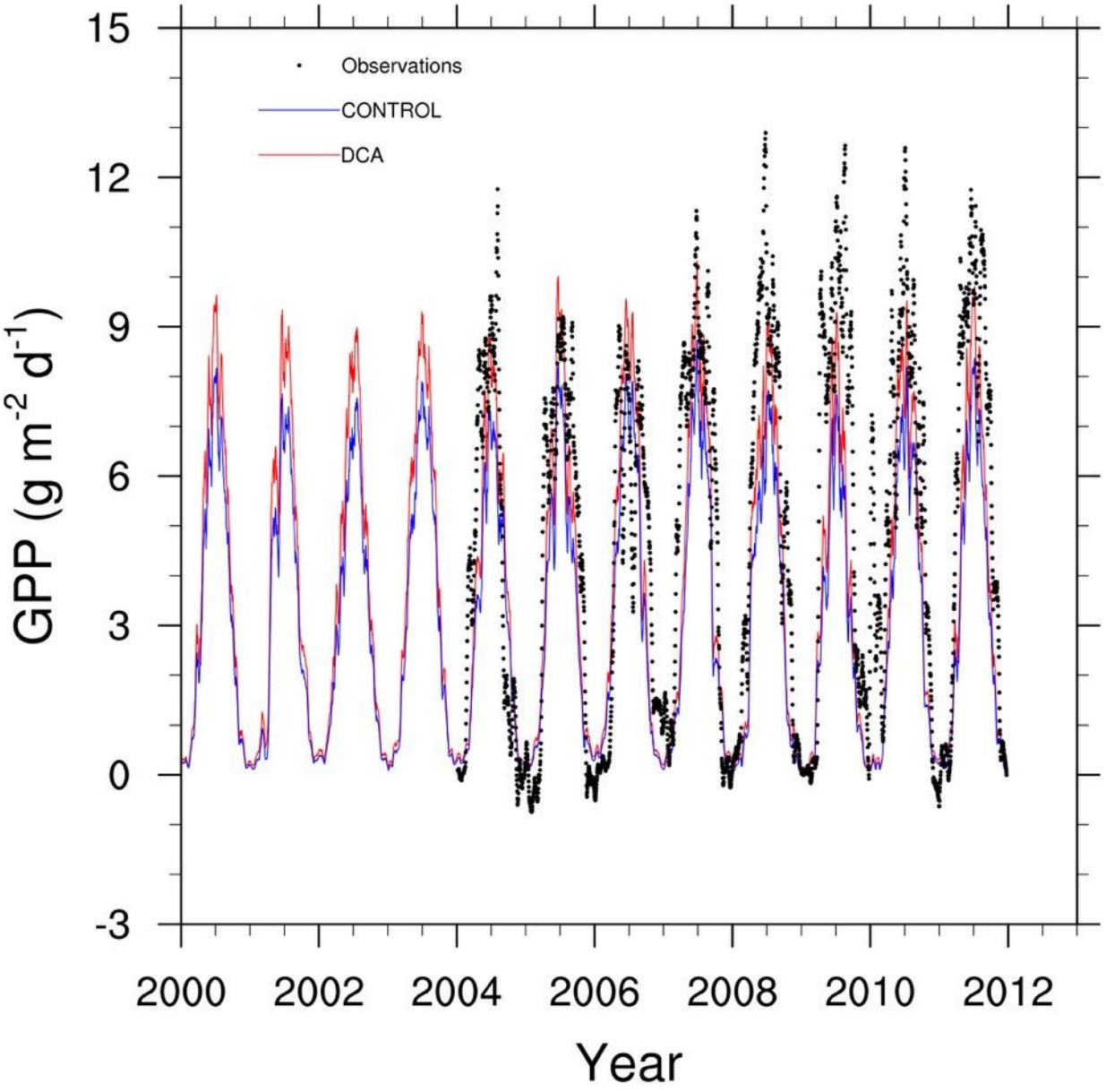

Figure 4.7. GPP of DCA (red line), CONTROL (blue line), and observations (black dots) at the CZ-BK1 site.

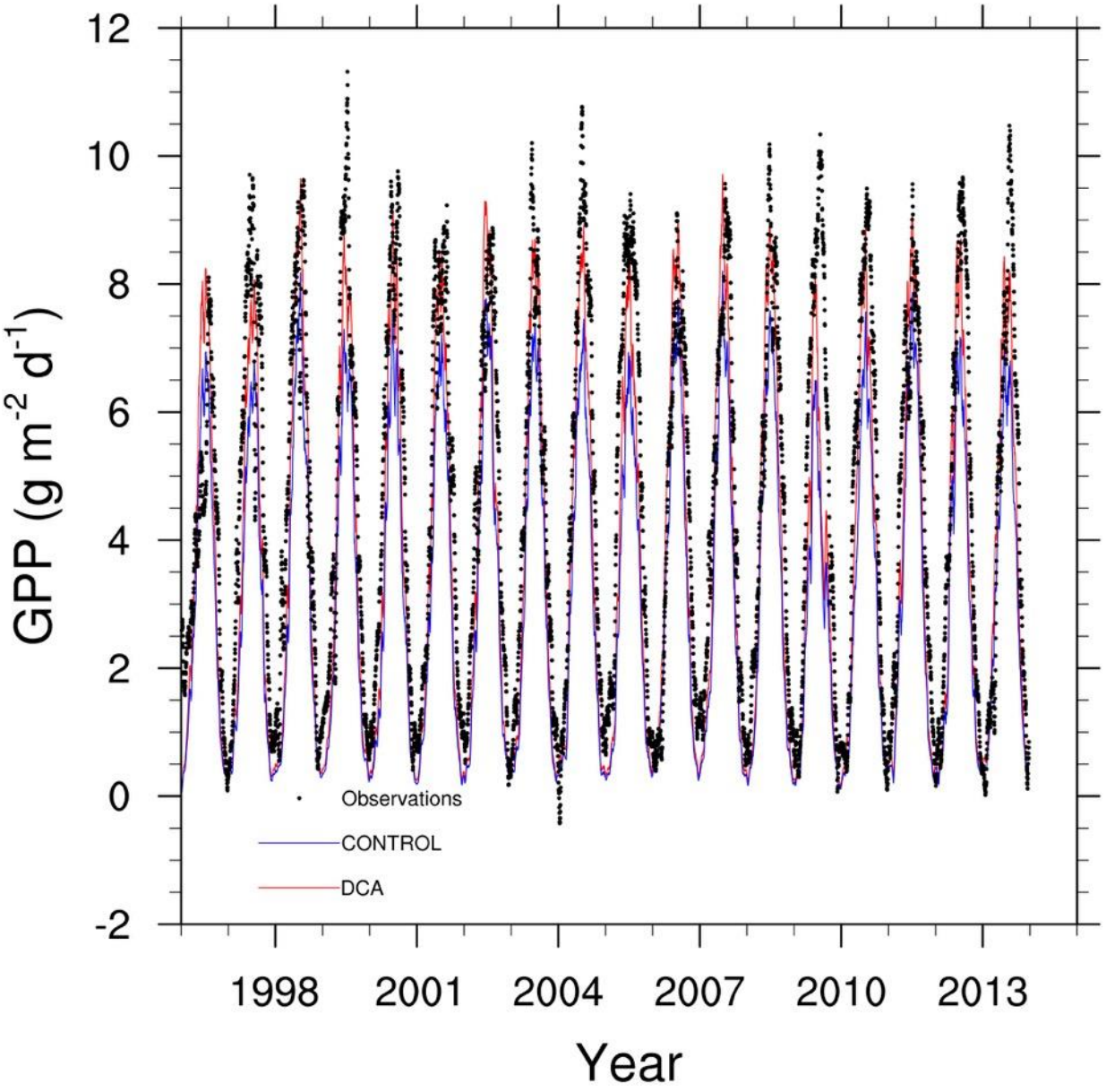

Figure 4.8. GPP of DCA (red line), CONTROL (blue line), and observations (black dots) at the NL-Loo site.

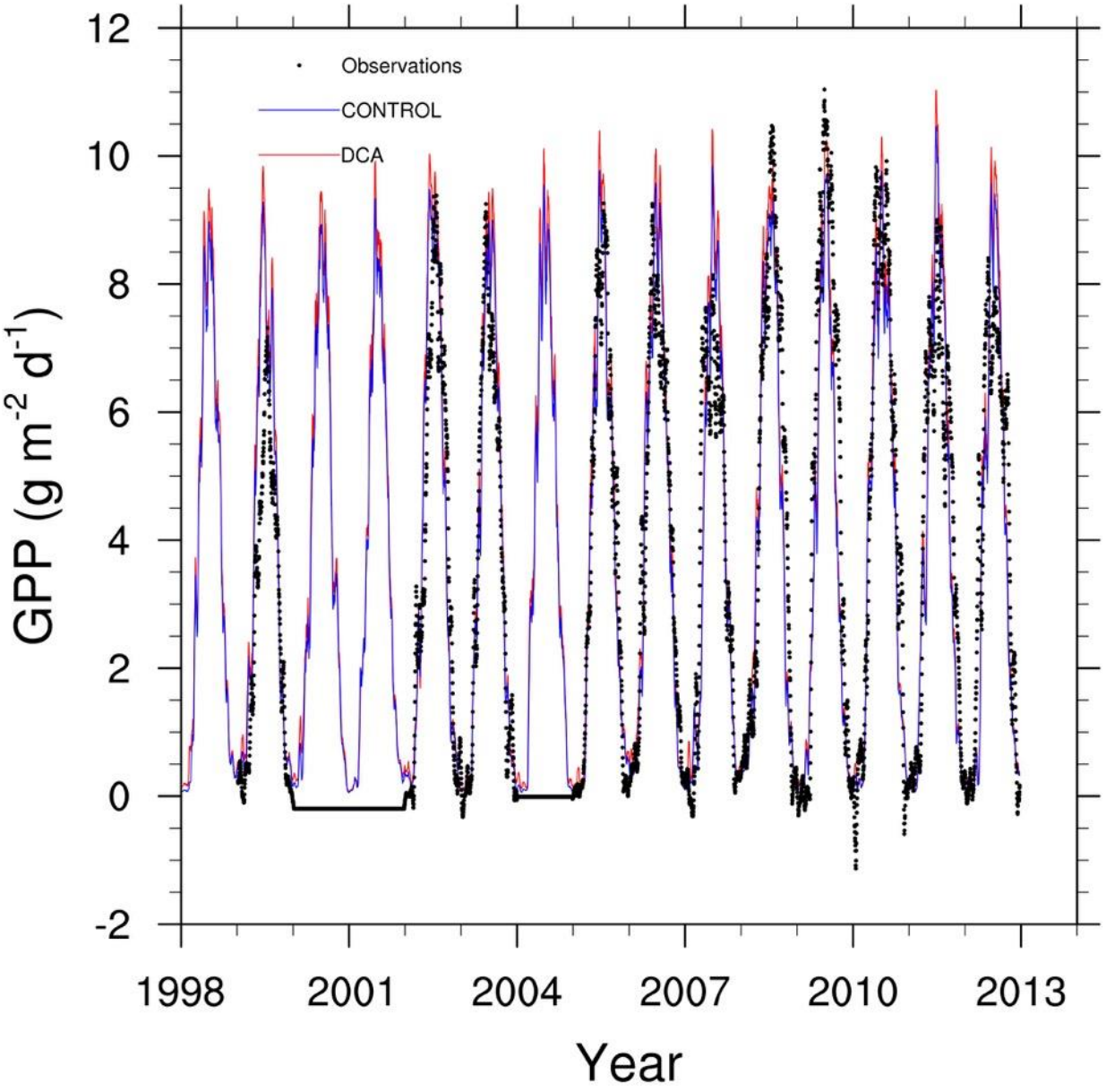

Figure 4.9. GPP of DCA (red line), CONTROL (blue line), and observations (black dots) at the IT-Ren site.

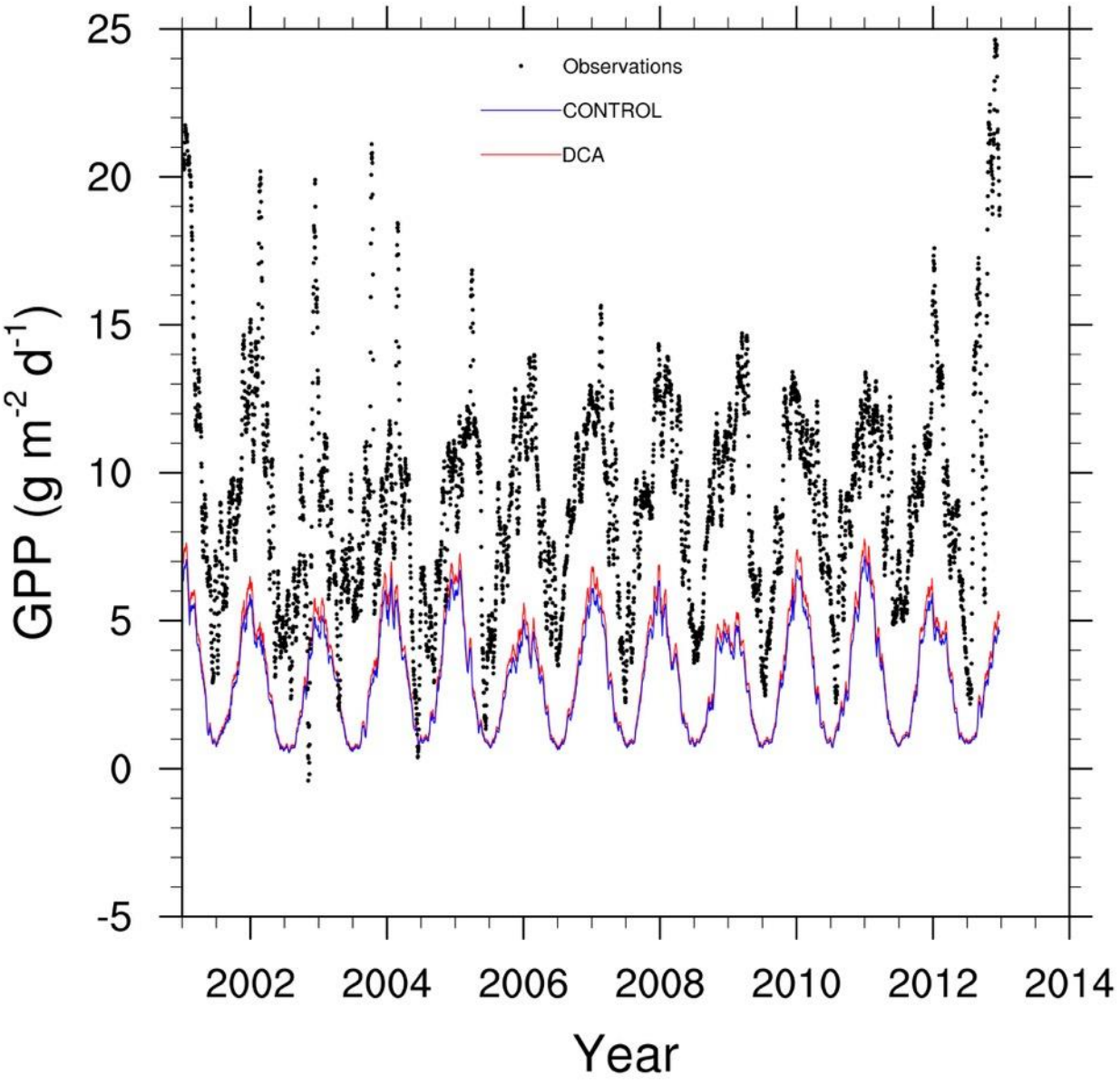

Figure 4.10. GPP of DCA (red line), CONTROL (blue line), and observations (black dots) at the AU-Tum site.

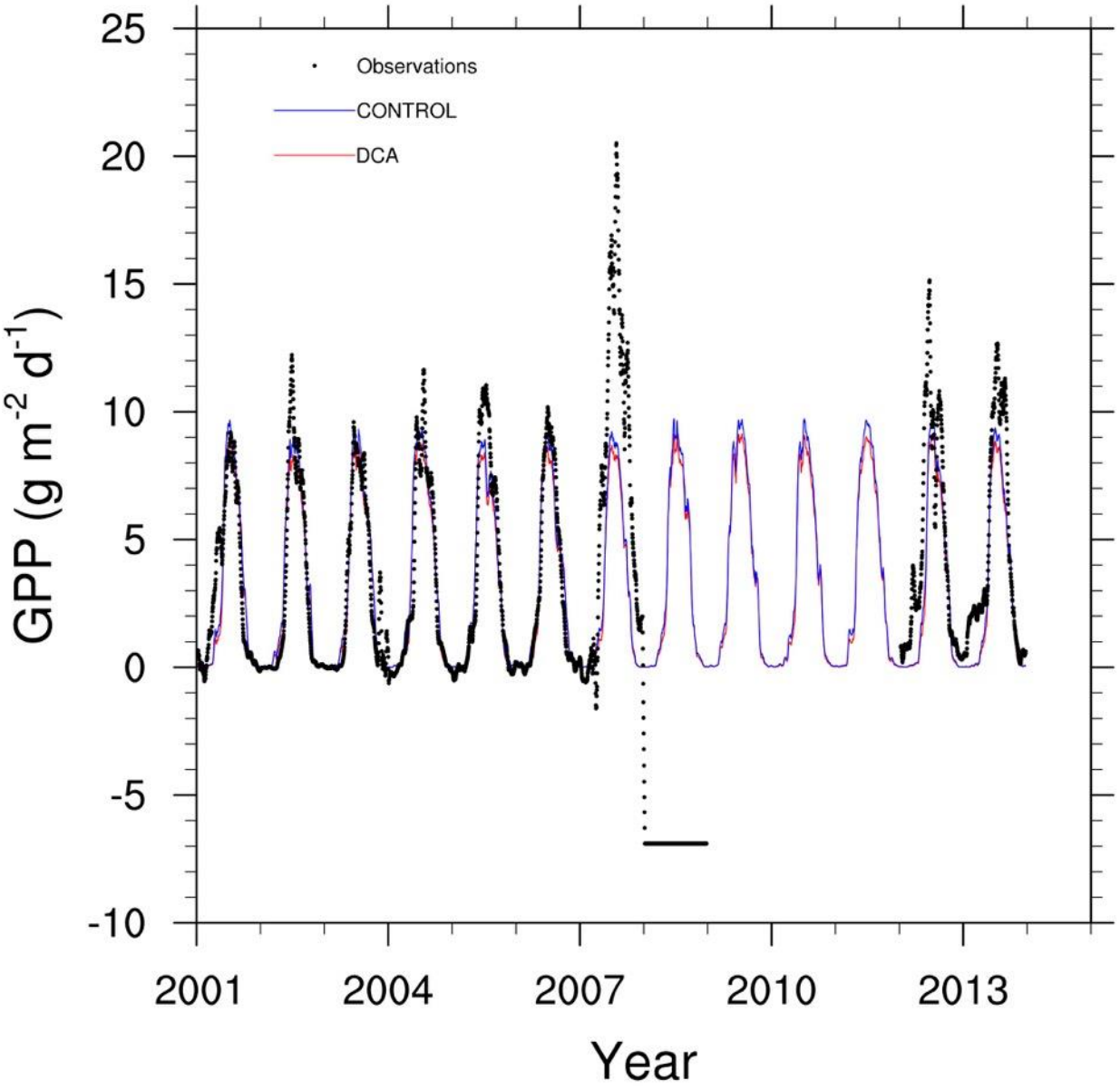

Figure 4.11. GPP of DCA (red line), CONTROL (blue line), and observations (black dots) at the US-Syv site.

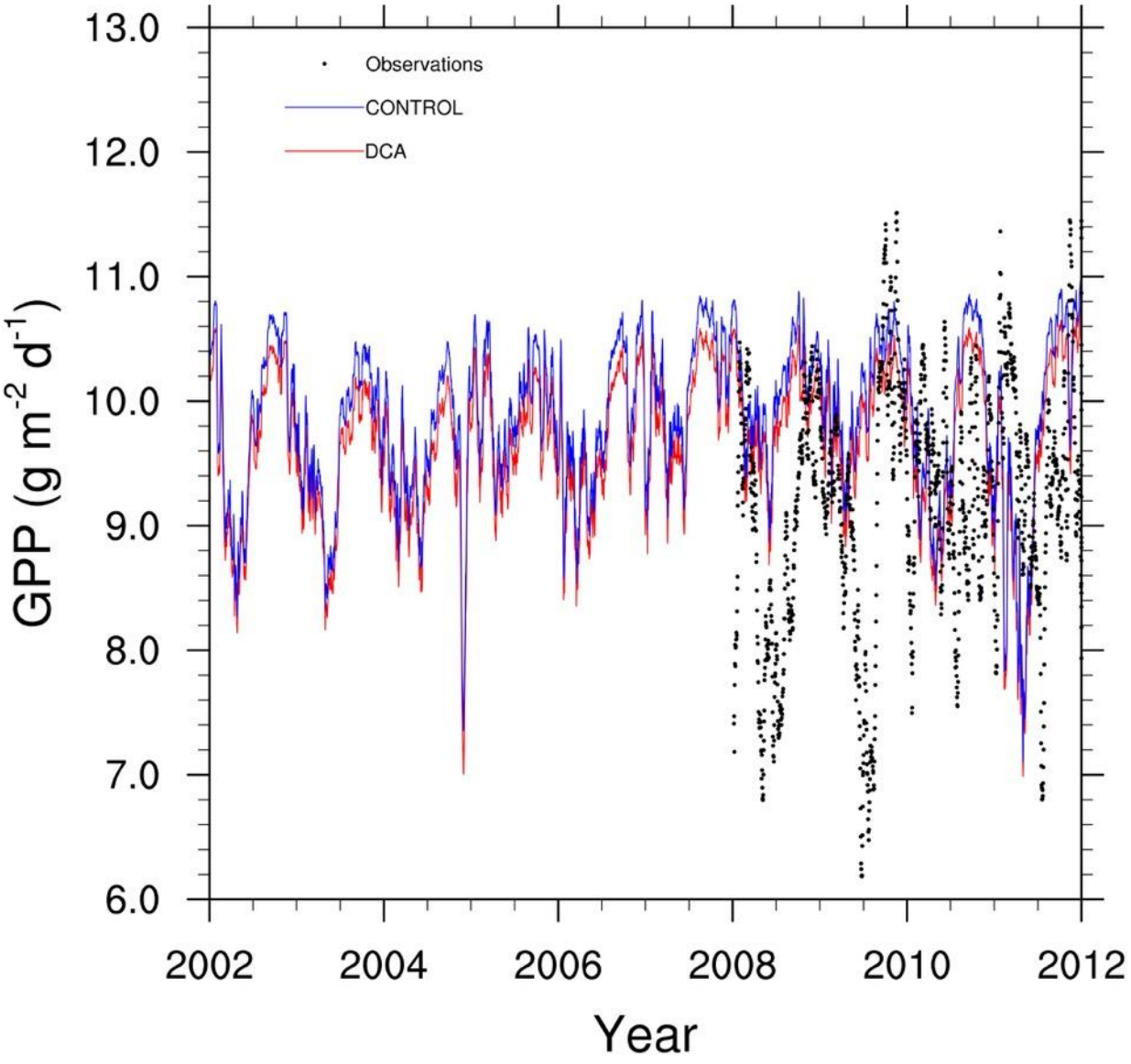

Figure 4.12. GPP of DCA (red line), CONTROL (blue line), and observations (black dots) at the BR-Sa1 site.

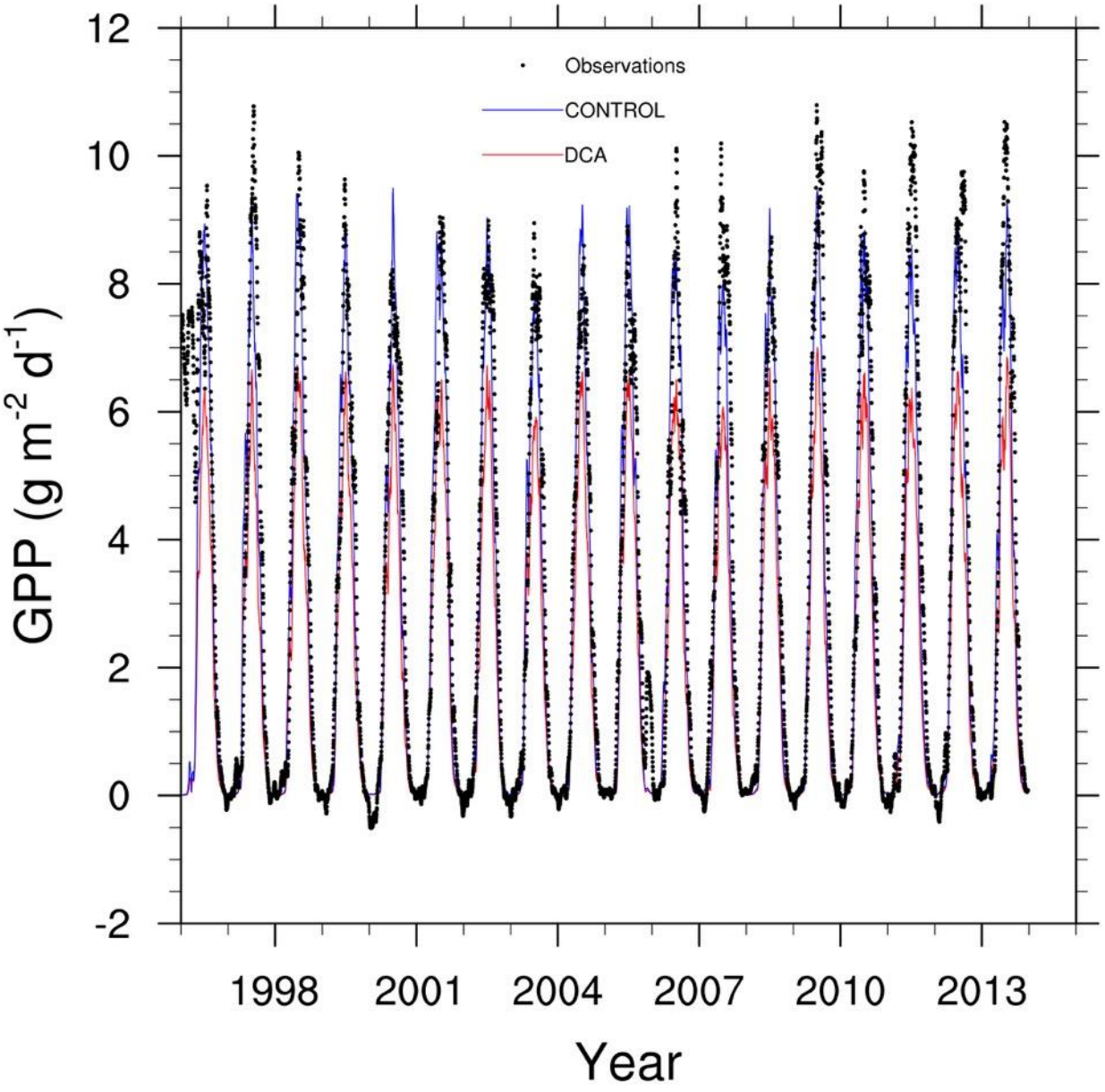

Figure 4.14. GPP of DCA (red line), CONTROL (blue line), and observations (black dots) at the FI-Hyy site.

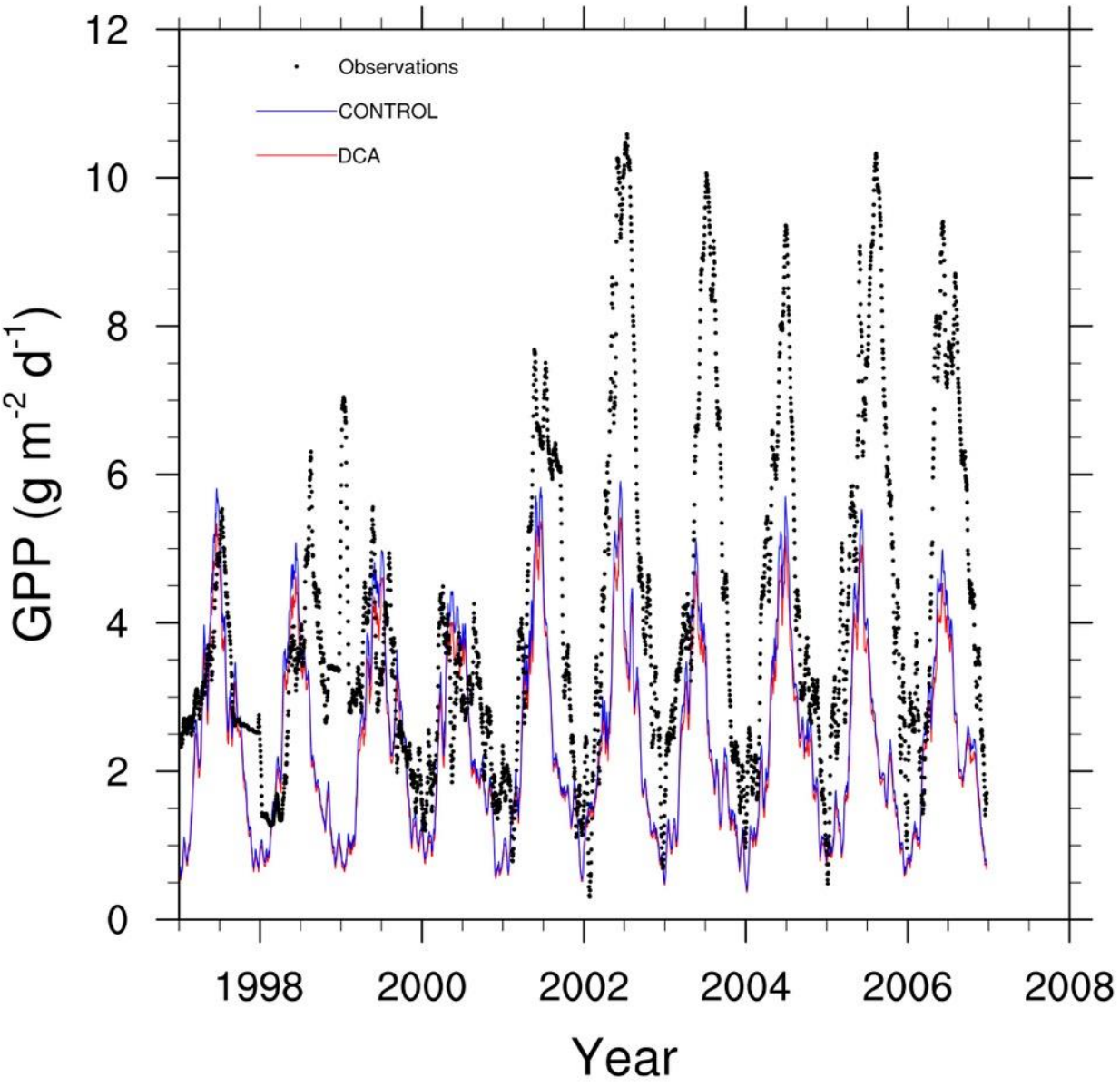

Figure 4.15. GPP of DCA (red line), CONTROL (blue line), and observations (black dots) at the US-Blo site.

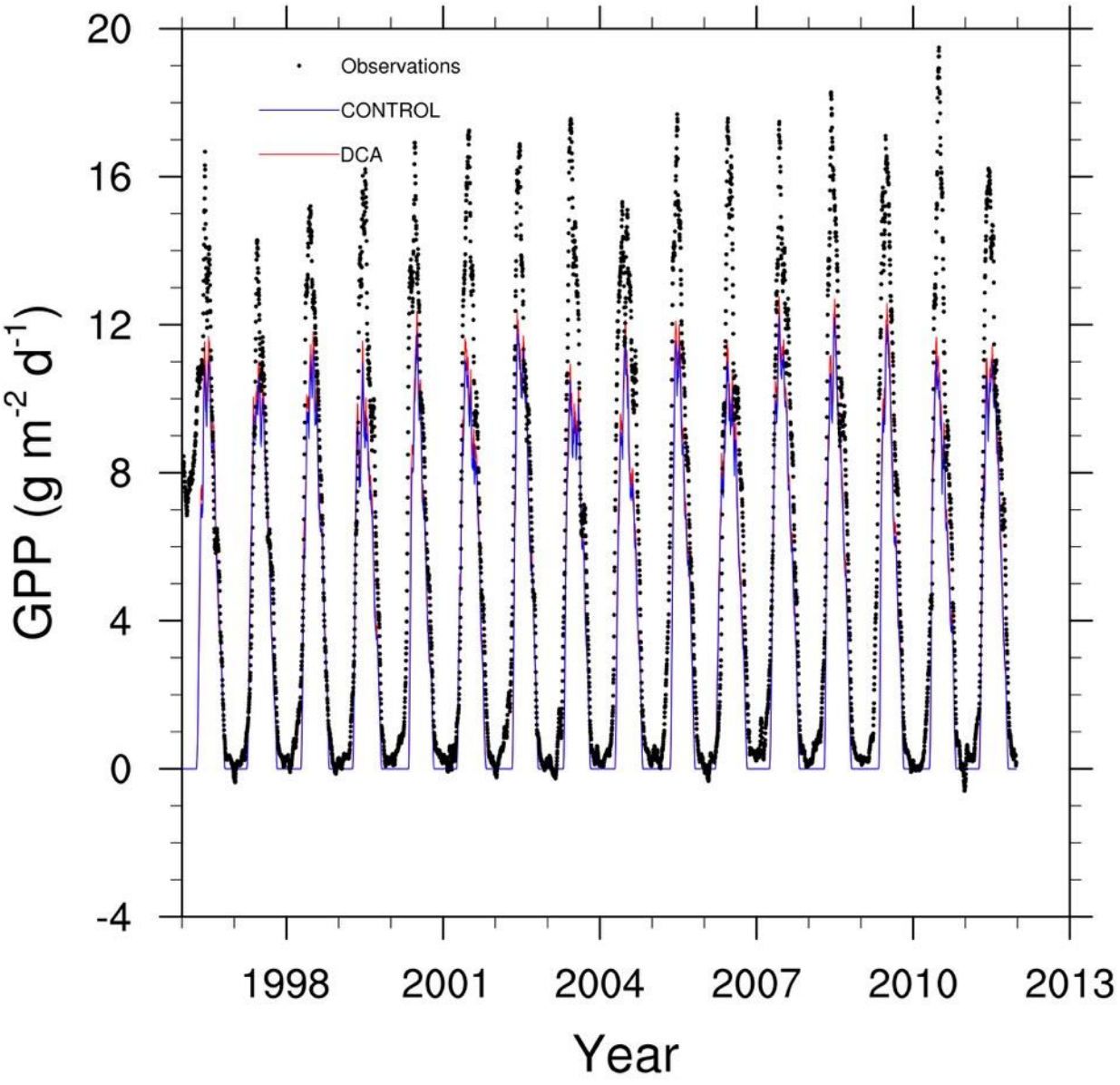

Figure 4.17. GPP of DCA (red line), CONTROL (blue line), and observations (black dots) at the DK-Sor site.

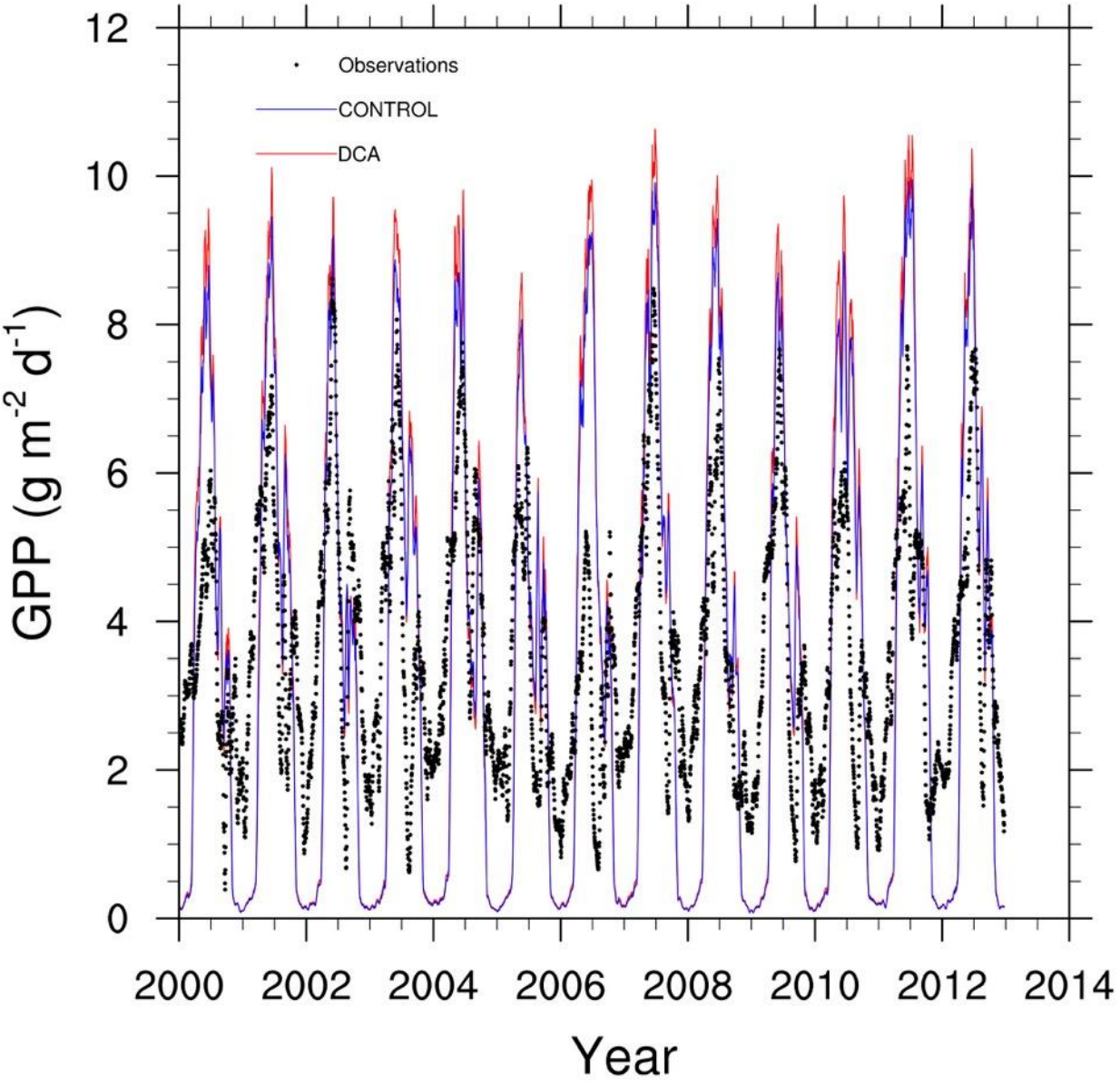

Figure 4.18. GPP of DCA (red line), CONTROL (blue line), and observations (black dots) at the FR-Pue site.

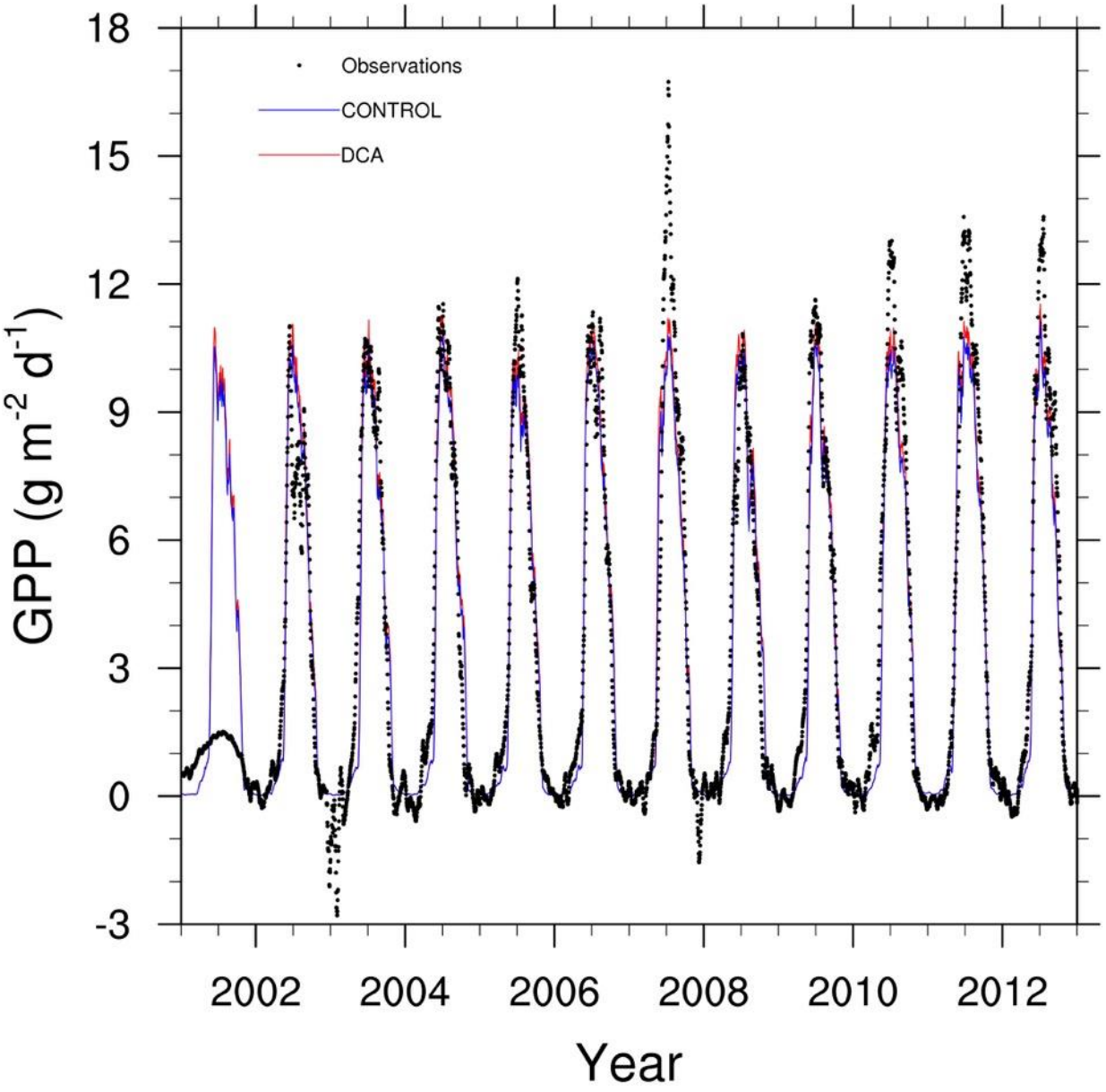

Figure 4.19. GPP of DCA (red line), CONTROL (blue line), and observations (black dots) at the US-Ha1 site.

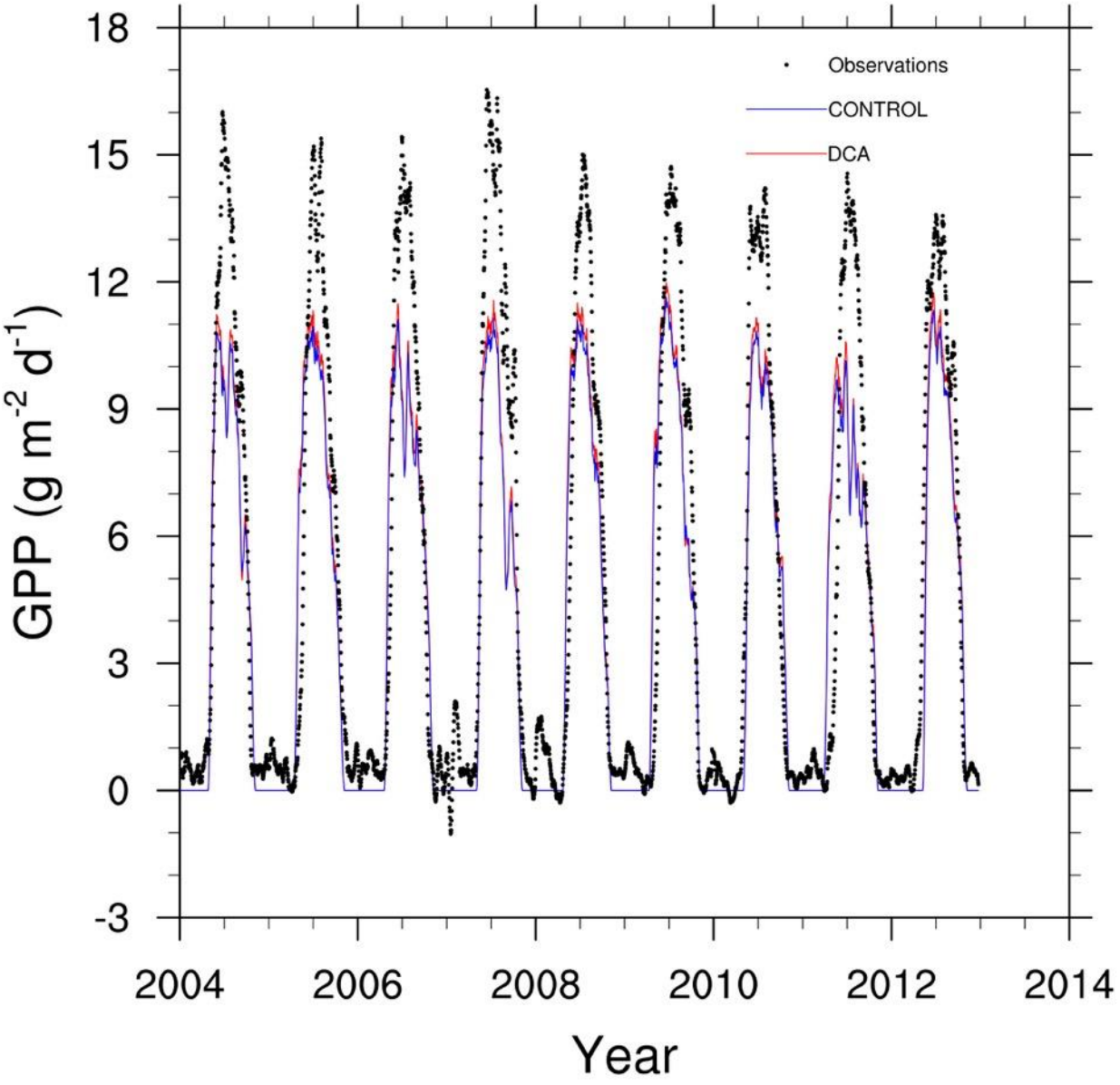

Figure 4.20. GPP of DCA (red line), CONTROL (blue line), and observations (black dots) at the US-Oho site.

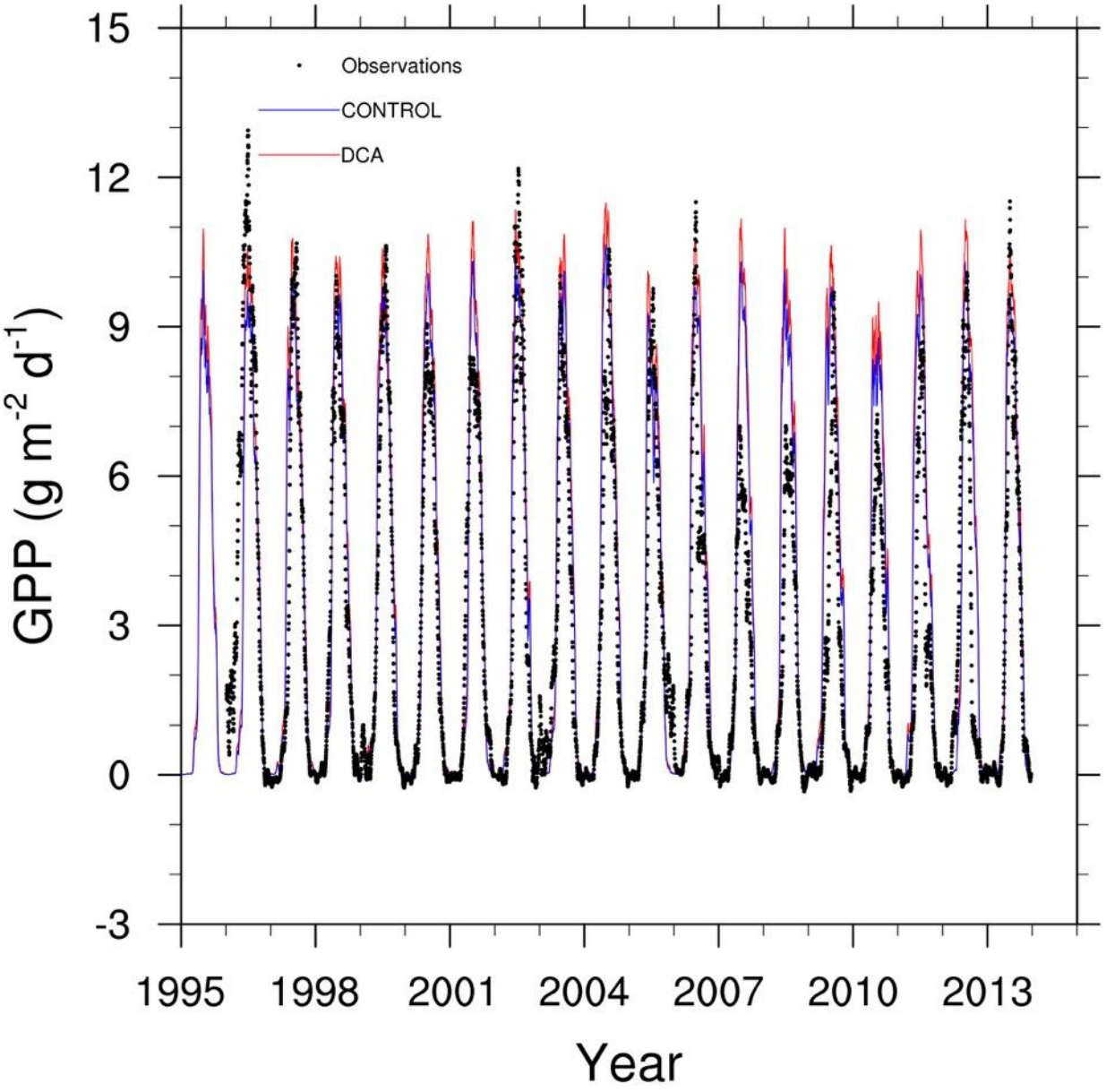

Figure 4.21. GPP of DCA (red line), CONTROL (blue line), and observations (black dots) at the US-PFa site.

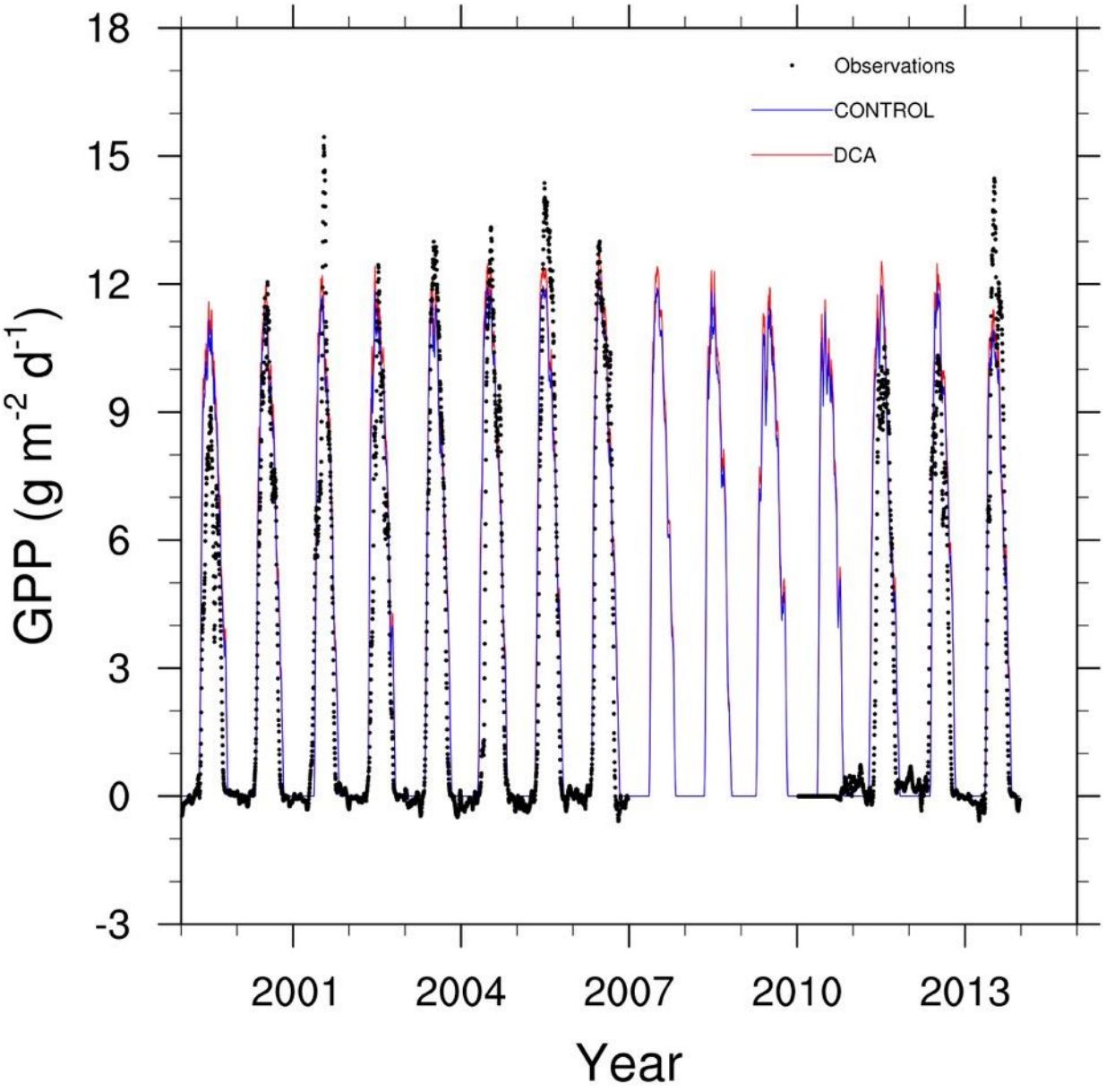

Figure 4.22. GPP of DCA (red line), CONTROL (blue line), and observations (black dots) at the US-Wcr site.

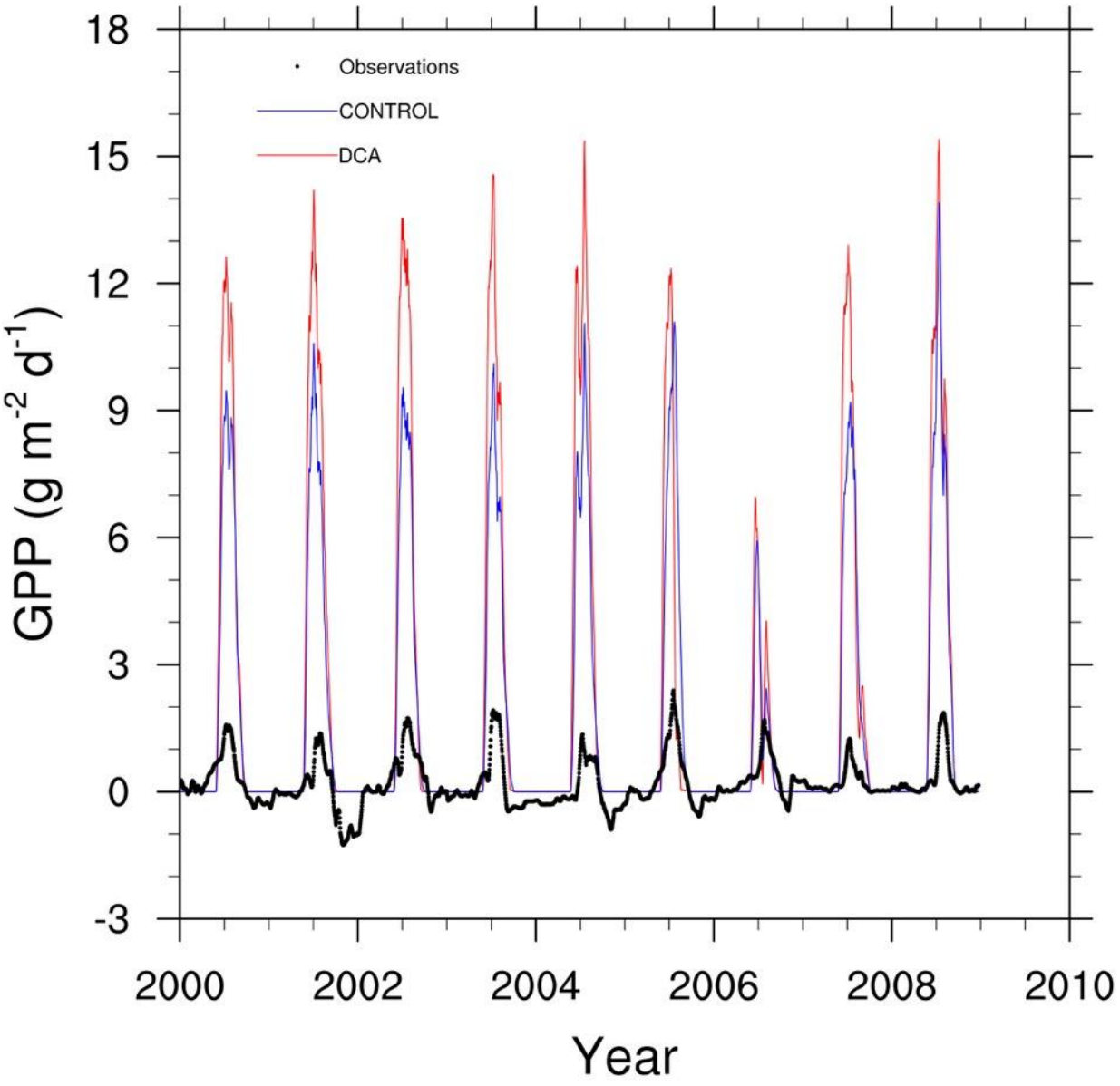

Figure 4.23. GPP of DCA (red line), CONTROL (blue line), and observations (black dots) at the DK-Zah site.

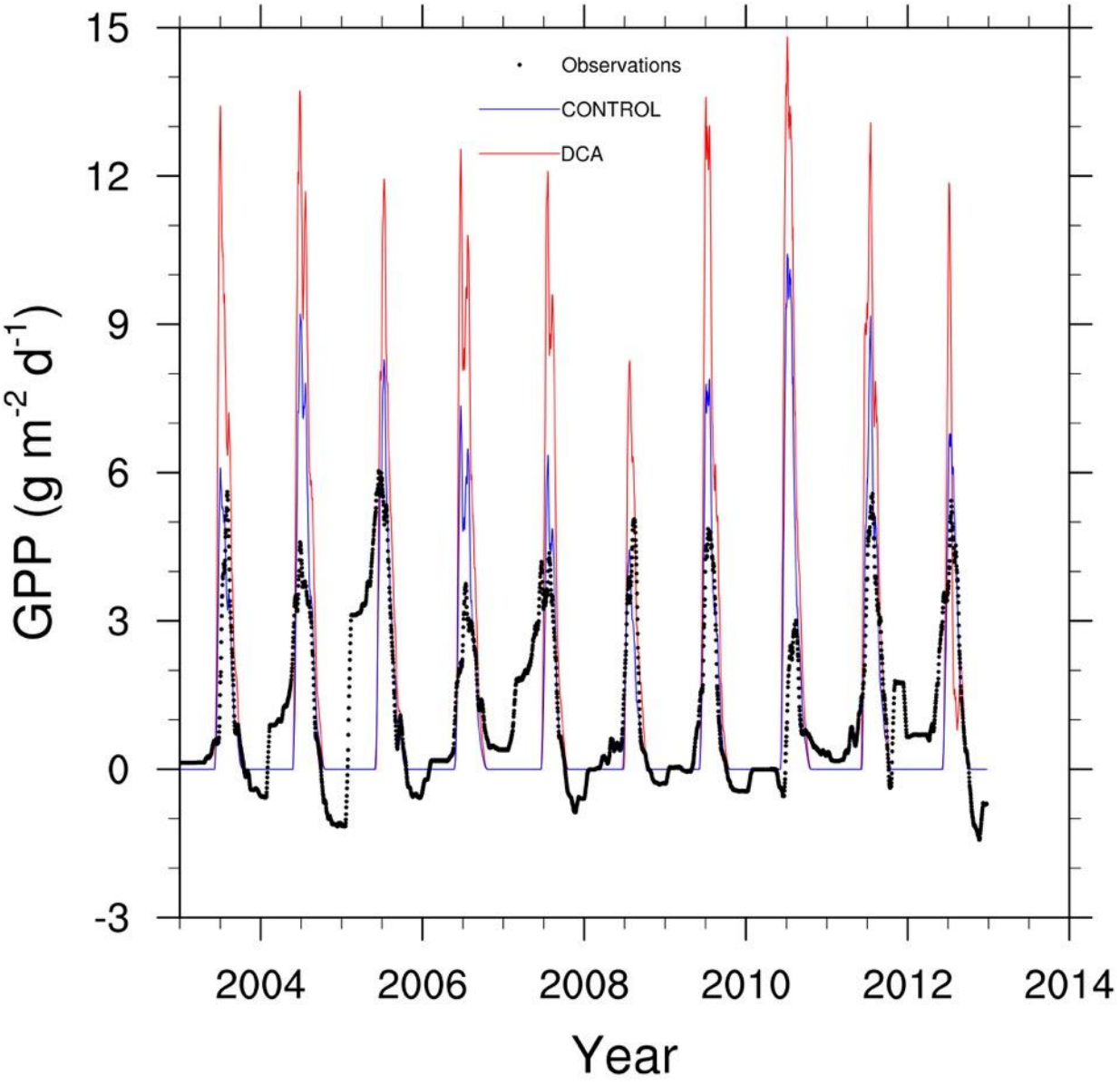

Figure 4.24. GPP of DCA (red line), CONTROL (blue line), and observations (black dots) at the RU-Cok site.

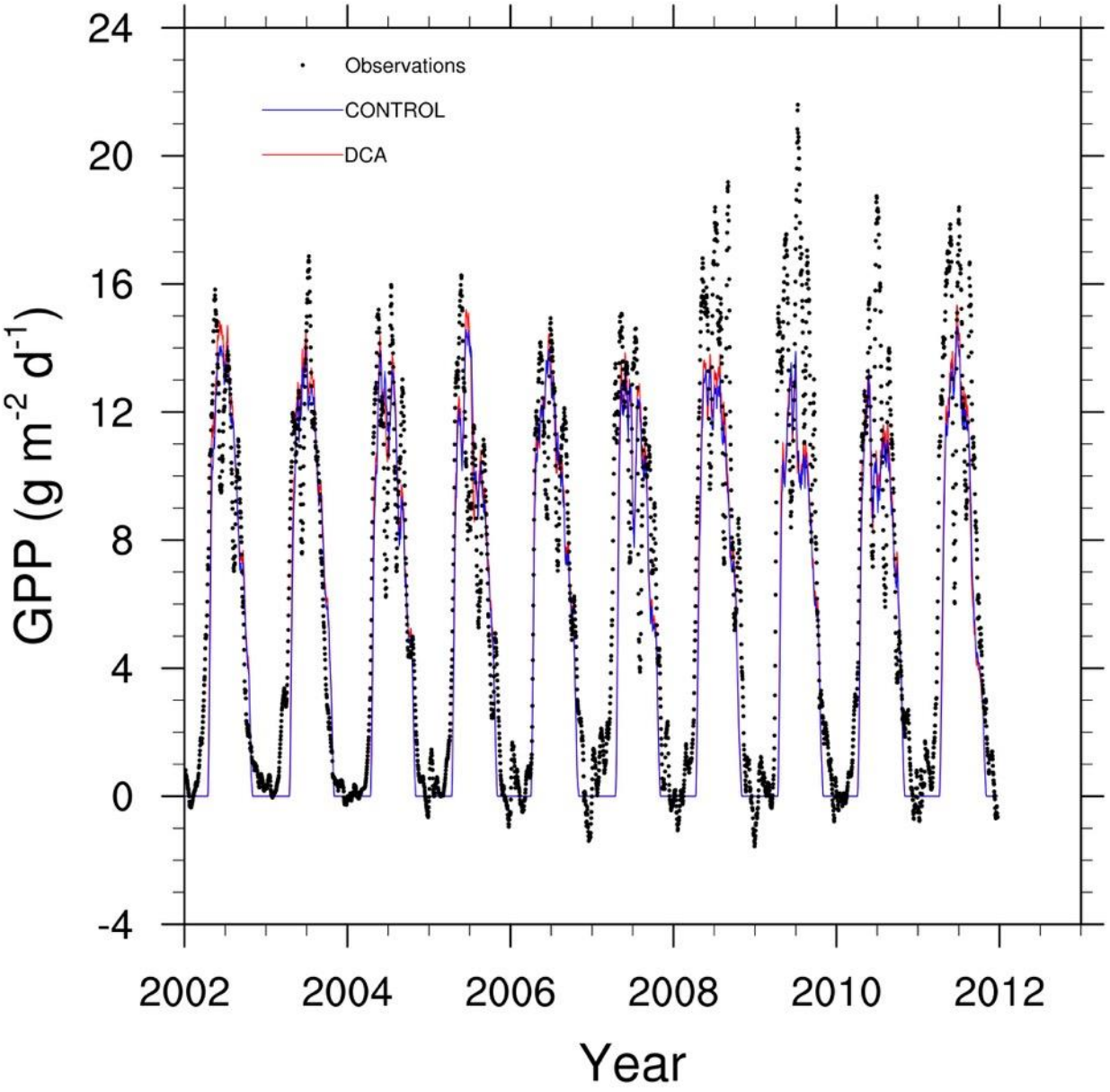

Figure 4.25. GPP of DCA (red line), CONTROL (blue line), and observations (black dots) at the AT-Nue site.

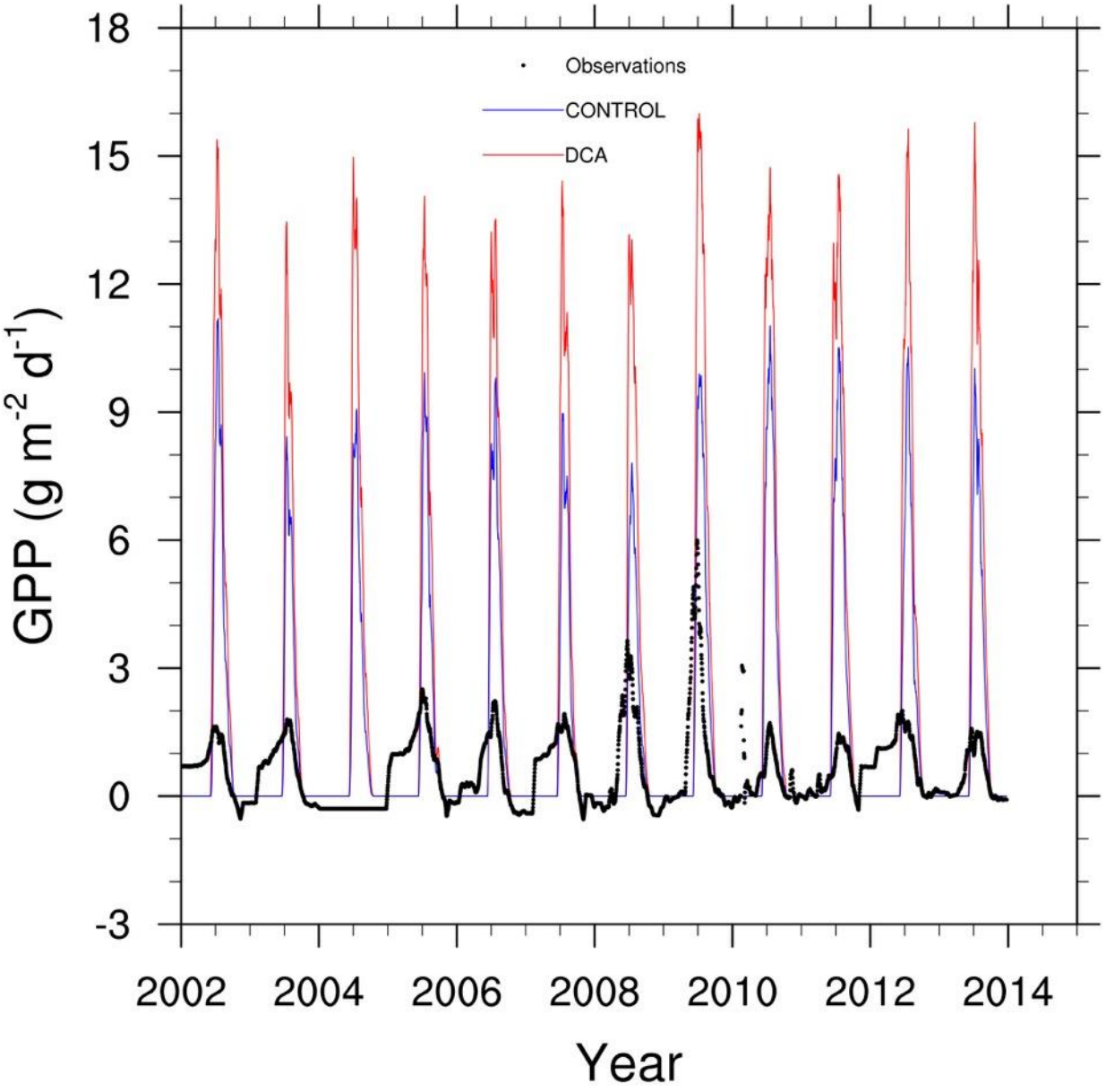

Figure 4.26. GPP of DCA (red line), CONTROL (blue line), and observations (black dots) at the RU-Sam site.

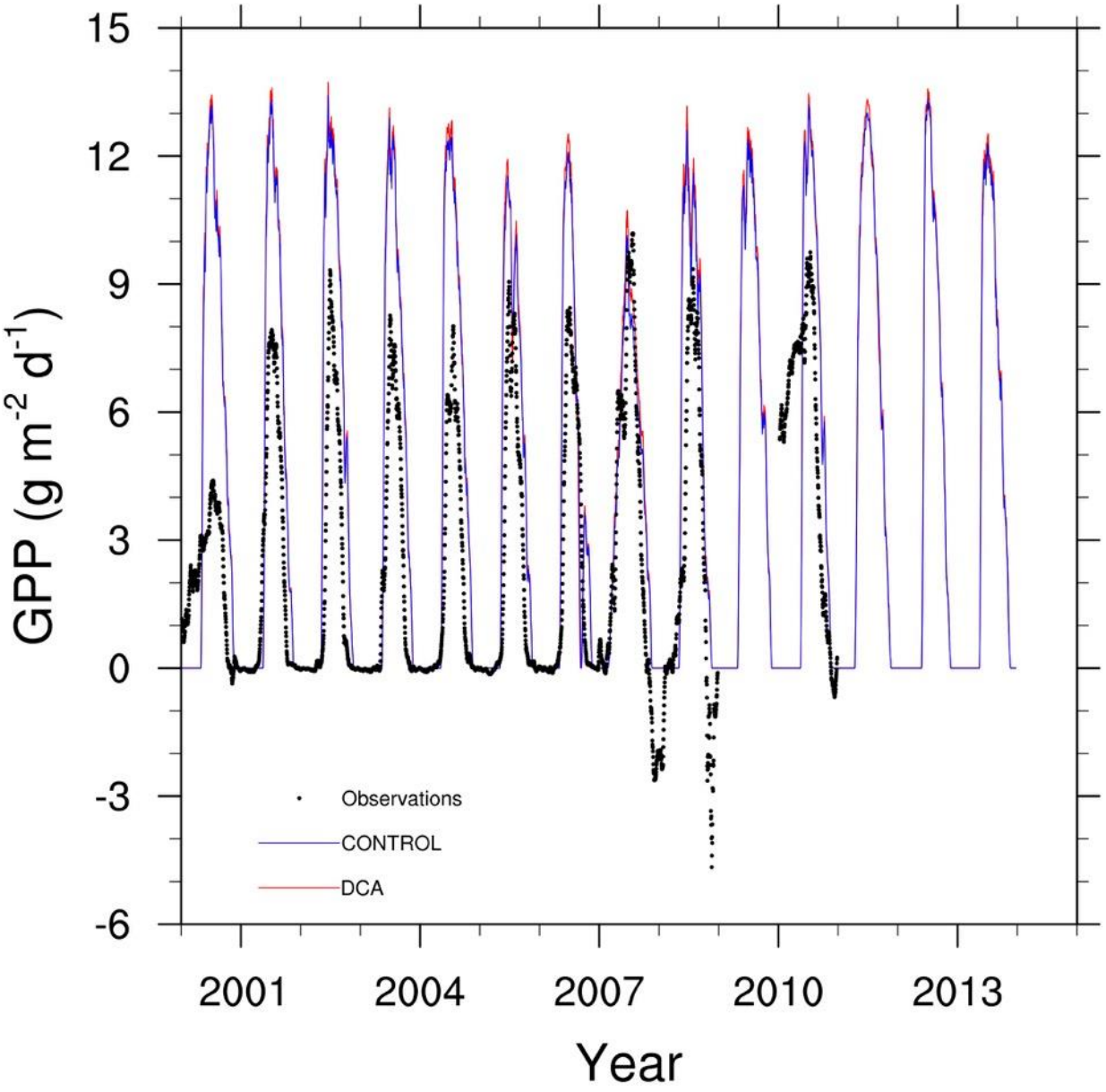

Figure 4.29. GPP of DCA (red line), CONTROL (blue line), and observations (black dots) at the US-Los site.

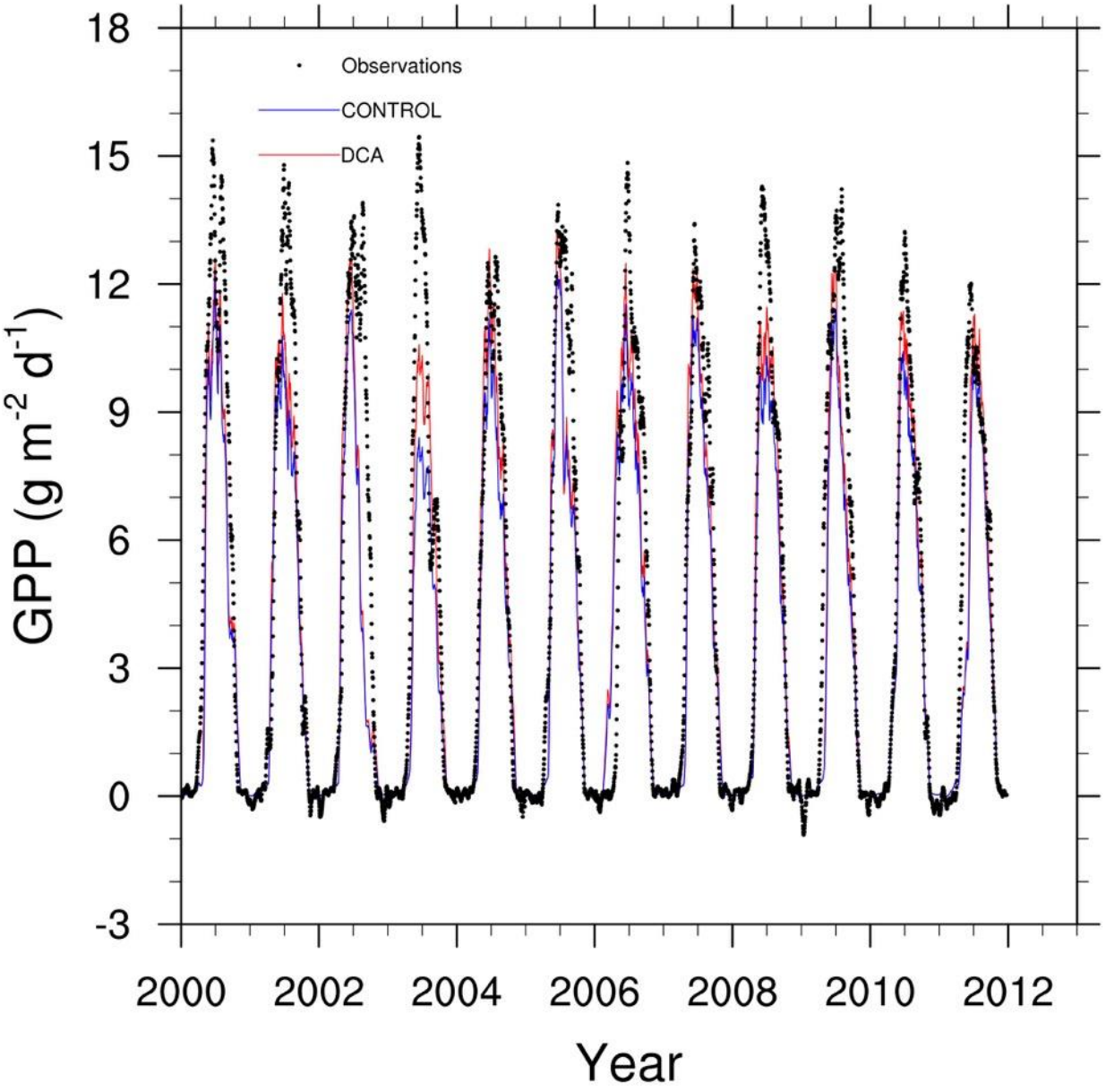

Figure 4.30. GPP of DCA (red line), CONTROL (blue line), and observations (black dots) at the DE-Hai site.

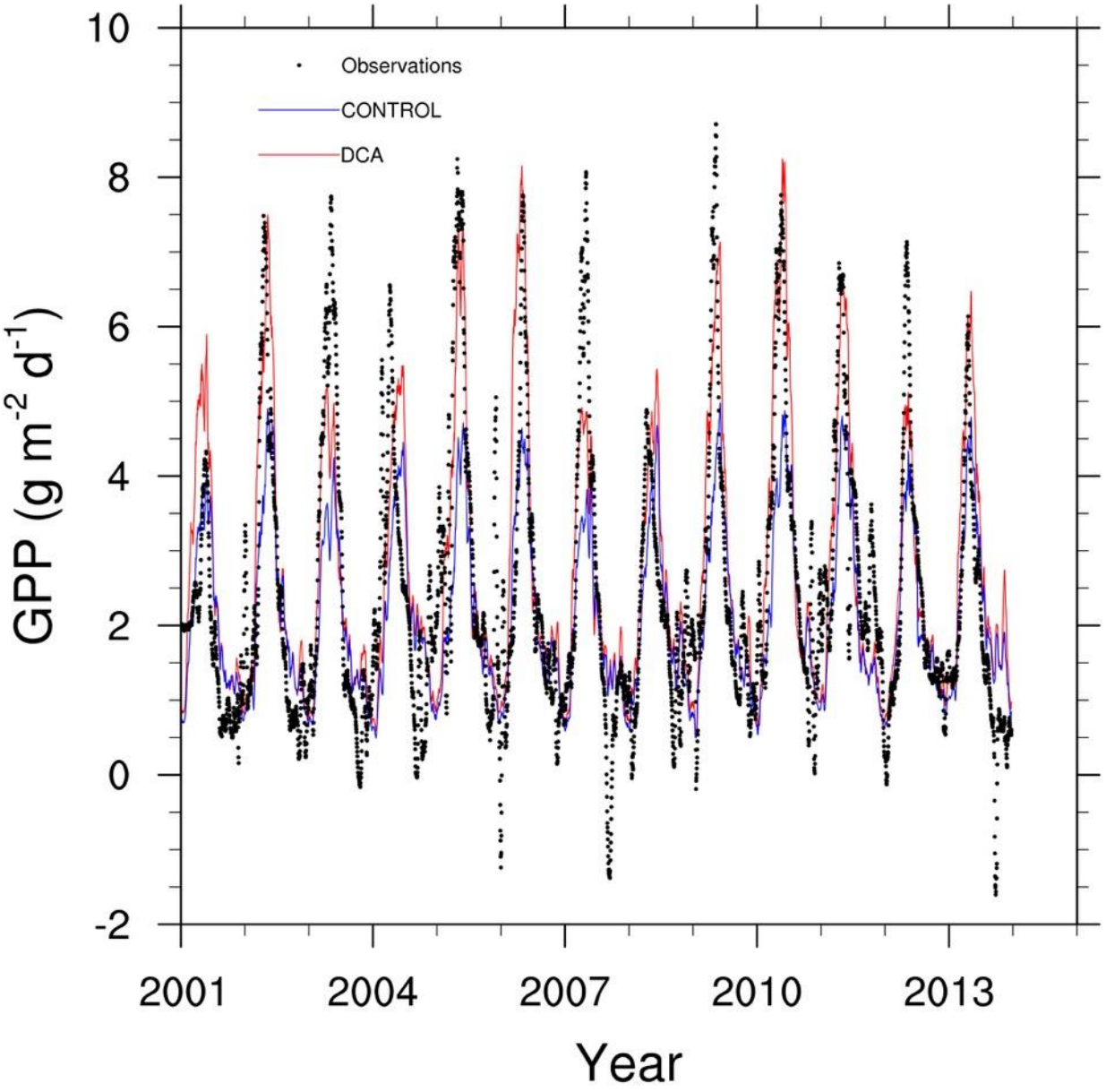

Figure 4.31. GPP of DCA (red line), CONTROL (blue line), and observations (black dots) at the US-Ton site.

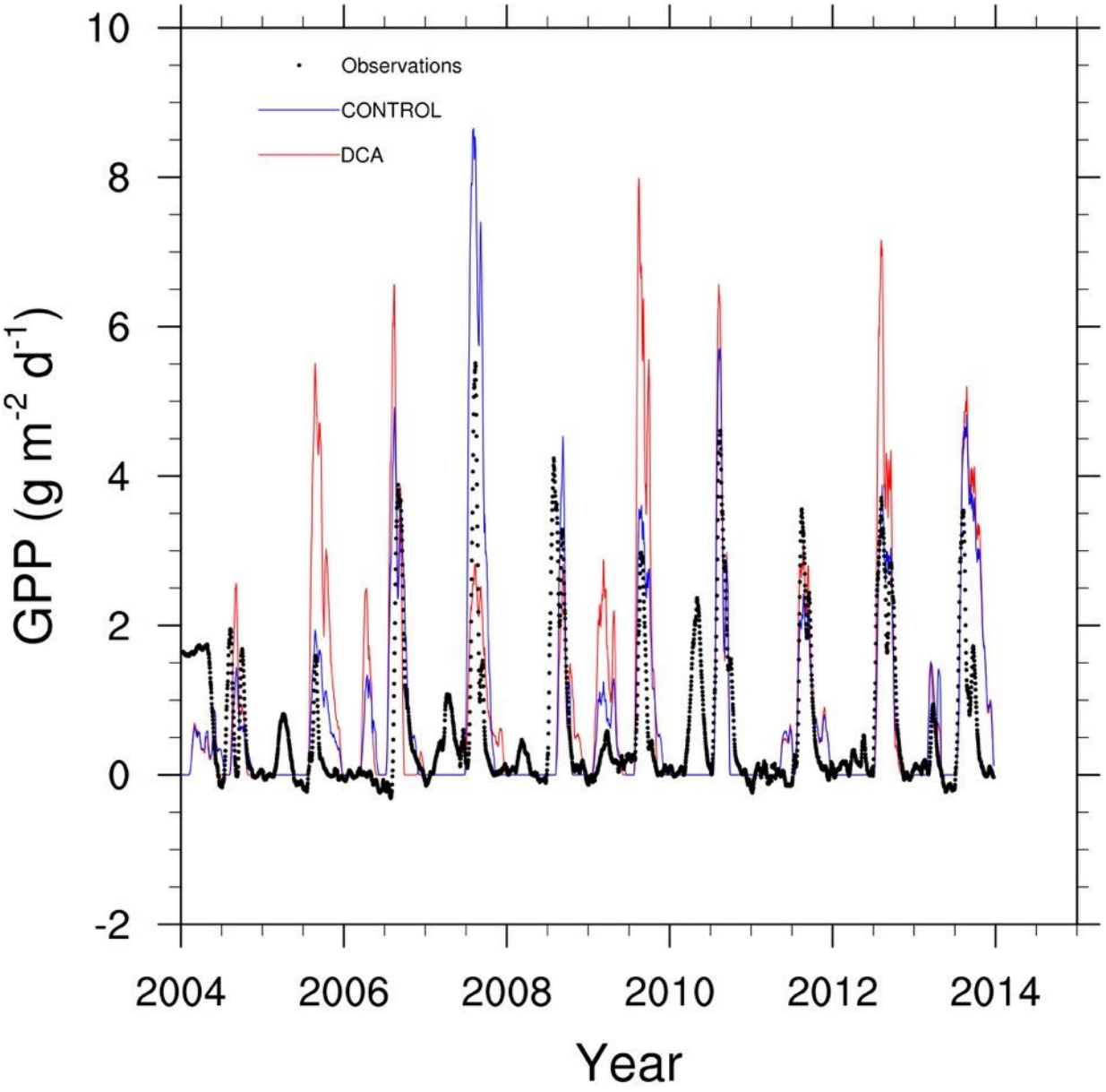

Figure 4.32. GPP of DCA (red line), CONTROL (blue line), and observations (black dots) at the US-Wkg site.

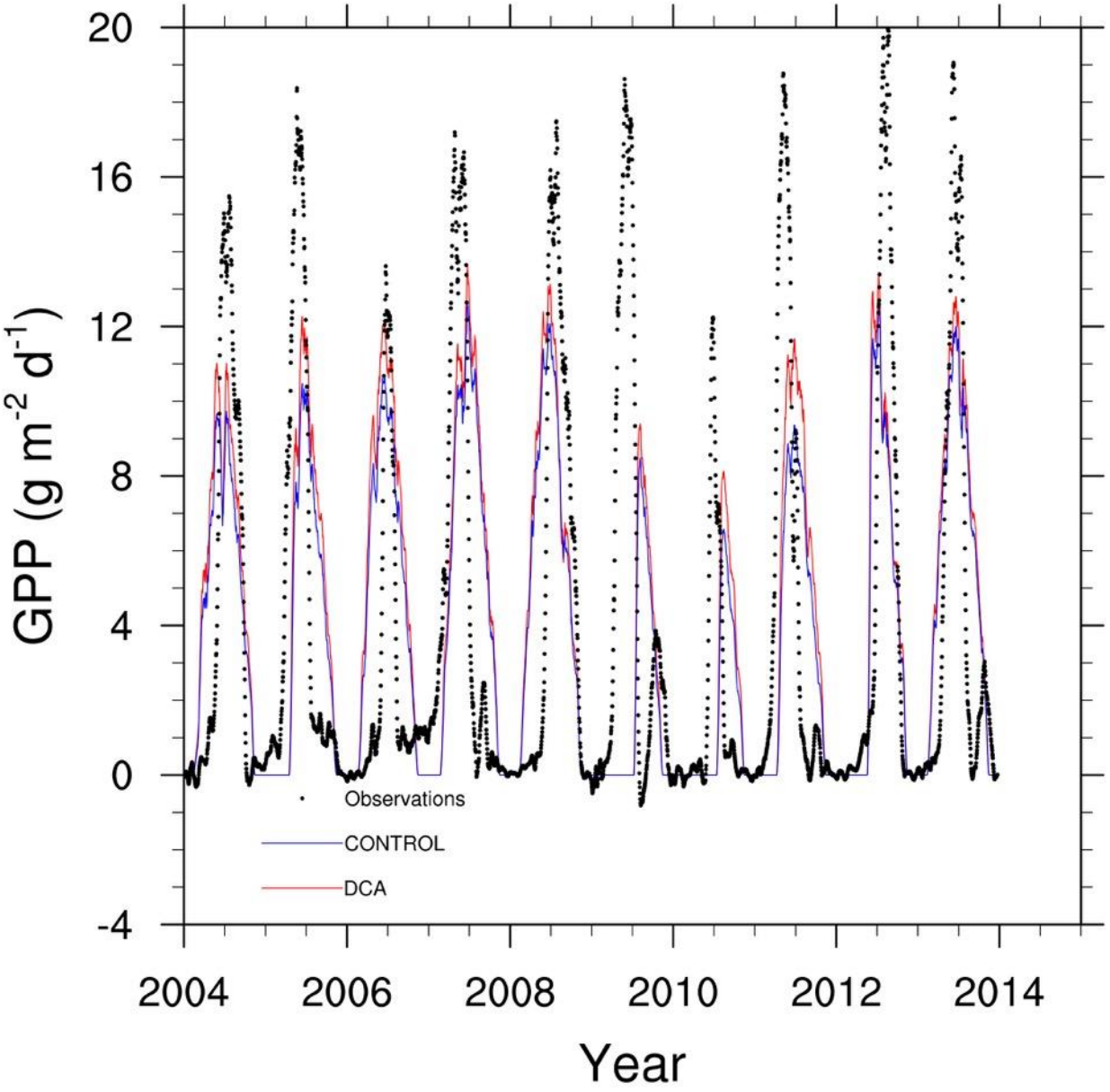

Figure 4.33. GPP of DCA (red line), CONTROL (blue line), and observations (black dots) at the BE-Lon site.

D. Forests Copyright and Licensing Information

E. Biogeosciences Copyright and Licensing Information

The following license and copyright agreement is valid for any article published by Copernicus Publications whose original manuscript was received from **10 December 2007** on.

Copyright

Creative Commons Attribution 3.0 License
Anyone is free:

to Share — to copy, distribute and transmit the work

to Remix — to adapt the work

Under the following conditions:
Attribution — The original authors must be given credit

For any reuse or distribution, it must be made clear to others what the license terms of this work are.

Any of these conditions can be waived if the copyright holders give permission.

Nothing in this license impairs or restricts the author's moral rights.

The full legal code of this license can be found at:
https://creativecommons.org/licenses/by/3.0/legalcode

Copyright transfers
Many authors have strict regulations in their contract of employment regarding their works. A transfer of copyright to the institution or company, as well as the reservation of specific usage rights, is typical. Please note that in the case of open-access publications in combination with a Creative Commons License, a transfer of the **copyright** to the institution is possible, as it belongs to the author anyway and is not subject to the publisher.

Any **usage rights** are regulated through the Creative Commons License. As Copernicus Publications uses the Creative Commons Attribution 3.0 License, anyone (the author, his/her institution/company, the publisher, as well as the public) is free to copy, distribute, transmit, and adapt the work as long as the original author is given credit (see above). Therefore, specific usage rights cannot be reserved by the author or his/her institution/company, and the publisher cannot include a statement "all rights reserved" in any published paper.

A copyright transfer from the author to his/her institution/company will be expressed in a special "Copyright Statement" at the end of the publication rather than on the first page in the article citation header. Authors are asked to include the following sentence: "The author's copyright for this publication is transferred to *institution/company*".

F. Journal of Advancing Modeling the Earth System Copyright and Licensing Information

All articles in the *Journal of Advances in Modeling Earth Systems* will be published under the terms of a Creative Commons License: All Research Councils UK (RCUK) and Wellcome Trust funded authors will be directed to the Creative Commons Attribution license (CC BY) in accordance with funder mandates effective on 1 April 2013. All other authors (non- RCUK and Wellcome Trust funded authors) will be directed to a choice of Creative Commons Attribution Non-Commercial NoDerivs license (CC BY NC ND license). Copyright on any research article published by a Wiley Open Access journal is retained by the author(s). Authors grant Wiley a license to publish the article and identify itself as the original publisher.

The Creative Commons Attribution License (CC BY) allows users to copy, distribute and transmit an article and adapt the article and make commercial use of the article. The CC BY license permits commercial and non-commercial re-use of an open access article, as long as the author is properly attributed.

Copyright on any research article published by a Wiley Open Access journal is retained by the author(s). Authors grant Wiley a license to publish the article and identify itself as the original publisher. Authors also grant any third party the right to use the article freely as long as its original authors, citation details and publisher are identified.

Use of the article in whole or part in any medium requires attribution suitable in form and content as follows: [Title of Article/Author/Journal Title and Volume/Issue. Copyright (c) [year] [copyright owner as specified in the Journal]. Links to the final article on Wiley's website are encouraged where applicable.

8 VITA

Beth Drewniak

Education
M.S., 2006, Atmospheric Sciences, University of Illinois, Urbana
B.S., 2002, Physics and Astronomy, University of Illinois, Urbana

Research and Professional Experience
Argonne National Laboratory Argonne, IL
Assistant Climate Scientist, Environmental Science Division 2014-present

- Designated task lead for DOE Energy Exascale Earth System Model (E3SM) project to expand the crop model within the E3SM Land Model (ELM) with additional crop types and farming management practices.
- Provided support for analyzing regional model output of temperature and precipitation extremes for the Regional Resiliency Assessment Program.
- Helped compare observed vs. modeled iron deposition and dissolved iron content in the ocean.

Computational Associate, Atmospheric Modeling, Environmental Science Division 2009-2014

- Investigated the impact on soil organic carbon and crop productivity from farming practices including plant date, residue management, fertilizer use, and land cover change with a land surface model, CLM, updated to include agriculture. Developed crop features are included in CLM4.5.
- Worked on dynamic land use capability in CLM to allow changes in land type over time such that carbon, water, and energy balance are maintained across multiple soil columns. Interests for this work also include adding additional management practices (e.g., tillage and irrigation) and crop types (including managed grasses) to the CLM framework.
- Organized a workshop on Urban Landscapes and Climate Change; currently working on methodology for permanent sensor deployment to create an urban observatory.
- Assisting the Air Force with the development of a Presumed to Conform List of activities to maintain compliance of criteria pollutants with air quality regulations.

Predoctoral Appointee, Environmental Science Division 2006-2009

- Integrated agriculture land representation, including maize, soybean, and spring wheat into the Carbon-Nitrogen version of the Community Land Model (CLM-CN). Incorporated dynamic roots, management practices, and a separate growth scheme with carbon and nitrogen allocation.
- Evaluated U.S. mercury contributions from China with the Chemical Transport Model (CTM), Model for Ozone and Related Chemical Tracers (MOZART).
- Provided support to Air Force Material Command (AFMC) for various projects including biodiesel emissions estimates, greenhouse gas inventory development, and technical support related to Aerospace Residual Risk.
- Evaluated air quality compliance in the Environmental Compliance Assessment and Management Program (ECAMP) audits at various AFMC bases.

- Participated in development of air quality and noise impact sections of energy-related Environmental Impact Statements (EIS).

University of Illinois Champaign, IL
Graduate Research Assistant, Atmospheric Sciences Department 2004-2006

- Evaluated the influence of climate on land cover and biogenic volatile organic carbon emissions from vegetation and nitrogen oxides from soil, with a modified version of the dynamic vegetation model, Integrated Biosphere Simulator, agricultural version (Agro-IBIS).
- Modified Agro-IBIS to include biogenic volatile organic carbon emissions from vegetation and NOx emissions from soil.
- Worked with the Global Biosphere Emissions and Interactions System (GloBEIS) model to estimate spatial changes in isoprene emissions from a new plant species distribution in the northern US forests.

Publications

Drewniak, B. A., "Simulating dynamic roots in the Energy Exascale Earth System Land Model", *Journal of Advances in Modeling Earth Systems*, 11, https://doi.org/10.1029/2018MS001334, (2019).

Wang, J., Bessac, J., Kotamarthi, R. Constantinescu, E., and Drewniak, B., "Internal variability of a dynamically downscaled climate over North America", *Climate Dynamics*, doi:10.1007/s00382-017-3889-1, (2017).

Drewniak, B., Gonzalez-Meler, M. A., "Earth System Model needs for including the interactive representation of nitrogen deposition and drought effects on forested ecosystems", *Forests*, 8, doi:10.3390/f8080267 (2017).

Levis, S., A. Badger, B. Drewniak, C. Nevinson, and X. Ren, "CLMcrop yields and water requirements: Avoided impacts by choosing RCP 4.5 over 8.5", *Climatic Change*, doi:10.1007/s10584-016-1654-9 (2016).

Mishra, U., B. Drewniak, J. D. Jastrow, R. M. Matamala, and U. W. A. Vitharana, "Spatial representation of organic carbon and active-layer thickness of high latitude soils in CMIP5 earth system models", *Geoderma*, http://dx.doi.org/10.1016/j.geoderma.2016.04.017 (2016).

Drewniak, B. A., U. Mishra, J. Song, J. Prell, and V. R. Kotamarthi, "Modeling the impact of agricultural land use and management on US carbon budgets," *Biogeosciences*, 12: 2119-2129 (2015).

Bilionis, I., B. A. Drewniak, and E. M. Constantinescu, "Crop physiology calibration in the CLM", *Geoscientific Model Development*, 8:1071-1083 (2015).

Drewniak, B., P. Snyder, A. L. Steiner, T. Twine, D. Wuebbles, "Simulated changes in biogenic VOC emissions and ozone formation from habitat expansion of Acer Rubrum (Red Maple)," *Environmental Research Letters*, 9:doi: 10.1088/1748-9326/9/1/014006 (2014).

Zeng, X., B. Drewniak, and E. Constantinescu, "Calibration of the Crop Model in the Community Land Model," *Geoscientific Model Development Discussion*, 6:379-398 (2013).

Drewniak, B., J. Song, J. Prell, R. Kotamarthi, and R. Jacob, "Modeling Agriculture in the Community Land Model," *Geoscientific Model Development*, 6: 495-515 (2013).

Drewniak, B., V. Kotamarthi, D. Streets, M. Kim, and D. Crist, "Estimates of Mercury Flux into the United States from Non-local and Global Sources: Results from a 3-D CTM Simulation," *Atmospheric Chemistry and Physics Discussion*, 8:19861-19890 (2008).

McCullough, P. R., J. E. Stys, Jeff A. Valenti, C. M. Johns-Krull, K. A. Janes, J. N. Heasley, B. A. Bye, C. Dodd, S. W. Fleming, A. Pinnick, R. Bissinger, B. L. Gary, P. J. Howell, and T. Vanmunster, "A Transiting Planet of a Sun-like Star," Astrophysical Journal, 648:1228-1238 (2006).

Manuscripts under review

Drewniak, B., Simulating dynamic roots in the Energy Exascale Earth System Land Model, submitted to JAMES.

Peer Reviewed Extended Abstracts

A. Mametjanov, B. Norris, X. Zeng, B. Drewniak, J. Utke, M. Anitescu, P. Hovland, "Applying Automatic Differentiation to the Community Land Model," *Proceedings of AD2012, the 6th International Conference on Automatic Differentiation*, 2012. Also Preprint ANL/MCS-P1993-0112, January 2012.

Non-Peer Reviewed Publications

Kotamarthi, V. R., Wang, J., and Drewniak, B.: Climate Assessments: A Summary for the State of Maine, Argonne National Laboratory, Lemont, IL, 2016.

Oleson, K.W., D.M. Lawrence, G.B. Bonan, B. Drewniak, M. Huang, C.D. Koven, S. Levis, F. Li, W.J. Riley, Z.M. Subin, S.C. Swenson, P.E. Thornton, A. Bozbiyik, R. Fisher, C.L. Heald, E. Kluzek, J.-F. Lamarque, P.J. Lawrence, L.R. Leung, W. Lipscomb, S. Muszala, D.M. Ricciuto, W. Sacks, Y. Sun, J. Tang, and Z.-L. Yang, 2013: Technical description of version 4.5 of the Community Land Model (CLM), NCAR Technical Note NCAR/TN-503+STR, 434 pp.

Chang, Y., M. MacDonell, and B. Drewniak, Review of Relevant Toxicity Data, Exposure Guidelines, and Environmental Pollution Cases to Support the Gwangyang Bay Area Project, Argonne National Laboratory, prepared for Research Institute of Industrial Science and Technology, Gwangyang Environment Research Department (December 2007).

Presentations

Drewniak, B., “Climate driven crop planting date in the ACME Land Model (ALM): Impacts on productivity and yield”, AGU Fall Meeting, New Orleans, LA, December 11-15, 2017.

Drewniak, B., “Climate driven planting date in the ACME Land Model”, CESM Workshop, Boulder, CO, June 19-22, 2017.

Drewniak, B., “Establishing a planting date for crops in the ACME Land Model (ALM)”, ACME Land Science Talk, April, 11, 2017.

Feng, Y., Drewniak, B., and Ito, A., “Spatial and Seasonal Variability in Soluble Iron Deposition and Contribution to Sea-surface Iron Distributions”, AGU Fall Meeting, San Francisco, CA, Dec. 12-16, 2016 (poster).

Drewniak, B., “New method to determine crop planting date in the ACME Land Model”, AGU, San Francisco, CA, December 12-16, 2016 (poster).

Drewniak, B., “Climate driven planting date in ALM”, ACME Fall Meeting, Denver, CO, November 9-11, 2016 (poster).

Drewniak, B., “New method to determine crop planting in ALM”, CESM Workshop, Breckenridge, CO, June 20-23, 2016 (poster).

Drewniak, B., “New method to determine crop planting in ALM”, ACME All Hands Meeting, Washington D.C., June 7-10, 2016 (poster).

Drewniak, B. A., “Dynamic root status and impacts on productivity and evapotranspiration”, CLM Working Group Meeting, Boulder, CO, February 8-11, 2016.

Drewniak, B. A., “Dynamic Root Distribution in the Community Land Model”, AGU, December 14-18, 2015.

Drewniak, B. A., “Dynamic Roots in ALM”, ACME Fall Meeting, Albuquerque, NM, November 2-4, 2015.

Drewniak, B. A., “Dynamic Root Distribution in CLM”, CESM Workshop, Breckenridge, CO, June 15-18, 2015.

Drewniak, B. A., “Dynamic Roots in CLM”, CLM Working Group Meeting, Boulder, CO, March 3-5, 2015.

Bilionis, I., B. A. Drewniak, and E. M. Constantinescu, “Calibrating Soybean Parameters using a Sequential Monte Carlo Scheme”, AGU, December 15-19, 2014.

Bilionis, I., B. Drewniak, and E. M. Constantinescu, "Calibration soybean parameters using a Sequential Monte Carlo scheme", CESM Workshop, Breckenridge, CO, June 16-19, 2014.

Drewniak, B., and U. Mishra, "Soil organic carbon response to cultivation in the Community Land Model", RCN FORECAST Workshop: Representing Soil Carbon Dynamics in Global Land Models to Improve Future IPCC Assessments, Breckenridge, CO, June 11-14, 2014.

Drewniak, B., and U. Mishra, "Soil carbon response to cultivation in the Community Land Model", DOE PI Meeting, Potomac, MD, May 12-14, 2014.

Drewniak, B., "Biogeochemical Cycles in the Community Land Model", Argonne Biology Seminar, Argonne, IL, March 27, 2014 (Invited).

Drewniak, B., "CLM Crops", iESM Meeting, College Park, MD, March 24-25, 2014.

Drewniak, B., "Soil organic response to harvested crops: a comparison between biogeochemistry model versions", CESM Land Model, Biogeochemistry, and Societal Dimensions Working Group Meeting, Boulder, CO, February 24-27, 2014.

Drewniak, B., F. Cheng, R. Jacob, and C. Catlett, "Urban Landscapes and Climate Change: Workshop Report", 2014 AMS Annual Meeting, Atlanta, GA, Feb. 3-7, 2014.

Drewniak, B. A. and U. Mishra, "Modeling cultivation impacts on soil organic carbon under different management practices with the Community Land Model", 2013 AGU Fall Meeting, San Francisco, CA, Dec. 9-13, 2012.

Drewniak, B., X. Zeng, E. Constantinescu, "Calibrating soybean parameters in CLM-Crop using an MCMC approach", CESM Workshop, Breckenridge, CO, June 17-20, 2013.

Drewniak, B. A., "Assessing the impacts of a new planting date scheme on crop productivity and yield in CLM-Crop", CESM Land Model, Biogeochemistry, and Societal Dimensions Working Group Meetings, Boulder, CO, February 19 - 22, 2013.

Drewniak, B., V. R. Kotamarthi, "Estimating the Sensitivity of CLM-Crop to Plant Date and Growing Season Length", 2012 AGU Fall Meeting, San Francisco, CA, Dec. 3-7, 2012. (Poster)

Constantinescu, E. M., B. A. Drewniak, X. Zeng, "Calibration of the crop processes in the climate community model", 2012 AGU Fall Meeting, San Francisco, CA, Dec. 3-7, 2012. (Poster)

Drewniak, B., X. Zeng, M. Anitescu, and V. R. Kotamarthi, "Parameter Sensitivity Evaluation of the CLM-Crop Model," CESM Workshop, Breckenridge, CO, June 18-21, 2012. (Poster)

Drewniak, B., J. Song, J. Prell, and V. R. Kotamarthi, "Integrating a dynamic root scheme in a land surface model," Scaling Root Processes: Global Impacts Workshop, Arlington, VA, March 6-9, 2012.

Zeng, X., B. Drewniak, A. Mametjanov, M. Anitescu, B. Norris, and V.R. Kotamarthi, "Crop parameter evaluation in CLM-Crop". CESM Land/BGC/Chemistry Climate/Societal Dimensions Working Group Meeting, Boulder, CO, February 27 - March 2, 2012.

Drewniak, B., X. Zeng, A. Mametjanov, M. Anitescu, B. Norris, and V.R., Kotamarthi, "Parameter sensitivity evaluation of the CLM-Crop model," 2011 AGU Fall Meeting, San Francisco, CA, Dec. 5-9, 2011. (Poster)

Drewniak, B., V. R. Kotamarthi, J. Prell, R. Jacob, and J. Song, "Agricultural impacts on soil carbon in CLM," Data Needs for Improving Model Representations of Soil Carbon Responses to Climate Change in Permafrost Regions Workshop, Argonne, IL, October 3-4, 2011.

Drewniak, B., "Transient Landunits in CLM," 16th Annual CESM Workshop, Breckenridge, CO, June 20-23, 2011. (Poster)

Drewniak, B., V. R. Kotamarthi, J. Prell, R. Jacob, and J. Song, "Estimating changes in soil organic carbon under selected agriculture residue and fertilizer management practices with the Community Land Model," 2010 American Geophysical Union Fall Meeting, San Francisco, CA, Dec. 13-17, 2010.

Drewniak, B., V. R. Kotamarthi, J. Prell, R. Jacob, and J. Song, "Agriculture land use in CLM : impacts of management on soil carbon," 15th Annual Community Climate System Model Workshop, Breckenridge, CO, June 28 - July 1, 2010.

Drewniak, B., V. R. Kotamarthi, R. Jacob, J. Prell, and J. Song, "Modeling Soil Organic Carbon for Agriculture Land Use Under Various Management Practices," 2009 American Geophysical Union Fall Meeting, San Francisco, CA, December 14-18, 2009. (Poster)

Drewniak, B., J. Song, J. Prell, R. Kotamarthi, and R. Jacob, "Modeling Impacts of Land Use Change and Agriculture Management on Soil Carbon," 14th Annual CCSM Workshop, Breckenridge, CO, June 15-18, 2009. (Poster)

Drewniak, B., J. Song, R. Kotamarthi, and R. Jacob, "Agriculture Land Surface Scheme and Dynamic Root Structure in CLM," 2009 Climate Change and Prediction Program Meeting, Bethesda, MD, April 6-9, 2009. (Poster)

Drewniak, B., V. R. Kotamarthi, R. Jacob, J. Prell, and J. Song, "Modeling Water and Carbon Budgets in Current and Future Agriculture Land Use," 2008 American Geophysical Union Fall Meeting, San Francisco, CA, December 15-19, 2008. (Poster)

Drewniak, B., V. R. Kotamarthi, R. Jacob, J. Song, I. Foster, "Agriculture Models in CLM," 13th Annual CCSM Workshop, Breckenridge, CO, June 17-20, 2008. (Poster)

Sponsor reports

Air Force Presumed to Conform Materials: Boilers, Runway Marking, Airfield Lighting, Signage, and Aerospace Ground Equipment; with Al Smith and Young-Soo Chang

Organization of Workshops

Urban Landscapes and Climate Change: from measurements to modeling, Argonne, IL, August 27-28, 2013 (organizing committee chair)

Scaling Root Processes: Global Impacts Workshop, Arlington, VA, March 7-9, 2012 (organizing committee)

Projects managed or directed

Evaluation of Microtopography Effects on the Terrestrial Biosphere and Hydrosphere Under Regional Climate Change (Laboratory Directed Research and Development) – 270K over 3 years
Collaborators: Satish Balay, Todd Munson, Barry Smith, and Y. Eugene Yan

Major program initiatives and proposals

Evaluation of Microtopography Effects on the Terrestrial Biosphere and Hydrosphere Under Regional Climate Change (Laboratory Directed Research and Development) – 270K over 3 years
Collaborators: Satish Balay, Todd Munson, Barry Smith, and Y. Eugene Yan

Manuscripts in Preparation

Lynch, D. J., G.G. McNickle, B. Drewniak, M. A. Gonzalez-Meler, and J. S. Brown, "A Cobb-Douglas optimization model for predicting dynamic above- and below-ground biomass production", in prep.

Professional Memberships
American Geophysical Union